

DISTRIBUTION STATEMENT A
Approved for Public Release
Distribution Unlimited



NLO 99

Contract F61775 - 99 - WFO80

NLO Materials Workshop

DERA Malvern UK

20-21 September 1999

**Reproduced From
Best Available Copy**

19991105 104

We wish to thank the following for their contribution to the success of this Conference:

European Office of Aerospace Research and Development

Air Force Office of Scientific Research

United States Air Force Research Laboratory

UK Ministry of Defence (International Research Collaboration Dept)

Defence Evaluation and Research Agency

DTIC QUALITY INSPECTED 4

AQF00-02-0422

REPORT DOCUMENTATION PAGE

Form Approved OMB No. 0704-0188

Public reporting burden for this collection of information is estimated to average 1 hour per response, including the time for reviewing instructions, searching existing data sources, gathering and maintaining the data needed, and completing and reviewing the collection of information. Send comments regarding this burden estimate or any other aspect of this collection of information, including suggestions for reducing this burden to Washington Headquarters Services, Directorate for Information Operations and Reports, 1215 Jefferson Davis Highway, Suite 1204, Arlington, VA 22202-4302, and to the Office of Management and Budget, Paperwork Reduction Project (0704-0188), Washington, DC 20503.

1. AGENCY USE ONLY (Leave blank)		2. REPORT DATE September 1999	3. REPORT TYPE AND DATES COVERED Conference Proceedings	
4. TITLE AND SUBTITLE Workshop on Nonlinear Optical Materials			5. FUNDING NUMBERS F61775-99-WF	
6. AUTHOR(S) Conference Committee				
7. PERFORMING ORGANIZATION NAME(S) AND ADDRESS(ES) DERA St. Andrews Rd., Malvern WR14 3PS England			8. PERFORMING ORGANIZATION REPORT NUMBER N/A	
9. SPONSORING/MONITORING AGENCY NAME(S) AND ADDRESS(ES) EOARD PSC 802 BOX 14 FPO 09499-0200			10. SPONSORING/MONITORING AGENCY REPORT NUMBER CSP 99-5080	
11. SUPPLEMENTARY NOTES				
12a. DISTRIBUTION/AVAILABILITY STATEMENT Approved for public release; distribution is unlimited.			12b. DISTRIBUTION CODE A	
13. ABSTRACT (Maximum 200 words) The Final Proceedings for Workshop on Nonlinear Optical Materials, 20 September 1999 - 21 September 1999 This is an interdisciplinary conference. Topics include growth, characterization, and applications of chalcopyrites and other nonlinear optical materials for use in the mid-IR.				
14. SUBJECT TERMS EOARD, Chalcopyrite materials, Non-linear Optical Materials			15. NUMBER OF PAGES Too many to count	
			16. PRICE CODE N/A	
17. SECURITY CLASSIFICATION OF REPORT UNCLASSIFIED	18. SECURITY CLASSIFICATION OF THIS PAGE UNCLASSIFIED	19. SECURITY CLASSIFICATION OF ABSTRACT UNCLASSIFIED	20. LIMITATION OF ABSTRACT UL	

NSN 7540-01-280-5500

Standard Form 298 (Rev. 2-89)
Prescribed by ANSI Std. Z39-18
298-102

NLO Materials Workshop

**Woodward Building, DERA Malvern
20-21 September 1999**

Monday 20 September

- 09.15 Registration and Coffee
- 09.45 Introduction and Welcome
 Jayne Ackroyd Manager EOP Dept DERA
- 10.00 NLO Materials – Key Technical Issues
 A W Vere DERA
- 10.15 ZGP – The DERA Programme
 C J Flynn DERA
- 10.35 ZGP annealing studies
 L L Chng DSO Singapore
- 10.50 Non-linear absorption and damage measurements in
 chalcopyrite crystals Shekar Guha AFRL/MLPO
- 11.05 ZGP –crystals: homogeneity region, real defects and optical
 quality V Voevodin R&D Center 'ATOM Tomsk
- 11.25 Break
- 11.45 Secondary ion mass spectrometry analysis
 of CdGeAs₂ J Solomon University of Dayton
- 11.55 Refractive Index measurements and phase-matching
 calculations in chalcopyrites D Zelmon AFRL/MLPO
- 12.10 Analysis of CGA using Thermal admittance spectroscopy
 Steven Smith University of Dayton, Research Institute
- 12.15 High Frequency ZGP Tandem OPO
 J A C Terry DERA

We would like to thank the following for their contribution to the Workshop:

European Office of Aerospace Research and Development
Air Force Office of Scientific Research
United States Air Force Research Laboratory
UK Ministry of Defence (International Research Collaboration Dept)
Defence Evaluation and Research Agency

- 12.45 Buffet Lunch
- 14.00 Recent Advances in chalcopyrites for
mid to far IR frequency conversion P Schunemann
- 14.20 NLO materials at IOM
A Gribenyukov. Institute of Optical Monitoring Tomsk
- 14.35 ZGP Growth and thermal treatment
G Verozubova IOM Tomsk Russia
- 14.50 Optical and electron transport properties of
ZnGeP₂ and CdGeAs₂
B Bairamov Ioffe Institute St Petersburg Russia
- 15.20 Tea
- 15.50 Identification of defects in ZGP by EPR/ENDOR
L Halliburton University of West Virginia
- 16.10 Theory of defects in chalcopyrites
R Pandey University of Michigan
- 16.40 Defect energy and band structure of ZGP
Keith Nash / Mike Fearn DERA Malvern
- 16.50 Tellurium-selenium alloys
M Ohmer Materials Labs WPAFB Dayton Ohio
- 17.00 Discussion – Chalcopyrites II
- 19.30 **Workshop Dinner**
(coach collection from hotels at approx 19.00)

Tuesday 21 September

- 09.00 Non-linear Optical Crystal development at AFRL materials
directorate N Fernelius AFRL/MLPO
- 09.30 Non-linear crystals for IR region in DTIM
L. Isaenko Institute of Monocrystals Novosibirsk
- 10.00 Spectroscopic properties of Pure and Rare-Earth-ion-doped
Non-linear Crystals for the mid IR
A Elisseev Institute of Monocrystals Novosibirsk
- 10.15 LiNbO_3 H Gallagher U. of Strathclyde
- 10.30 Growth and Characterisation of photorefractive materials
C Finnan University of Strathclyde
- 10.45 Coffee
- 11.00 Laboratory visits (or free discussion period)
- 12.30 Lunch
- 13.30 Developments in PPLN fabrication
P Smith University of Southampton
- 13.50 Growth of phosphates and arsenates for periodic poling
R Ward/K Hutton University of Oxford
- 14.10 Tunable quasi-phase-matched SHG of a CO_2 laser
in GaAs Shekar Guha AFRL/MLPO
- 14.30 Periodically -poled BaTiO_3
P Schunemann Lockheed Martin, Nashua
- 14.50 Panel discussion - Quasi-phase matching
- 15.20 Tea and informal discussion session on issues arising from
the workshop and debate on future research
- 16.00 Workshop closes. (The room will be available for informal
discussion groups until 17.00)

Title	First Name	Last Name	Company/University	Country	WorkPhone	FaxNumber	EmailAddress
Prof	Bakhych	Bairamov	A I Ioffe Physico-Technical Institute	Russia	+7 (812) 247-9140	+7 (812) 247-1017	bairamov@bahish.ioffe.rssi.ru
Dr	David	Burlage	Cleveland Crystals	USA	+1-216-486-6100 x3026	+1-216-486-6103	db@clevelandcrystals.com
Dr	David	Titterton	DERA Farnborough	UK	+44(0)1252-393264	+44(0)1252-392007	
Ms	Jayne	Ackroyd	DERA Malvern	UK	+44(0)1684-896607	+44(0)1684-896715	
Dr	Doug	Burgess	DERA Malvern	UK	+44(0)1684-895177	+44(0)1684-895603	
Dr	Ian	Elder	DERA Malvern	UK	+44(0)1684-896139	+44(0)1684-896270	
Dr	Mike	Fearn	DERA Malvern	UK	+44(0)1684-895371	+44(0)1684-894428	
Mr	Colin	Flynn	DERA Malvern	UK	+44 (0)1684-894360	+44(0)1684-894311	cjflynn@dera.gov.uk
Mr	Mike	Harris	DERA Malvern	UK	+44(0)1684-894099	+44(0)1684-894428	
Dr	Keith	Nash	DERA Malvern	UK	+44(0)1684-894746	+44(0)1684-896150	
David	Orchard		DERA Malvern	UK	+44(0)1684-895377		
	Payne		DERA Malvern	UK	+44(0)1684-895766	+44(0)1684-896270	
Mr	Phil	Smith	DERA Malvern	UK	+44(0)1684-894243	+44(0)1684-894311	
Dr	Phil	Soan	DERA Malvern	UK	+44(0)1684-896336	+44(0)1684-896270	
Ms	Lesley	Taylor	DERA Malvern	UK	+44(0)1684-894231	+44(0)1684-894311	ltaylor@dera.gov.uk
	Johnny	Terry	DERA Malvern	UK	+44(0)1684-896295	+44(0)1684-896270	
Dr	Tony	Vere	DERA Malvern	UK	+44(0)1684-894583	+44(0)1684-894311	awvere@dera.gov.uk
Prof	Ludmila	Isaenko	Design & Technolical Inst of Monocrystals	Russia	+7-3832-333-843	+7-3832-333-843	lisa@lea.nsk.su
Dr	Leng Leng	Chng	DSO National Labs	Singapore	c/o DERA Malvern		clenglen@dso.org.sg
Mr	Jim	Telfer	Hilger Crystals	UK	+44(0)1843-231166 x100	+44(0)1843-290310	jim@hilger-crystals.co.uk
Mr	John	Ingleby	Ingcriys Laser Systems Ltd	UK	+44(0)1494-482541	+44(0)1494-2873	jingleby@netcomuk.co.uk
Dr	Alexander	Eliseev	Institute of Mineralogy & Petrography	Russia	+7-3832-332-409	+7-3832-333-843	alex@elis.nsk.ru
Dr	Alexander	Gribenyukov	Institute of Optical Monitoring	Russia	+7-3822-259589	+7-3822-258950	alexandre@losiom.tomsk.ru
Dr	Galina	Verozubova	Institute of Optical Monitoring	Russia	+7-3822-259589	+7-3822-258950	galina@losiom.tomsk.ru
Dr	Tom	Pollak	Lockheed Martin	USA	+1-603-885-4405	+1-603-885-0207	thomas.m.pollak@lmco.com
Dr	Pete	Schunemann	Lockheed Martin	USA	+1-603-885-5401	+1-603-885-0207	peter.g.schunemann@lmco.com
Dr	Ravi	Pandey	Michigan Tech University	USA	+1-906-487-2831	+1-906-487-2933	pandey@mtu.edu
Dr	Valeri	Voevodin	R&D Centre "ATOM"	Russia	+7-3822-413636	+7-3822-413636	voevodin@elefot.tsu.ru
Dr	James	Solomon	University of Dayton	USA	+1-937-656-5712	+1-937-656-7788	james.solomon@ml.afri.af.mil
Dr	Keith	Hutton	University of Oxford	UK	+44(0)1865-272223	+44(0)1865-272400	k.hutton1@physics.ox.ac.uk
Dr	Roger	Ward	University of Oxford	UK	+44(0)1865-272355	+44(0)1865-272400	r.ward2@physics.ox.ac.uk
Dr	Peter	Smith	University of Southampton	UK	+44(0)1703-592809	+44(0)1703-593149	pgs@orc.soton.ac.uk
Mr	Craig	Finnan	University of Strathclyde	UK	+44(0)141-548-3165	+44(0)141-553-4162	craig.j.finnan@strath.ac.uk
Mr	Hugh	Gallagher	University of Strathclyde	UK	+44(0)141-548-4015	+44(0)141-552-2891	h.g.gallagher@strath.ac.uk
Dr	Larry	Halliburton	University of West Virginia	USA	+1-304-2933422 x1442	+1-304-293-5732	lhallibu@www.edu
Dr	Nils	Femelius	Wright Patterson AFB	USA	+1-937-255-4474 x3217	+1-937-255-4913	nils.femelius@ml.afri.af.mil
Dr	Shekhar	Guha	Wright Patterson AFB	USA	+1-937-252-3132 x3022	+1-937-252-0418	shekhar.guha@afri.af.mil
Dr	Melvin	Ohmer	Wright Patterson AFB	USA	+1-937-255-4474 x3233	+1-937-255-4913	melvin.ohmer@ml.afri.af.mil
Dr	Steven	Smith	Wright Patterson AFB	USA	+1-937-255-4474 x3221	+1-937-255-4913	steven.smith@afri.af.mil
Dr	David	Zelmon	Wright Patterson AFB	USA	+1-937-255-4474 x3231	+1-937-255-4913	david.zelmon@afri.af.mil
Dr	Martin	Stickley	EOARD, London	USA	+44(0)171-514-4354	+44(0)171-514-4960	mstickley@eoard.af.mil

Bulk Optical Materials at DERA Malvern

- 1965 Laser materials CaWO_4 Ruby YAG
- 1966 NLO Materials LiNbO_3 LiTaO_3
- 1967 New NLO programme -wide materials survey
tungsten bronzes BSN SBN, KLN and others
Chalcogenides Ag_3AsS_3 AgGaSe_2 AgGaS_2
- 1970's Expanding programme
Solution growth KDP, KTN
Bulk growth (CZ and Bridgman) CdTe CdSeTe

DERA

Notes

Welcome

To the

Non-linear Optical Materials Workshop

DERA Malvern
20 September 1999

Jayne Ackroyd
Business Group Manager EO Protection

DERA

Workshop Benefits

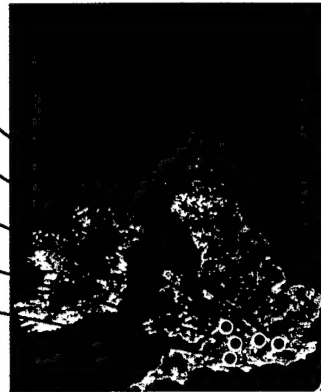
- ⌘ Collaboration
- ⌘ Ideas Exchange
- ⌘ Best use of funding and resources

Enjoy!

DERA

What is DERA?

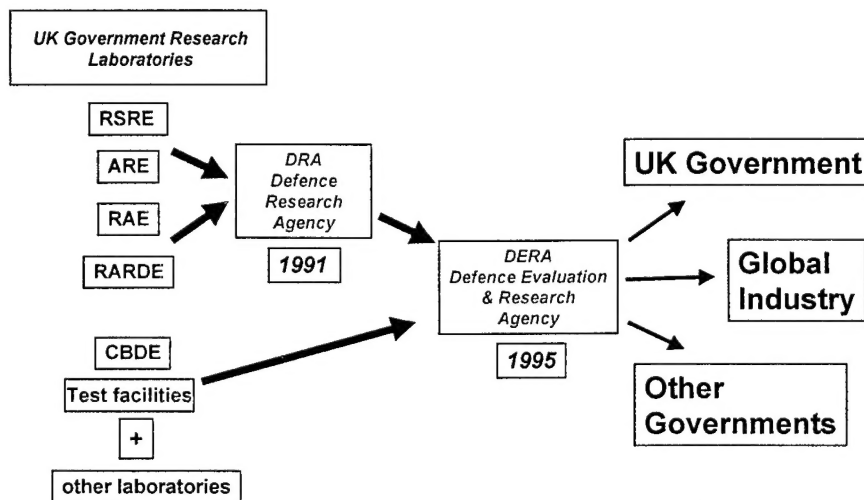
- The largest Research and Technology organisation of its kind in Europe
- £1 billion turnover
- Owned by the UK Government
- Our mission is:
 - to be the main advisor to the UK Government on technology issues
 - to create wealth by technology transfer to industry



May 1999

DERA

DERA Evolution



May 1999

DERA

Bulk Optical Materials at DERA Malvern

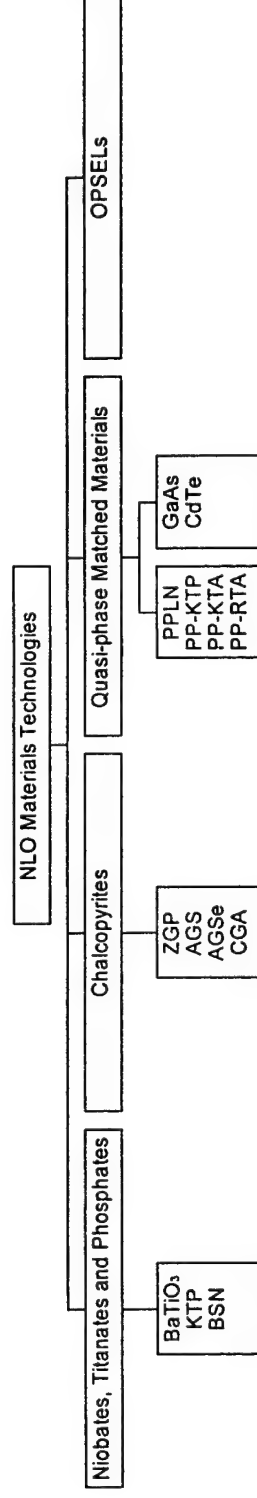
- 1985-90 Slow contraction of programmes
Laser growth concentrated on eye-safe lasers
YLF and related materials
Alternatives to YAG e.g YAP
- 1985-90 Declining interest in NLO Materials
Too difficult and limited markets
- 1992 Improved growth technology and emergence of
ZGP, AgGaSe₂ as potential high power OPO
and SHG materials reinvigorates NLO
programme

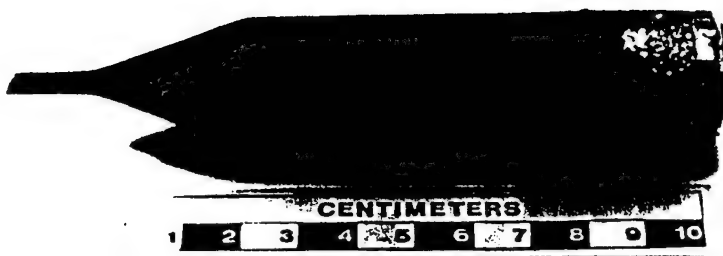
NLO Materials - What Next?

- A short Introduction to the range, content and key issues for discussion at the Workshop and beyond

- A W Vere
DERA Malvern

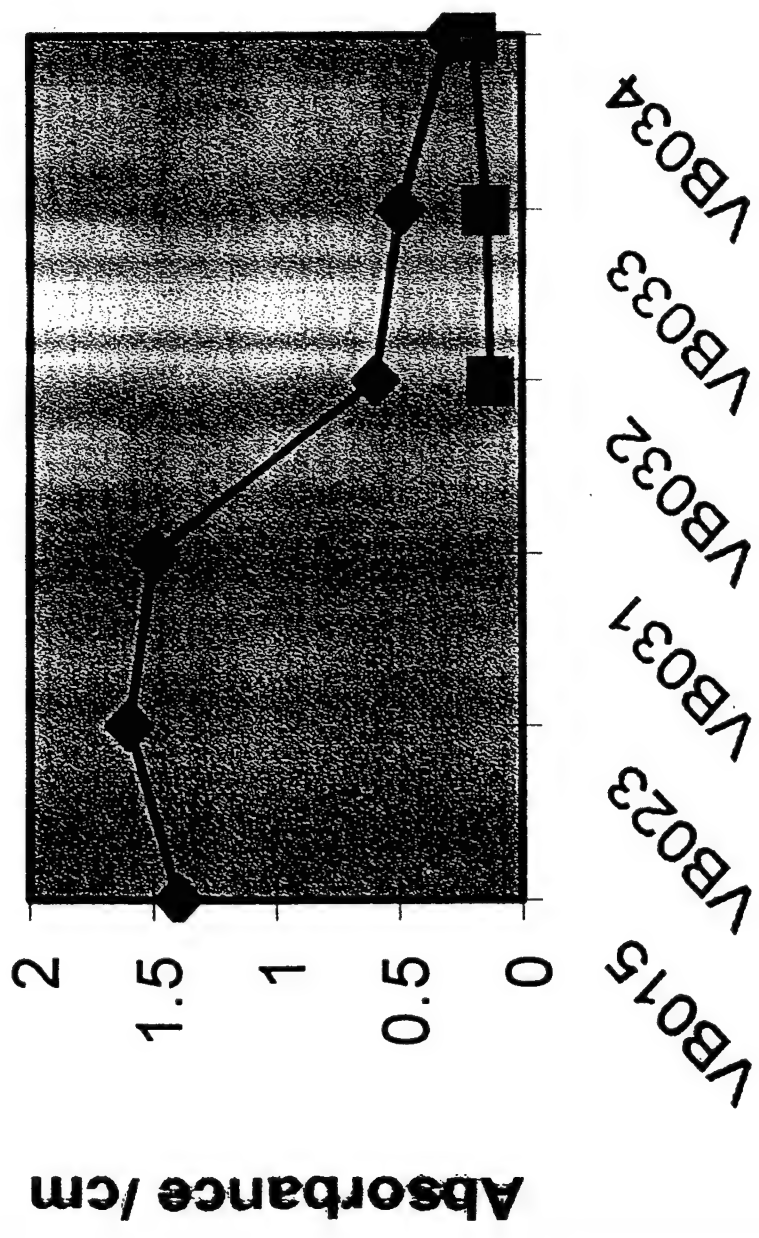
NLO Materials





DERA

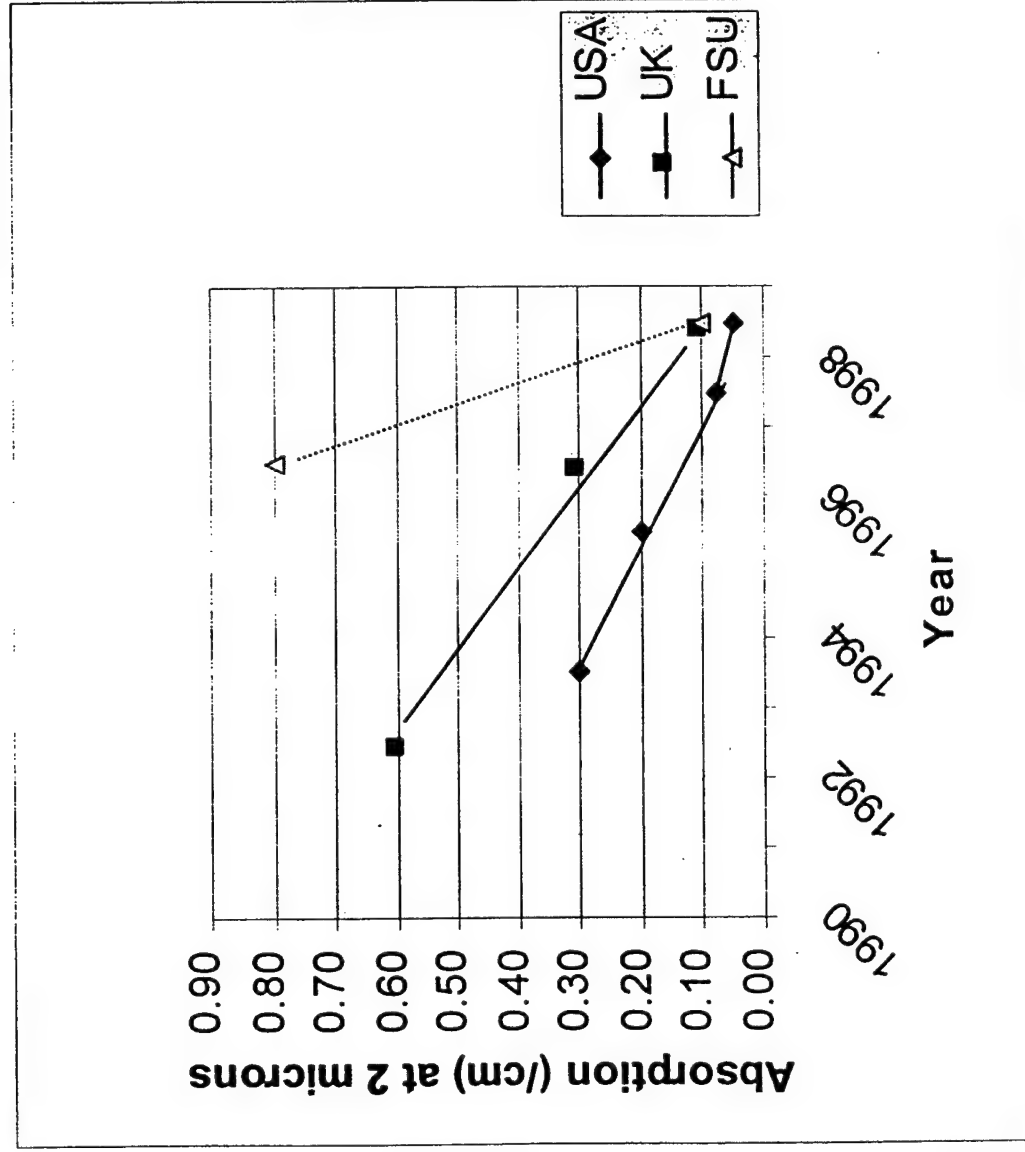
2 micron absorbance



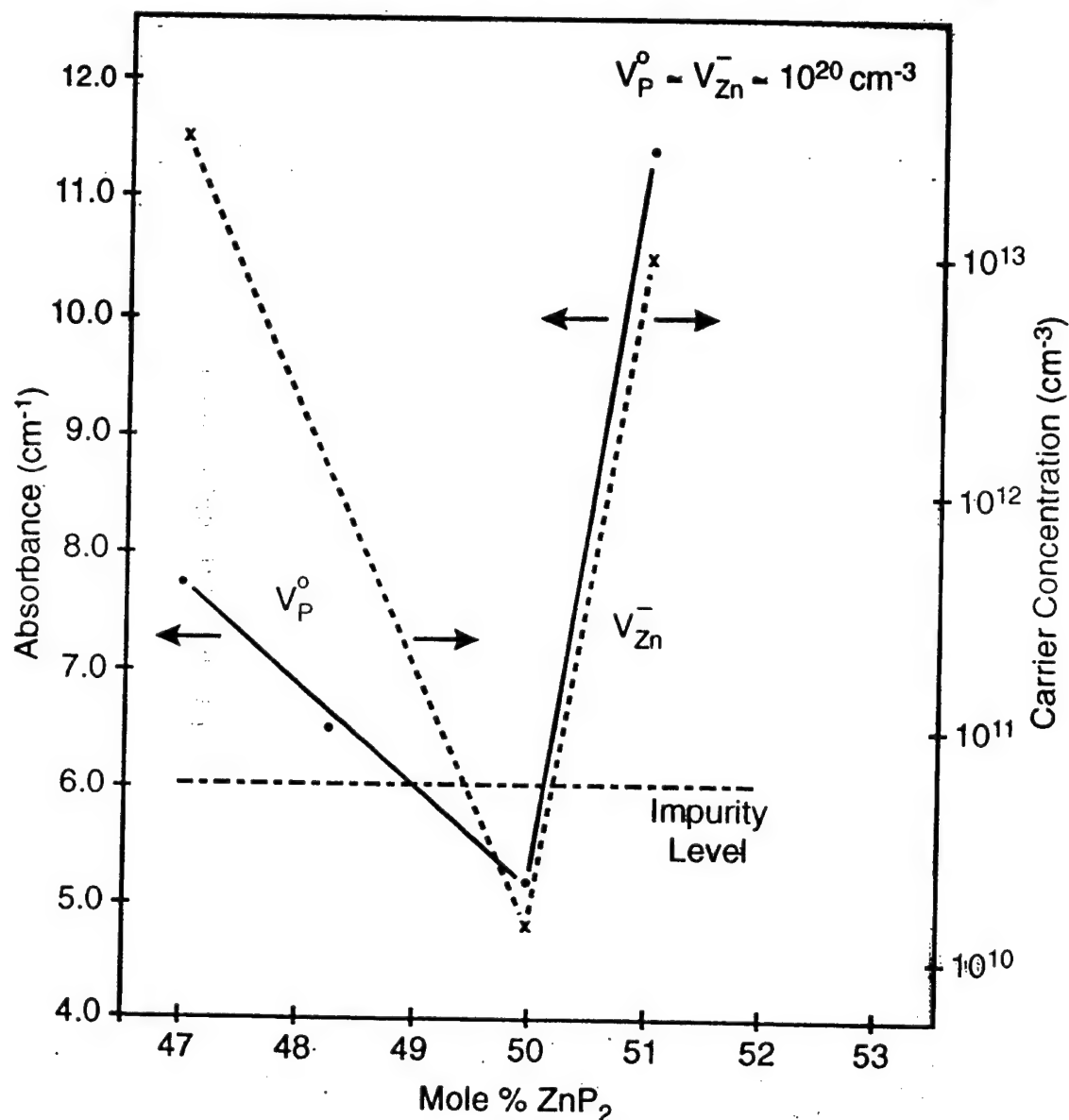
Crystal No.

DERA

2 micron absorption in ZGP



Variation of Absorbance and Carrier Concentration with Stoichiometry



- P G Schunemann, Control of Stoichiometry in Semiconductor Heterostructures (Workshop – Bad Suhl, Germany, 1995)
- x---x V S Grigor'eva et al, Sov Tech Phys Lett **1** No 2 (1975) 61
- Impurity Level (Hypothetical)

DERA

ZnGeP2: DERA Malvern Programme

Tony Vere, Colin Flynn, Phil Smith
DERA Malvern

DERA

Key Properties of ZnGeP_2

- High vapour pressure ($P_{\text{P}_2} \sim 10^{10}$ over melt)
- High melting point (1028 °C)
- Brittle fracture mode
- Thermal expansion coefficient ($5.0 \cdot 10^{-6} \parallel c, 7.8 \cdot 10^{-6} \perp c$)
- Potential precipitation problems
- Band edge optical absorption tail

DERA

Growth programme: OBJECTIVE

- Grow single crystal ZGP
- Low absorption ($< 0.1 \text{ cm}^{-1}$ at $2.128 \mu\text{m}$)
- Understand optical absorption/scattering mechanisms
- Fabricate optical parametric oscillator (OPO) element for use in mid IR.

DERA

Growth programme: HISTORY

- Initially, starting material produced by Wafer Tech
- Vertical Bridgman (VB) & Horizontal Bridgman (HB) produced crystals with mosaic cracking for a few years
- VB now producing good single crystal (PBN crucibles, [016] seed, insulation around seed holder)
- HB improving but abandoned due to VB success
- Collaboration with Institute of Optical Monitoring (IOM), Tomsk
- Starting material now obtained from IOM

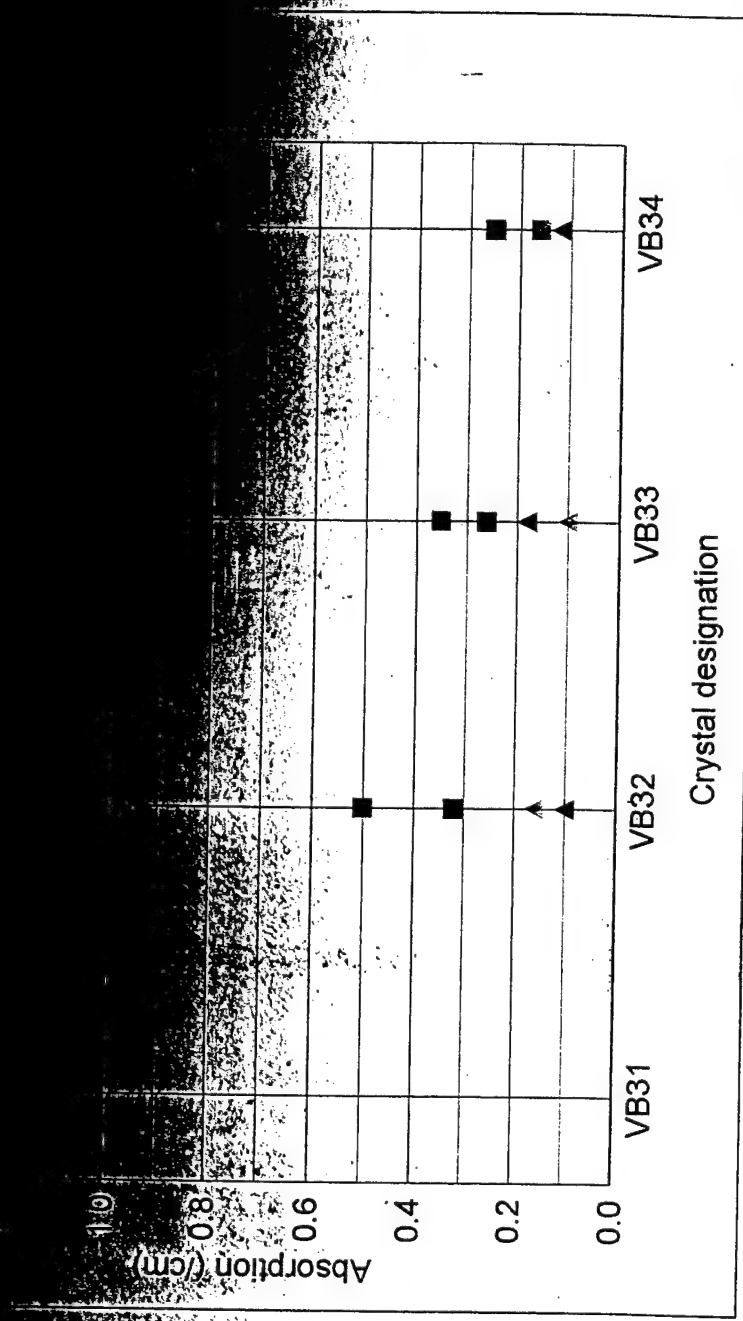
DERA

Comparison of starting materials

- Glow Discharge Mass Spectrometry (GDMS) data for IOM and Wafer Tech starting material.

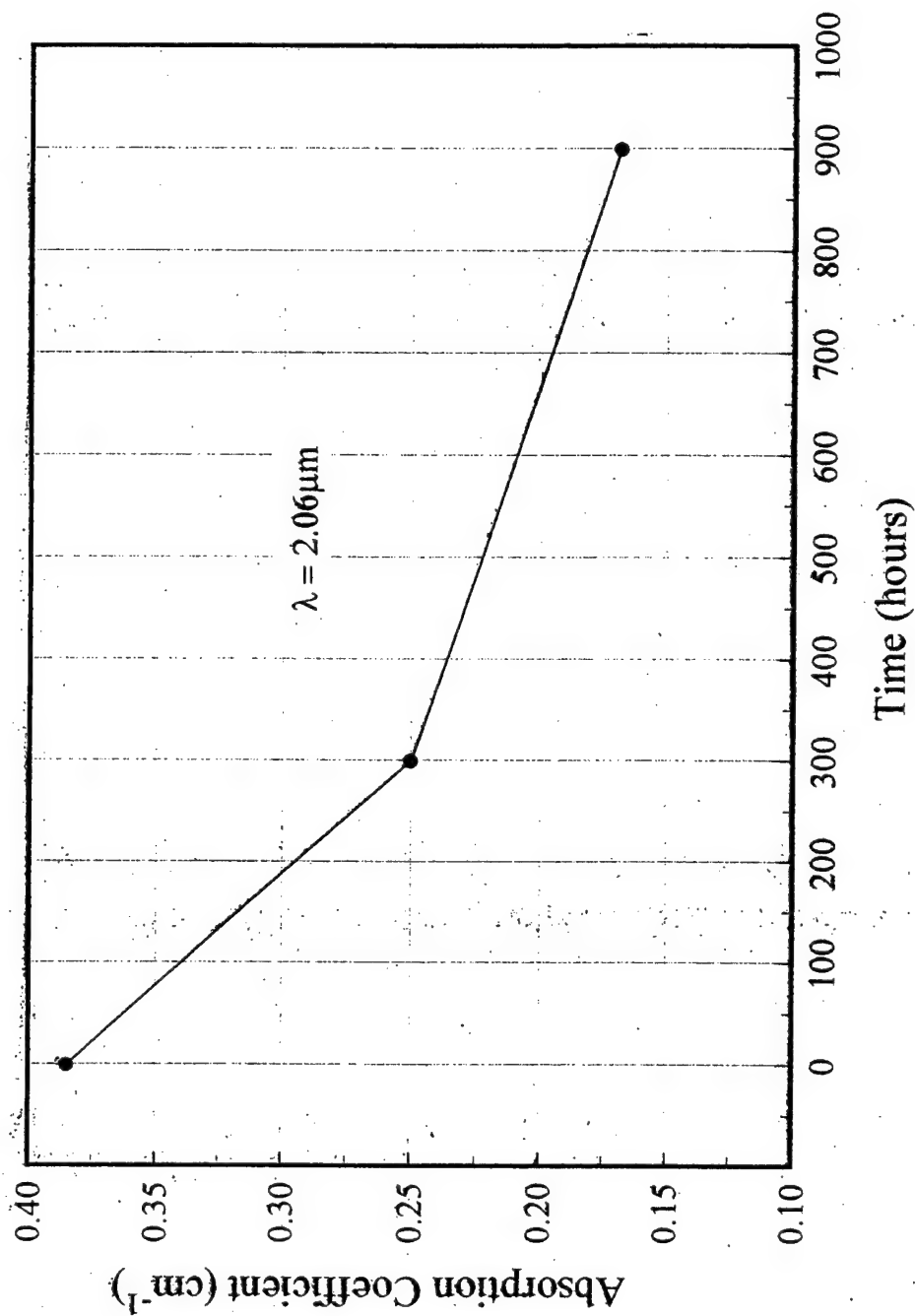
Element	ppb by atom	
	IOM	Wafer Tech
S	120	<20
Mn	29	200
Fe	24	280

DERA



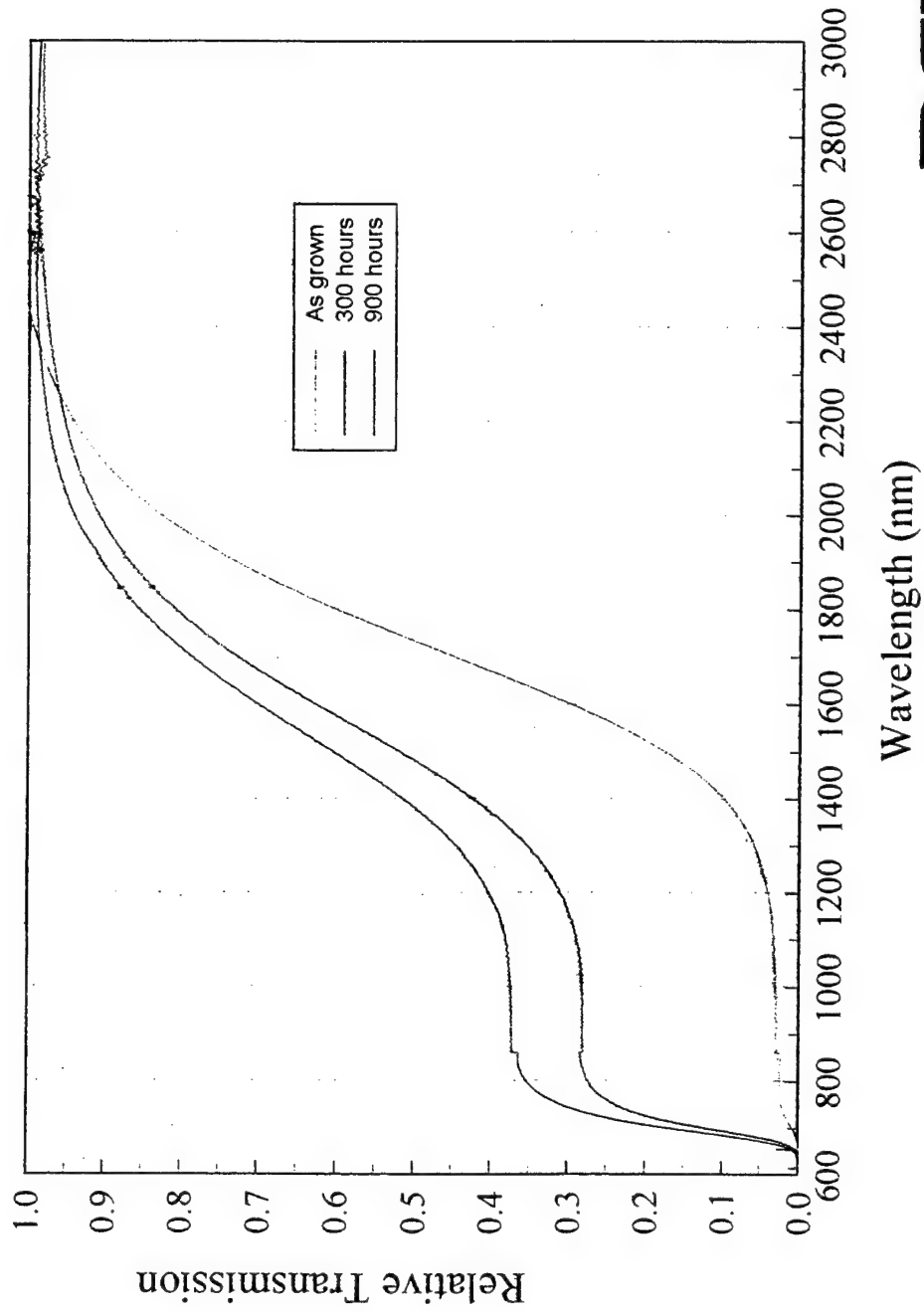
DERA

Variation of absorption coefficient with annealing time



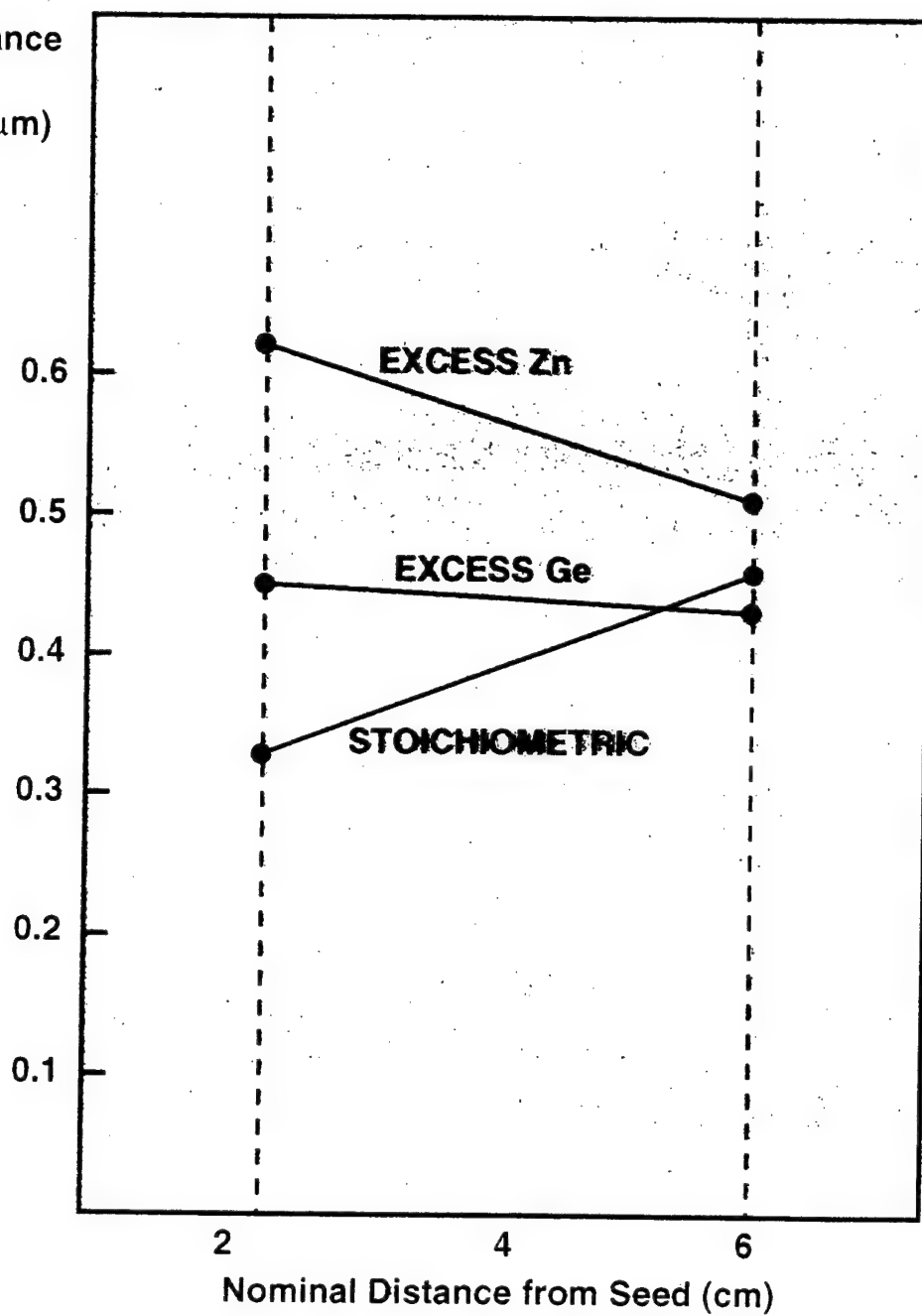
DERA

Effect of annealing on the transmission of ZGP



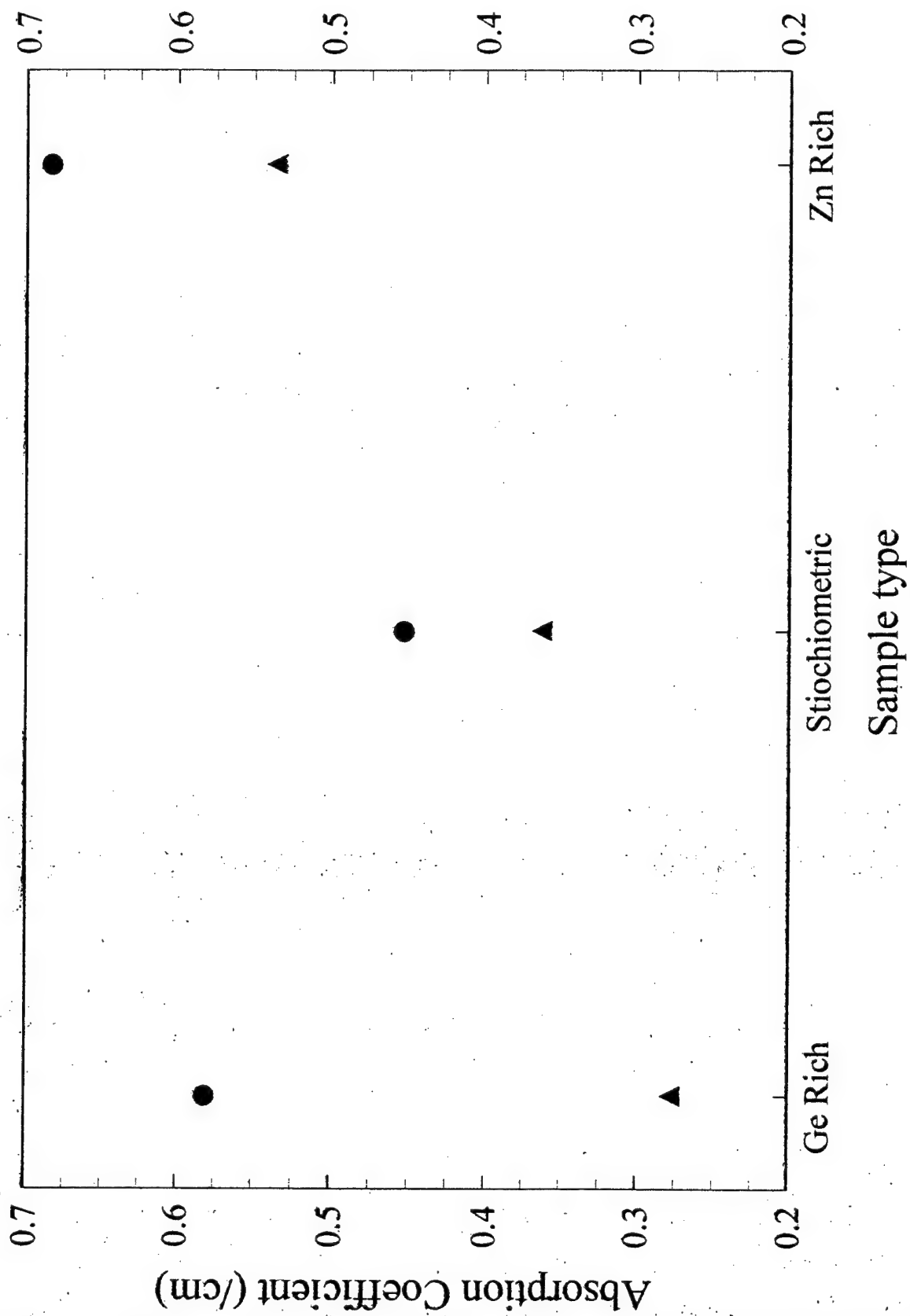
DERA

Absorbance
 cm^{-1}
($\lambda=2.05\mu\text{m}$)

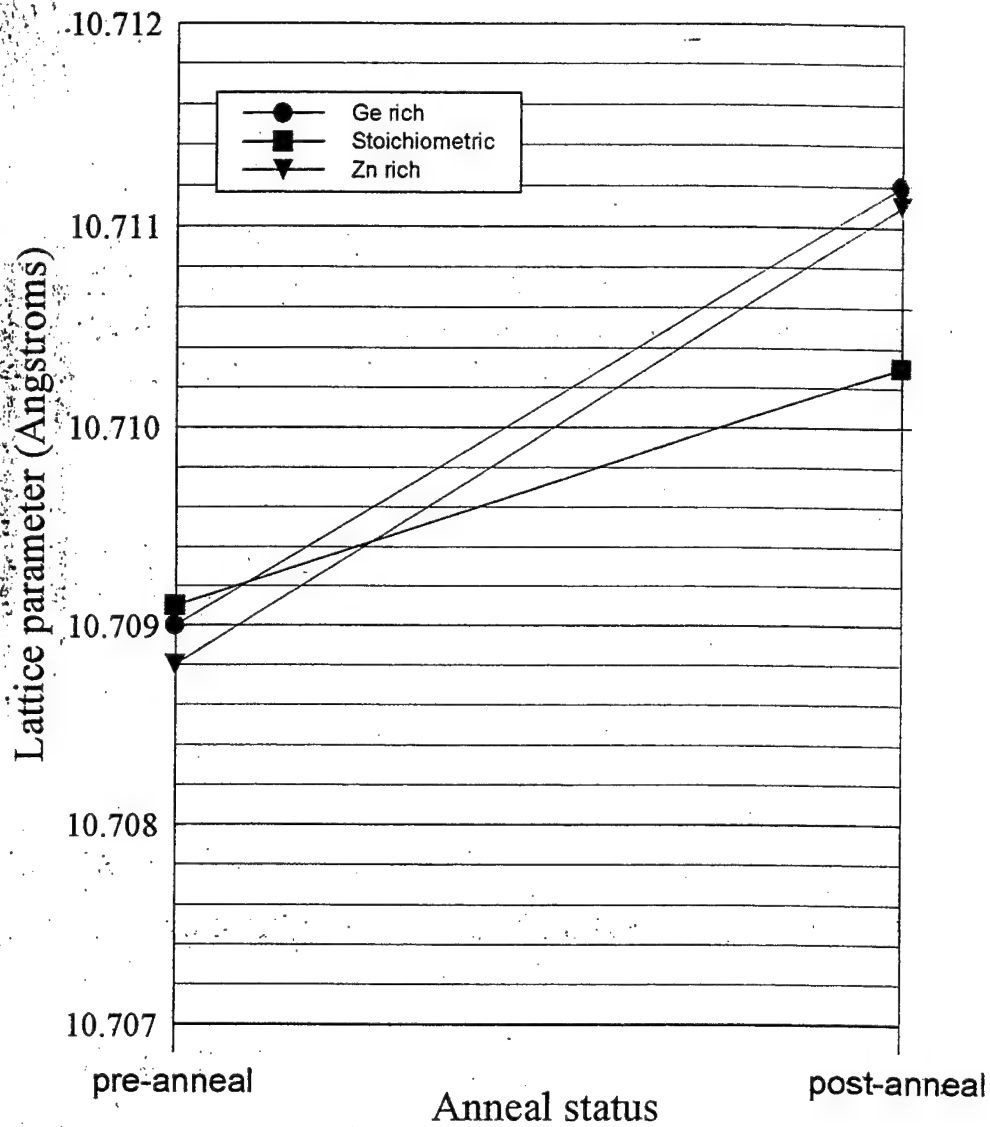


DERA

Absorption coefficient at 2.06 microns

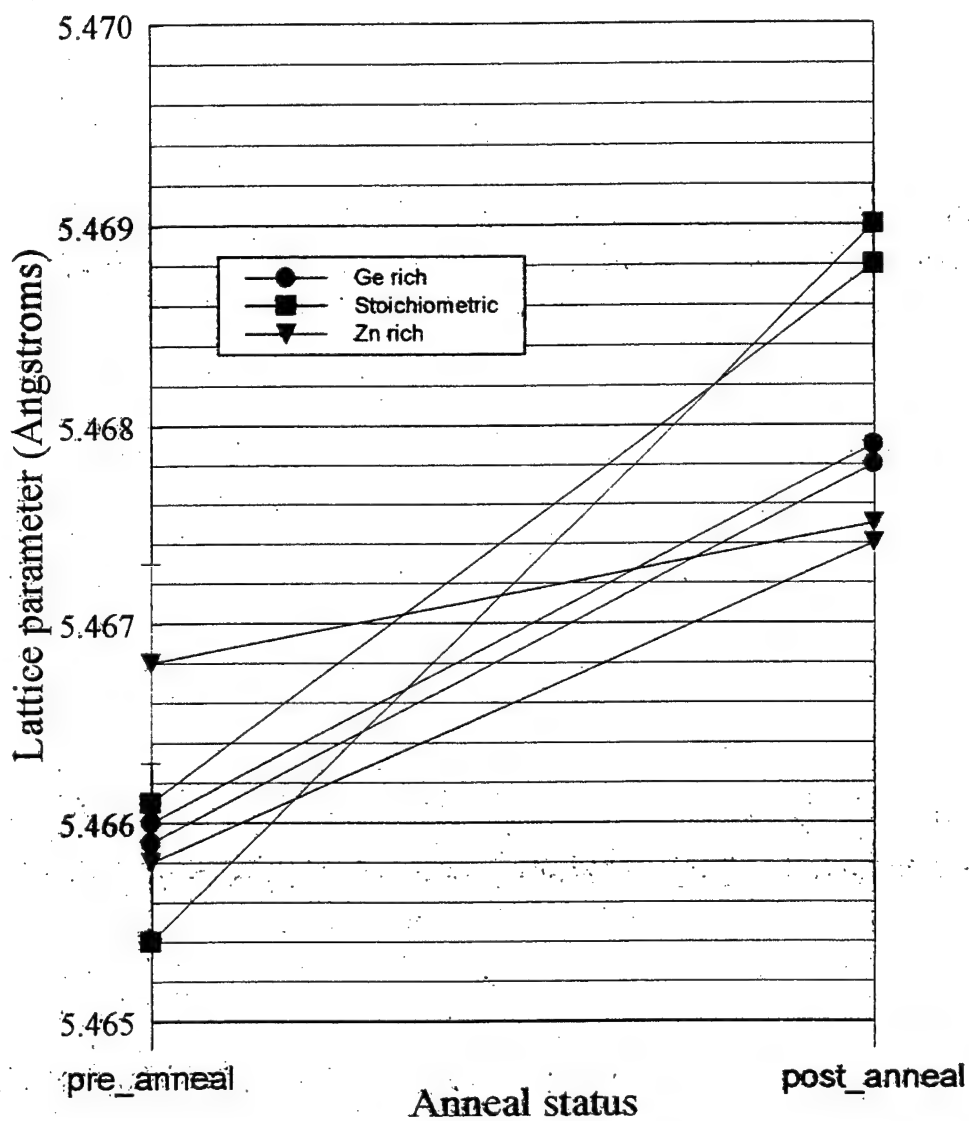


Lattice parameter for $\langle 001 \rangle$ direction
in first-to-freeze, c-axis slices



DERA

Lattice parameter for $\langle 100 \rangle$ & $\langle 010 \rangle$ directions
in first-to-freeze, c-axis slices



DERA

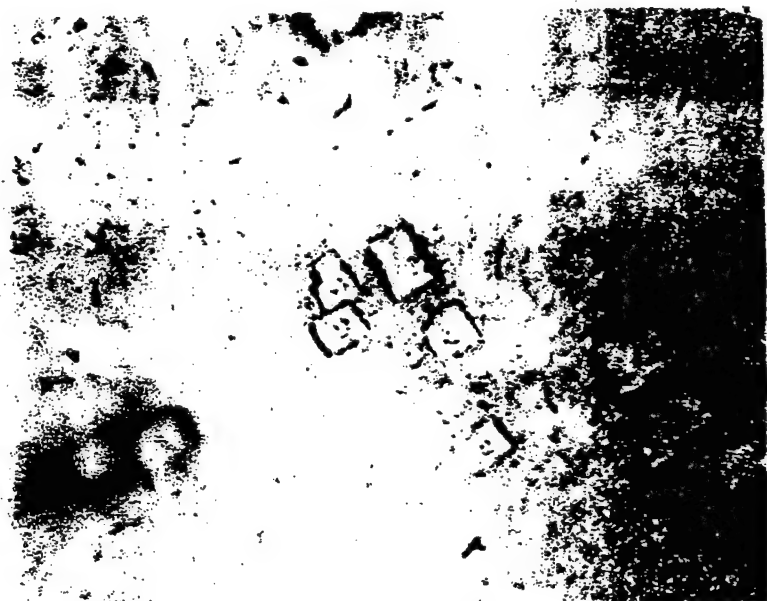
100 μm

DERA

12



10



Summary

- Growing good quality single crystal ZGP
- Need to control stoichiometry of starting charge to avoid precipitation
- Absorption coefficient 'bottoming out' but still worthwhile pursuing annealing studies
- Now need to concentrate programme on identifying causes of absorption

DERA

ZGP Annealing Studies

L L Chng, Y-W Lee and H-G Ang

DSO National Laboratories, Singapore

C J Flynn, P C Smith and A W Vere

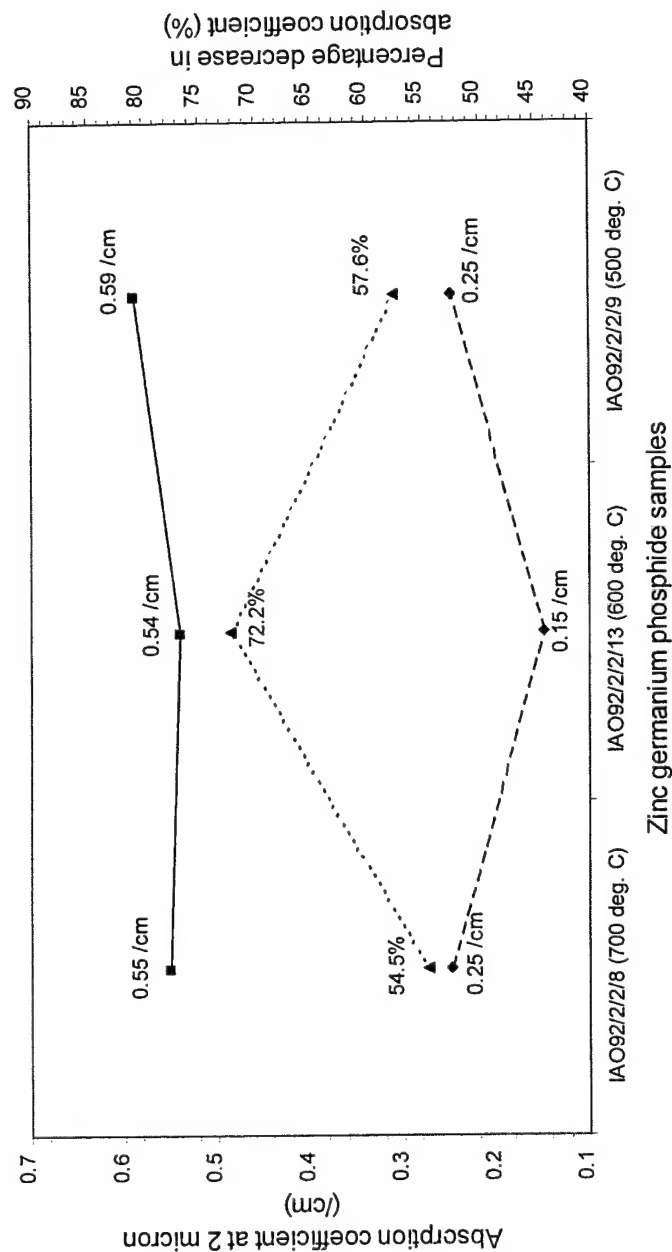
DERA Malvern UK



DSO NATIONAL
LABORATORIES

Effect of Annealing Temperature on the Optical Absorption of IAO Zinc Germanium Phosphide Samples

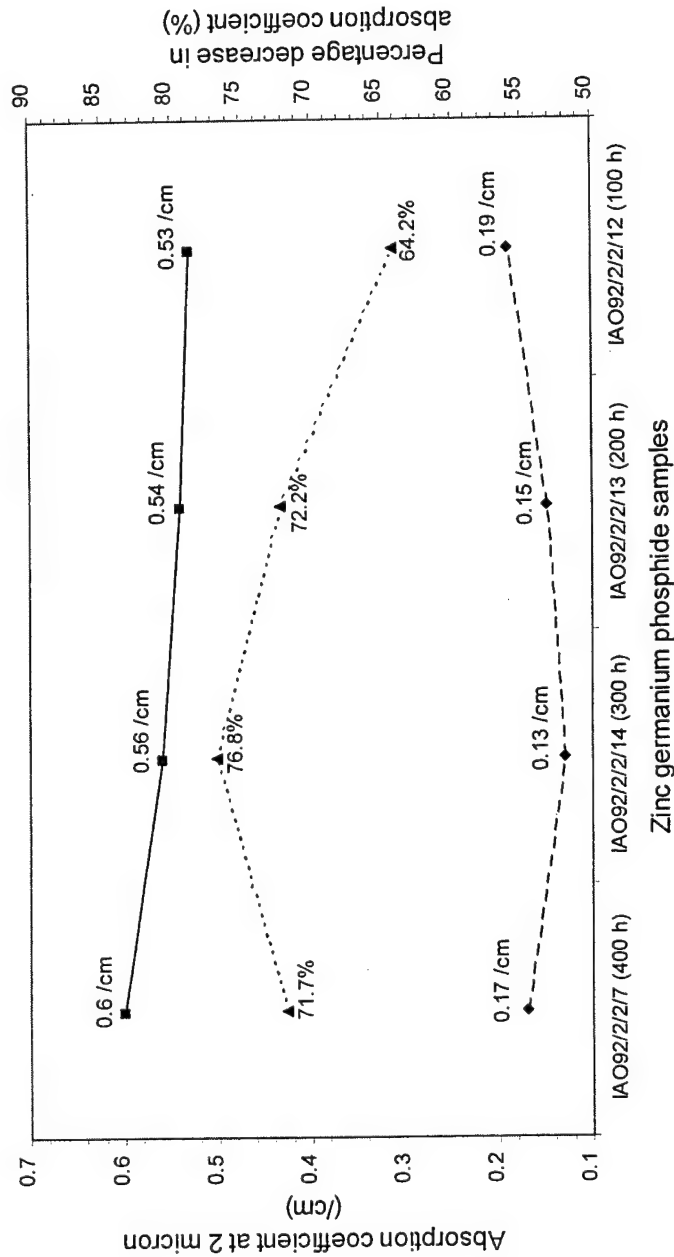
Effect of Annealing Temperature on the Absorption Coefficient at 2 micron



—■— Absorption coefficient before thermal anneal
 - - -◆- - Absorption coefficient after thermal anneal
 ...▲... Percentage decrease in absorption coefficient after thermal anneal

Effect of Annealing Time on the Optical Absorption of IAO Zinc Germanium Phosphide Samples

Effect of Annealing Time on the Absorption Coefficient at 2 micron



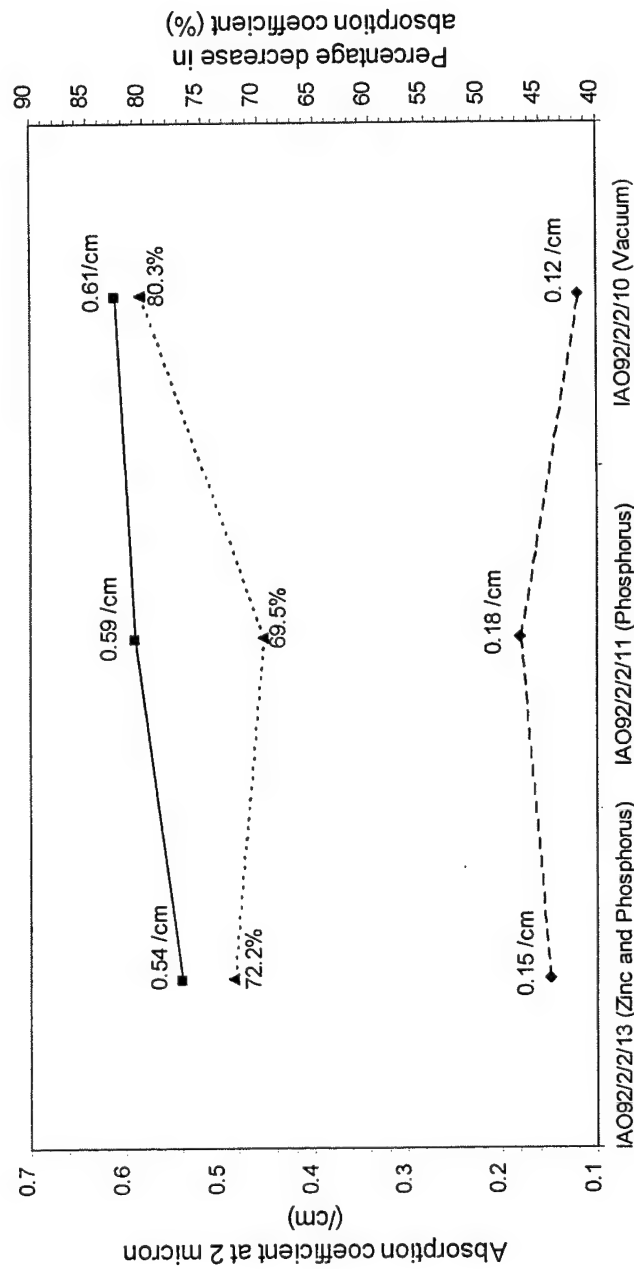
—■— Absorption coefficient before thermal anneal
 - - - ♦ - - Absorption coefficient after thermal anneal
 ... ▲ ... Percentage decrease in absorption coefficient after thermal anneal



DSO NATIONAL
LABORATORIES

Effect of Annealing Vapour Pressure on the Optical Absorption of IAO Zinc Germanium Phosphide Samples

Effect of Annealing Vapour Pressure on the Absorption Coefficient at 2 micron

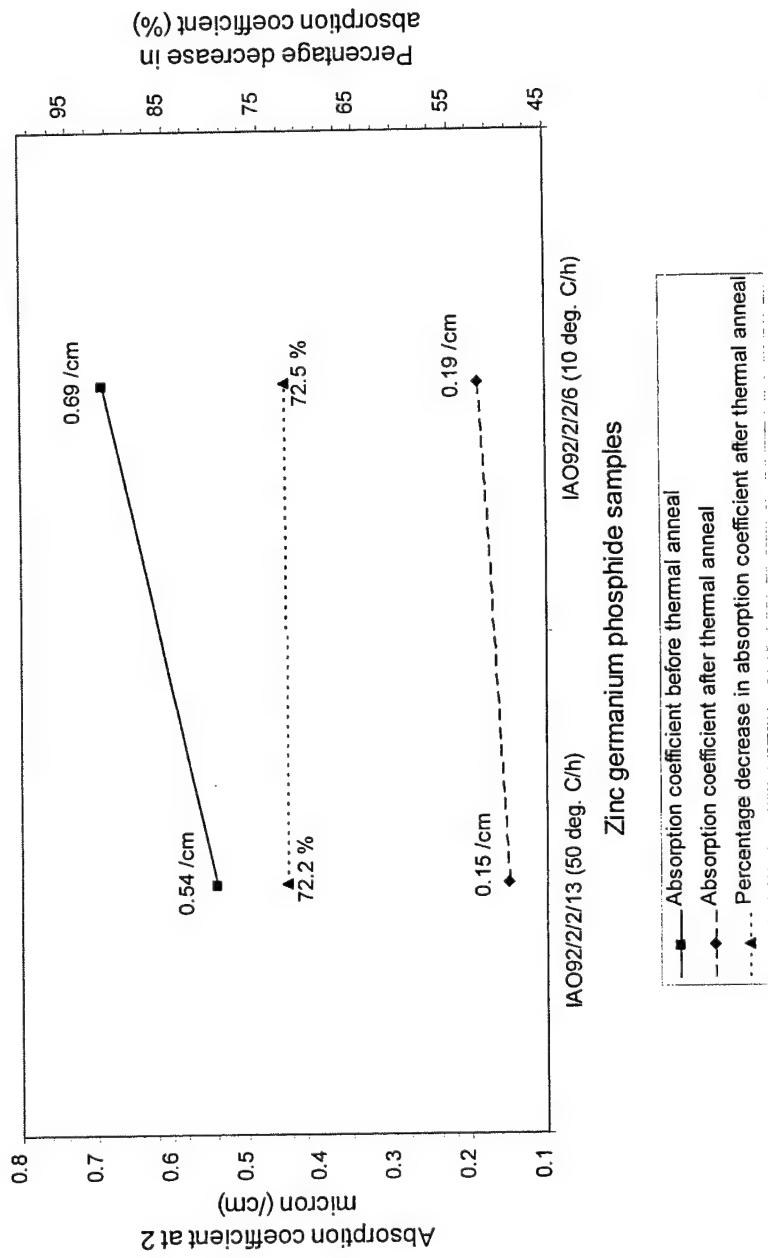


Zinc germanium phosphide samples



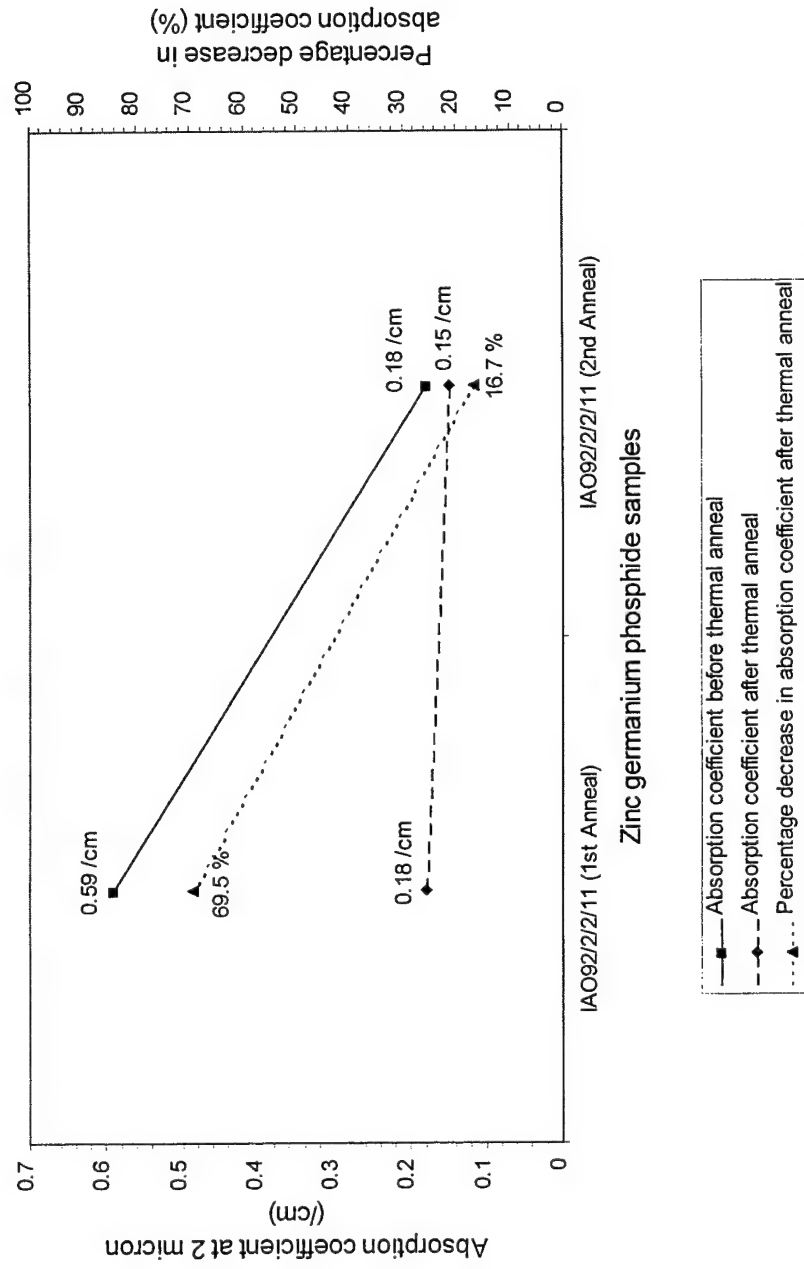
Effect of Annealing Heating/Cooling Rate on the Optical Absorption of IAO Zinc Germanium Phosphide Samples

Effect of Annealing Heating/Cooling Rate on the Absorption Coefficient at 2 micron



Effect of Re-Annealing on the Optical Absorption of IAO Zinc Germanium Phosphide Samples

Effect of Re-Annealing on the Absorption Coefficient at 2 micron

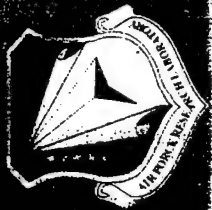


Reduction of the Near-Infrared Absorption of Zinc Germanium Phosphide Through Post-Growth Annealing Treatment

- Optimal annealing temperature of ZGP is 600°C.
- Optimal annealing time should be 200 - 400 h.
- Optimal annealing atmosphere is vacuum.
- Thermal annealing of zinc germanium phosphide decreased the 2- μm optical absorption by at least 50%.
- Rate of heating and cooling ZGP did not affect the percentage decrease in the 2 μm absorption coefficient.
- Re-annealing ZGP reduced further the 2 μm absorption coefficient.



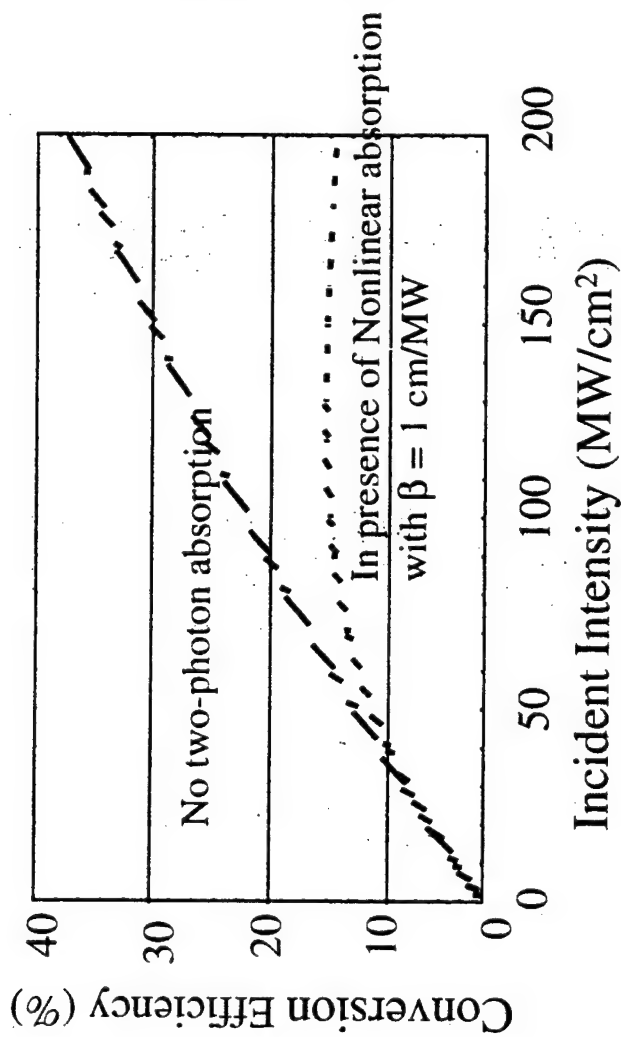
**DSO NATIONAL
LABORATORIES**



Shekhar Guha, Michael Eaton, F. Ken Hopkins and Melvin C. Ohmer
AFRL/MLP
Wright Patterson Air Force Base, OH 45433-7702

shekhar.guha@afrl.af.mil

NLO99 Workshop, DERA, Malvern, UK, 20 - 21 September, 1999



$$\frac{dA_1}{dz} = -i\kappa A_1^* A_2$$

$$\frac{dA_2}{dz} = -i\kappa A_1^2 - \beta(A_2 A_2^*) A_2$$

Presence of two-photon absorption limits high power generation

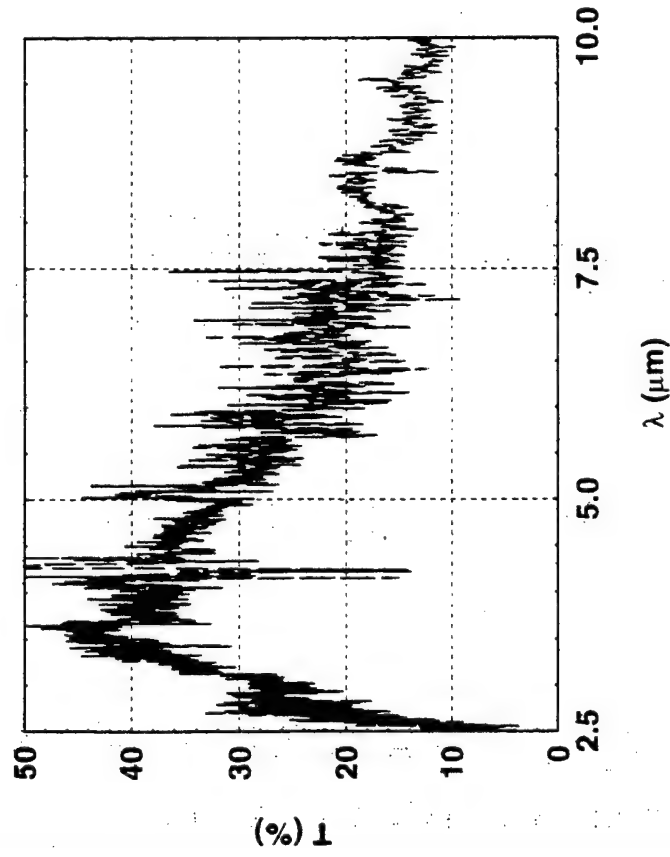


Sample name	Sample thickness (μm)	Carrier concentration (10^{16} cm^{-3})	Absorption coefficient (cm^{-1})			
			300 K		90 K	
				\perp		\perp
2G	974	0.4	2.5	2.8	0.6	0.1
4Q	912	4.9	19	9	8.5	4.2
4M	934	6.9	22	9	11	0.6
4O	957	7.8	32	18	10	0.6

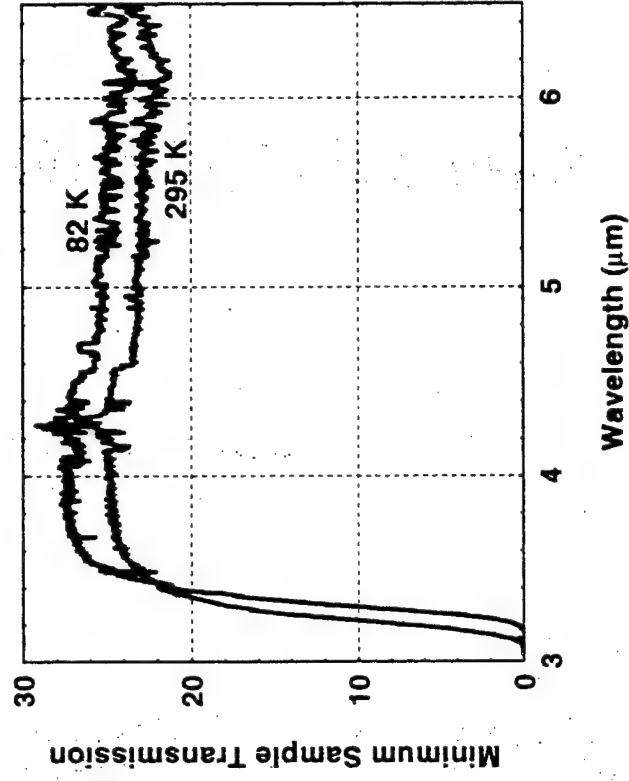
Sample size: $\sim 1 \text{ cm} \times 1 \text{ cm} \times 1 \text{ mm}$
c axis in the polished face



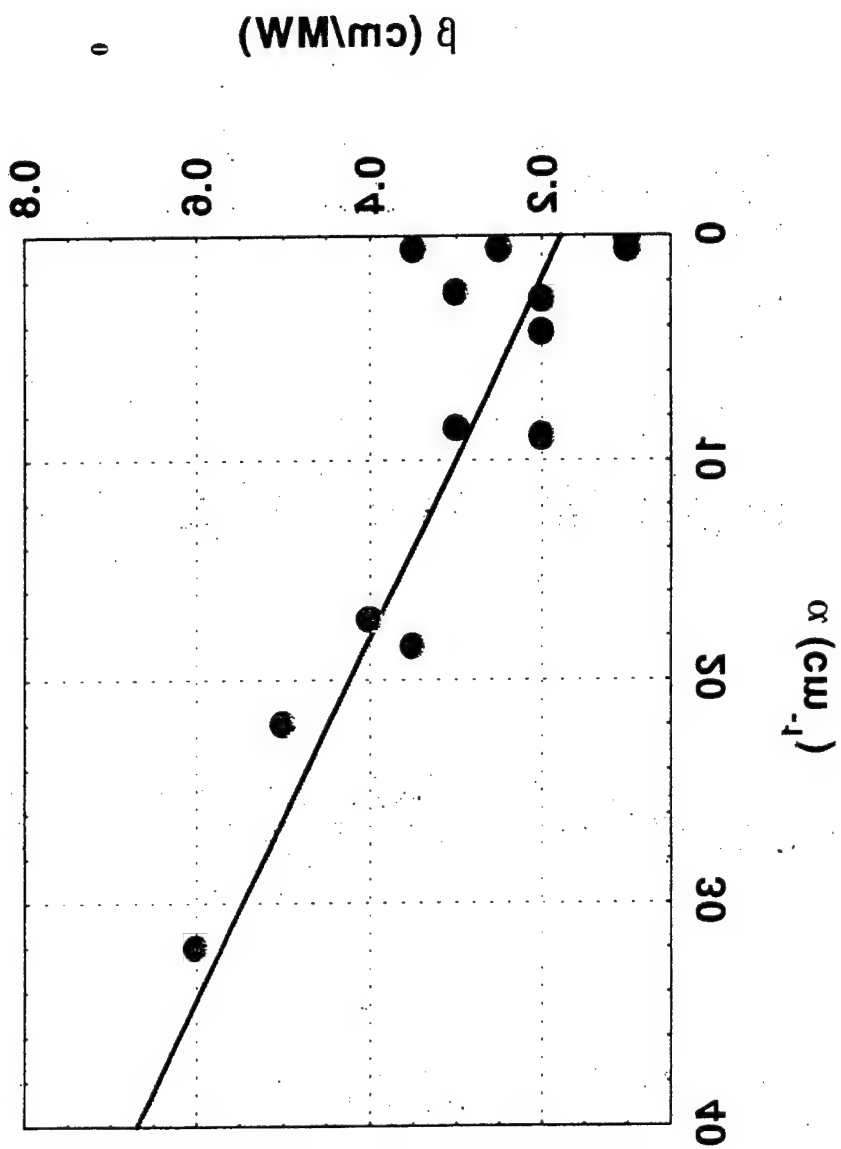
CGA (S 106)



CdGeAs₂ sample 2



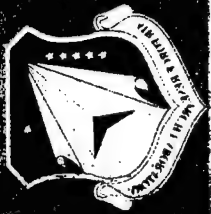
Bandgap of CGA increases with temperature increase



- Temperature Dependence
- Anisotropy

4O	0.6	0.4	1	0.32
4W	0.2	0.5	1.2	0.1
4Q	0.32	0.5	0.5	0.3
5G	0.3	0.5	0.52	0.1
		T		T
Sample	300 K		30 K	

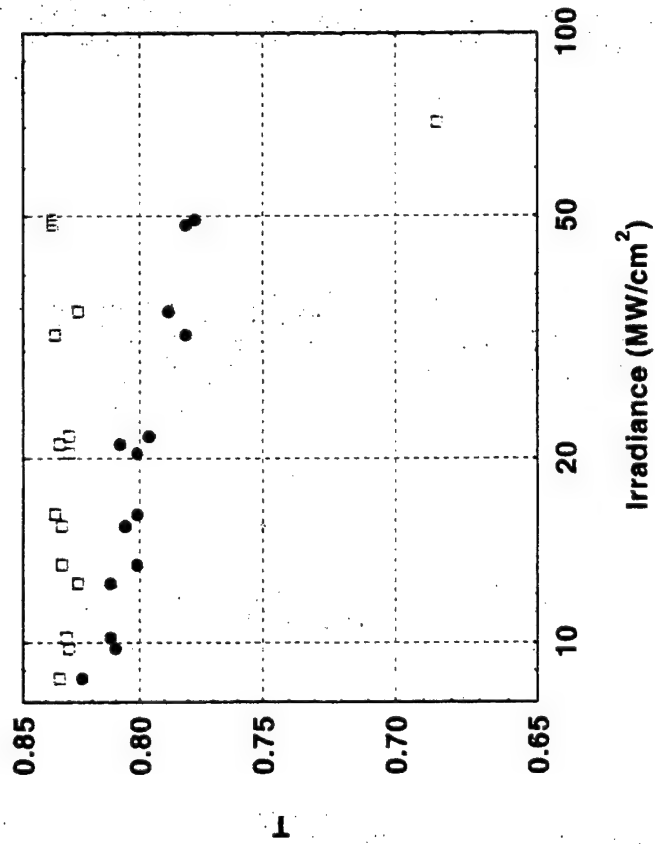
β (cm/Wm)





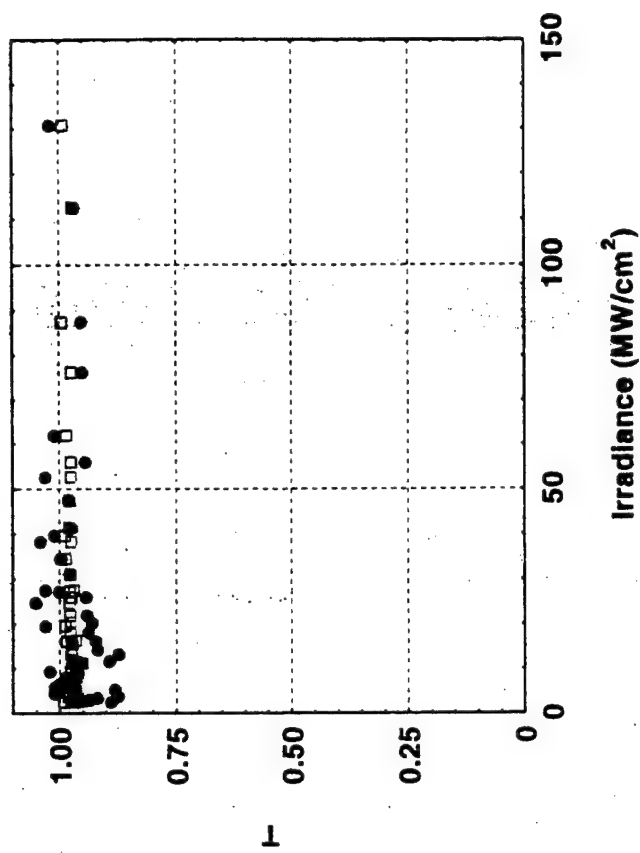
2.09 μm

ZGP (91M)

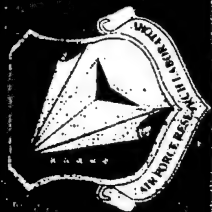


2.94 μm

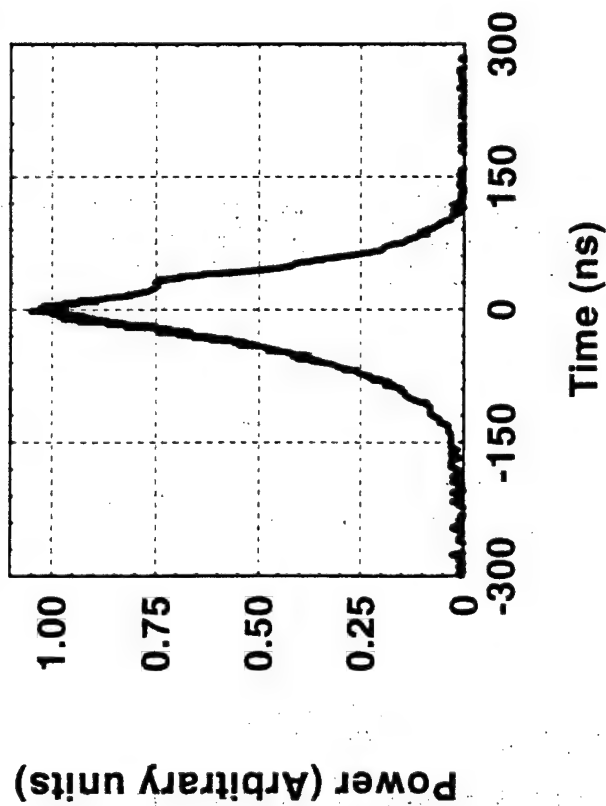
ZGP (91M)



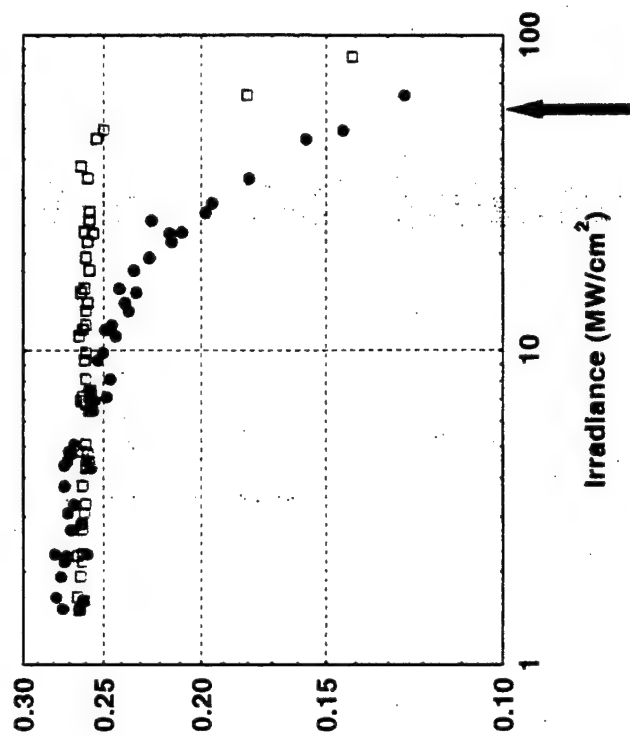
Nonlinearity and damage in ZnGeP_2 observed at 2.09 μm but not at 2.94 μm



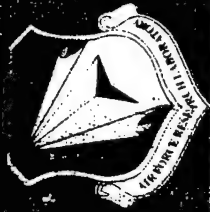
Shape of 2.94 μm short pulse



CGA sample S106
2.94 μm



Effective Nonlinearity < 0.05 cm/MW



Sample Number (6M/MW)	Coating status	Linear Absorption (cm-1)		Nonlinear Absorption <i>cm²/W</i>	
		Ordinary	Extraordinary	Ordinary	Extraordinary
92H	Uncoated	0.29	1.04	0.04	0.12
92N	Standard AR	0.33	0.70	0.08	0.35
92P	Standard AR	0.32	0.69	0.06	0.20
92Q	ARDO52x98	0.30	0.75	0.12	0.25

Strong anisotropy in the NLA of ZnGeP_2 is observed

ZGP - crystals: homogeneity region, real defects and optical quality

R@D Center ATOM
(Advanced Technologies for Optical Materials)

Semiconductor Material Science Laboratory
Siberian Physico-Technical Institute at Tomsk State University

Crystals	GaSe	ZnGeP ₂	CdGeAs ₂	Tl ₃ AsSe ₃
Transparency region, μm	0.7-16	2.1 2.5-8 10	2.5-16	2-17
Optical losses in transparency region, cm^{-1}	< 0.1	< 0.2 < 0.1 0.2	< 0.2	< 0.1
Monocrystals size				
diameter, mm	30	30	20	40
length, mm	100	80	50	80
Nonlinear elements size, $\text{mm} \times \text{mm} \times \text{mm}$	$\leq 20 \times 20 \times 20$	$\leq 15 \times 15 \times 25$	$\leq 10 \times 10 \times 15$	-

MOLTECH Corp. (USA), EKSMA (Lithuania), ELAN (St.-Petersburg, Russia) and other.

Chronology of ZnGeP₂ researches in Siberian Physico-Technical Institute

1973 - 1975 - Coping the ZnGeP₂ technology developed in Ioffe PTI

1978 - beginning the works on development new technology of ZnGeP₂ growing (V.G.Voevodin)

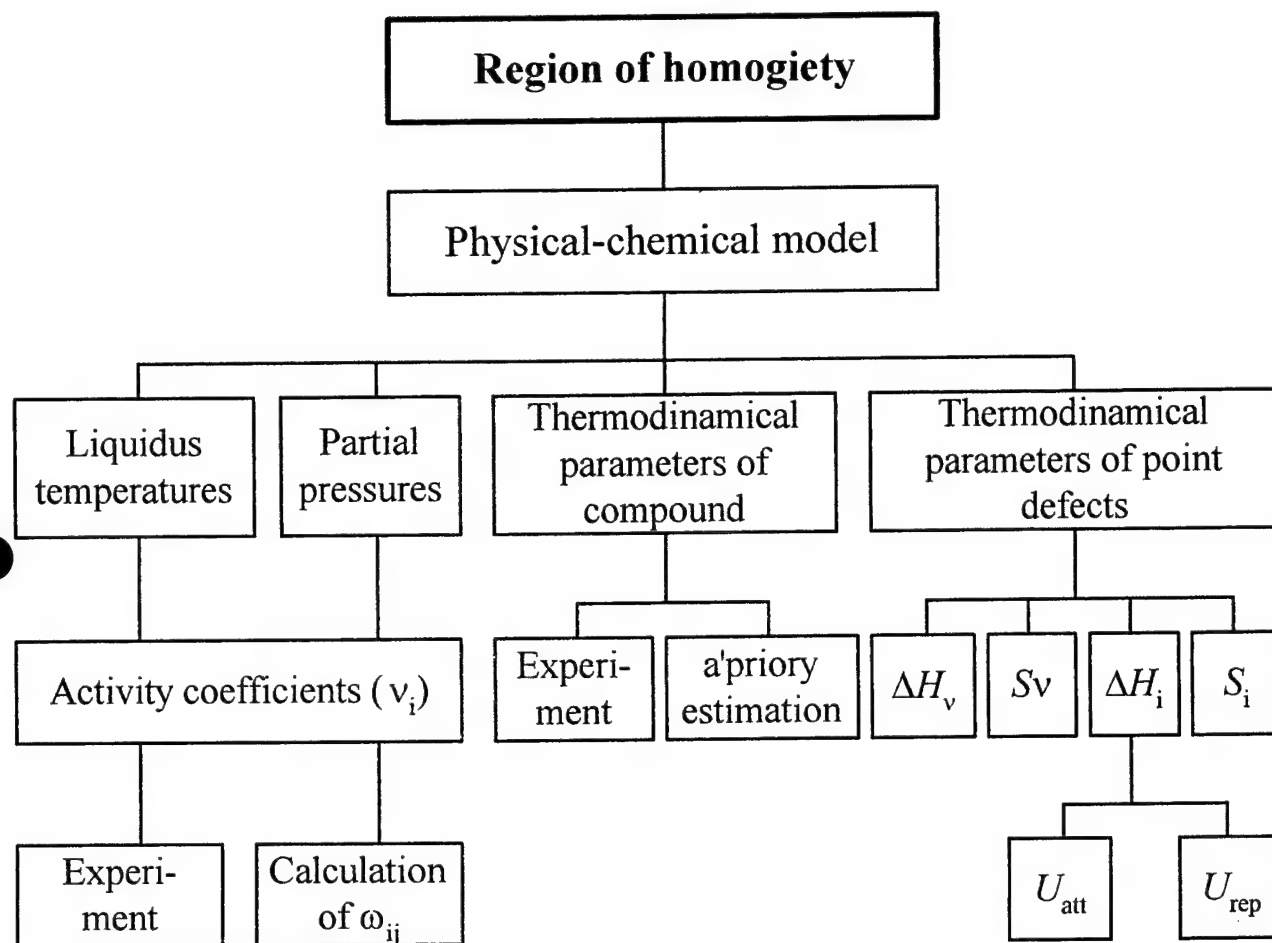
1980 - producing large ZnGeP₂ single-crystal ingots of high optical quality ($\alpha < 0.1 \text{ cm}^{-1}$ @ 2.5 - 8.5 mkm)

1982 - 1986 - the cycle of main publications on PFC in ZnGeP₂ (SPTI, IAO, IGP, IAP)

1986 - 1988 transfer the ZnGeP₂ technology to SD "Optika" (now IOM) together with the equipment and part of servicing staff

1990 - present - together with R&D Centre "ATOM" team-work on the solving of the following problems:

- thermodynamical calculations of ZnGeP₂ homogeneity region;
- clearing up the nature of defects in ZnGeP₂;
- search the reliable ways of reduce the optical losses in the range $\lambda < 2.5 \text{ mkm}$



Formation of the neutral vacancies in ZnGeP_2

Table II. Entropies and enthalpies of neutral vacancies in ZnGeP_2

Element	Zn	Ge	P
Entropy in J/(mol K)	41.6	54.4	52.4
Enthalpy in kJ/mol	18.3	28.9	16.8

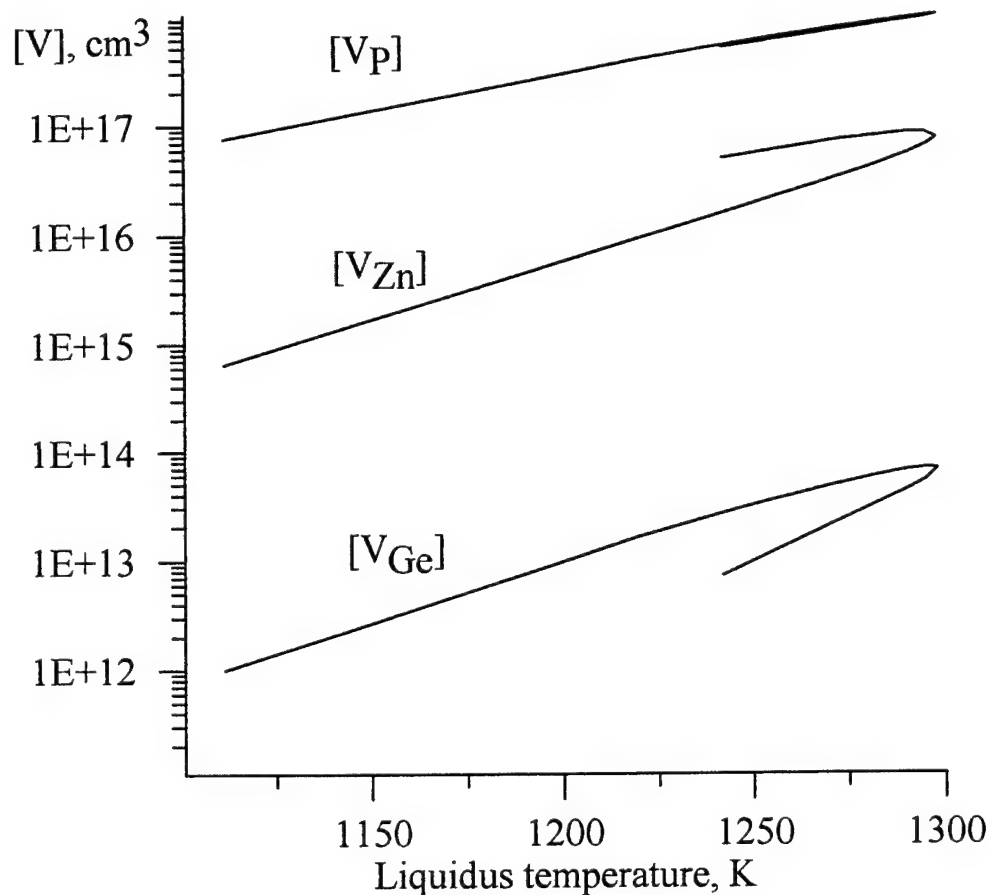


Fig. 3. The neutral vacancies concentration in ZnGeP_2 as a function of liquidus temperature; cut Ge - ZnP_2 .

8

The ionised vacancies concentrations in ZnGeP_2

Ionisation energy $E_{\text{IM}} = I_{\text{M}}(m^*/m)(z/\epsilon + 5C/6)^2$, $C = 1/\epsilon_0 - 1/\epsilon$ (11)

where I_{M} is first ionisation potential of atom M, z is effective charge, ϵ is static dielectric constant, ϵ_0 is high-frequency dielectric constant.

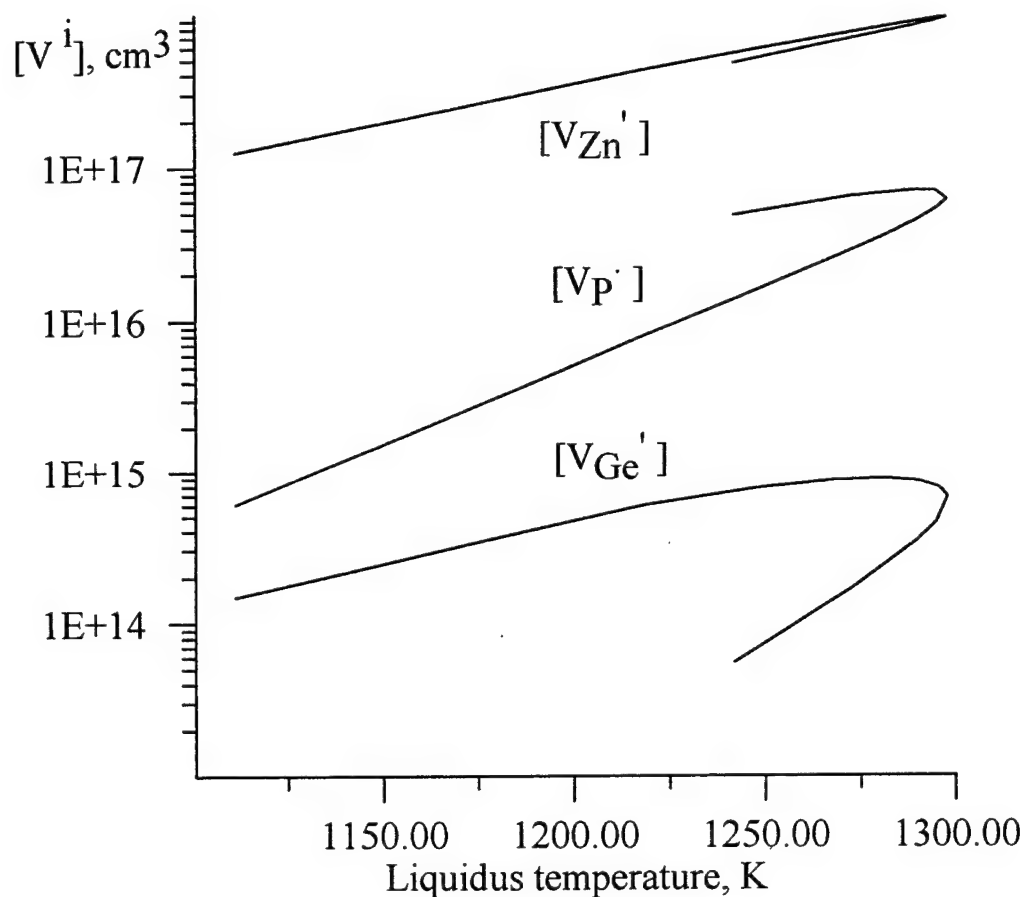


Fig. 4. The ionised vacancies concentration in ZnGeP_2 as a function of liquidus temperature; cut Ge - ZnP_2 .

92

Results of estimation of interstitials concentrations

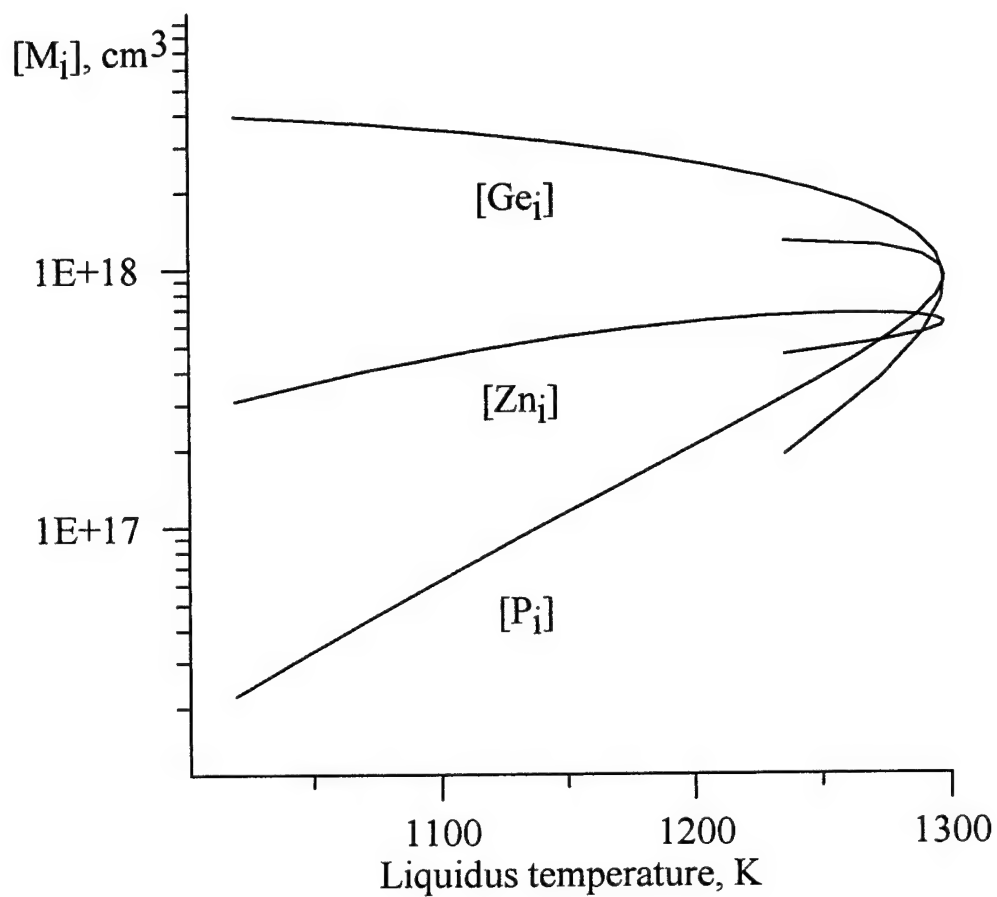


Fig. 5 Interstitials concentration in ZnGeP_2 as a function of liquidus temperature; Ge - ZnP_2 - cut

Results of simulation of the region of homogeneity formation

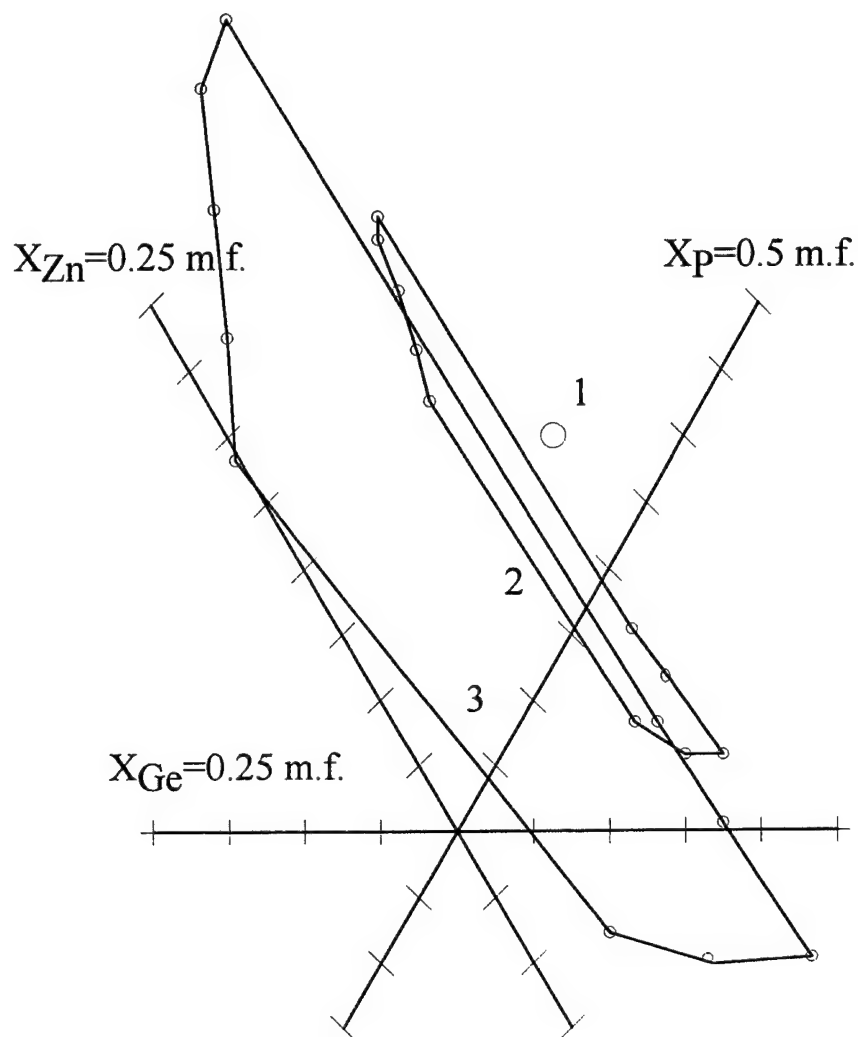


Fig. 6. ZnGeP_2 region of homogeneity, estimated as deviation of corresponding concentrations of point defects.

T, K: 1 - 1298; 2 - 1270; 3 - 1210.

Axes correspond to

$X_{\text{Zn}}=0.25$ mol fractions, $X_{\text{Ge}}=0.25$ mol fractions, $X_{\text{P}}=0.5$ mol fractions.

Value of scale deviation is 0.0003 mol %.

14

Optical losses in ZGP at $\lambda < 2.5 \mu$

Versions
of main reason
for the losses

- A: photoionization of deep acceptors (V_{zn} ?) [Brudnyi ao]
- B: light scattering by microinclusions of Zn and Ge [Voevodin ao]
- C: light scattering by β -ZGP clusters or photoionization of Zn_{Ge} - Ge_{Zn} antisite pairs [Shimony ao, J. Cryst. Growth, 198/199 (1999) 583-587]

Post-growth treatment of ZGP for losses decreasing

- | | | |
|---------------------------------|---------------|-------|
| 1. Annealing at 500-550°C | [Rud' ao] | A. B? |
| 2. Electron (e-) irradiation | [Brudnyi ao] | C? |
| 3. Laser & 1.06 μ annealing | [Voevodin ao] | B. |
| 4. γ -irradiation | [Shuneman ao] | A. B? |
| 5. Ultrasonic treatment | [Voevodin ao] | B. C? |

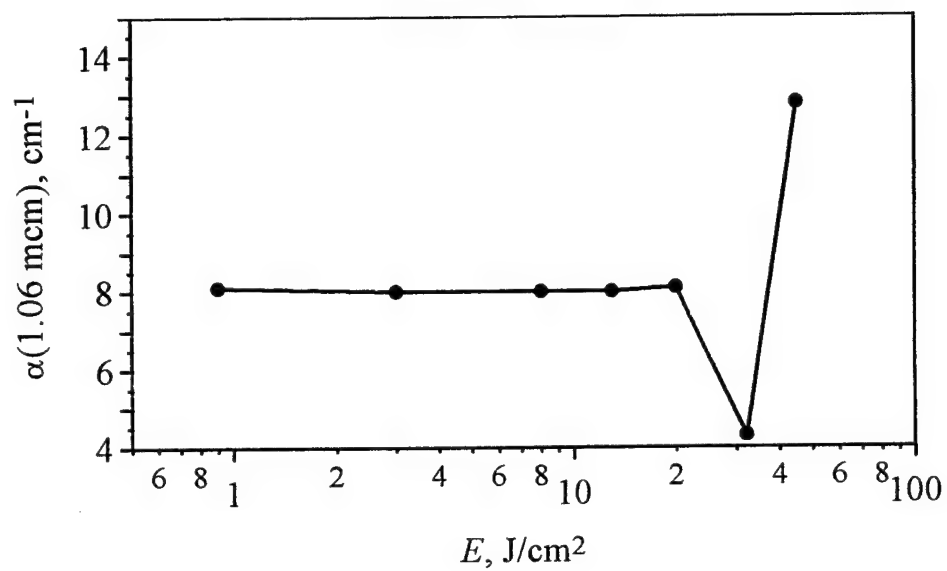
LT-annealing of ZGP crystals

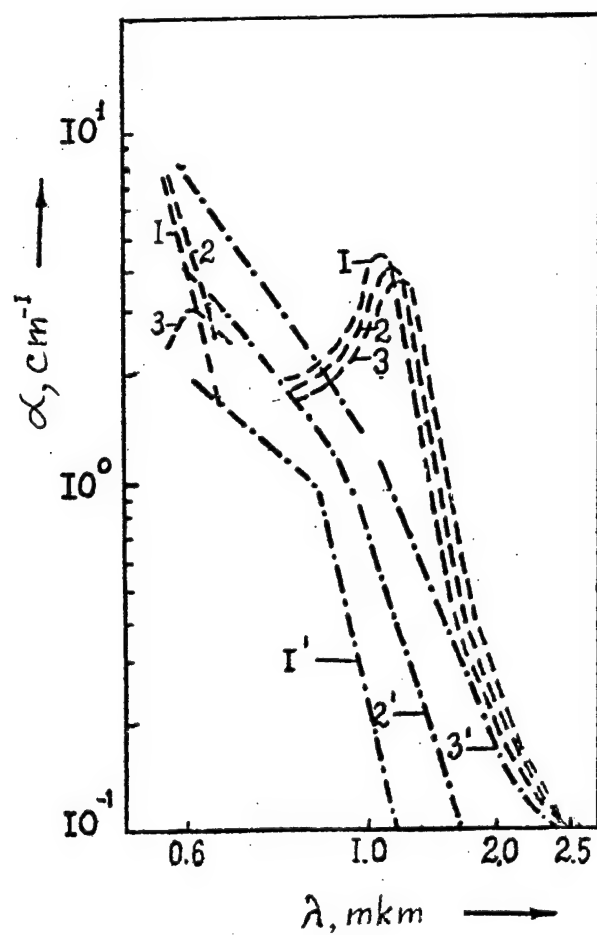
Sample #	As-grown			Condition of LTA	Annealed		
	α, cm^{-1} ($\lambda=2.5 \mu$)	α, cm^{-1} ($\lambda=5 \mu$)	N_d, cm^{-2}		α, cm^{-1} ($\lambda=2.5 \mu$)	α, cm^{-1} ($\lambda=5 \mu$)	N_d, cm^{-2}
187	0.5	0.3	10^6	550°C 150 h ZGP powder	0.2	0.01	$3 \cdot 10^5$
165	1.0	0.7	$5 \cdot 10^4$	550°C 150 h 2 at P ₄	0.3	0.07	10^5
282	0.8	0.3	10^5	550°C 150 h 1.3 at P ₄	0.3	0.1	$8 \cdot 10^4$
273	1.8	1.8	$5 \cdot 10^4$	550°C 150 h 2 at P ₄	0.05	0.04	$3 \cdot 10^4$

Ultrasonic treatment of ZGP crystals

Sample #	As-grown				After treatment			
	α, cm^{-1} ($\lambda=2.5 \mu$)	α, cm^{-1} ($\lambda=5 \mu$)	N_d, cm^{-2}	N_i, cm^{-2}	α, cm^{-1} ($\lambda=2.5 \mu$)	α, cm^{-1} ($\lambda=5 \mu$)	N_d, cm^{-2}	N_i, cm^{-2}
188	1.8	1.8	10^5	$2 \cdot 10^2$	1.3	1.3	$7 \cdot 10^4$	10^2
306	0.8	0.6	$6 \cdot 10^4$	$2 \cdot 10^3$	0.5	0.4	$4 \cdot 10^4$	10^3

Absorption coefficient of ZnGeP_2 at wavelength $\lambda = 1.06 \text{ mcm}$
versus energy density of pulsed laser radiation ($\tau = 1 \text{ ms}$)





Calculated spectra of light losses in ZnGeP_2 with microinclusions of Zn (1-3) and Ge (1'-3').

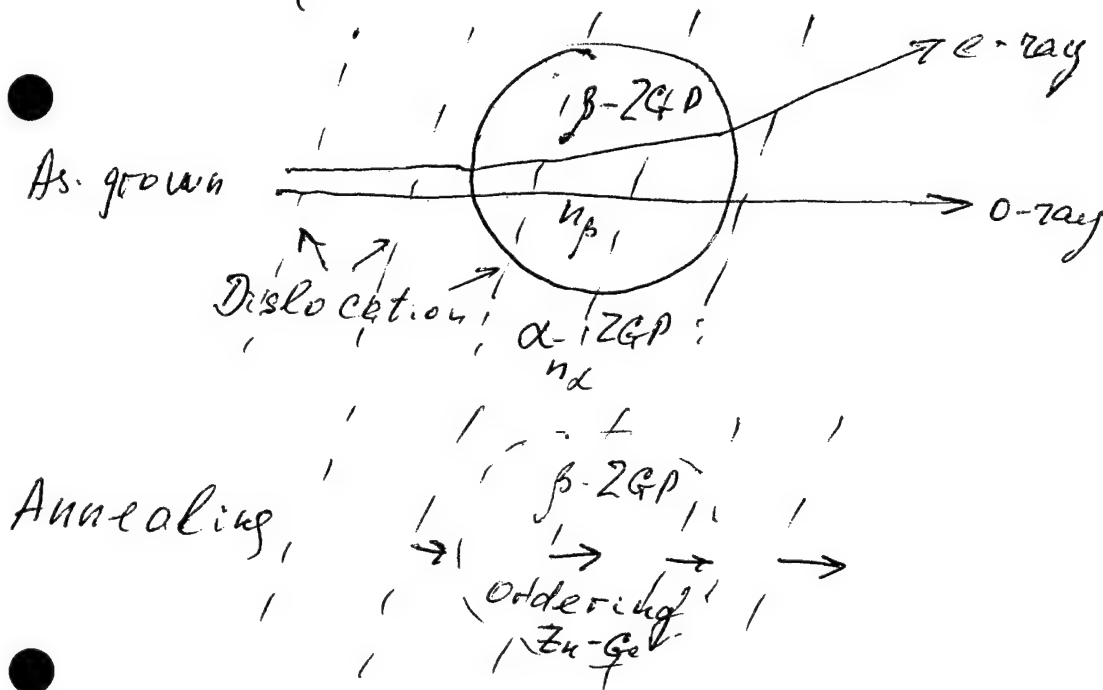
Diameter of inclusions is : 1, 1' - 200 Å; 2, 2' - 400 Å; 3, 3' - 600 Å;

Volume fraction is $C=10^{-6}$

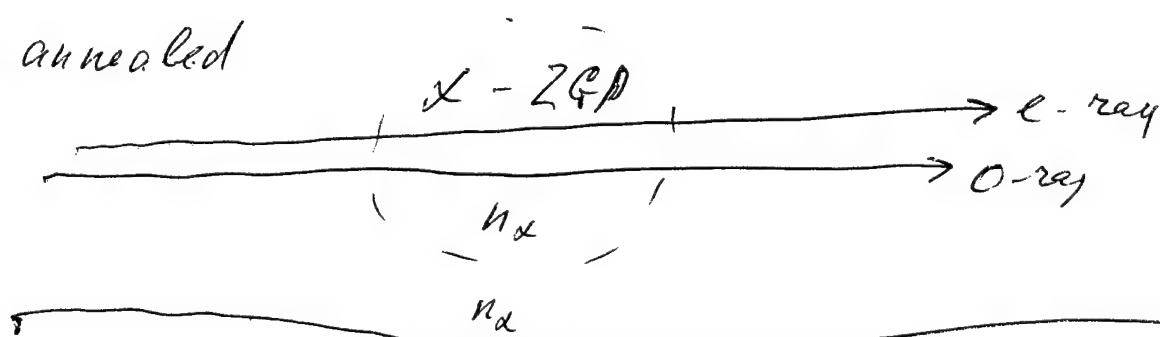
LASER@1.06 μ ANNEALING MODEL



LT(550°C)-ANNEALING MODEL



Post-annealed



SIMS Analysis of CdGeAs₂

J. S. Solomon*
University of Dayton Research Institute
Dayton, OH 45469-0167
USA

* Work supported by the Materials and Manufacturing Directorate
Air Force Research Laboratory/United States Air Force

Main Features of SIMS

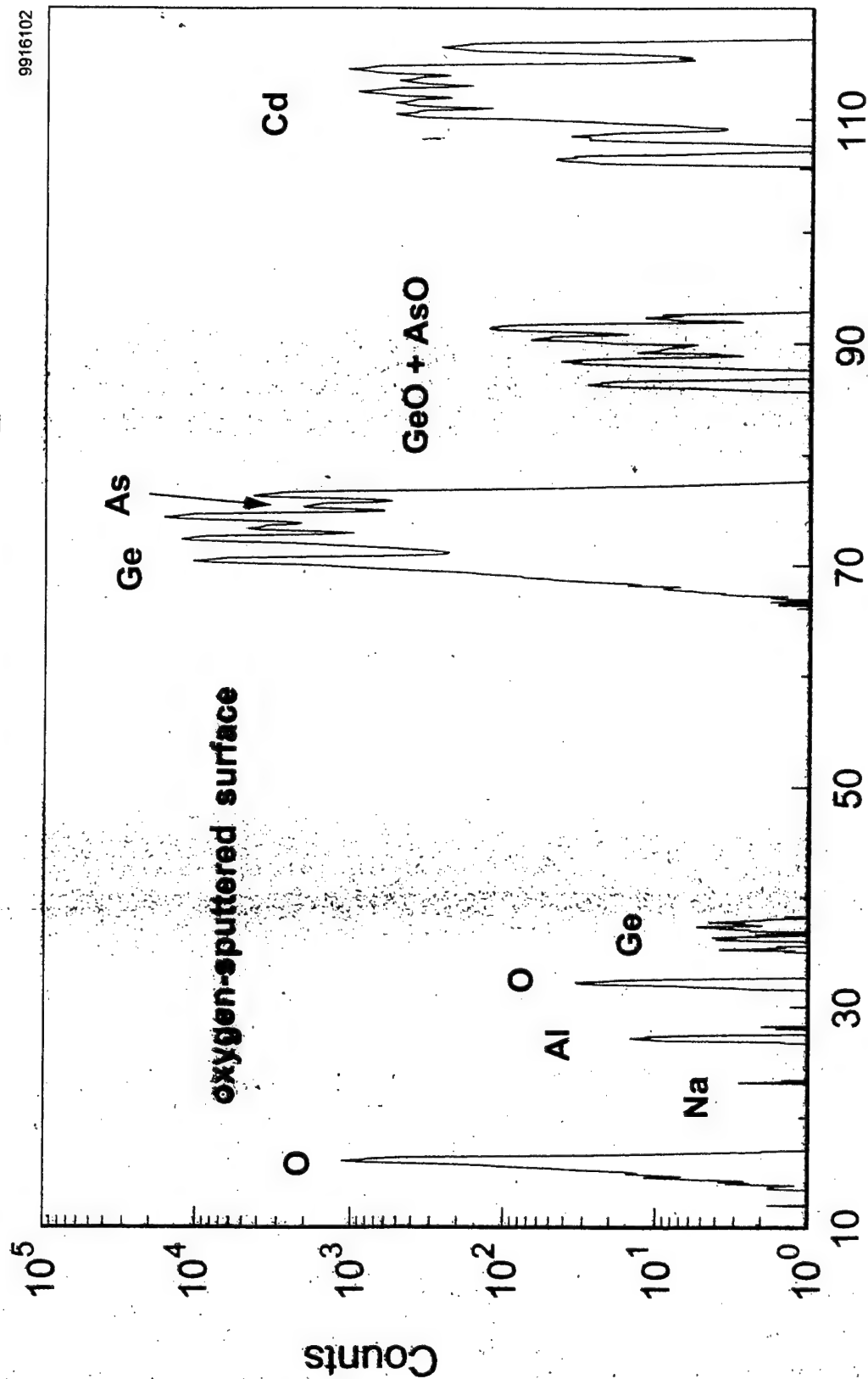
POSITIVE:

- Information depth in the "monolayer range"
- Detection of all elements and isotopes
- Extremely high elemental sensitivity for many elements
- Quantitative (with standards)

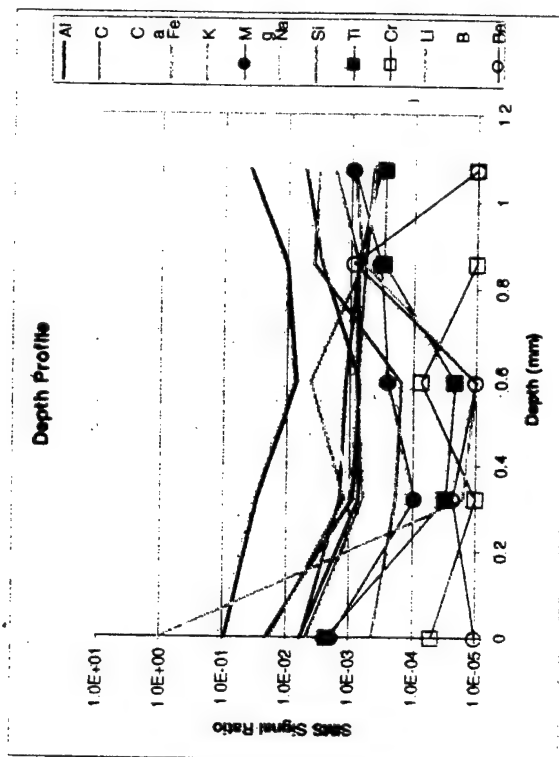
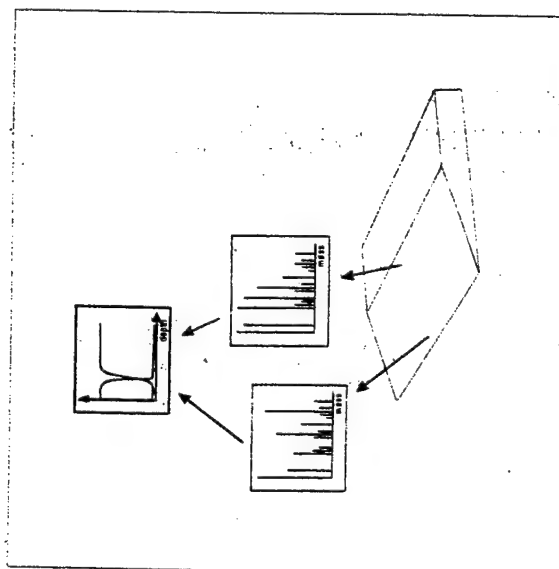
NEGATIVE:

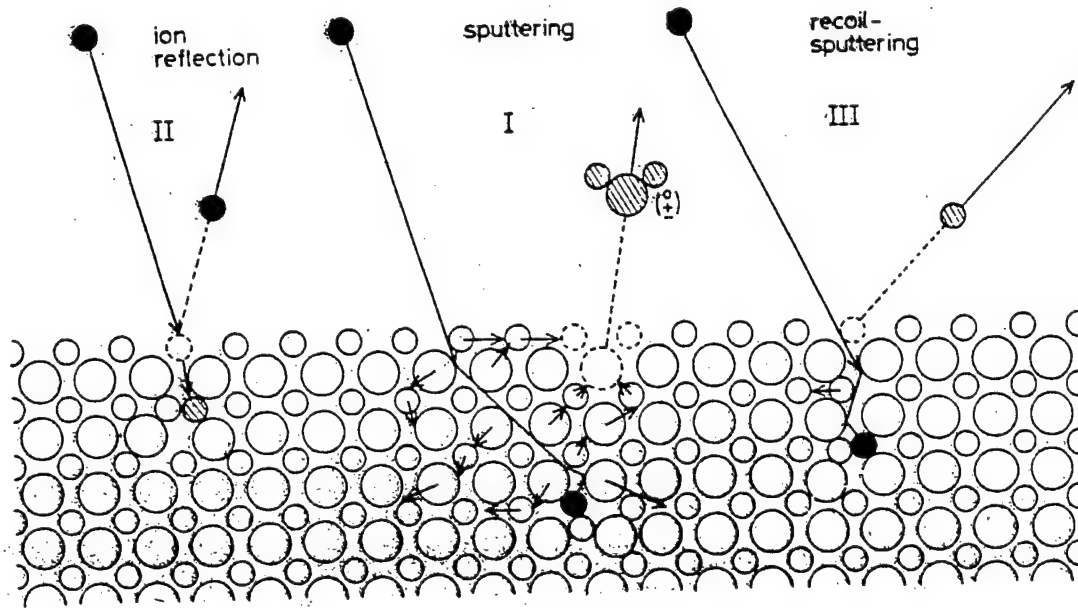
- Large differences in sensitivity for many elements
- No unified model to explain process.
- Process highly dependent on
Instrumental Parameters
Matrix composition
- Quantification difficult in mixed matrixes
- Destructive

10 keV O₂ → CdGeAs₂



SIMS Analysis of ZnO







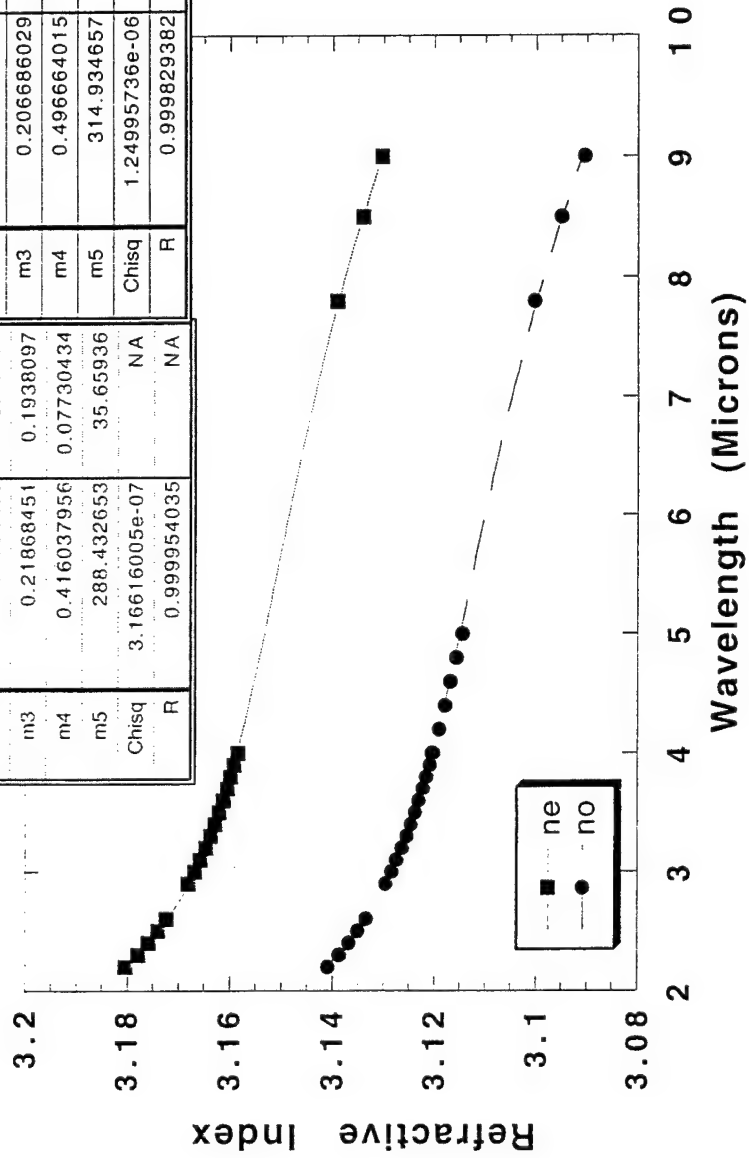
Materials and Manufacturing Directorate
Sensor Materials Branch AFRL/MLPO

Refractive Indices of Zinc Germanium Phosphide from 2-9 Microns and Implications for Phase Matching in Optical Parametric Oscillators

David E. Zelmon, David L. Small, and

Peter G. Schunemann

Refractive Indices-ZGP DAVE S + me-9/9/99

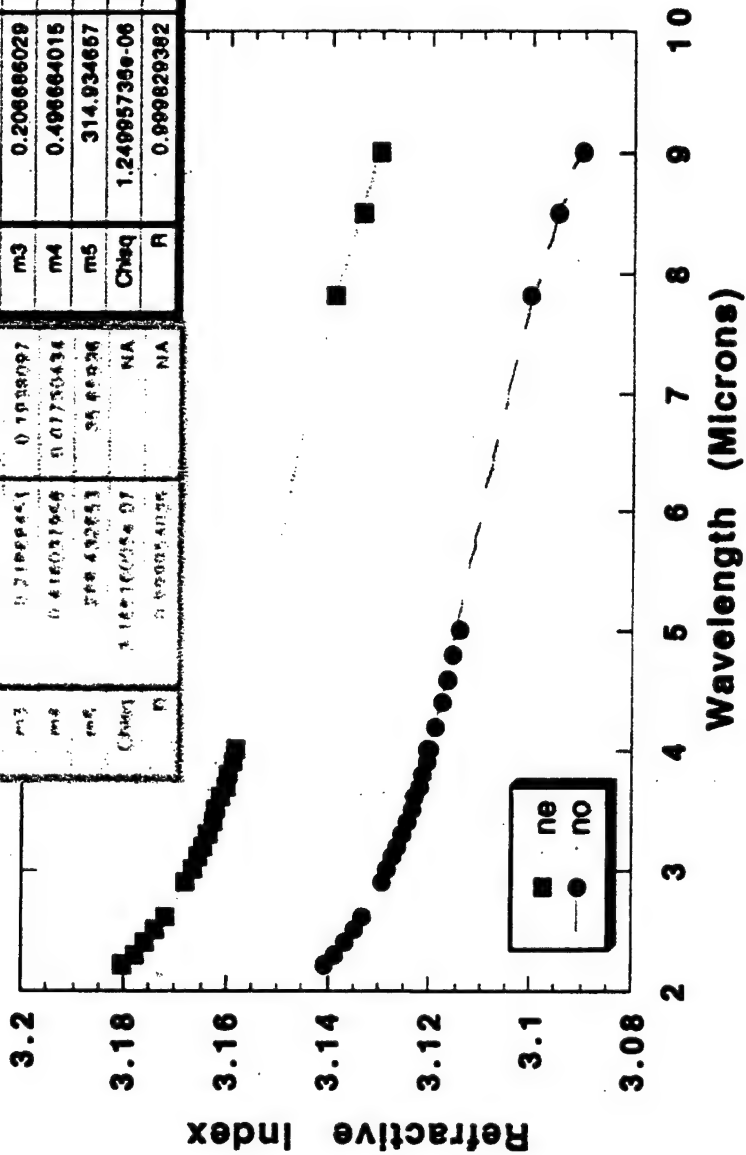


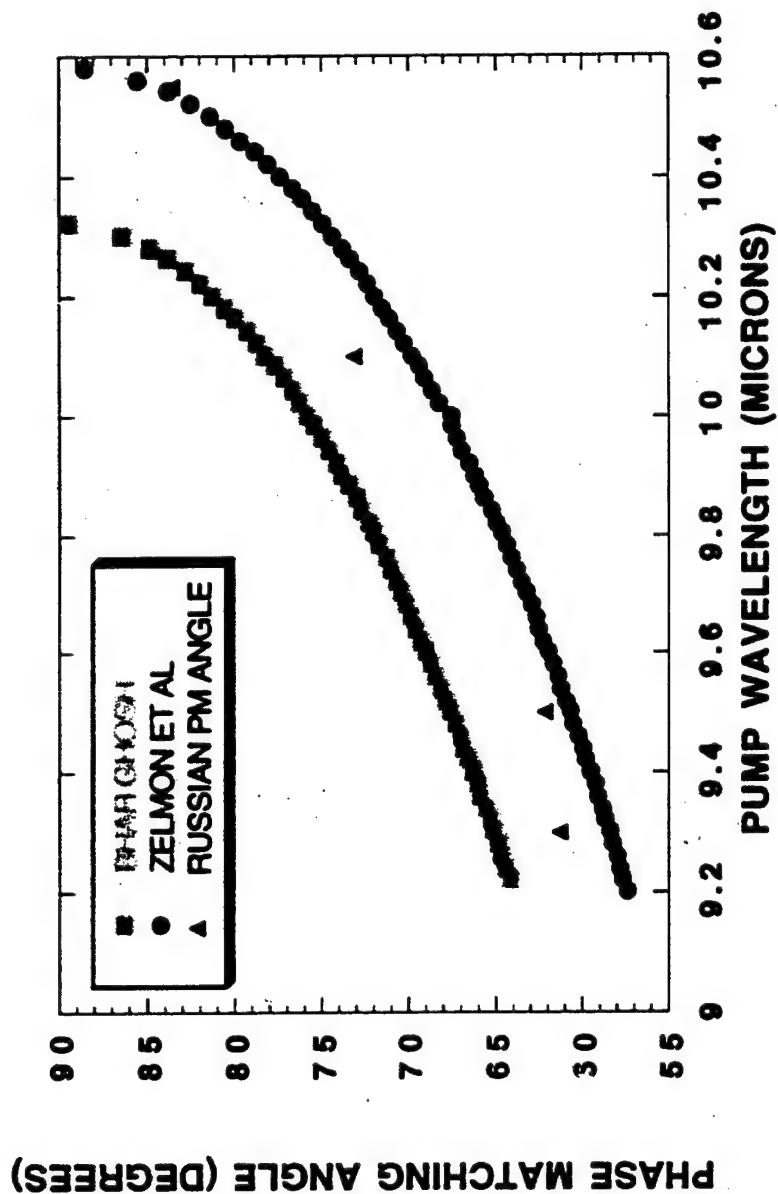
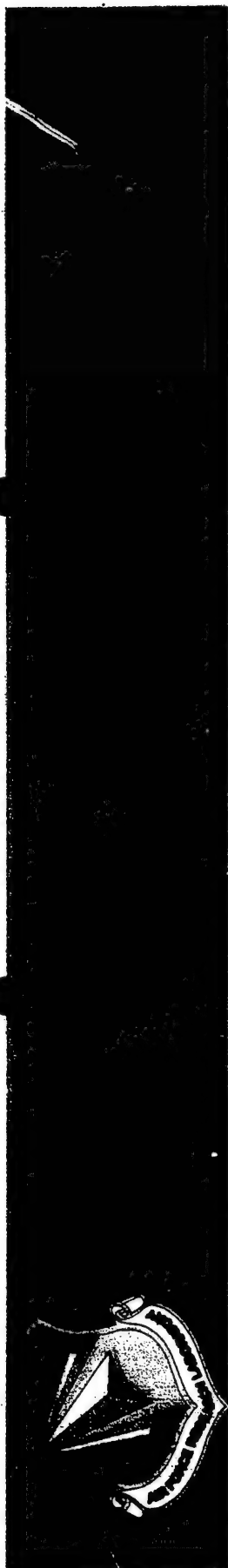
y = sqrt(m1+m2*m0^ 2/(m0^ 2-...				
ne	Value	Error		
m1	6.33463522	3.42104		
m2	3.61682203	3.41727		
m3	0.21868451	0.1938097		
m4	0.416037956	0.07730434		
m5	288.432653	35.65936		
Chisq	3.16616005e-07	NA		
R	0.999954035	NA		

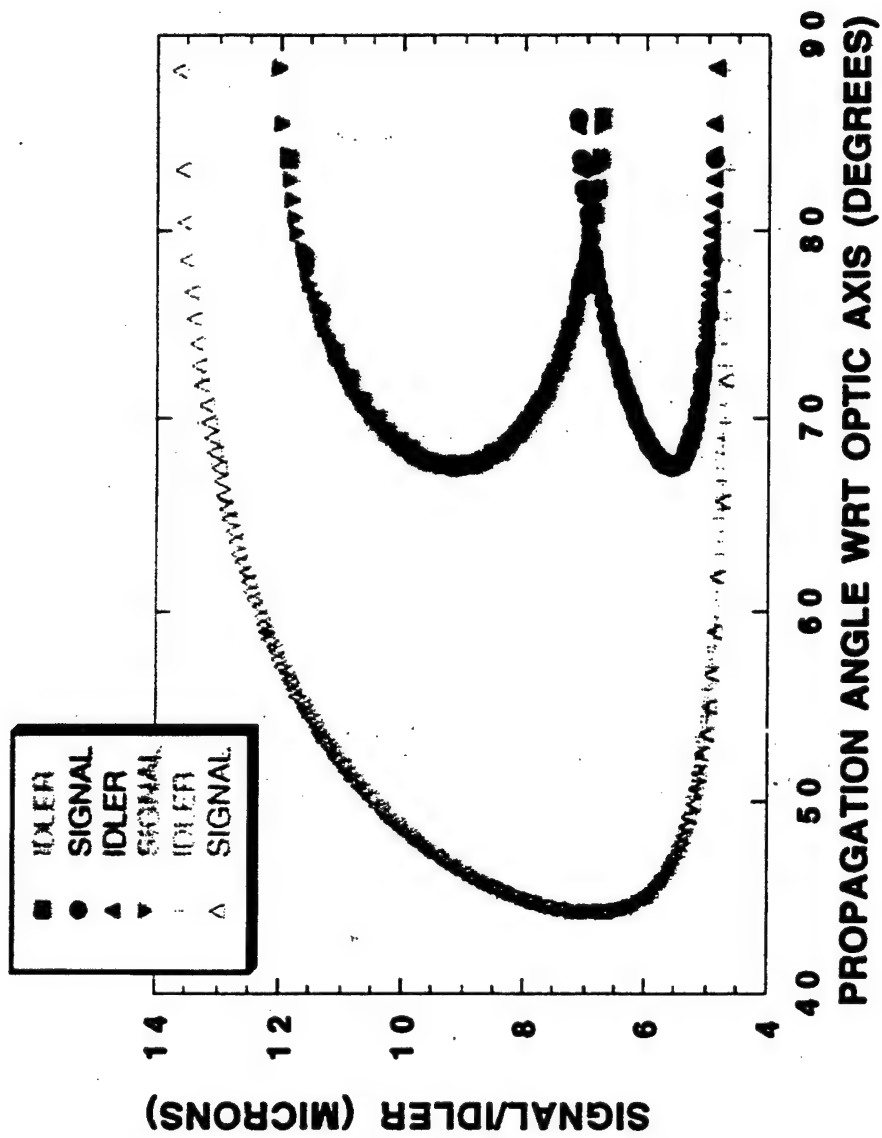
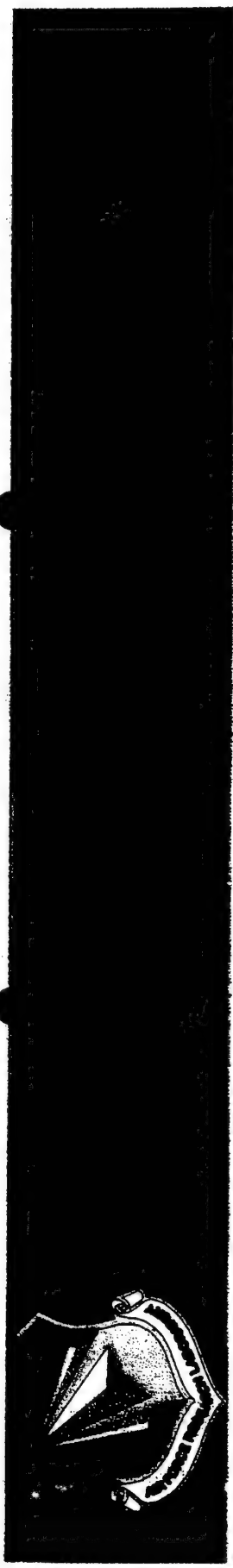
y = sqrt(m1+m2*m0^ 2/(m0^ 2-...				
no	Value	Error		
m1	6.16504	5.270687		
m2	3.55150249	5.265372		
m3	0.206686029	0.2885603		
m4	0.496664015	0.1568017		
m5	314.934657	69.0479		
Chisq	1.24995736e-06	NA		
R	0.999829382	NA		

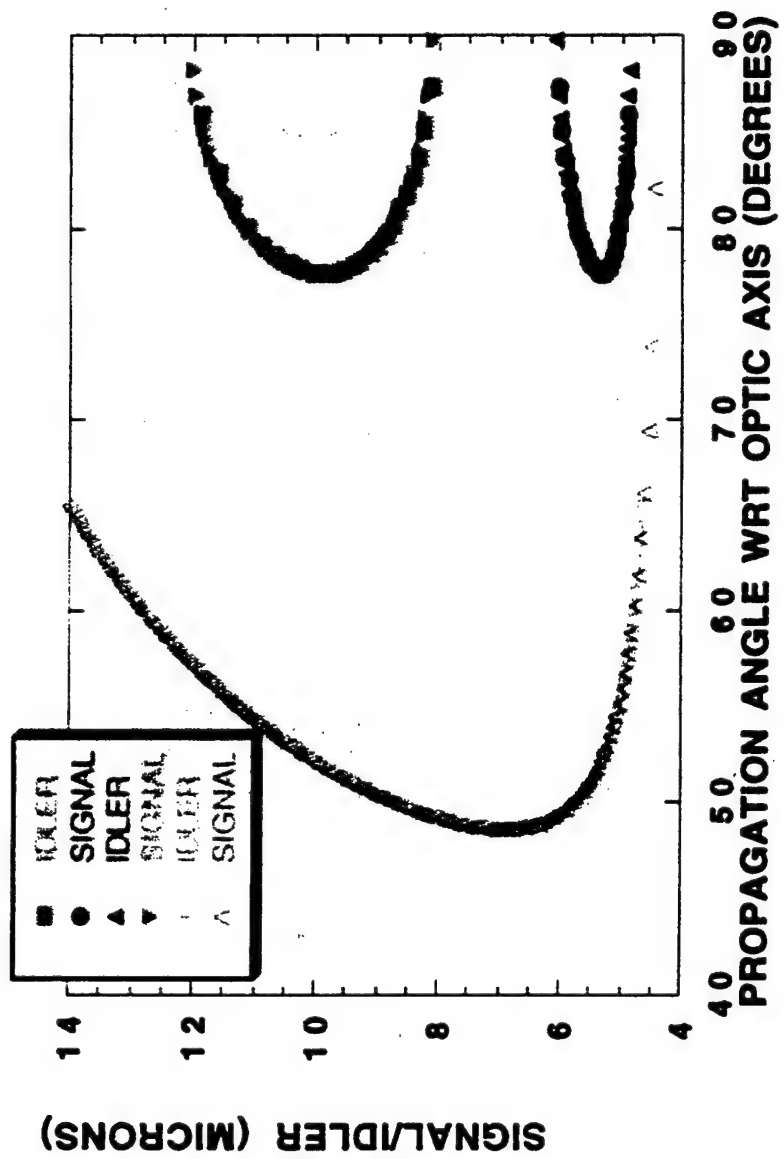
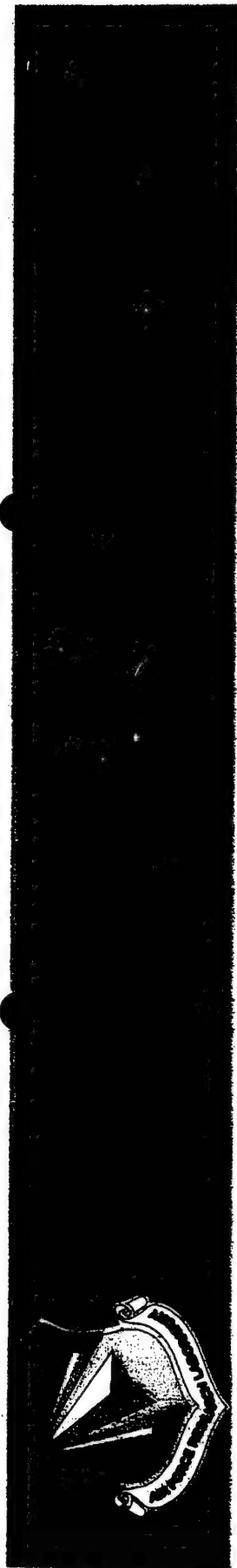


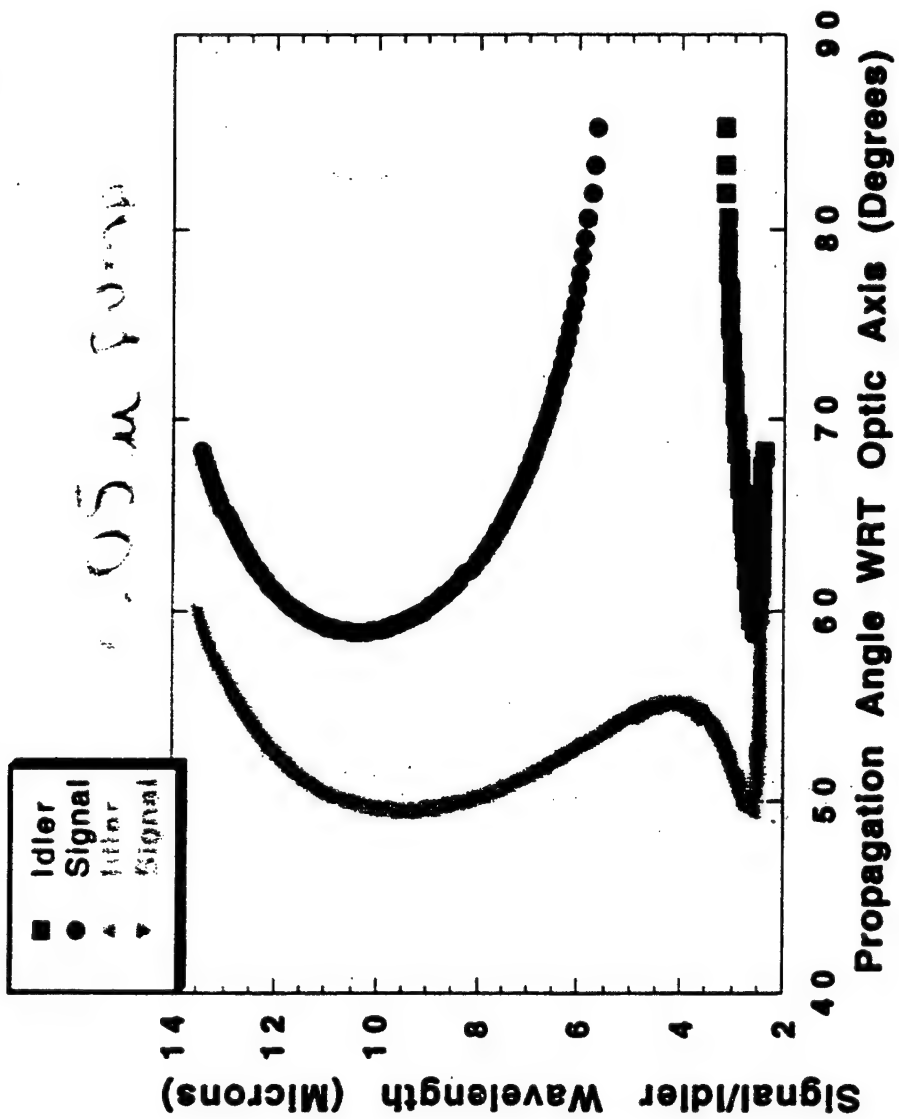
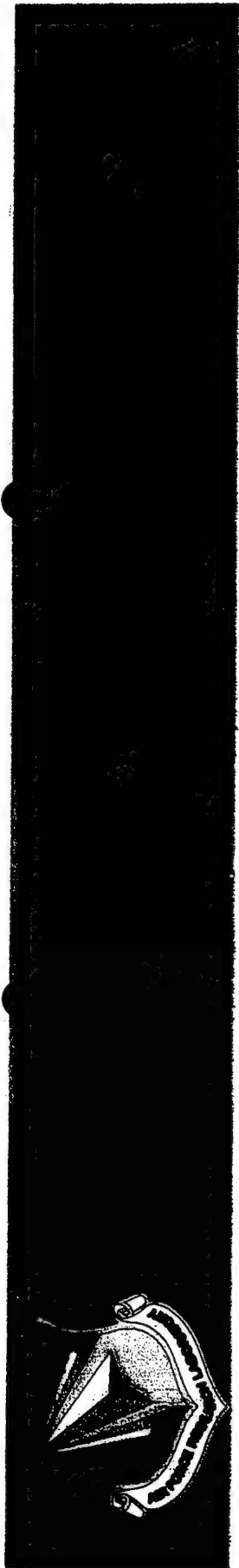
y = exp(m1+m2*m0^2/(m0^2-2))		
no	Value	Error
m1	6.16504	5.270897
m2	3.55150249	5.265372
m3	0.206896029	0.2885603
m4	0.498664015	0.1568017
m5	314.934657	69.0479
ChiSq	1.24995739e-06	NA
R	0.999829382	NA









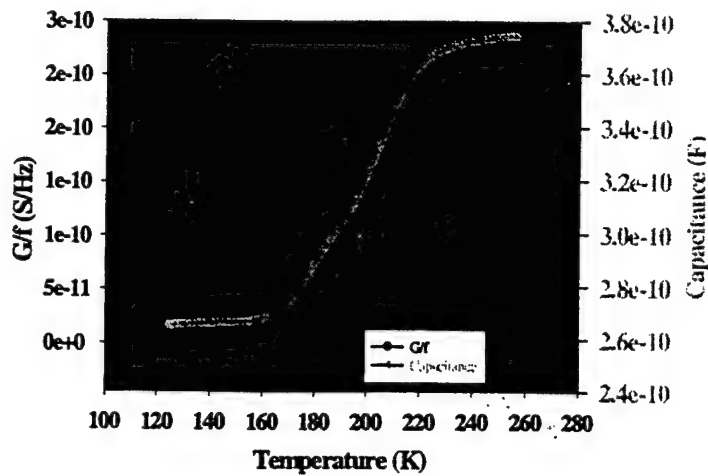


Analysis of CdGeAs₂ using thermal
admittance spectroscopy

Steven Smith

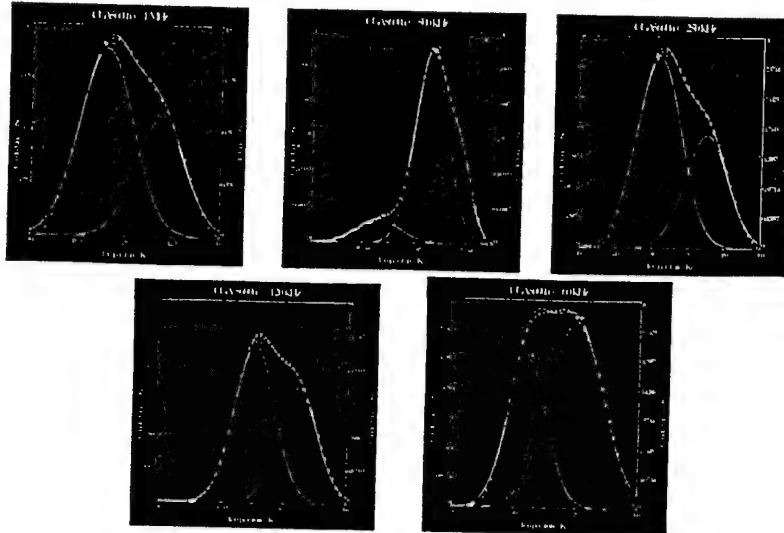
University of Dayton Research Institute

Principles of TAS

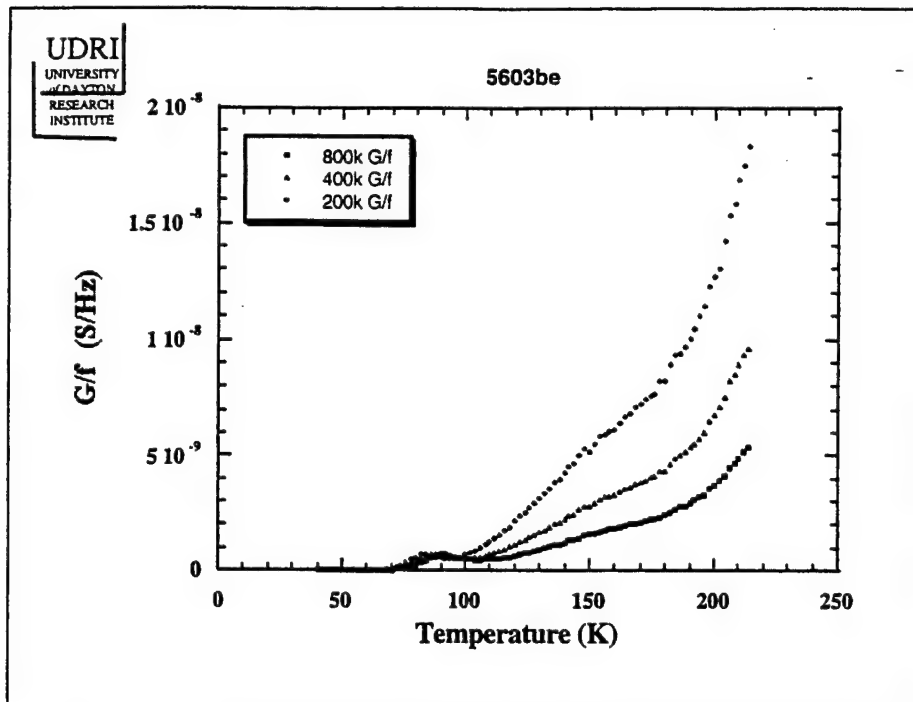


Thermal Admittance Spectroscopy (TAS) measures the response of a Schottky diode as a function of frequency and temperature. The resulting peaks in the conductance spectrum, or inflection points in the capacitance spectrum, can be used to determine the thermal activation energy(s) of the defects (impurities). Both spectra are shown in this slide.

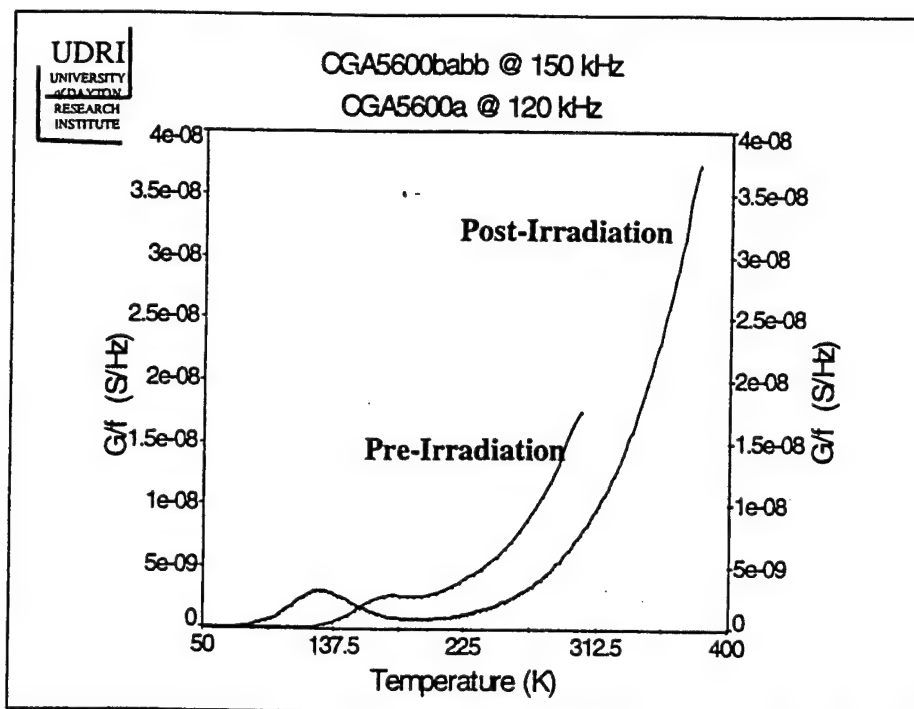
CGA5600a (4Q)



Fitting the peak in the TAS spectrum of specimen 5600 (4Q) demonstrates that more than one defect is responsible for the peak. The evolution of the shape demonstrates the relative response of the defects as a function of frequency.



TAS spectra of specimen 5603 (4N) differs significantly from those of 5600 and 5601. A deeper level is evidenced by the broad 'bump' in the spectra around 150 K.



Comparison of the TAS spectra before and after electron irradiation of specimen 5600. A slight shift to lower energy is noted by the position of the peak in the post-irradiation spectrum.

UK UNCLASSIFIED

High rep rate Tandem OPO

NLO Materials Workshop

20 - 21 September 1999

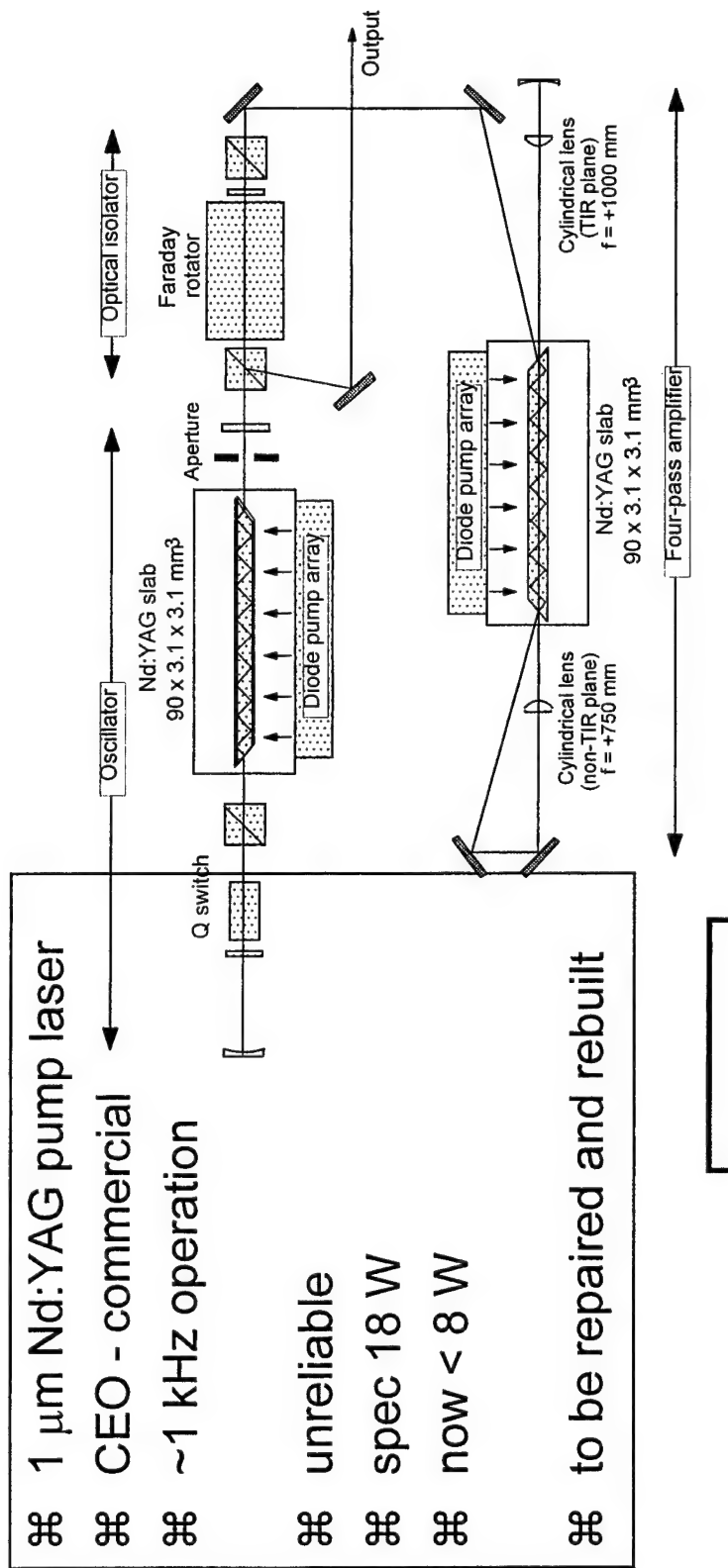
DERA Malvern

J A C Terry

© Crown copyright 1999. Published with the permission of the Defence Evaluation and Research Agency on behalf of the Controller of HMSO

DERA

Experimental - 3



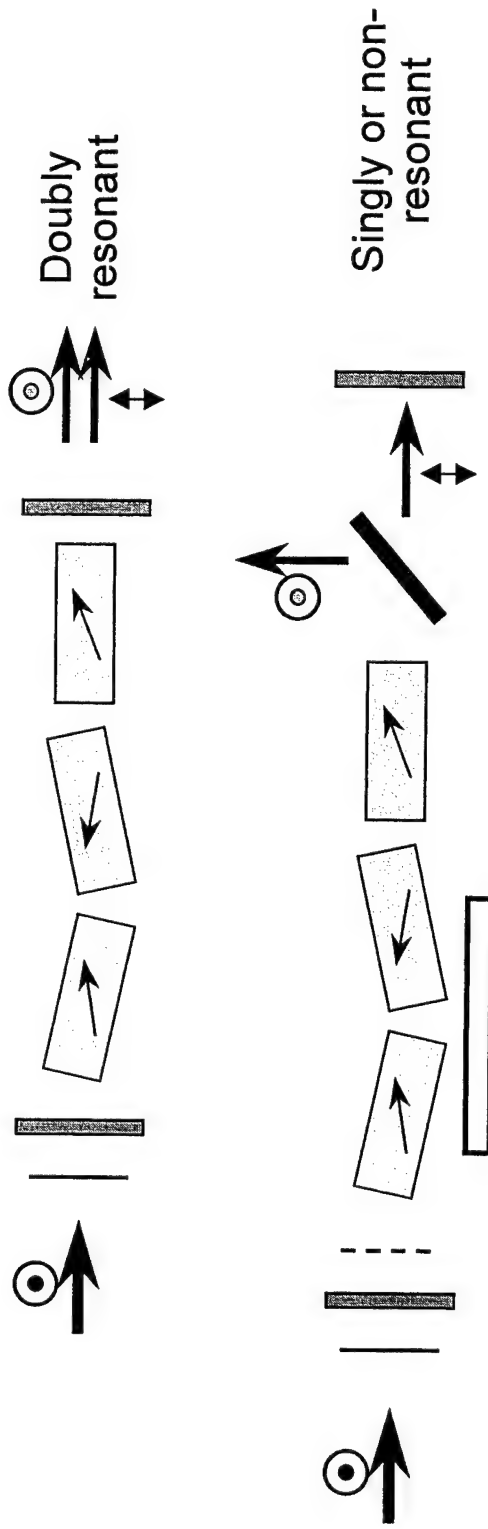
- ⌘ 1 μ m Nd:YAG pump laser
- ⌘ CEO - commercial
- ⌘ ~1 kHz operation
- ⌘ unreliable
- ⌘ spec 18 W
- ⌘ now < 8 W
- ⌘ to be repaired and rebuilt

DERA

UK UNCLASSIFIED

Experimental - 4

⌘ 1st OPO - wavelength doubler (3 KTP crystals)



DERA

Experimental - 5

⌘ WD power and efficiencies

⌘ Doubly resonant

⌘ 2.2 W (both polarisations)

⌘ P_{th} - 3.9 W, s.e. - 45 %, σ - 7 %

⌘ Singly resonant

⌘ 2.3 W ('single' polarisation)

⌘ P_{th} - 3.7 W, s.e. - 36 %, σ - 11 %

⌘ Non-resonant

⌘ 2.4 W ('single' polarisation)

⌘ P_{th} - 4.5 W, s.e. 44 %, σ - 14 %

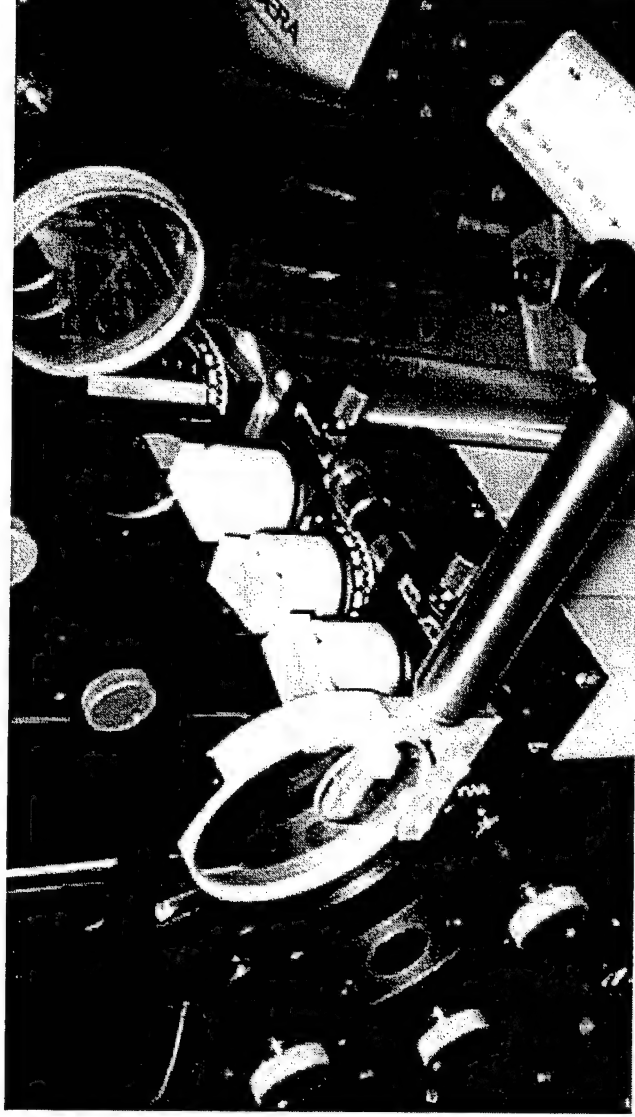
⌘ Beam quality

⌘ $M^2 \sim 1.5 \times 2.3$ (better in walk-off plane)

DERA

● ●
UK UNCLASSIFIED

Experimental - 6



DERA

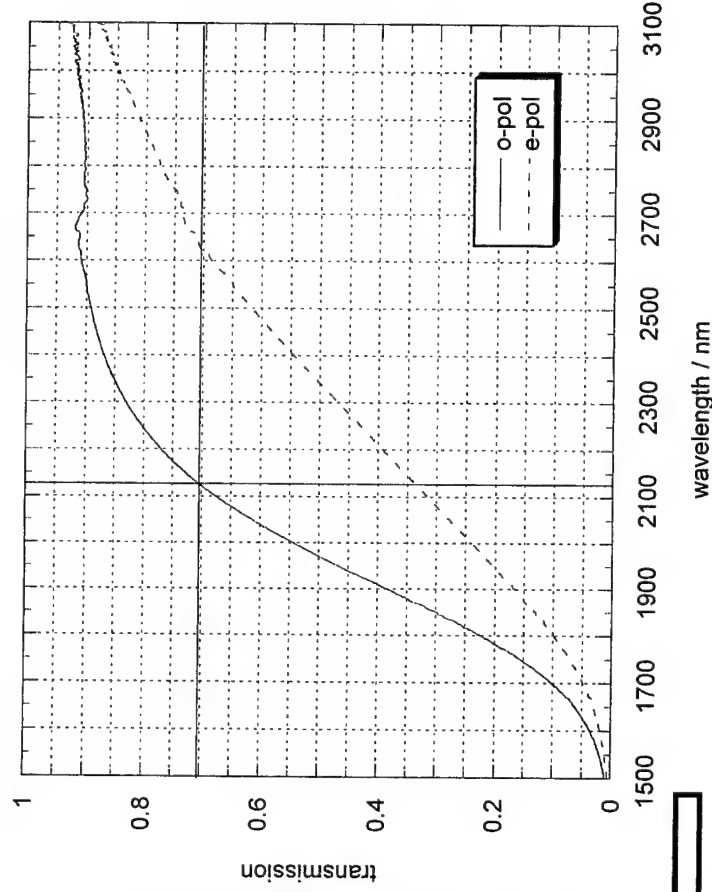
20-21/9/99

NLO materials workshop - High rep rate Tandem OPO

UK UNCLASSIFIED

Experimental - 7

Polarised transmission of coated ZGP sample VB34/2/2/2/3



⌘ DERA ZGP crystal

⌘ 6.5 x 6.5 x 18 mm³

⌘ nominally $\theta = 53$, $\phi = 0$

⌘ actually $\theta = 90$, $\phi = 53$

⌘ AR coated

⌘ 2.1, 3.5-4.0 μm

DERA

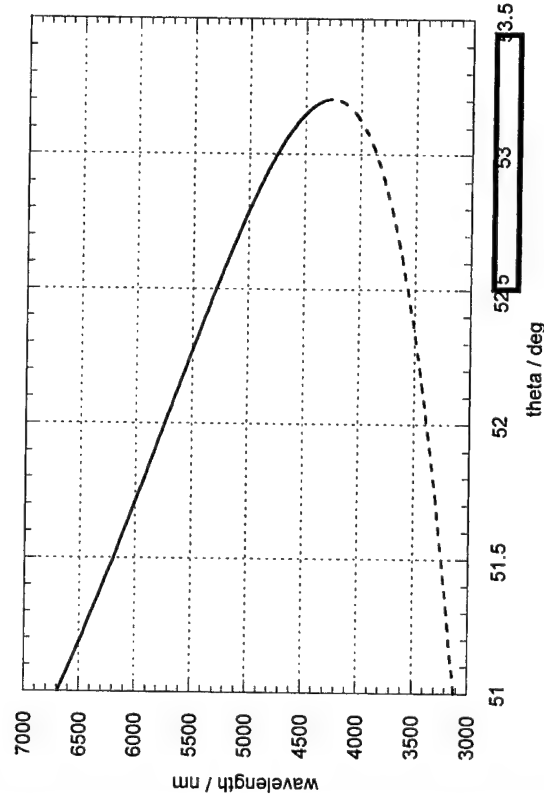
UK UNCLASSIFIED

Experimental - 8

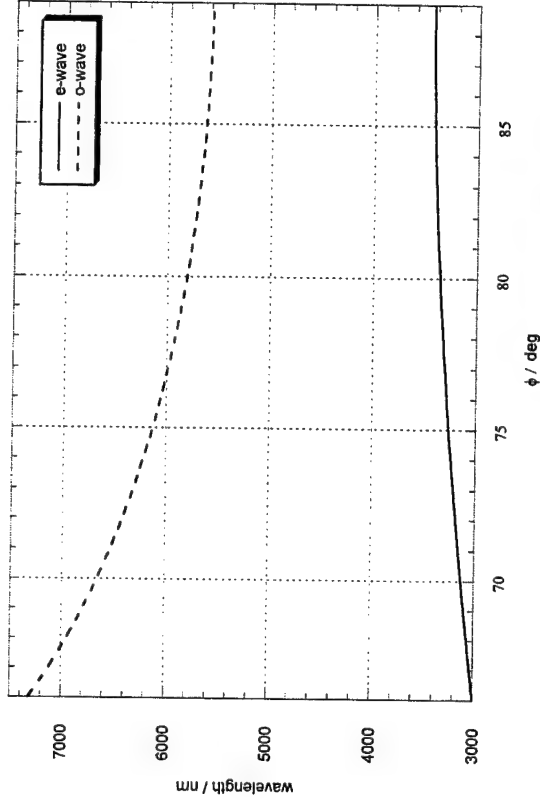
⌘ ZGP phasematching

- ⌘ type I - generated waves both have same polarisation plane
- ⌘ type II - generated waves have orthogonal polarisation planes

Type I phasematching for 2128 nm pumped ZGP ($\phi = 0$)



Type II phasematching for 2128 nm pumped ZGP ($\phi = 90$)



DERA

Experimental - 9

⌘ Output power, slope efficiency and threshold

⌘ v incident power

⌘ $P_{th} \sim 350 \text{ mW}$

⌘ s.e.

⌘ total $\sim 16.5 \%$

⌘ signal $\sim 10 \%$

⌘ idler $\sim 6.5 \%$

⌘ v unabsorbed power

⌘ $P_{th} \sim 250 \text{ mW}$

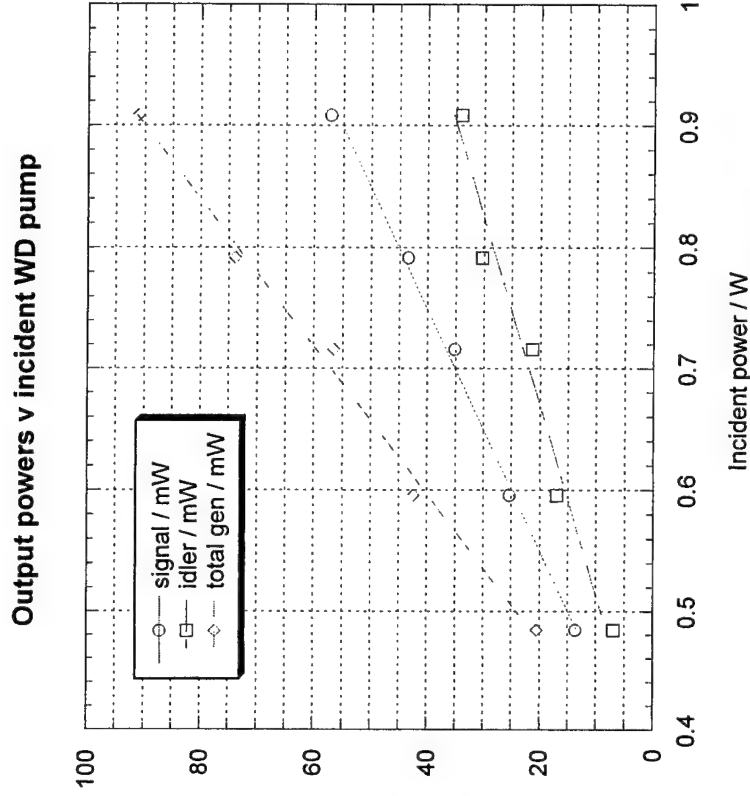
⌘ s.e.

⌘ total $\sim 23.5 \%$

⌘ signal $\sim 14.5 \%$

⌘ idler $\sim 9 \%$

⌘ Maximum output ~~100 mW~~
for $\sim 900 \text{ mW}$ incident ($2 \mu\text{m}$)



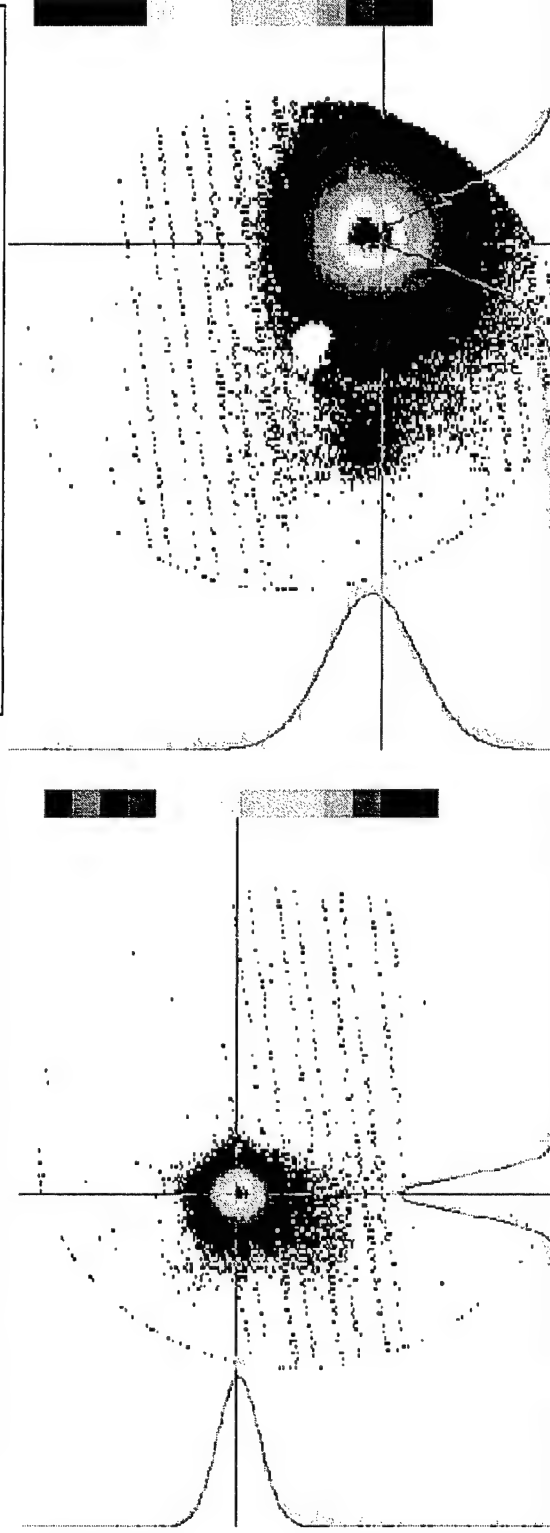
DERA

UK UNCLASSIFIED

Experimental - 10

⌘ Signal - 3.4 μm
⌘ $M^2 \sim 2.4$

⌘ Idler - 5.7 μm
⌘ $M^2 \sim 4.8$



DERA

UK UNCLASSIFIED

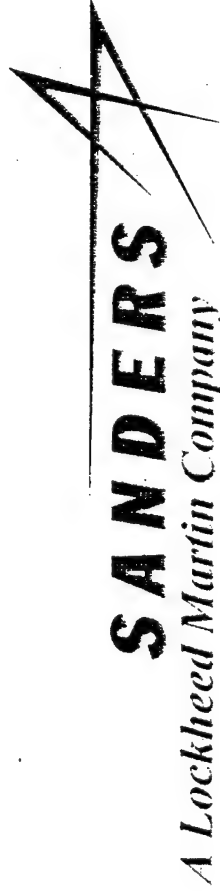
Summary

- ⌘ Operation of a tandem OPO system has been demonstrated at ~1 kHz rep rate
- ⌘ Device (wavelength doubler) with bulk NLO material demonstrated to operate with ~ 10 mJ energy per pulse
- ⌘ Demonstration of the utility of DERA ZGP
 - ⌘ In this case wrongly orientated, but reasons for this understood
- ⌘ Target of 1 W in band 4 not met
 - ⌘ Further experiments required to understand the limitations of this technology, especially thermal effects

DERA

Recent Advances in Chalcopyrites for Mid- to Far-IR Frequency Conversion

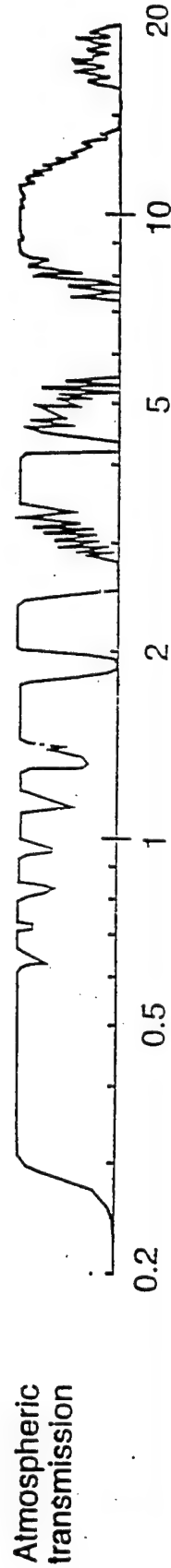
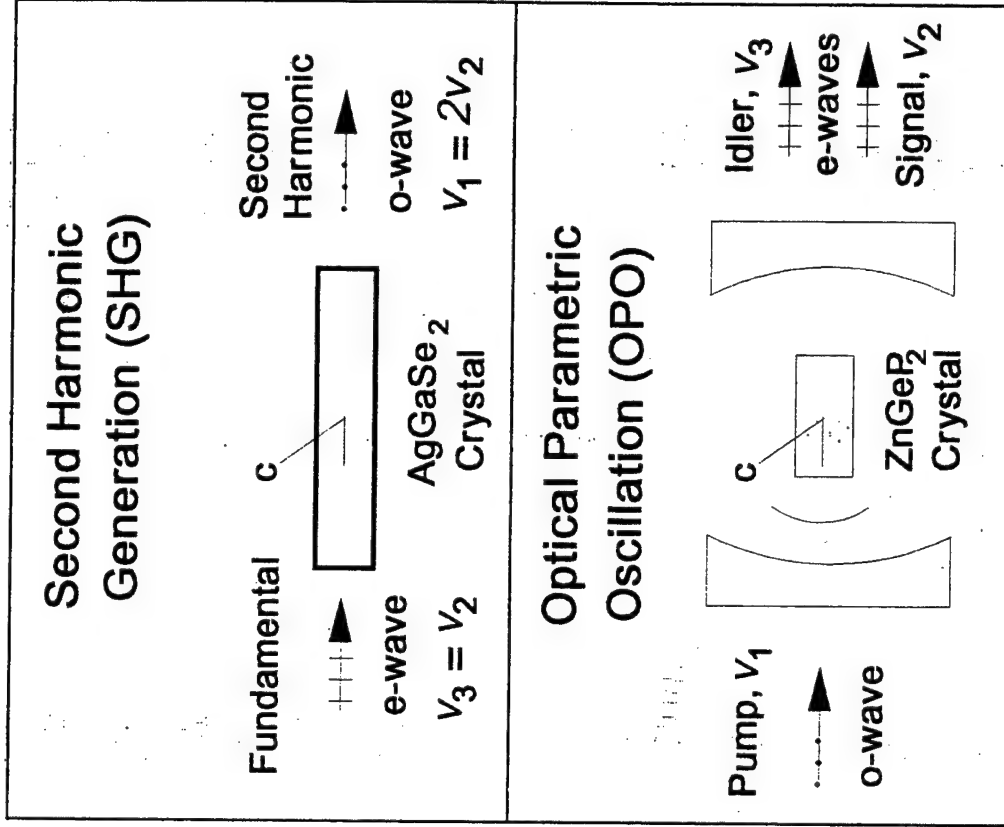
P. G. Schunemann and T. M. Pollak



Presented at the 1999 Nonlinear Optical Materials
Workshop, (NLO 99), DERA, Malvern, UK, Sept. 20, 1999

Work supported L.N. Durvasula at DARPA (via the Air Force Research Laboratory Materials Directorate
contract No. F33615 -94-C-5415) and Sanders Internal R&D Funding

- For the past 10 years we have focused on crystal growth and processing of bulk chalcopyrites for nonlinear optical (NLO) frequency conversion:
 - Frequency doubling of CO₂ Lasers (SHG)
 - "Wavelength doubling" of 2um solid state lasers (OPO)
- The Goal:
 - Produce efficient mid-IR lasers operating in regions of high atmospheric transmission
- Applications:
 - Laser radar, remote sensing, etc.



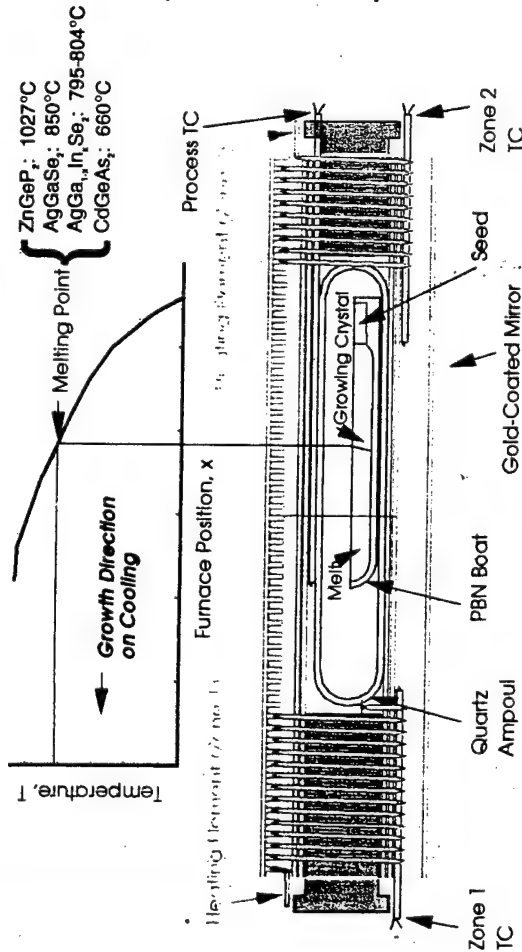
2 μ m-pumped OPO's

- Material of Choice: ZnGeP₂
 - Highest NLO Coefficient with sufficient band gap ($d_{14}=75$ pm/V)
 - High Thermal Conductivity (0.35W/cmK)
 - Reduced Losses ----> Efficient, High Power Output
- Alternatives for better performance:
 - **None:** Continue to Reduce ZnGeP₂ Near-IR Absorption

CO₂ Doubling

- Material of Choice: AgGaSe₂
 - Respectable NLO Coefficient (39 pm/V)
 - Wide transparency and phase-matching range (.78-18 μ m)
 - Low absorption Losses
- Alternatives for better performance:
 - CdGeAs₂: Highest Nonlinearity ($d_{14}=236$ pm/V) \blacktriangleright Reduce Absorption Loss
 - Ag(Ga,In)Se₂: Adjust Birefringence for Noncritical Phase-Matching (NCPM)
 - ABX₂: Continue Search for New Materials

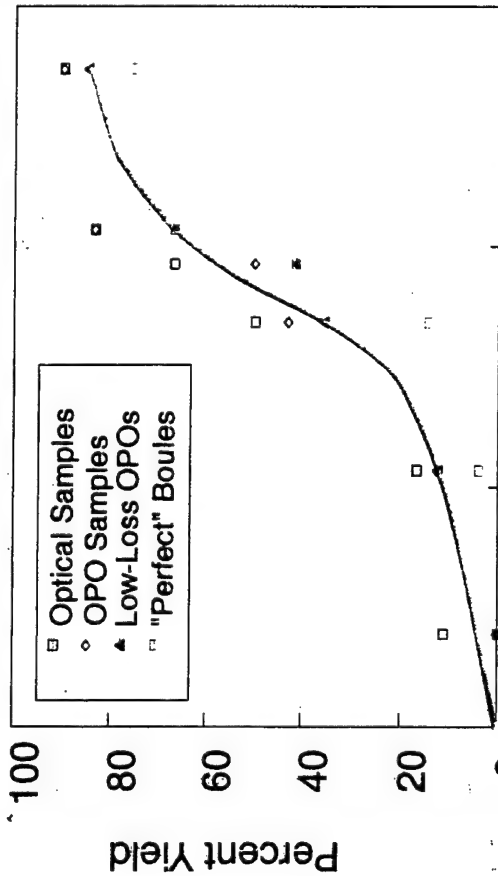
Horizontal gradient freeze growth led to advances in NLO chalcopyrites



HGF Approach: Key Aspects

- **Low thermal gradients**
 - Minimize vapor transport
 - Eliminate cracking due to anisotropic thermal expansion
- **Transparent Furnace**
 - Simplifies the seeding process
 - Allows *in situ* monitoring of the S/L interface shape & position
 - Facilitates interactive growth (secondary grains can be re-melted)
- **Seeded growth**
 - Eliminates initial polycrystallinity due to supercooling
 - Optimizes orientation to accommodate negative c-axis thermal expansion
 - Enables growth along phase matching direction for max. device length & yield

Improved Single Crystal Yield

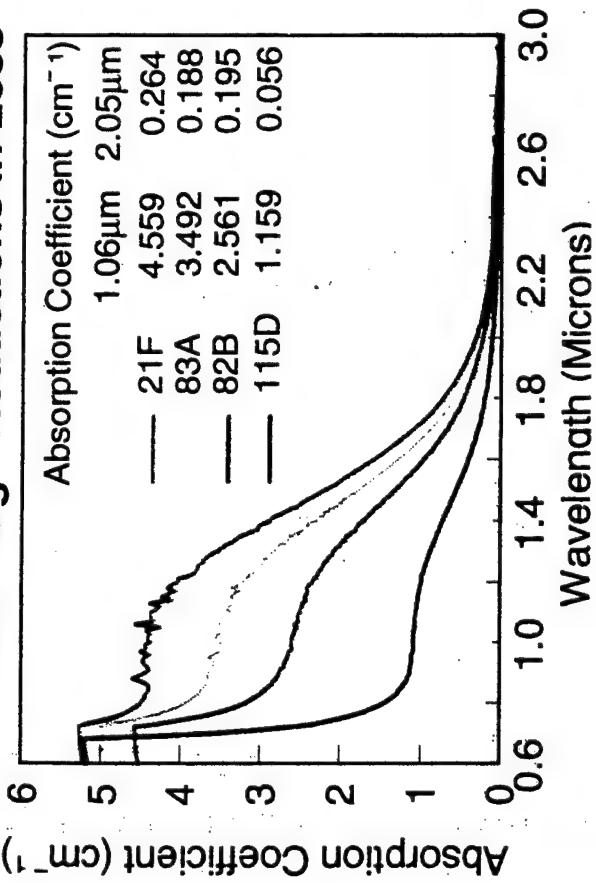


Dec-88 Sep-91 Jun-94 Mar-97
Program Time Line

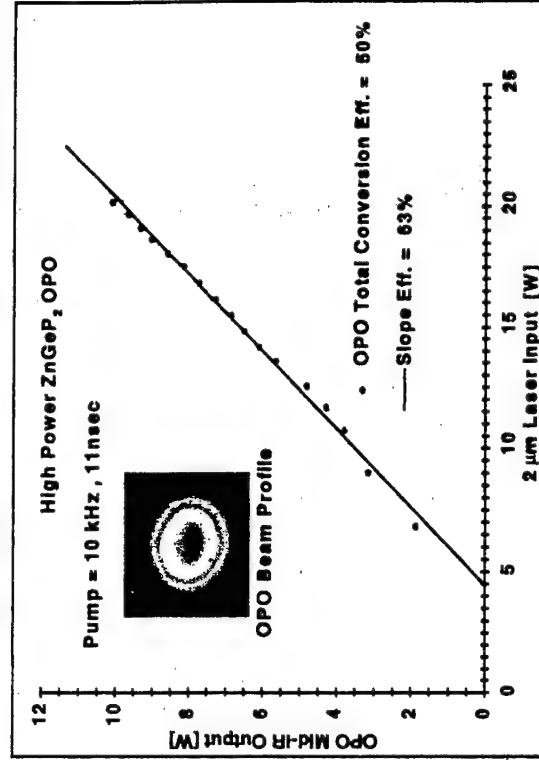
Sealed-Up Crystal Growth



Breakthrough Reductions in Loss

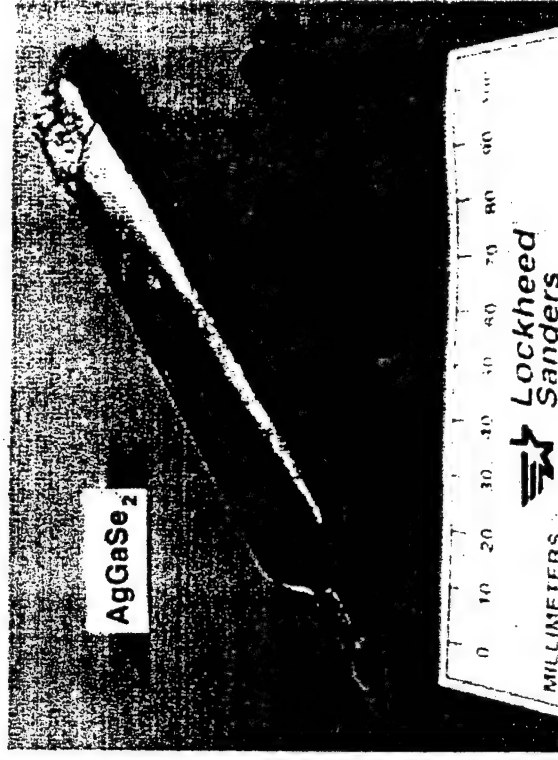
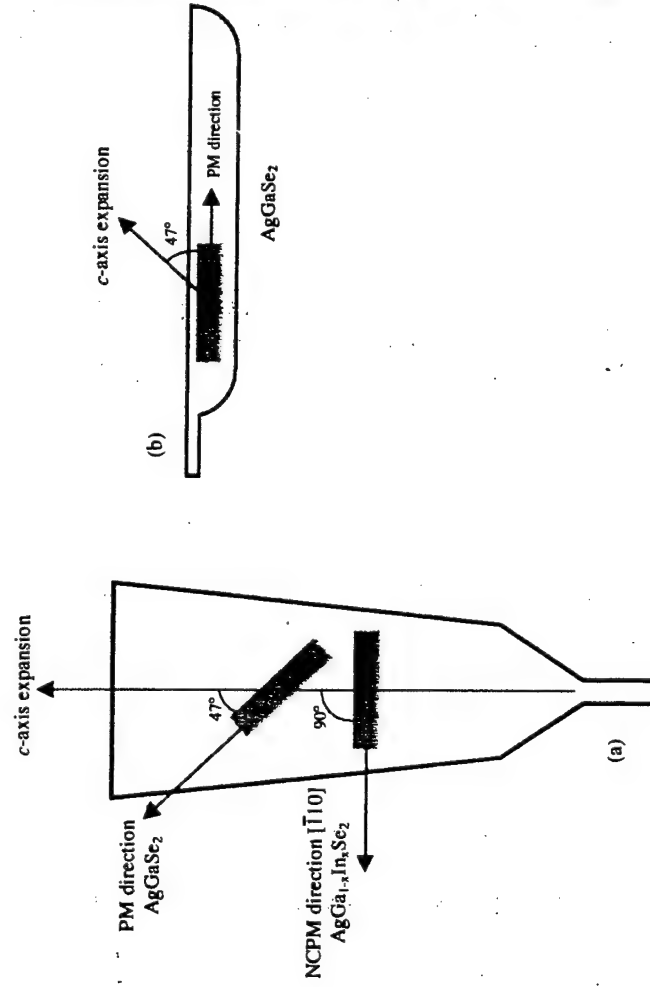


Enhanced OPO Performance

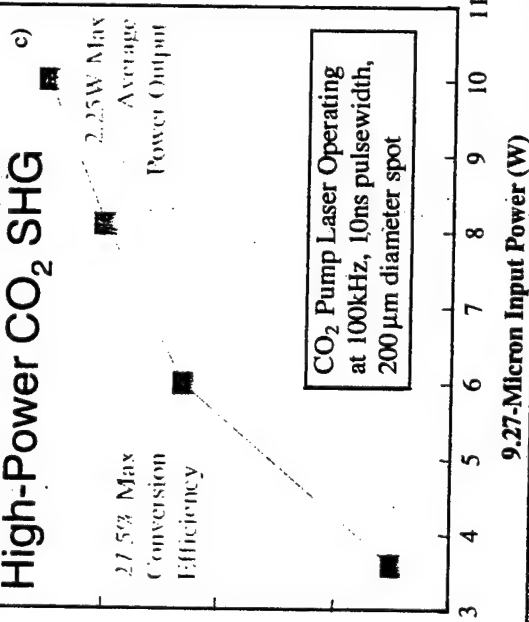
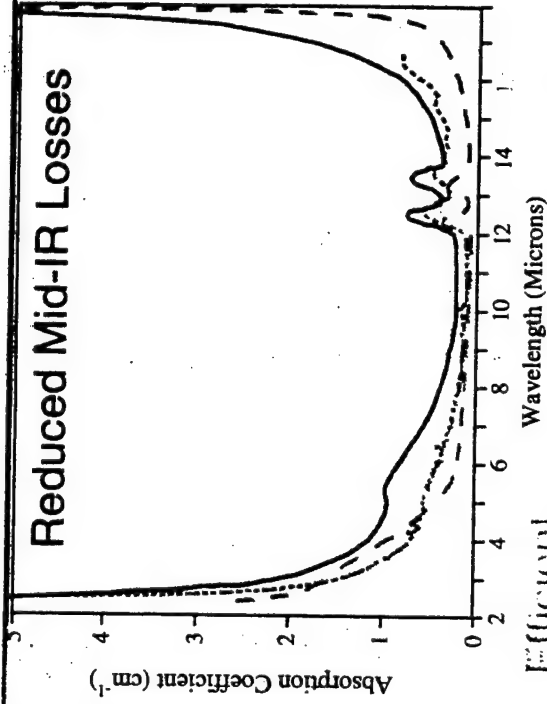
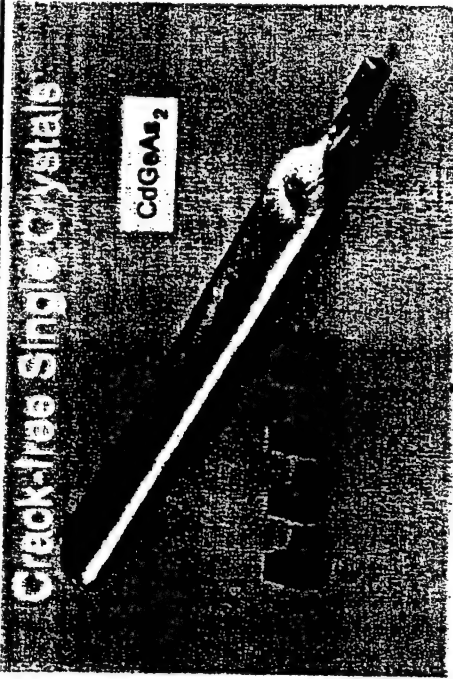


“Phase-Matched” Crystal Growth of AgGaSe₂

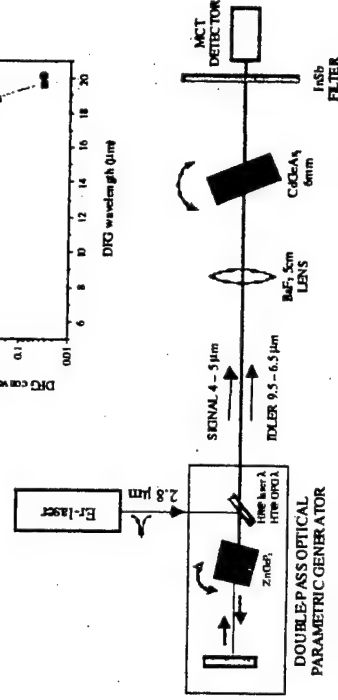
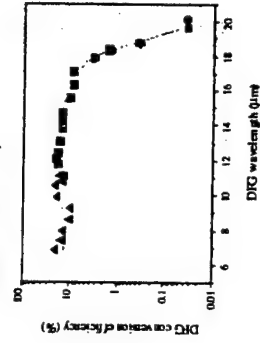
- Vertical Bridgman growth of AgGaSe₂ requires seeding along c-axis for unconstrained thermal expansion during cool-down
- The Horizontal Gradient Freeze (HGF) technique allows “phase-matched” growth along device orientation, yielding longer interaction lengths and minimal waste



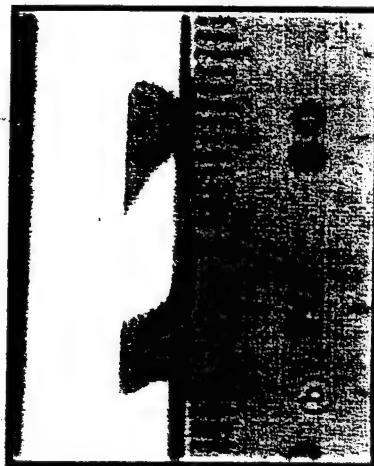
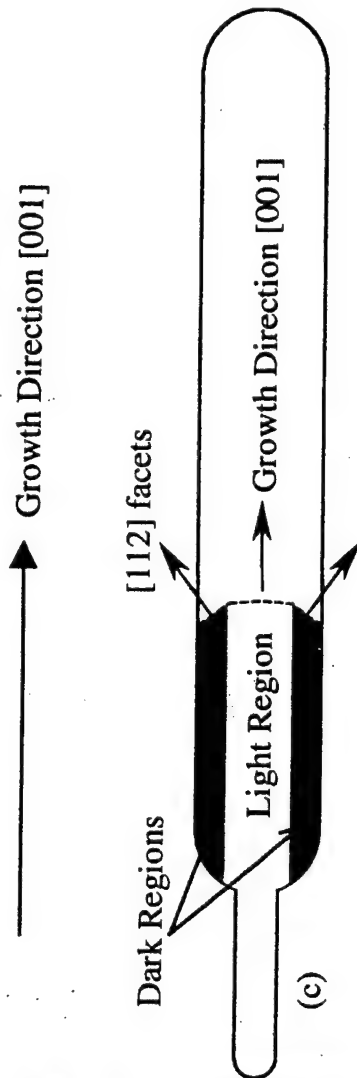
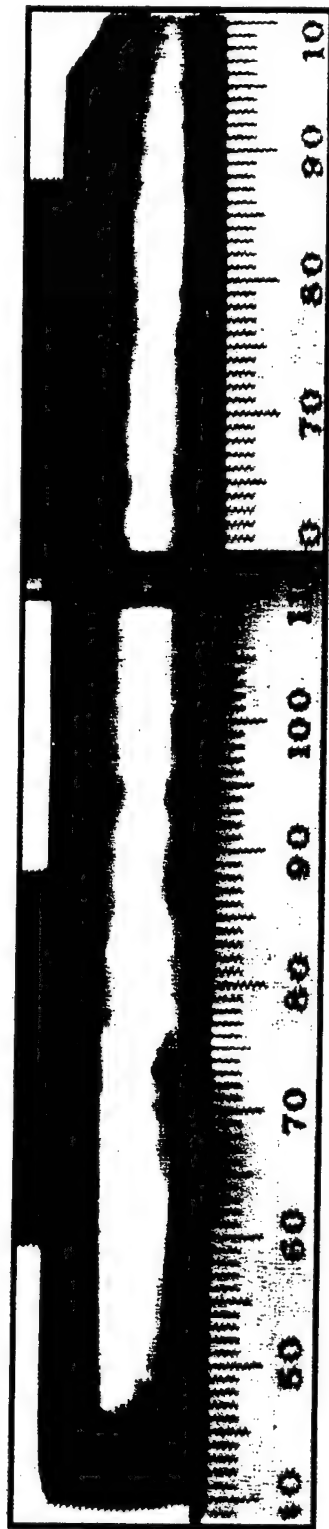
CdGeAs₂: Development Milestones



Efficient
Long-Wave
DFG



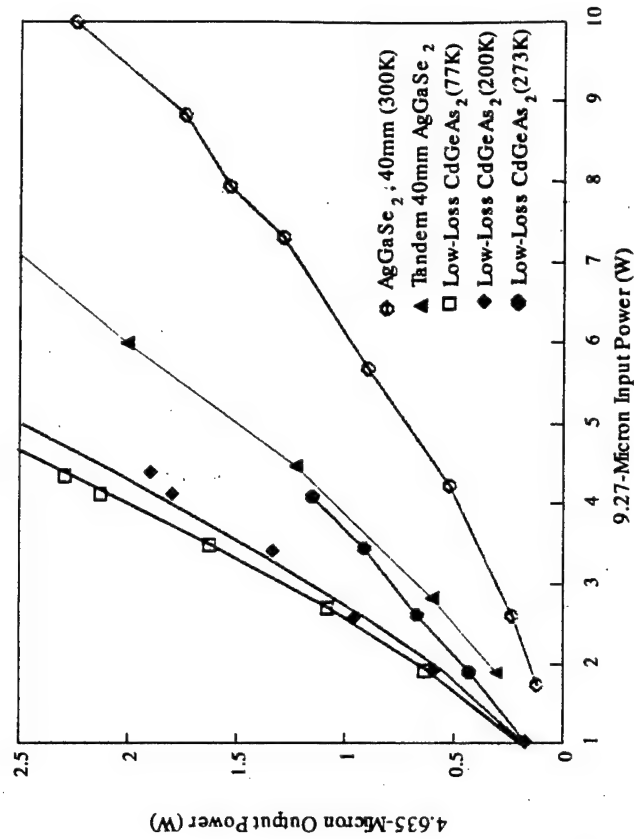
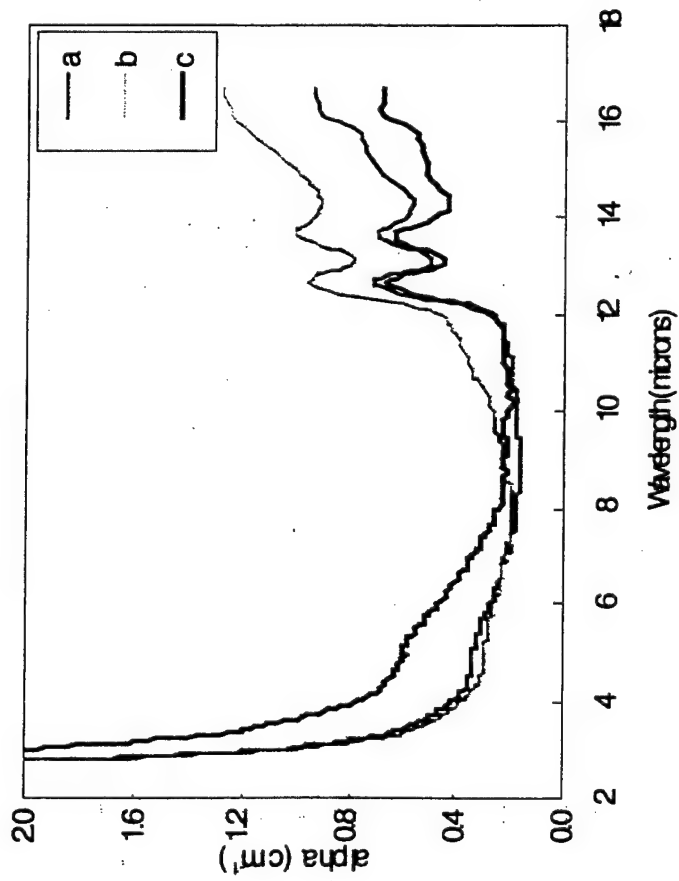
Segregation of Absorbing Defects in CdGeAs₂



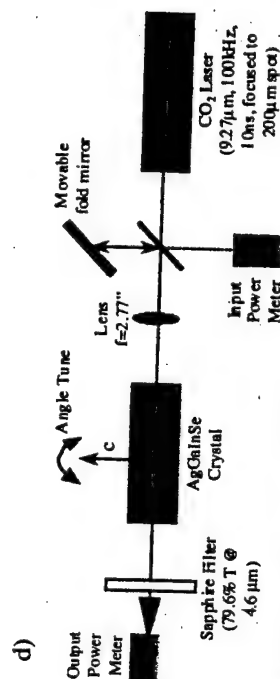
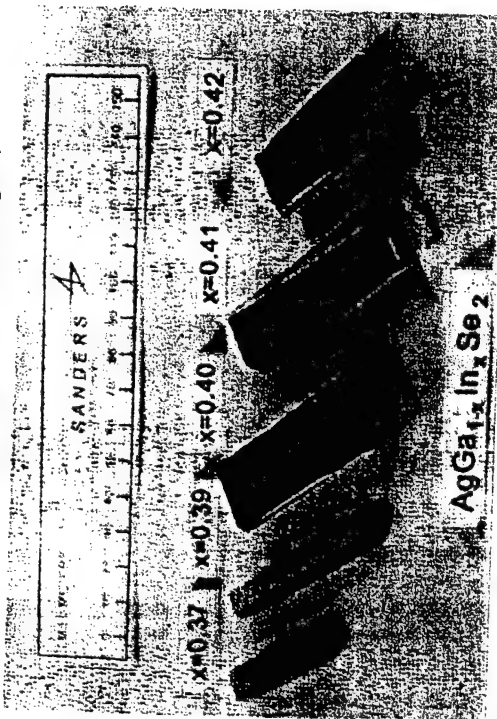
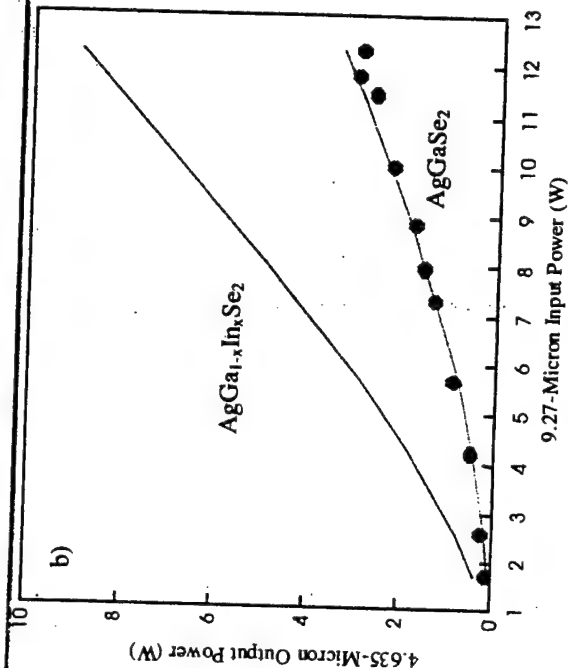
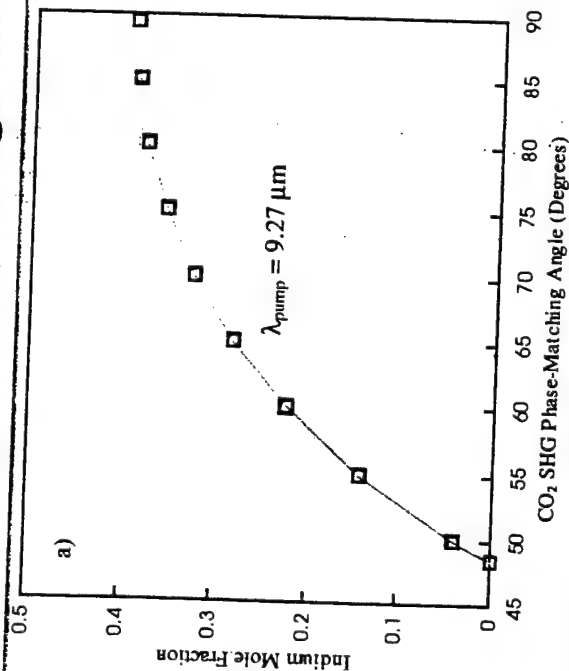
CdGeAs₂: Recent Advances

Reduced Mid-IR Absorption
(Low-Loss Central Core)

Efficient CO₂-Doubling:
 $\eta = 53\%$ at 77K
 $\eta = 28\%$ at 273K

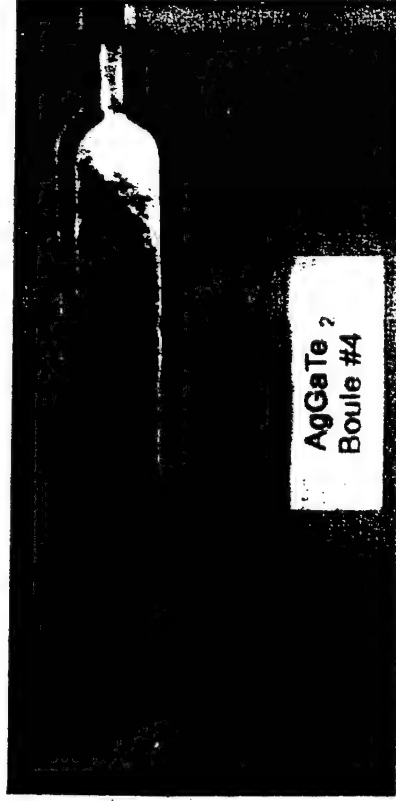
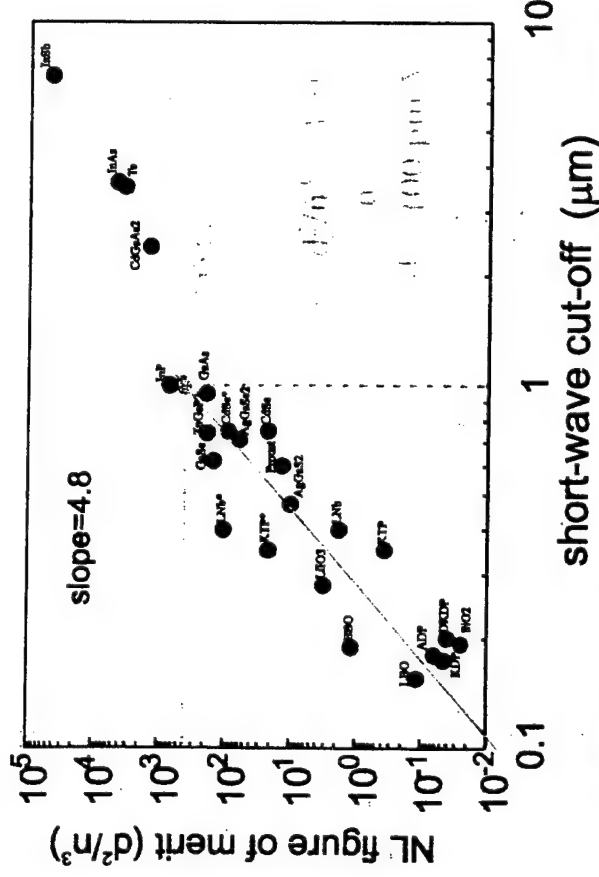


AgGa_{1-x}In_xSe₂: Engineered Birefringence for NCPM



NCPM at $x=0.42$ (melt)
Reflection & Scattering Losses $\rightarrow \eta = 1.8\%$

AgGaTe₂: a promising new nonlinear optical crystal



- Motivation:
 - Telluride analog of AgGaS₂ & AgGaSe₂
 - Substitution by Te should triple the NL coefficient and shift the transparency range further into the IR (~1-20 μm)
- Objectives of Research:
 - Produce large, crack-free single crystals
 - Determine if birefringence is sufficient for phasematching
- Approach:
 - HGF Growth in Transparent Furnace
 - Fabricate prism, measure Δn

Summary

- Recent crystal growth advances have established chalcopyrites as the NLO materials of choice for mid- to far-IR laser frequency conversion:
 - Large crack-free single crystals (up to 16x28x140mm³) of ZnGeP₂, AgGaSe₂, and CdGeAs₂ can be reproducibly grown by the HGF technique
 - Substantial reductions in absorption and/or scattering losses have been achieved by feed purification, compositional control, & post-growth annealing
 - Improved crystal quality has resulted in outstanding NLO device performance
- The birefringence of mixed crystals (AgGa_{1-x}In_xSe₂) can be engineered to achieve non-critical phase-matching (NCPM)
- The search for new materials has led to promising NLO crystals such as AgGaTe₂, CdGa₂S₄, and CdGa₂Se₄
- Dy³⁺:CaGa₂S₄ was demonstrated as the first sulfide mid-IR laser host

Development of Technology of ZnGeP₂ Single Crystal at

Institute for Optical Monitoring SD RAS

By Alexander I. Gribenyukov, Galina A. Verozubova, and Valentina V. Korotkova

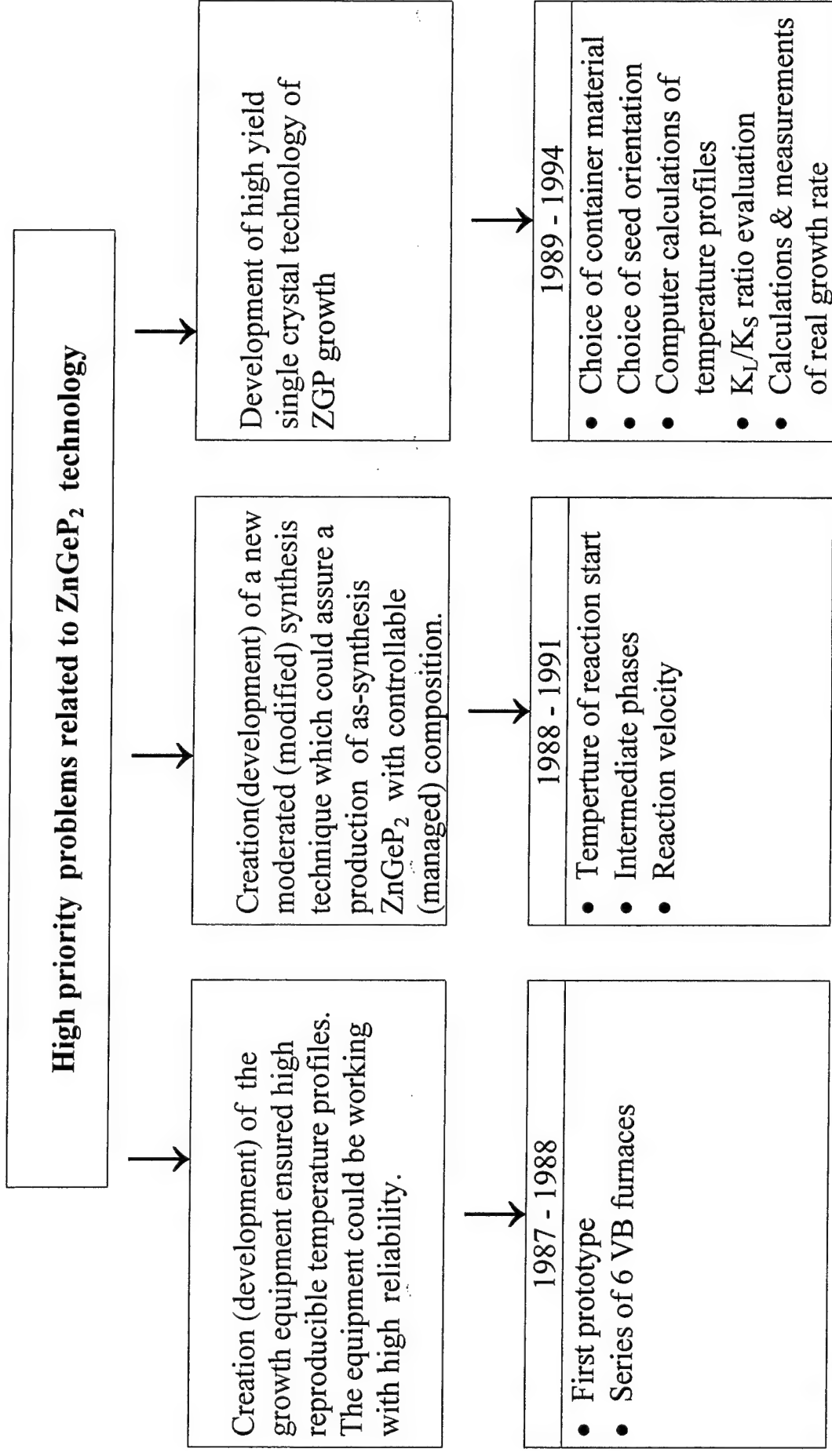
Laboratory of Optical Spectroscopy

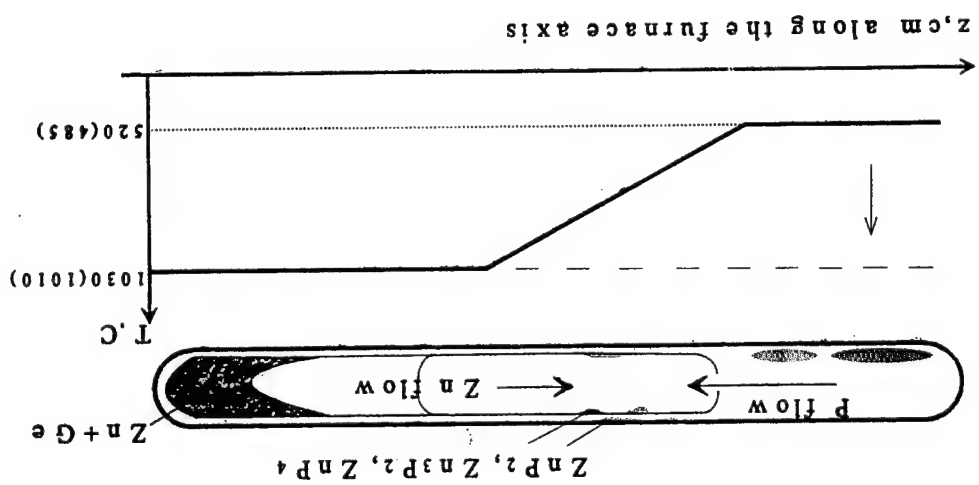
Institute for Optical Monitoring

Tomsk Branch of Siberian Division

Russian Academy of Sciences

IOM	The main directions of IOM activity & interests	<ul style="list-style-type: none"> • Theoretical and experimental investigations of climatic and ecological changes under effect of natural and human factors •
	The basic theme of the noted direction of IOM's activity	<ul style="list-style-type: none"> • Development of new techniques and technologies for environment remote sounding •
	Divisions of the basic theme	<ul style="list-style-type: none"> • Development of optical monitoring systems based on new generation of tunable coherent radiation sources working in the middle IR spectral range. •
	The main task	Provision of IOM works on development and multiplication of the new optical systems by optical materials needed
LOS IOM	The basic theme	Development of high yield and reliable technologies for production optical materials with controllable physical properties
	The main points of contents of basic theme	<ol style="list-style-type: none"> 1. Development of high yield technology of single crystal growth 2. Investigations of possibilities of controllable manage by physical properties of material due to purposeful changes (variations) of technological parameters on all stages of crystals production – at synthesis, at crystal growth, at postgrowth annealing



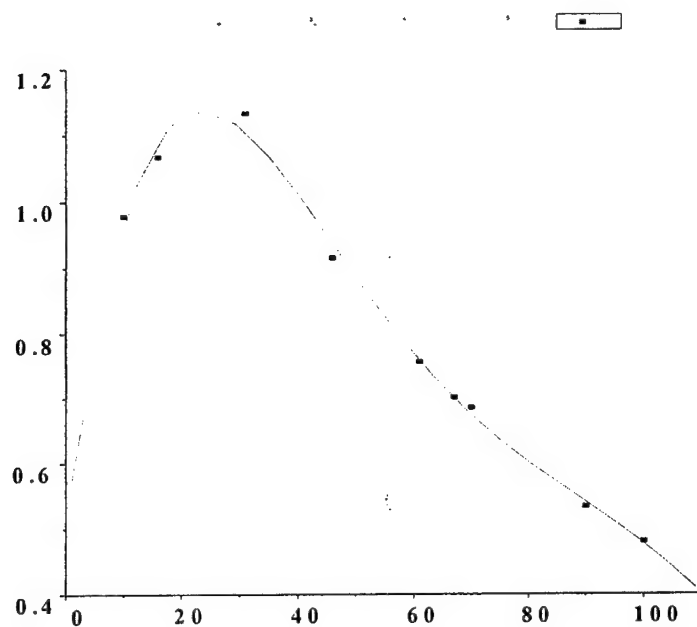


TR9, P_4 and Zn flows in non-isothermal closed synthesis system.

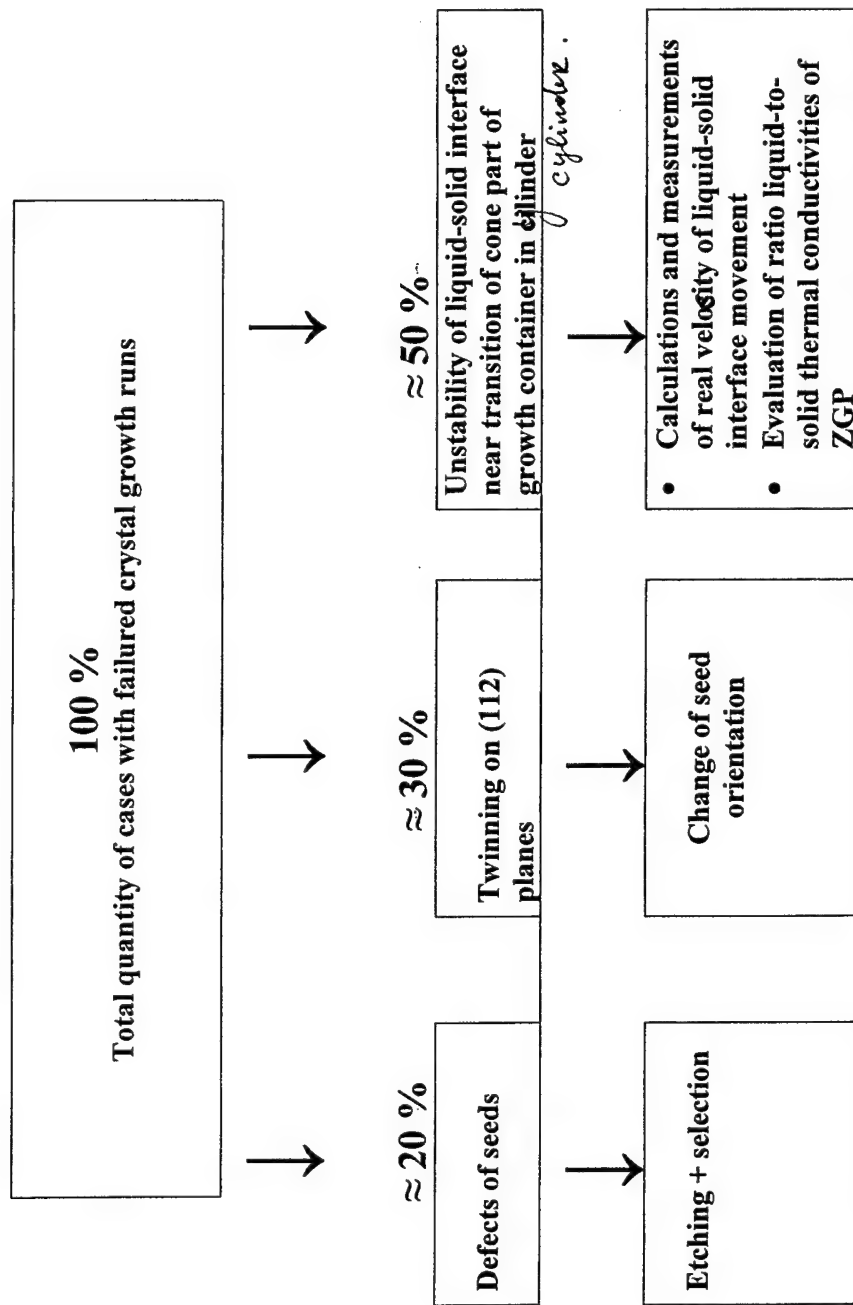
**TR10 – Time dependence of expenditure velocity of P4 vapour
under pressure of 10-12 atm with Zn-Ge melt at 1010 C .**

Hot zone temperature - 1010 °C

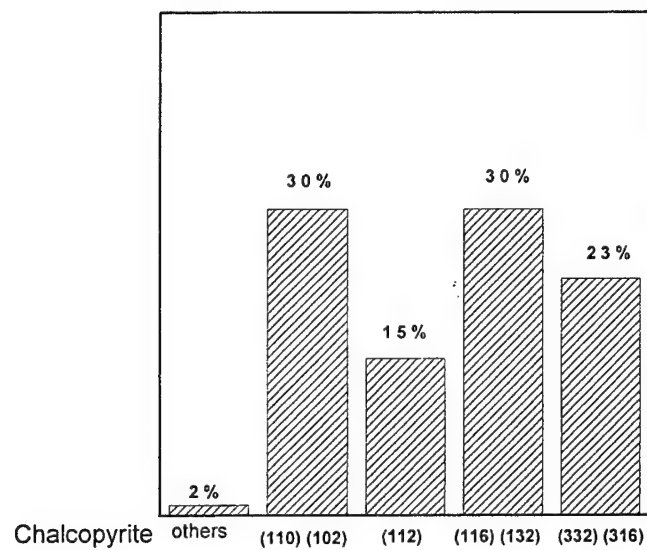
Cold zone temperature - 515 °C ($P_{P4} = 10$ atm)



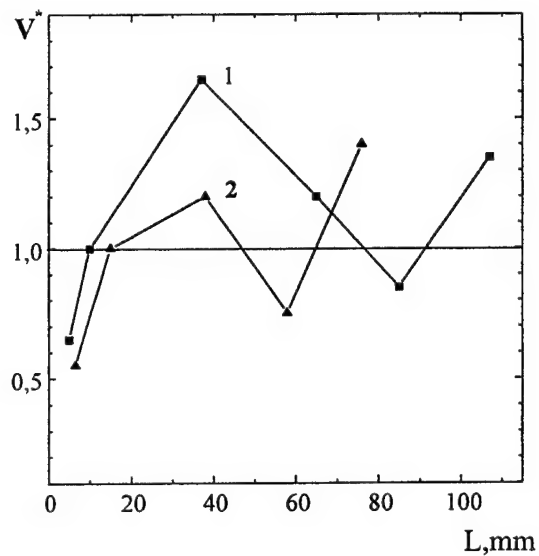
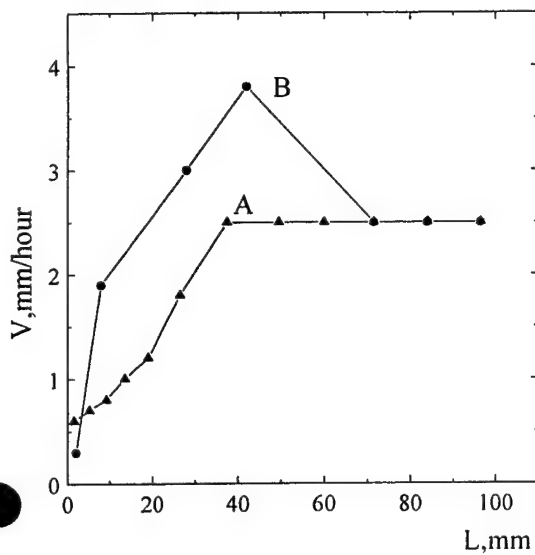
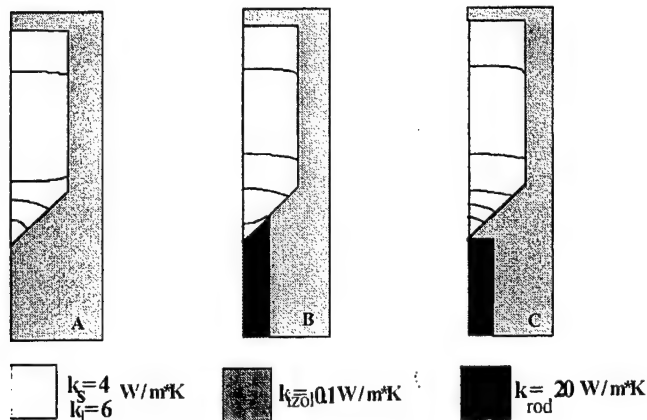
Distribution of growth failures on causes



TR12 – Probability distribution of ZGP crystalline blocks enlarged along growth axis in VB-method with spontaneous nucleation.



TR14 – The image of growth container surrounding structure for computer calculations.



GF method:

The isotherm crystallization rate for container with A and B surrounding structure.

Cooling rate – 1 °/hour.

VB method:

Distribution of isotherm crystallization rate (in units of mechanical movement rate) along crystal axis.

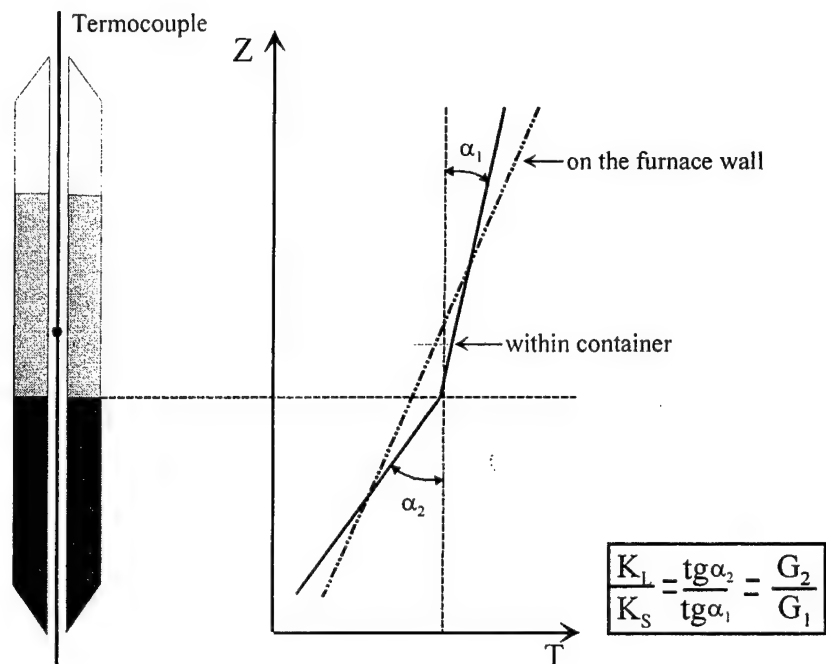
A-type of surrounding structure, $\varnothing_{\text{furnace}} = 6 \text{ mm}$;

1 – calculation's data, $\varnothing_{\text{ampoule}} = 3 \text{ mm}$;

2 – experiment's data, $\varnothing_{\text{ampoule}} = 2 \text{ mm}$;

steady

TR15. Diagram of stady state temperature distribution

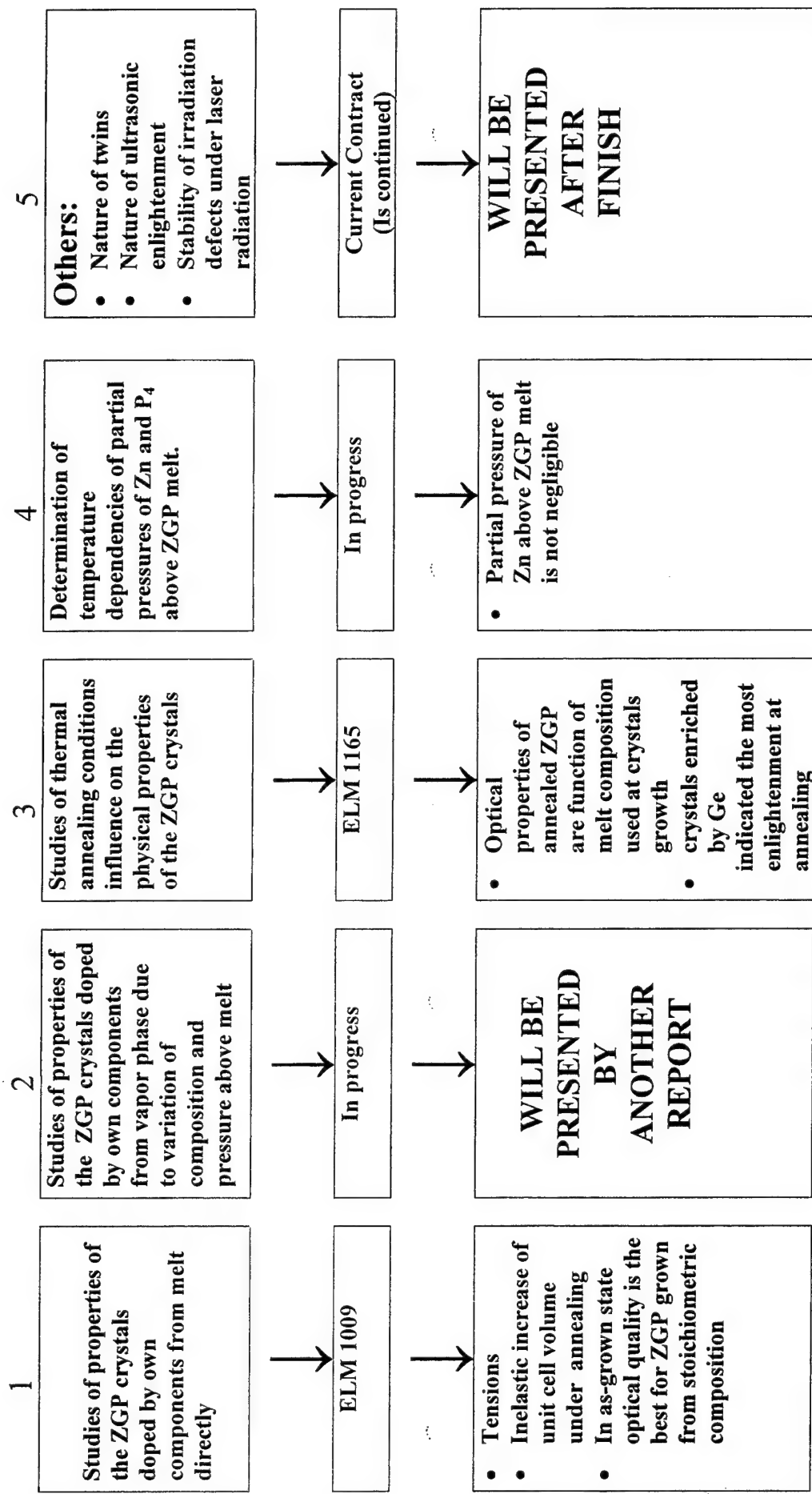


Material	Linear regression coefficients				Calculated values	
	Ts	Gs	TL	GL	T _{mel}	K _L /K _s
Ge	942.42	4.6	940.51	2.7	937 ± 1	1.7 ± 0.1
GeP ₂	2009.9	16.24	1807.53	12.9	1027 ± 1	1.3 ± 0.1

Literature data for Ge : K_L/K_s = 2.93 [3]

Corrected ratio for ZnGeP₂ : K_L/K_s = 2.3

The Second Long-term Program



TR17 Some Results of investigations of ZGP crystals doped from melt. Measurements were made in DERA. The crystals were grown in IOM

Crystal	Dopant (P ₄ -pres. atm)	Temperat -gradient DT/dx, °C/cm	Unit cell volume, Å ³	Unit cell volume difference (V _{lrf} - V _{ftf}) Å ³	Absorpt. coeff. at 2.06 μm cm ⁻¹	Absorpt. coeff. difference α _{lrf} - α _{ftf} cm ⁻¹	Derivative da/dV, cm ⁻¹ Å ⁻³	Unit cell volume after annealing Å ³	Absorpt. coeff. after annealing cm ⁻¹
89/3 ftf	0.2 wt%Ge	5.2	319.94861	-0.03872	0.431	0.016		320,234	0.27 -meas. <u>0.298-calc.</u>
89/3 ltf	(7.5)	15.4	319.90989		0.449				
91/2 ftf	Stoich	1.5	319.92818		0.332			320,332	0.36 -meas. <u>0.764-calc.</u>
91/2 ltf	(7.1)	7.5	320.04824	+0.12000 6	0.461	0.129	<u>+1.07</u>		
93/3 ftf	0.2 wt%Zn	2.5	319.98361		0.615			320,190	0.53-meas. <u>1.11-calc</u>
93/3 ltf	(3.8)	>20	319.93989	-0.04372	0.510	-0.105	<u>+2.4</u>		

Seeds orientation is (116) for all grown crystals.

Annealing result in an increase of unit cell volumes, but expected change of absorption coefficient with the unit cell volume indicated only for sample enriched by Ge.

**ZGP GROWTH FROM MELT:
THE VAPOUR PHASE COMPOSITION AND CRYSTAL
PROPERTIES**

**G.A. Verozubova
A.I. Gribenyukov
Yu. F. Ivanov***

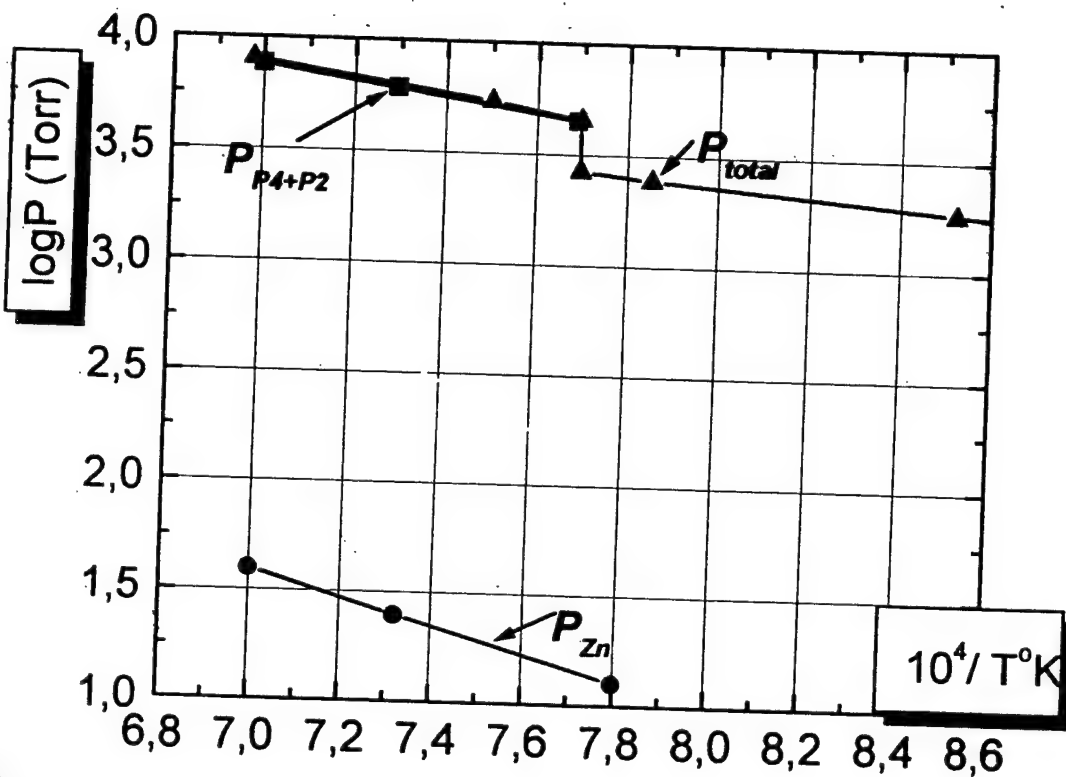
**Institute for Optical Monitoring SD RAS
*Tomsk Polytechnical University**

in collaboration with A.Vere, DERA, Malvern

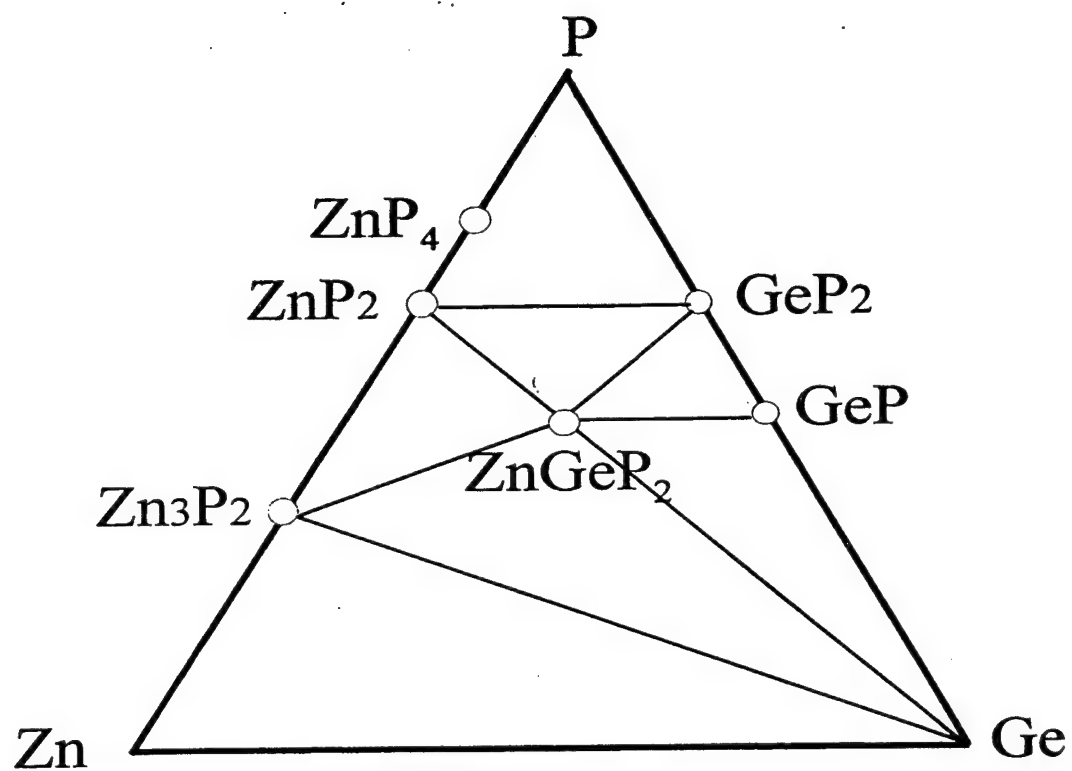
***The work was fulfilled under financial support
DERA, United Kindom***

327°C – ZnGeP₂ starts to decompose

1038°C – ZnGeP₂ melting point (Seb Fiechter, 1996)



The total pressure above ZnGeP₂ - P_{total} (Buehler, 1971) and partial pressures of Zn - P_{Zn} and P - P_{P4+P2} calculated from the regular solution theory (Roenkov, 1975): $P_{Zn} = 18$ Torr at 1068°C



The Zn-Ge-P phase triangle

Experimental details

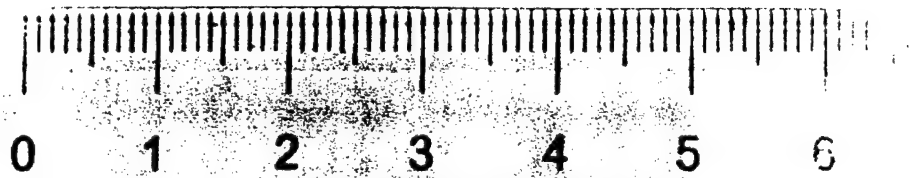
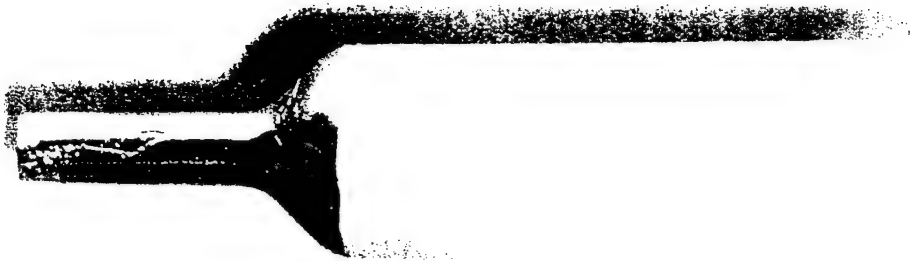
Synthesis: modified two-temperature technique, allowing to produce more than 500 gms of the material in one process

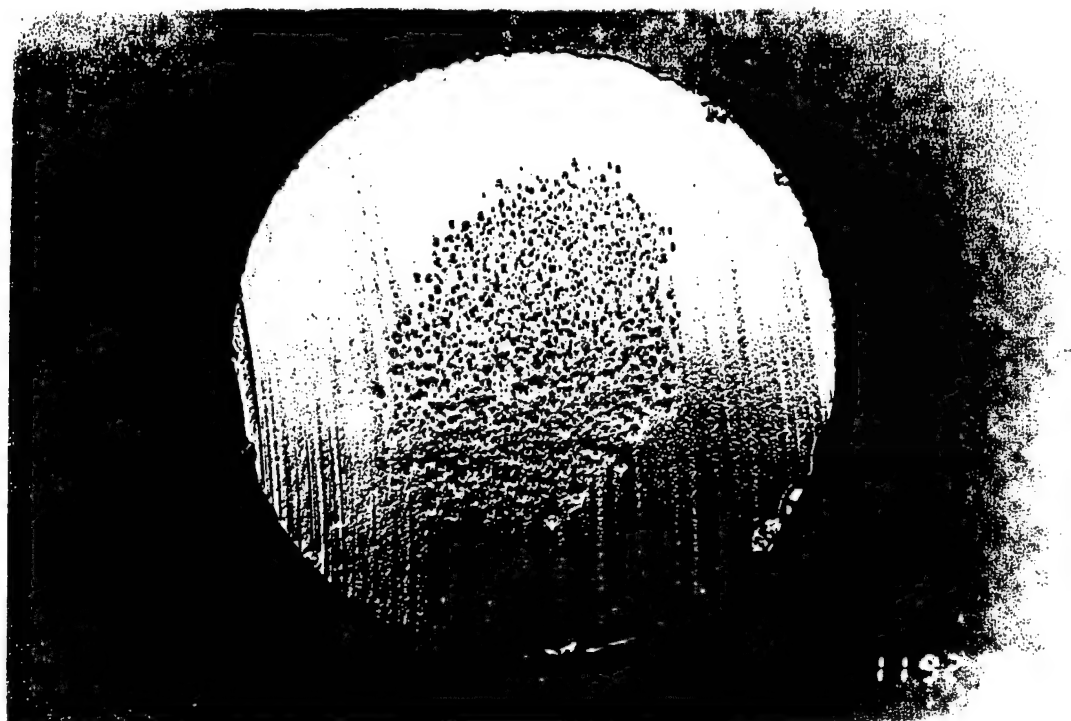
Growth: vertical Bridgman technique, (100) seeds

TABLE 1. Crystal growth conditions.

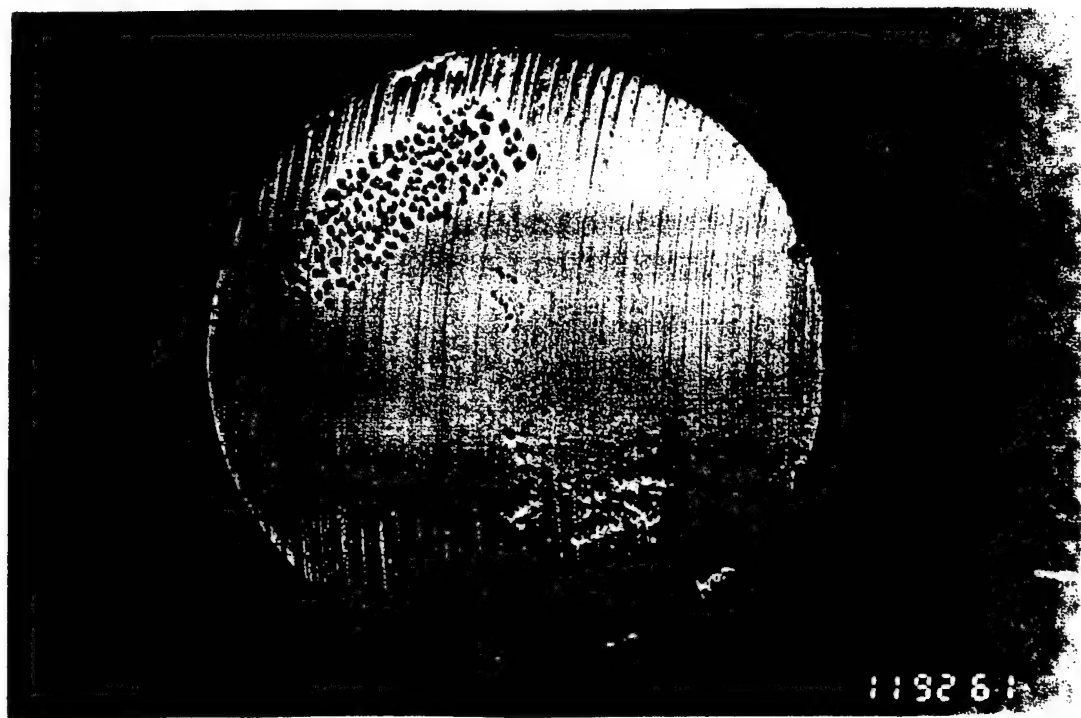
NUMBER OF CRYSTAL	HOT ZONE TEMPERATURE °C	COLD ZONE TEMPERATURE °C	PHOSPHORUS CHARGE (g)	ZINC CHARGE (g)	PHOSPHORUS PRESSURE (atm)	ZINC PRESSURE (atm)	REMARKS
1	1060	990	6	0.5	6.9	1.1	Gas pockets
2	1060	1000	3.5	10	7.2	-	No pockets Single phase
3	1060	950	10	0.5	-	-	Ge eutectic on the top of the crystal

* P_{P_4} (P_{Zn}) - pressures of phosphorus (zinc), created by additional charges of P (Zn), and calculated from the ideal gas law.

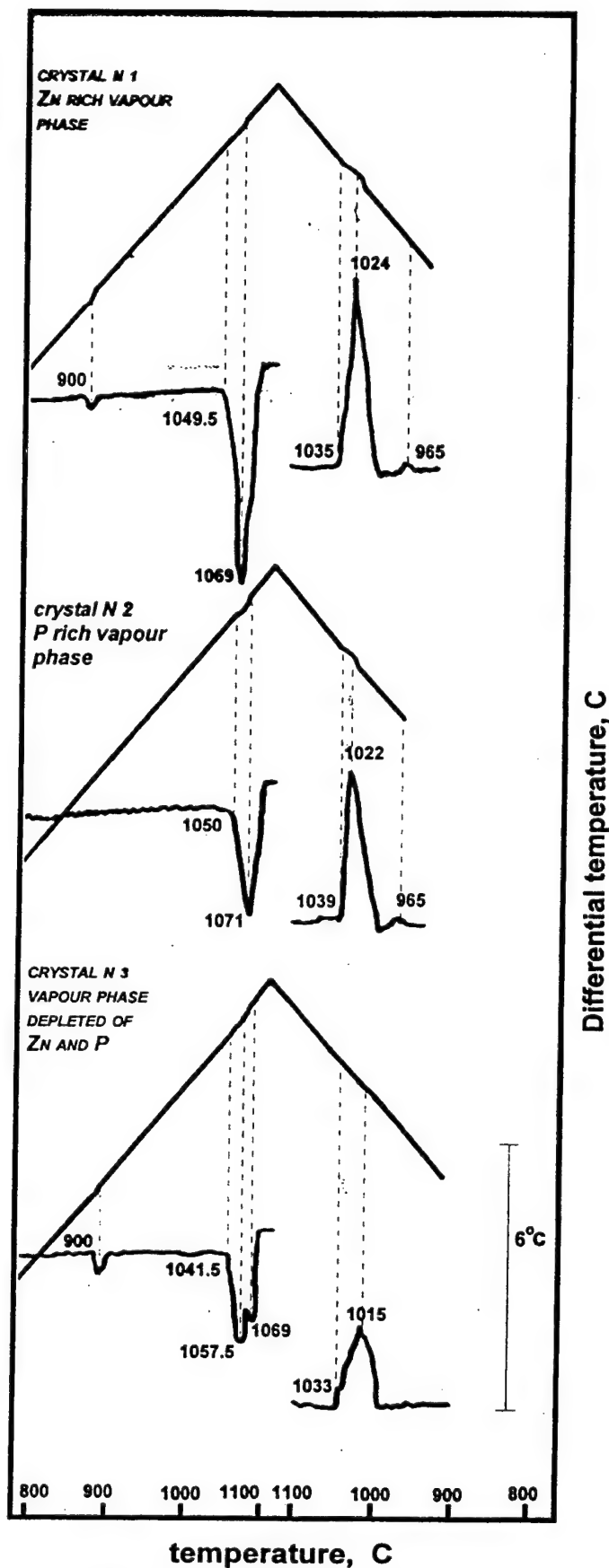




1 cm

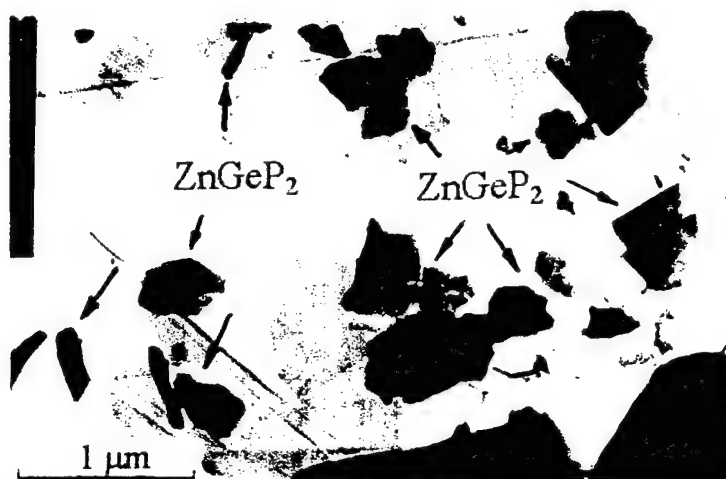


ZnGeP₂ slices after chemical etching



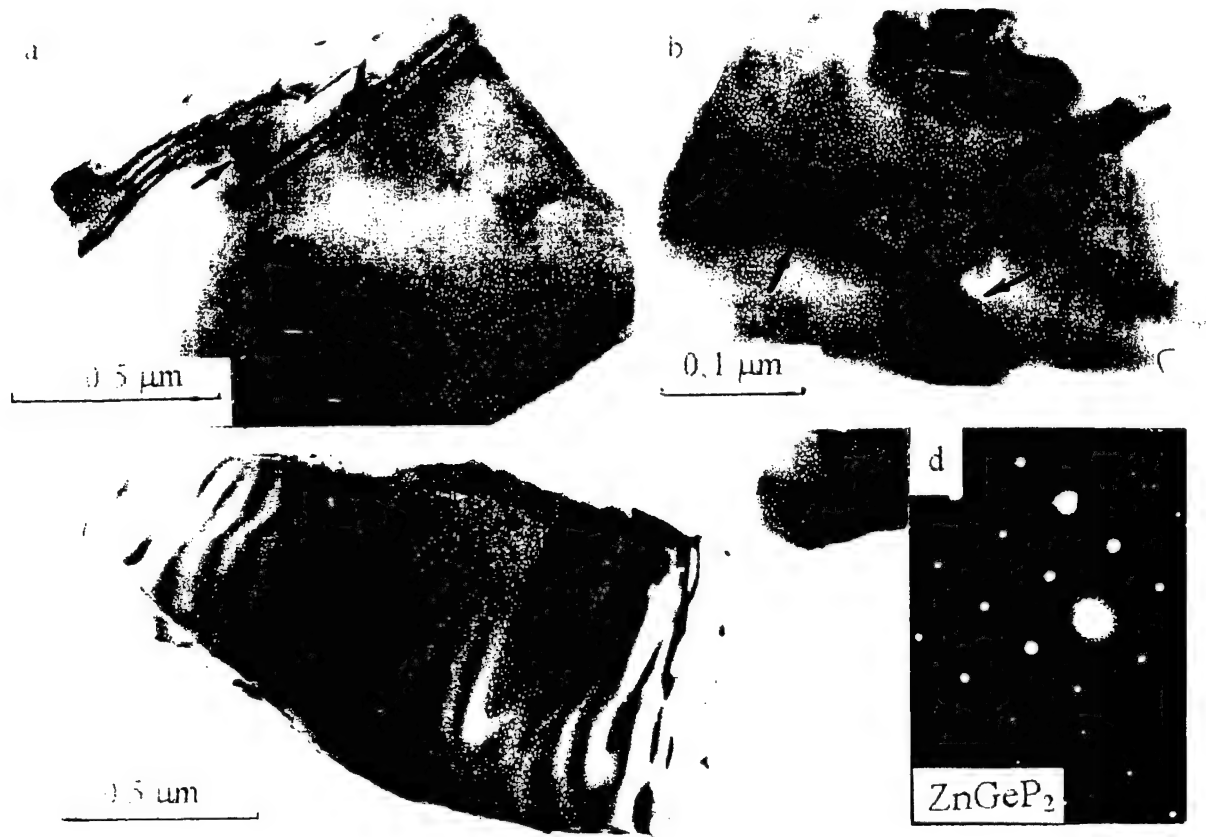
DTA curves of ZGP grown under various pressures of Zn and P

Experimental details: the weight of the studied samples - 0.5 g, heating and cooling rates - 7.5 deg/min
reference material - Al_2O_3 , speed of the paper movement - 1 mm/min

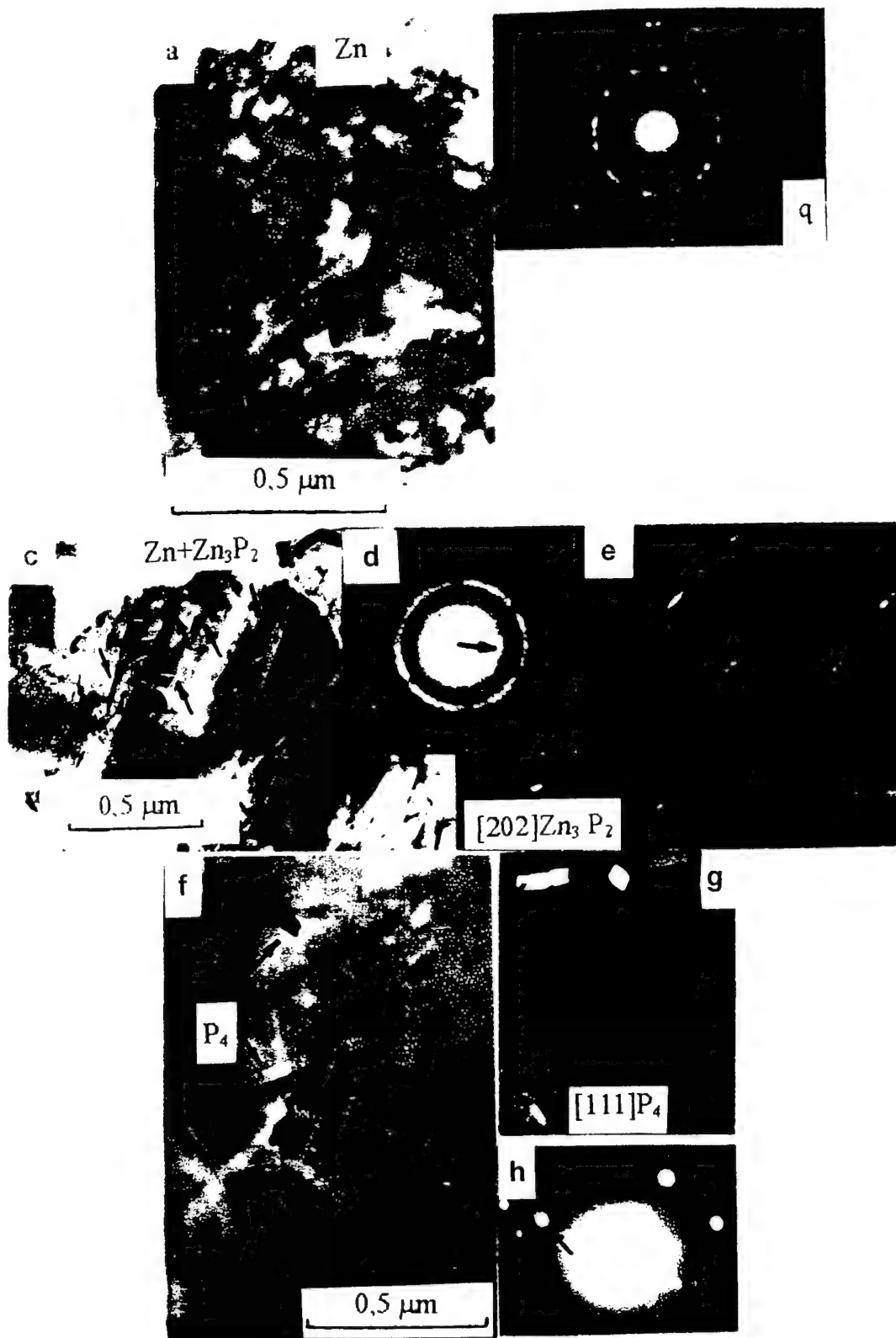


Fragments of failure (damage) of the bulk ZGP specimen
arranged on the carbon substrate

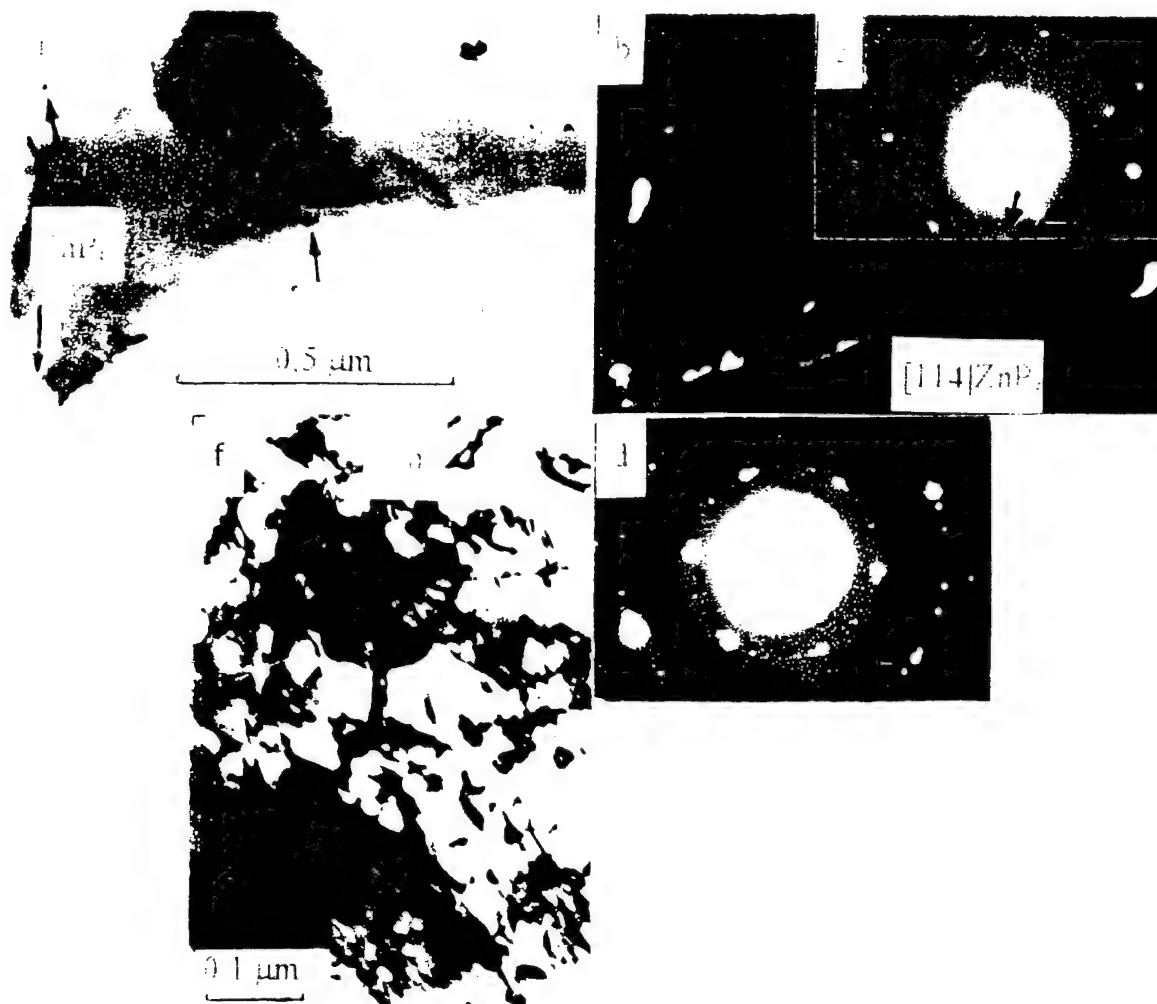
*Electron microscope EM-125
Accelerating voltage 125 kV
Working Magnification 65-85 000
Resolution 7-10Å*



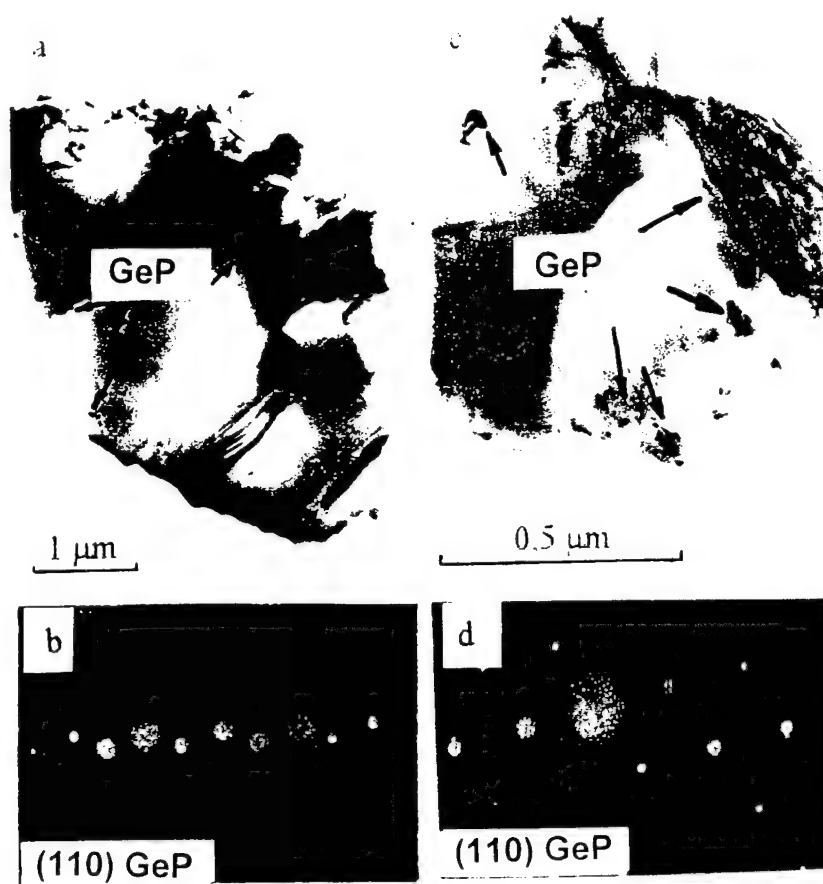
Microscopic image of ZnGeP_2



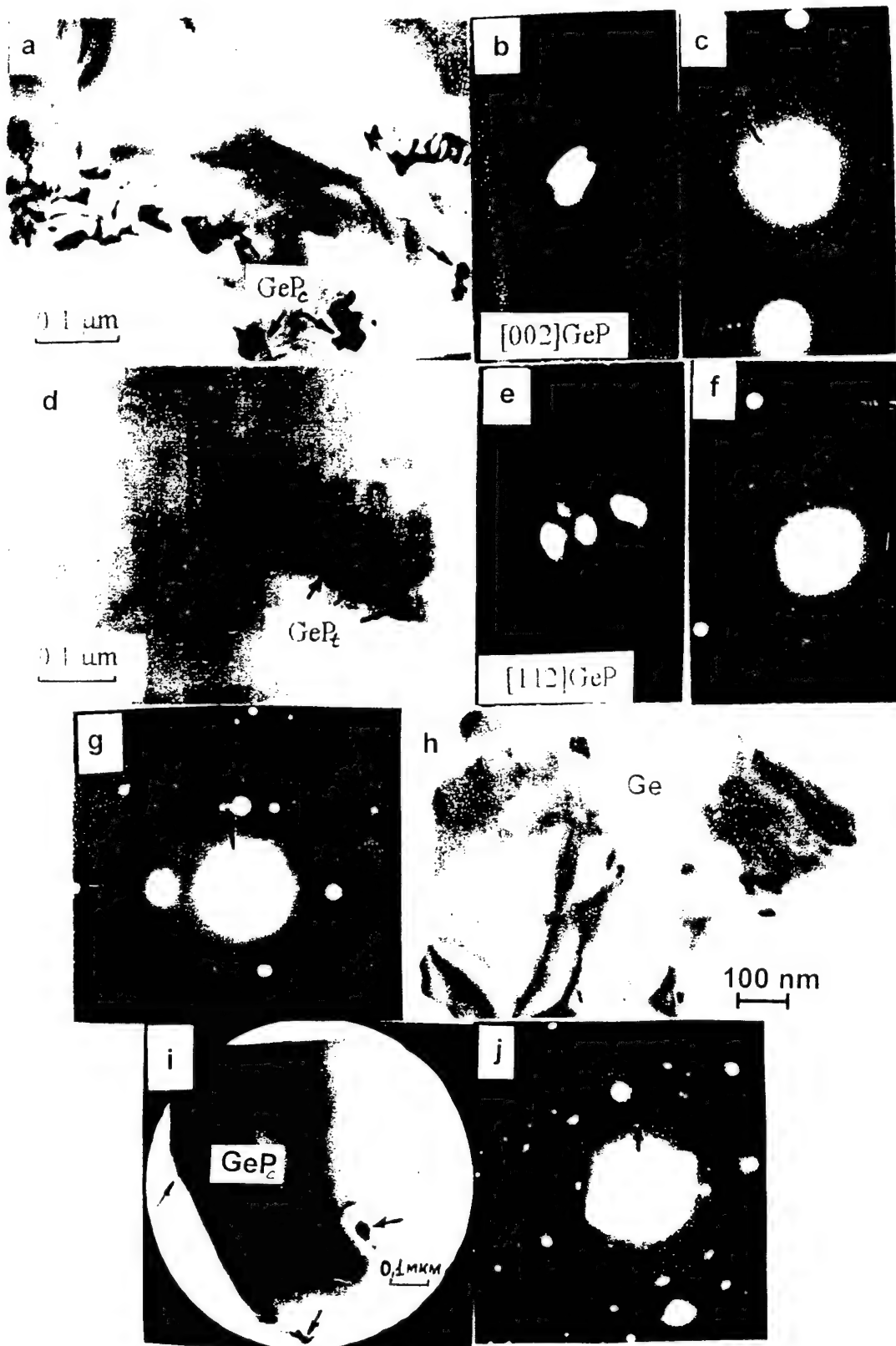
Microscopic image of ZnGeP_2 grown under Zn rich vapour phase (as- grown crystal N1)



Microscopic image of ZnGeP₂ grown under Zn rich vapour phase (annealed crystal N1)



Microscopic image of ZnGeP₂ grown under the phosphorus pressure of 7.2 atm (crystal N2)



Microscopic image of ZnGeP₂ grown under the vapour phase depleted of volatile components (crystal N3)

TABLE 2. The vapour phase composition during growth and the phase composition of precipitates.

NUMBER OF CRYSTAL	P_{P_4} ATM	P_{Zn} ATM	EXTERNAL VIEW OF THE GROWN CRYSTAL	PHASE COMPOSITION OF PRECIPITATES	SIZES OF PRECIPITATES
1	6.9	1.1	Gas pockets	Zn	Ø 1-1.5 mkm
				Zn_3P_2 ZnP_2	10 nm×1 mkm
				P	25×300 nm
2	7.2	-	No pockets Single phase top	GeP cubic	Ø 0.2-0.3 mkm
					Ø 80-90 nm
3	-	-	Ge eutectic on the top of the crystal	GeP cubic	Ø 5 nm
				GeP tetragonal	15×45 nm
				Ge	Ø 8 nm

* P_{P_4} (P_{Zn}) - pressures of phosphorus (zinc), created by additional charges of P (Zn), and calculated from the ideal gas law.

Chemical point of view:

Dissociation reaction for the melted ZGP (Seb. Fiechter, 1996)



Mass action law for the dissociation reaction of the melted ZGP:

$$K_P(T) \sim P_{Zn} P_{P_4}^{(0.5-0.25x)}$$

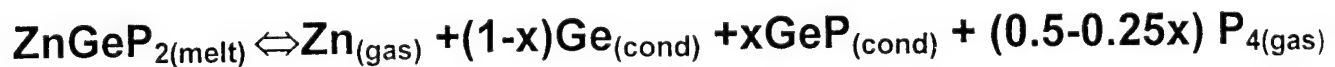
TABLE 2. The vapour phase composition during growth and the phase composition of precipitates.

NUMBER OF CRYSTAL	P_{P_4} ATM	P_{Zn} ATM	EXTERNAL VIEW OF THE GROWN CRYSTAL	PHASE COMPOSITION OF PRECIPITATES	SIZES OF PRECIPITATES
1	6.9	1.1	Gas pockets	Zn	Ø 1-1.5 mkm
				Zn_3P_2 ZnP_2	10 nm×1 mkm
				P	25×300 nm
2	7.2	-	No pockets Single phase top	GeP cubic	Ø 0.2-0.3 mkm
					Ø 80-90 nm
3	-	-	Ge eutectic on the top of the crystal	GeP cubic	Ø 5 nm
				GeP tetragonal	15×45 nm
				Ge	Ø 8 nm

* P_{P_4} (P_{Zn}) - pressures of phosphorus (zinc), created by additional charges of P (Zn), and calculated from the ideal gas law.

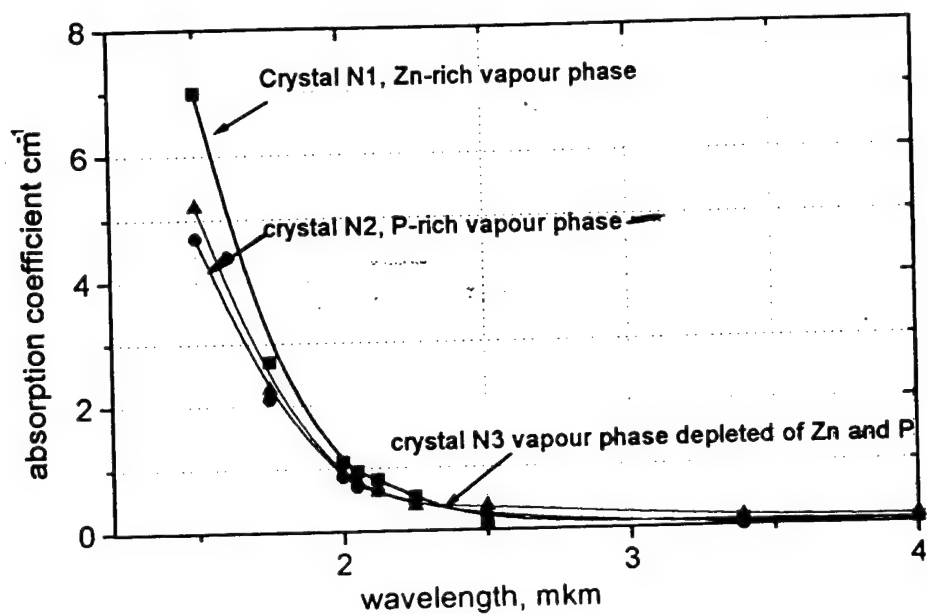
Chemical point of view:

Dissociation reaction for the melted ZGP (Seb. Fiechter, 1996)

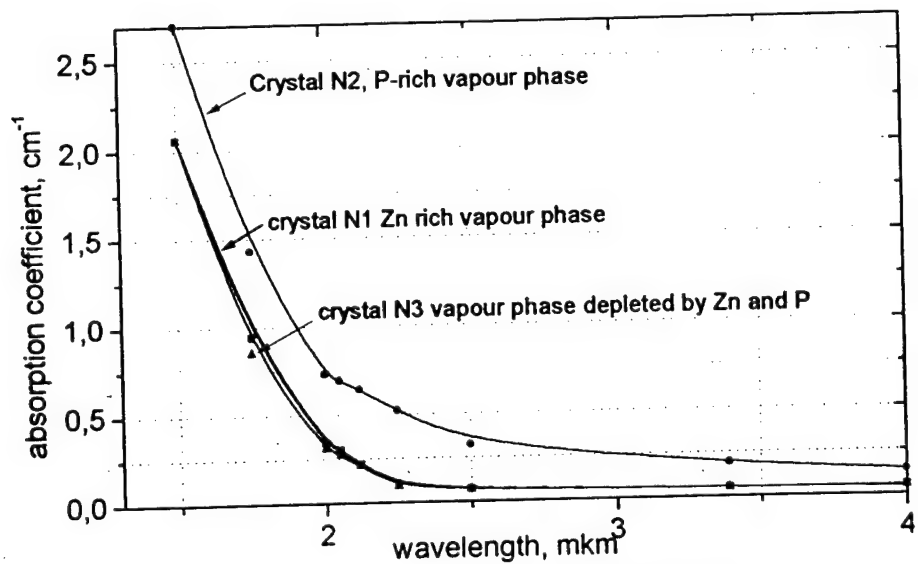


Mass action law for the dissociation reaction of the melted ZGP:

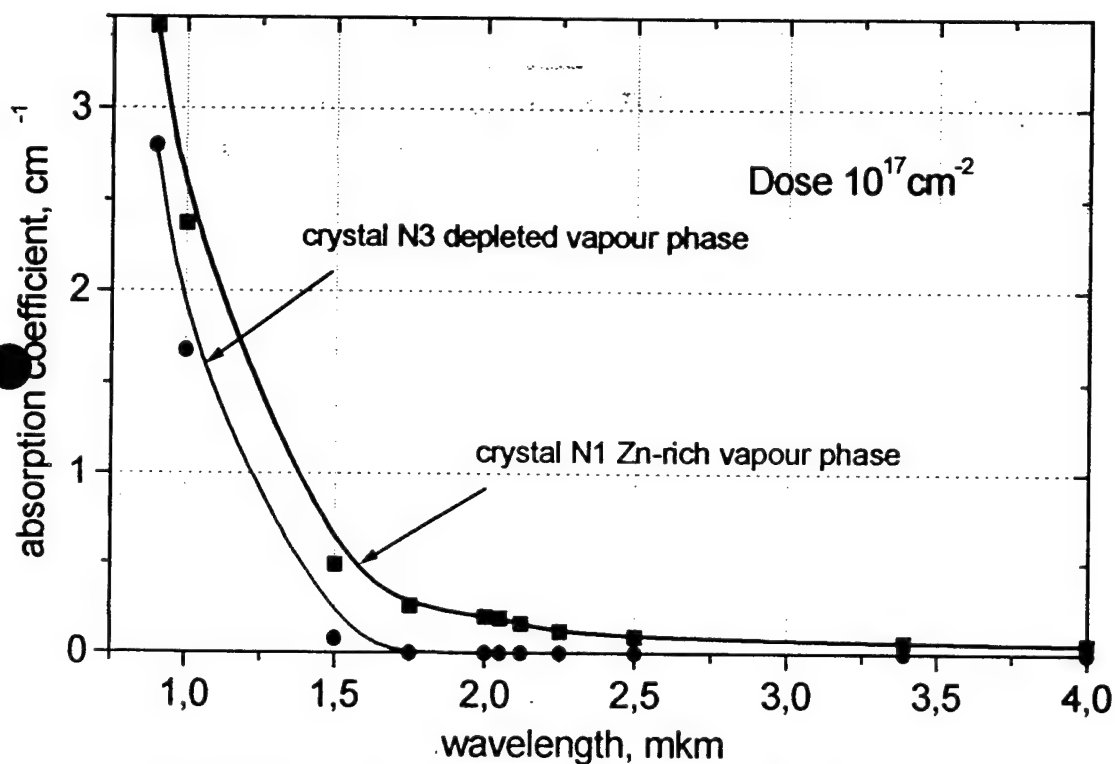
$$K_P(T) \sim P_{Zn} P_{P_4}^{(0.5-0.25x)}$$



Absorption coefficient spectra for as-grown crystals
Slices were cut from the middle part of the ingot



Optical absorption spectra after annealing
(vacuum, $T=600^{\circ}\text{C}$, duration 300 hours)
Slices were cut from the middle part of the ingots



Absorption coefficient spectra of ZnGeP_2 after irradiation
 slices were cut from the middle part of ingots, *thickness is 6 mm*

Conclusions

To study the influence of the vapour phase composition during growth on crystal properties three single crystals were grown from one starting material but under varied vapour phase composition.

1. DTA have shown the different composition of these crystals: their melting points are different. For the Zn and Ge rich crystals it is lowered as compared to the crystal grown with the P excess only.
2. All three crystals have the second phase particles. The second phase composition correlates with the vapour phase composition.
3. For the most part the second phase particles have a drop (splintery) form and nanometer sizes. In individual cases the second phase precipitations as the submicron – micron's areas (Zn or $\text{Zn} + \text{Zn}_x\text{P}_y$) are found.
4. As a rule, the nanodimensional particles are located along boundary of areas of the crystal fracture, being responsible for the brittle cracks in ZGP.
5. ZnGeP_2 fragments free from the second phase particles have high elastic stress fields whereas fragments containing the latter particles are free from stresses. This could possibly indicate that the crystal areas having a high level of elastic stress fields are the places of the second phase particle formation.
6. The different improvement of the crystals grown with Zn-rich vapour phase and vapour phase depleted of volatile components on irradiation is apparently related to the different volume fraction of the second phase particles or their sizes. The lowest absorption at $2\text{ }\mu\text{m}$ attained by irradiation is $< 0.01\text{ cm}^{-1}$.

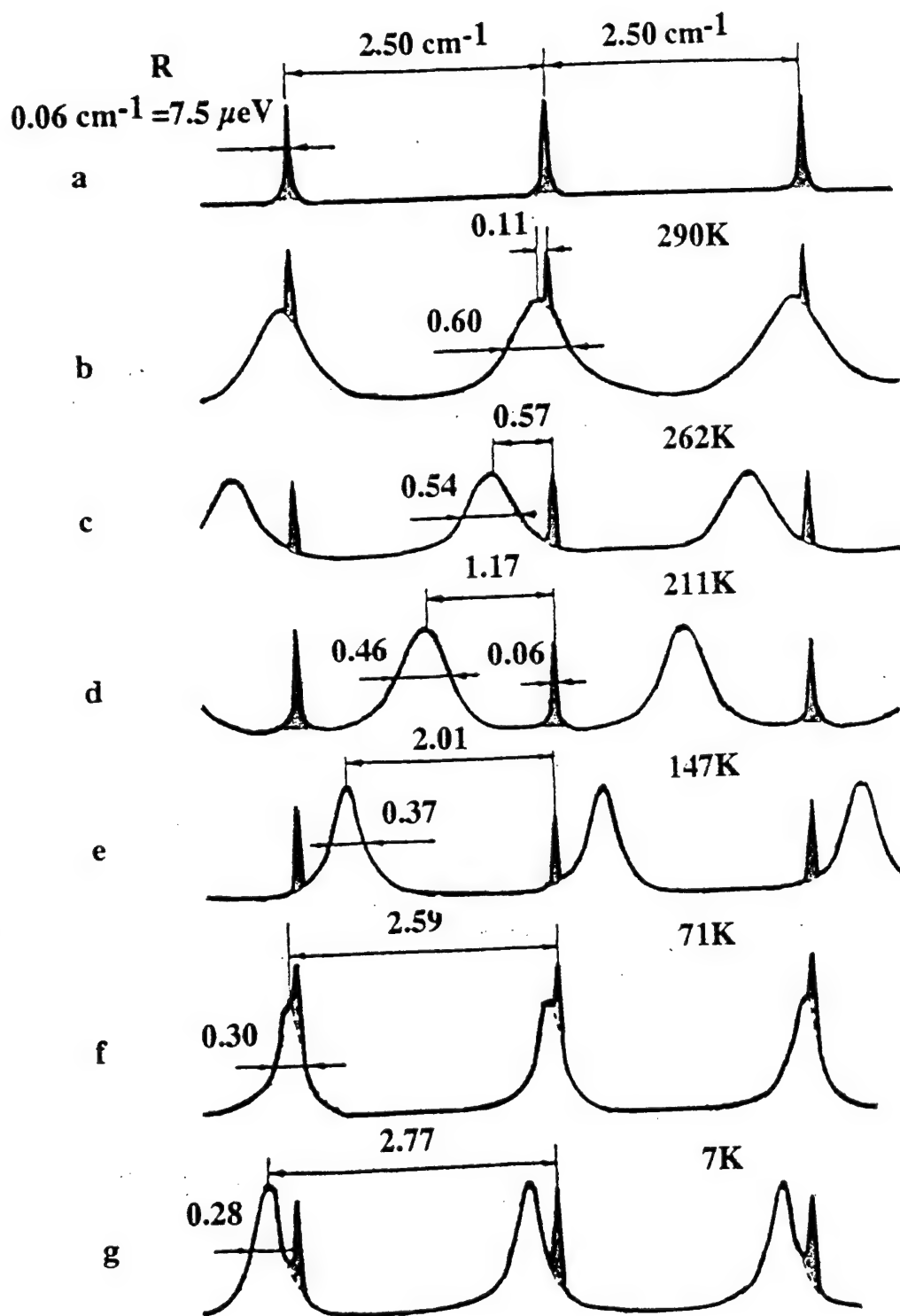
**Inelastic Light Scattering
by Free Electron Gas
and Coupled Electron-Phonon Excitations
in Advanced Semiconductor Structures**

Bahish H Bairamov

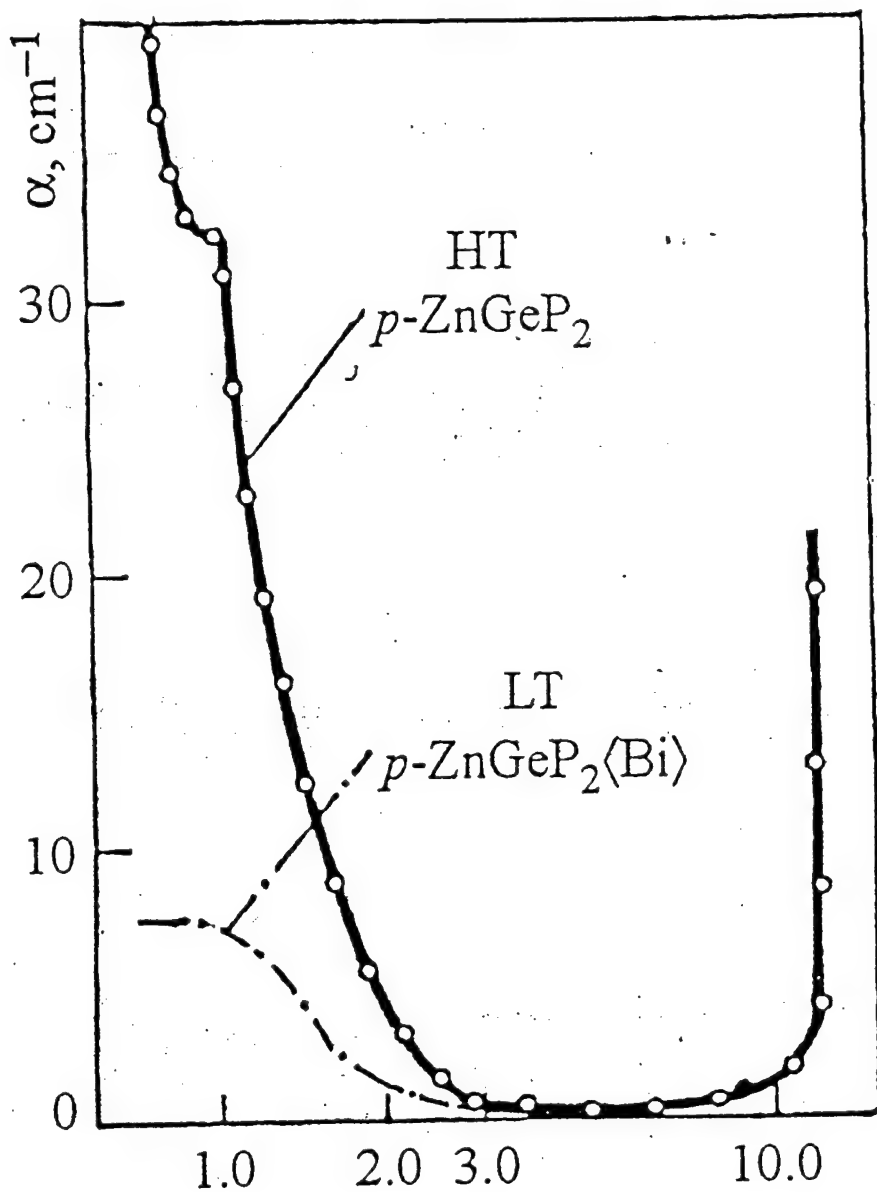
**A F Ioffe Physico-Technical Institute
Academy of Sciences of the Russia**

194021, St Petersburg, Russia

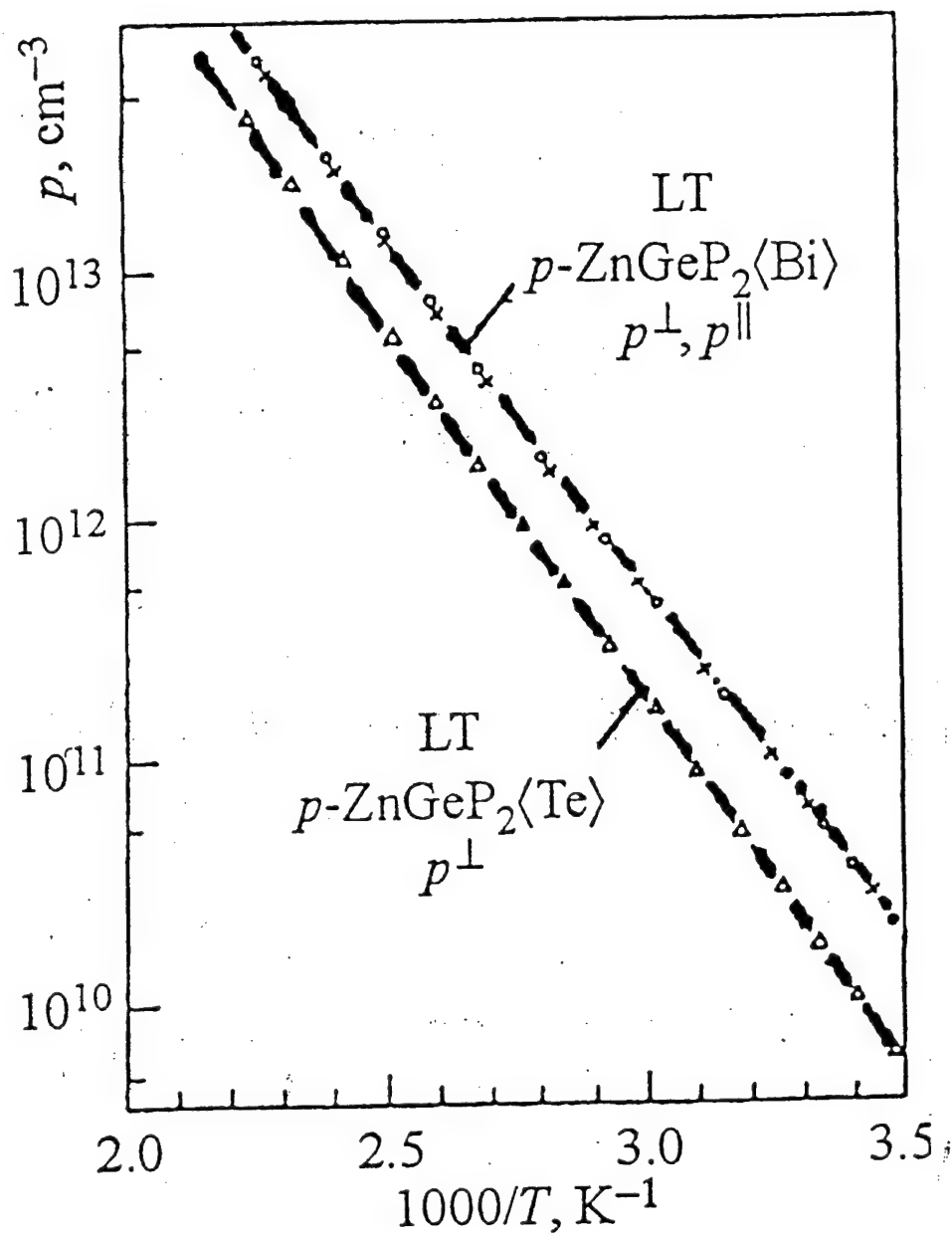
High resolution light scattering by LO phonons in semi-insulating GaP ($n < 10^{12} \text{ cm}^{-3}$) in the temperature range 7 - 290K



a) instrumental profile with a spectral resolution of 0.06 cm^{-1}
b-g) interference spectra of the light scattering by LO-phonons
various temperatures



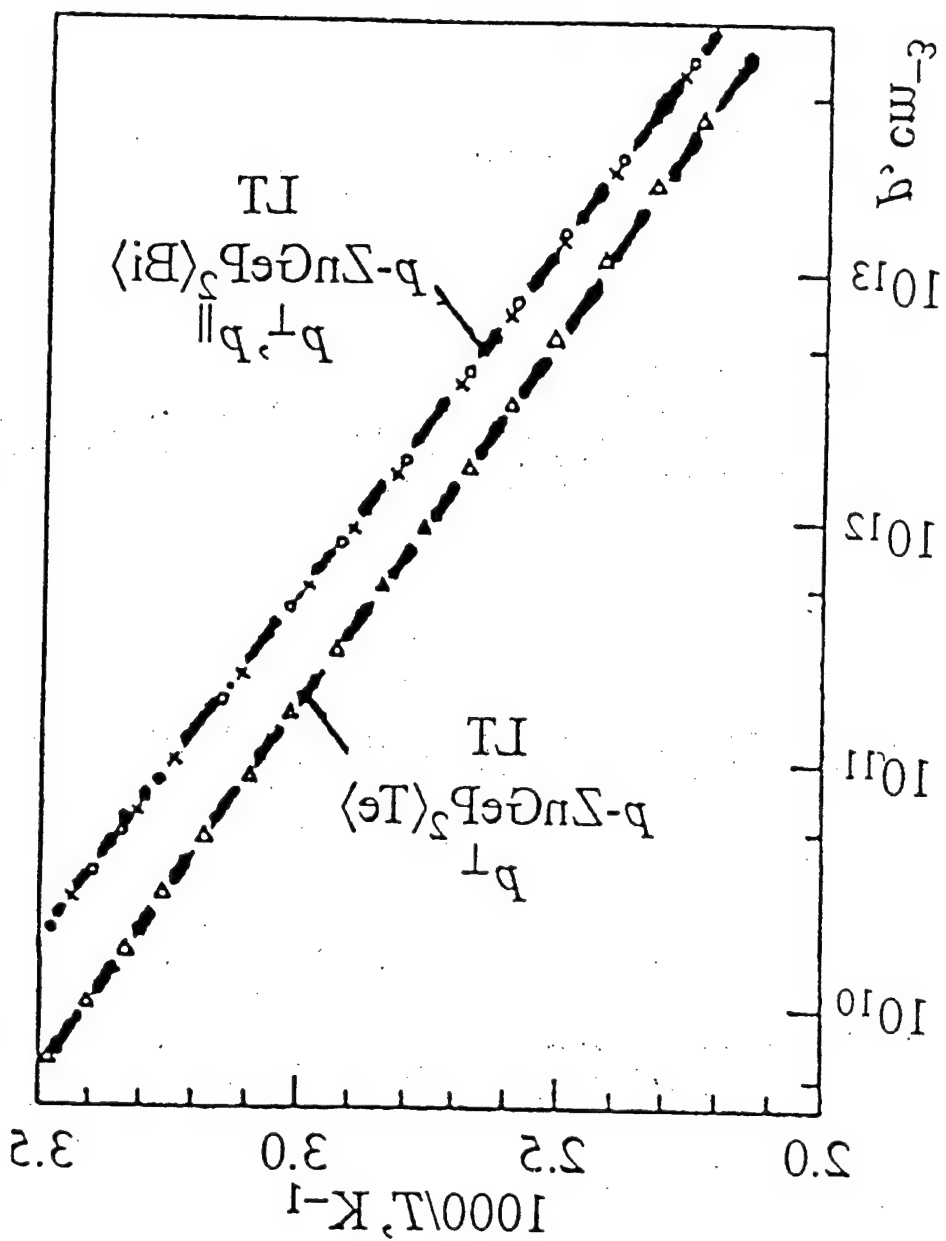
Optical absorption spectra
of the LT grown $\text{ZnGeP}_2\langle\text{Bi}\rangle$
and HT grown $p\text{-ZnGeP}_2$ single crystal
obtained by standard technique.

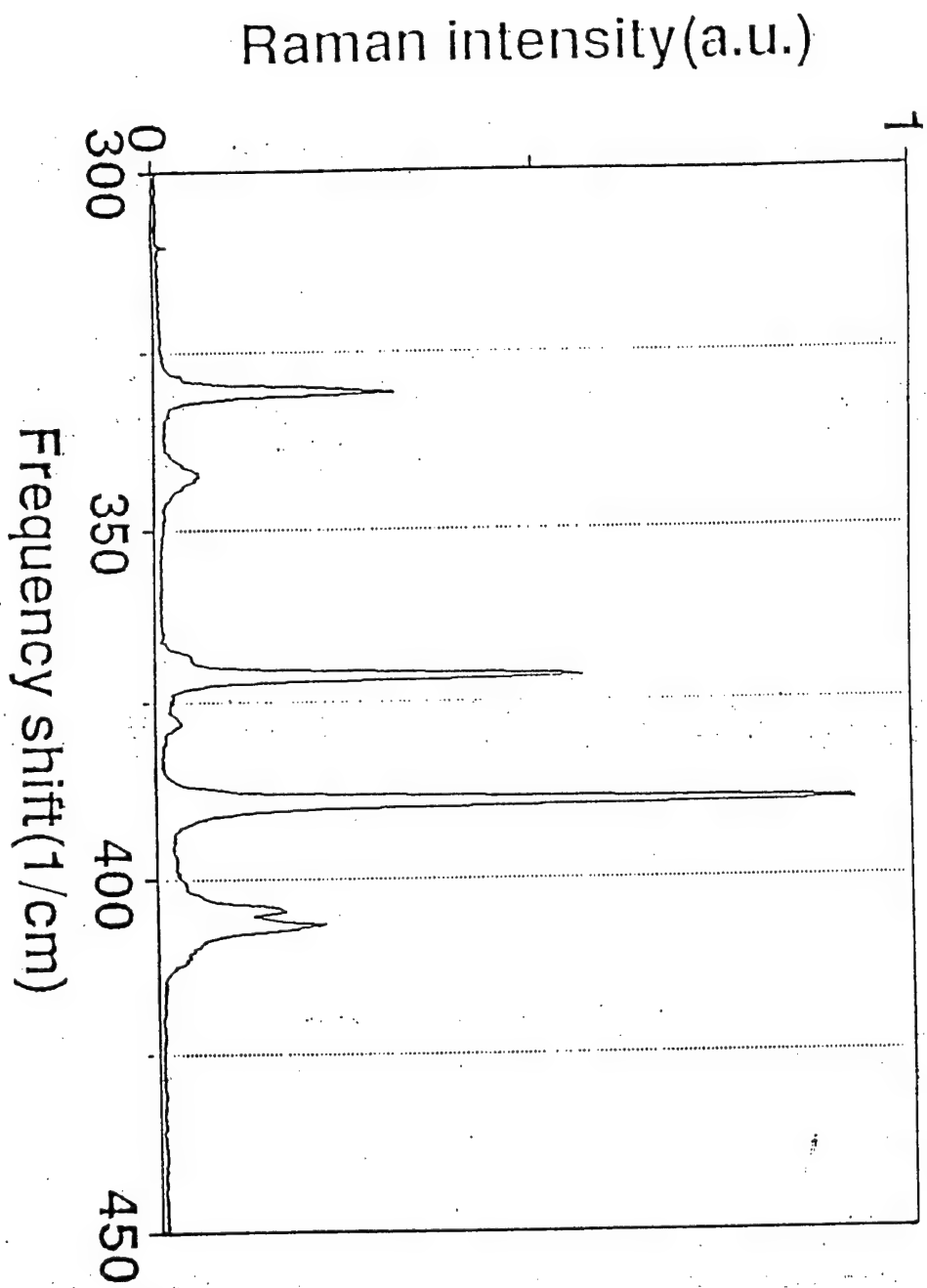


Temperature dependence
 of the hole concentrations
 of the two LT grown $p\text{-ZnGeP}_2\langle\text{Bi}\rangle$ and $\langle\text{Te}\rangle$
 samples.

Symbols: \times and Δ for p^\parallel , \circ for p^\perp .

Symbols: \times and Δ for p_{\parallel} , \circ for p_{\perp} .
of the two LT grown $p\text{-ZnGeP}_2$ $\langle\text{Bi}\rangle$ and $\langle\text{Te}\rangle$
of the hole concentrations
Temperature dependence





Raman spectra of p-ZnGeP₂ single crystals grown by low temperature method. T = 8 K. Excitation with the 514.5 nm line of an Ar⁺ laser, 100 mW, with slits width 0.9 1/cm.

Table IV. Symmetry assignments and frequencies of the optical phonons (in cm^{-1}) in ZnO γ_2 obtained from the Raman scattering (RS) and infrared reflection (IR)

Symmetry of the mode	ZB	Frequencies			
		RS ^a	RS ^b	RS ^c	IR ^d
CP		T = 300 K	T = 300 K	T = 300 K	T = 8 K
Γ_5	$[X_5]$	94 (TO+LO)	96 (TO+LO)	94 (TO+LO)	93.2
Γ_3	$[W_2]$	112	119	121	118.2
Γ_5	$[W_4]$	142 (TO+LO)	142 (TO+LO)	143 (TO) 144 (LO)	141.3 143.4
				166*	
Γ_5	$[W_3]$	202 (TO) 204 (LO)	201 (TO) 202 (TO+LO) 203 (LO)	204 (TO) 205 (TO+LO) 206 (LO)	198 206.5
Γ_3	$[W_2]$		248	249	
Γ_1	$[W_1]$	327	328 328 Γ_5 (TO+LO)	329 328 Γ_5 (TO) 330 Γ_5 (LO)	327.4 334
Γ_4	$[W_2]$	339 (TO)	338 (TO) 357 (LO) 346 (TO+LO)	341 (TO) 350 (LO+TO) 361 (LO)	340 354.5
			357 (LO)	364.5 (LO)	341.6 360
Γ_5	$[W_4]$	368 (TO) 374 (LO)	369 (TO) 374 (TO+LO) 377 (LO)	369 (TO) 377 (LO)	368.5 375 377?
Γ_3	$[X_3]$		390		
Γ_5	$[\Gamma_{15}]$	385 (TO) 402 (LO)	387 (TO) 393 $\Gamma_5 + \Gamma_4$ (TO)	387 (TO) 405 (LO) 395 $[q\Gamma_4(\text{TO})]^{***}$	389 404.3
Γ_4	$[\Gamma_{13}]$	399 (TO) 408 (LO)	401 (TO)	401 (TO) 411 (LO)	400.3? 407 412?
			403 Γ_5 (LO) 406 $\Gamma_5 + \Gamma_4$ (TO) 408 Γ_4 (LO)	396 $[q\Gamma_4(\text{TO})]$ 408 $[q\Gamma_5(\text{LO}), q\Gamma_4(\text{LO})]$	405.2

* References 53.

^b References 52 and 56.

^c References 50.

^d References 49 and 5).

^e our results.

EPR AND ENDOR CHARACTERIZATION OF
DONORS AND ACCEPTORS IN ZnGeP_2

Larry E. Halliburton
Kevin T. Stevens
Nancy C. Giles

Physics Department
West Virginia University

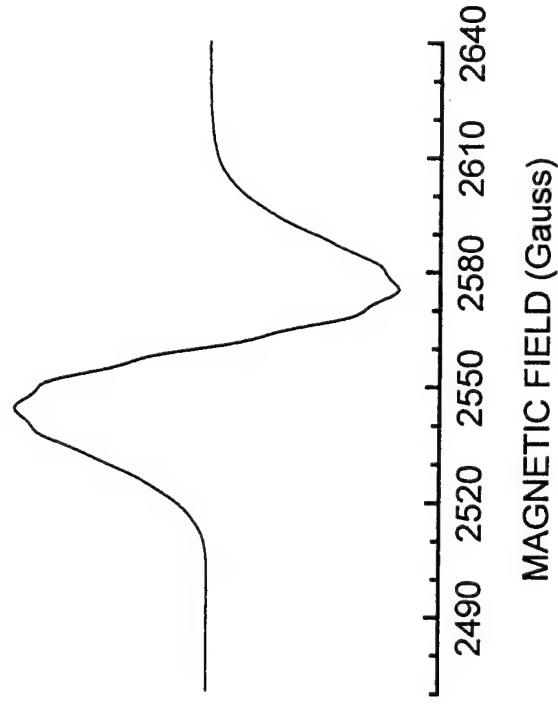
Nonlinear Optical Materials Workshop
DERA
Malvern, UK
September 20 – 21, 1999

Work supported by Air Force Office of Scientific
Research (in conjunction with the Materials
Directorate at Wright-Patterson AFB) and by the
National Science Foundation.

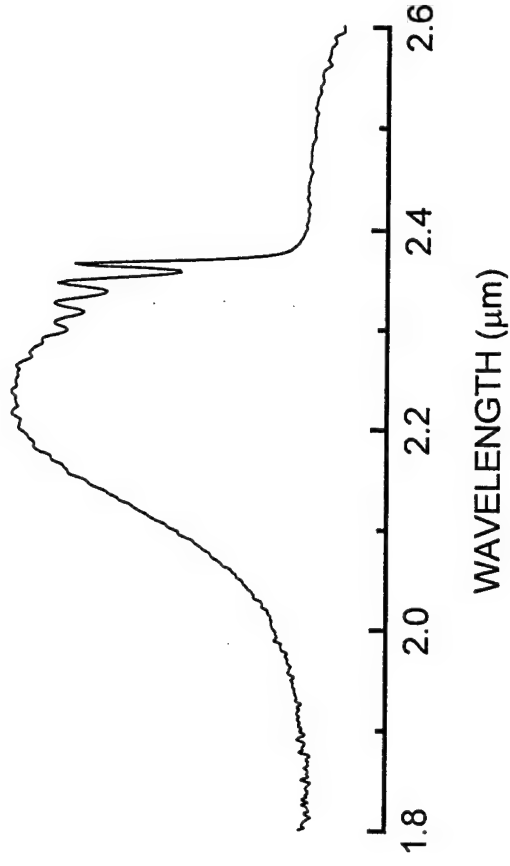
Work performed in cooperation with Lockheed Sanders.

Ni^{2+} in AgGaSe_2

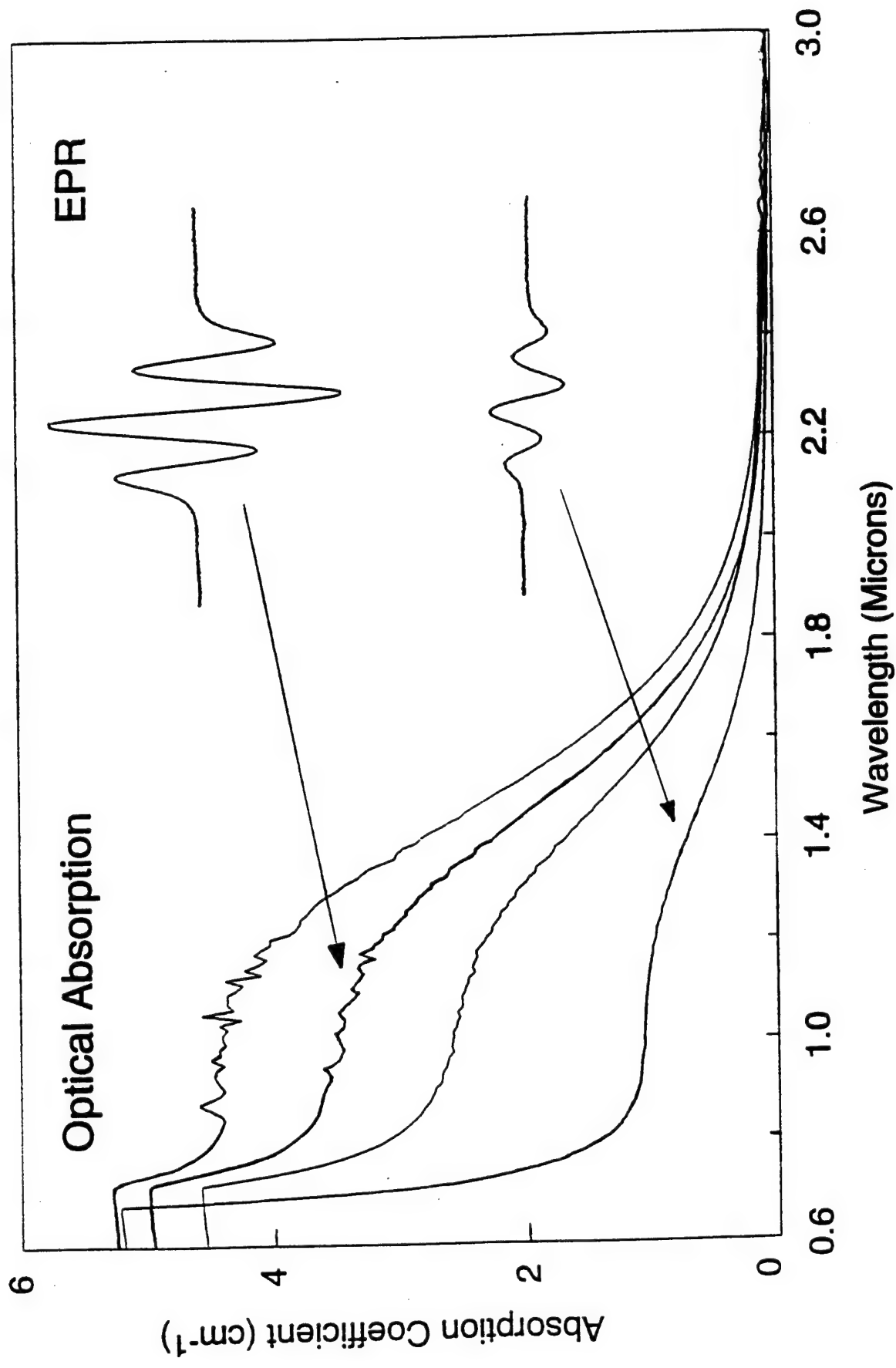
Electron Paramagnetic Resonance



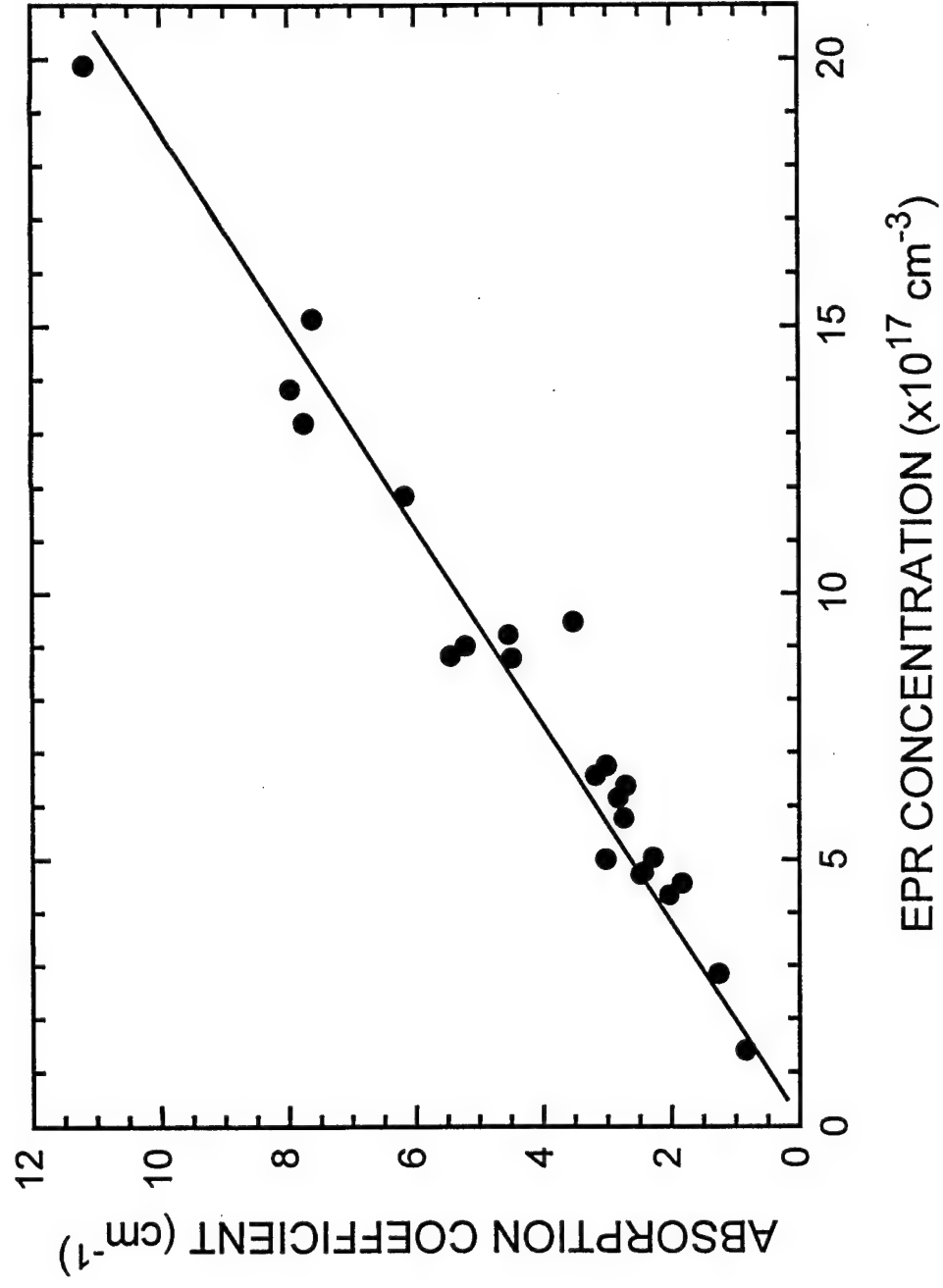
Infrared Absorption



Correlation of Optical Absorption with EPR Signals from the Zinc Vacancy



V_{Zn} EPR Intensity versus Absorption at $1\ \mu m$



SUMMARY OF DONOR AND ACCEPTOR PROPERTIES

1. Zinc vacancies are the dominant acceptor in ZnGeP_2 .

- Both V_{Zn}^- and $V_{\text{Zn}}^{=}$ charge states are present.
- There is no spectroscopic evidence to date for V_{Zn}^0 in as-grown crystals.

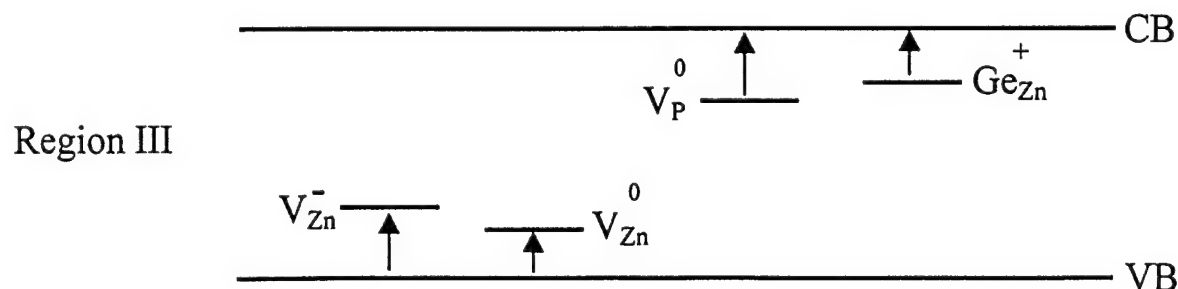
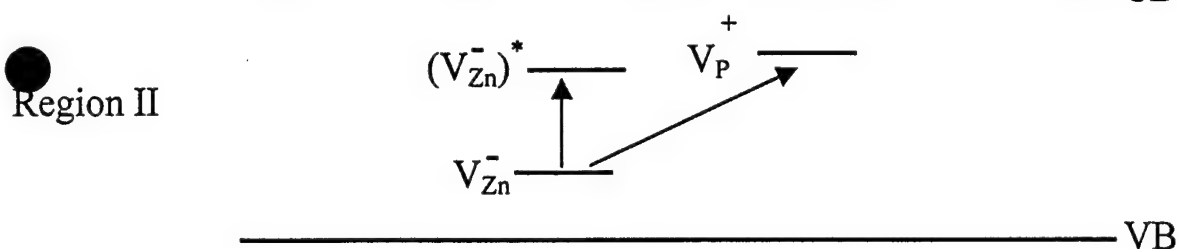
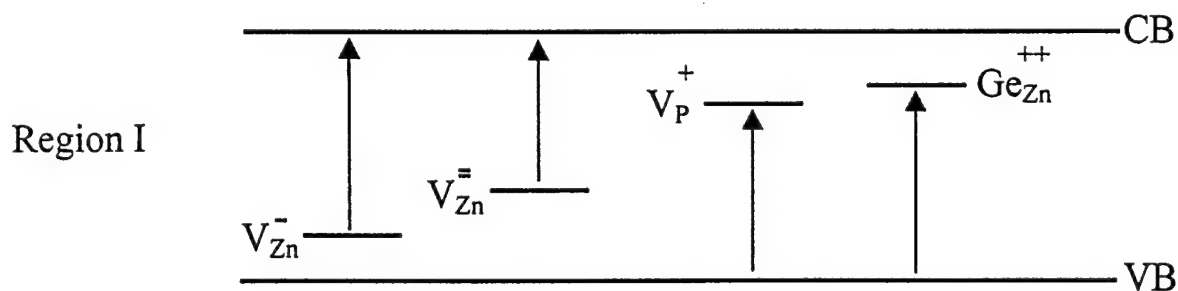
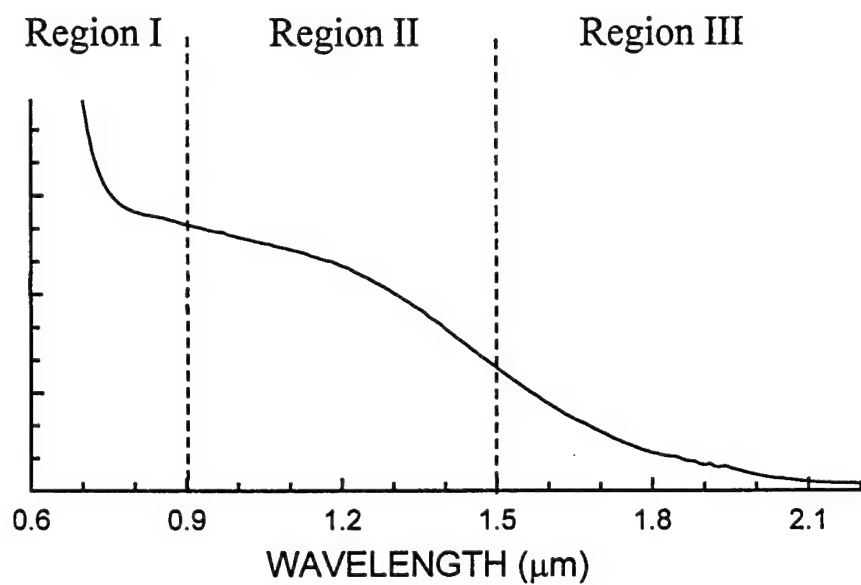
2. Dominant donors are phosphorus vacancies and germanium antisites.

- V_{P}^+ and $\text{Ge}_{\text{Zn}}^{++}$ in the dark.
- V_{P}^0 and Ge_{Zn}^+ with light.

3. Effect of laser light:

- 633 nm -- increases V_{Zn}^- signal
creates V_{P}^0 and Ge_{Zn}^+ signals
- 1064 nm -- decreases V_{Zn}^- signal
creates V_{P}^0
does not create Ge_{Zn}^+

Possible Optical Absorption Mechanisms



Recent Advances in Chalcopyrites for Mid- to Far-IR Frequency Conversion

P. G. Schunemann and T. M. Pollak

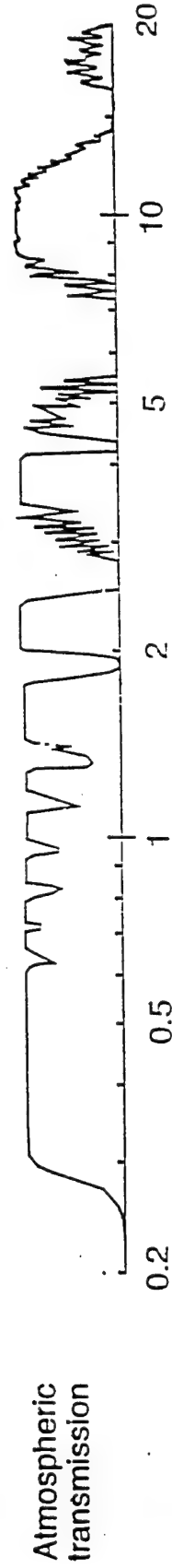
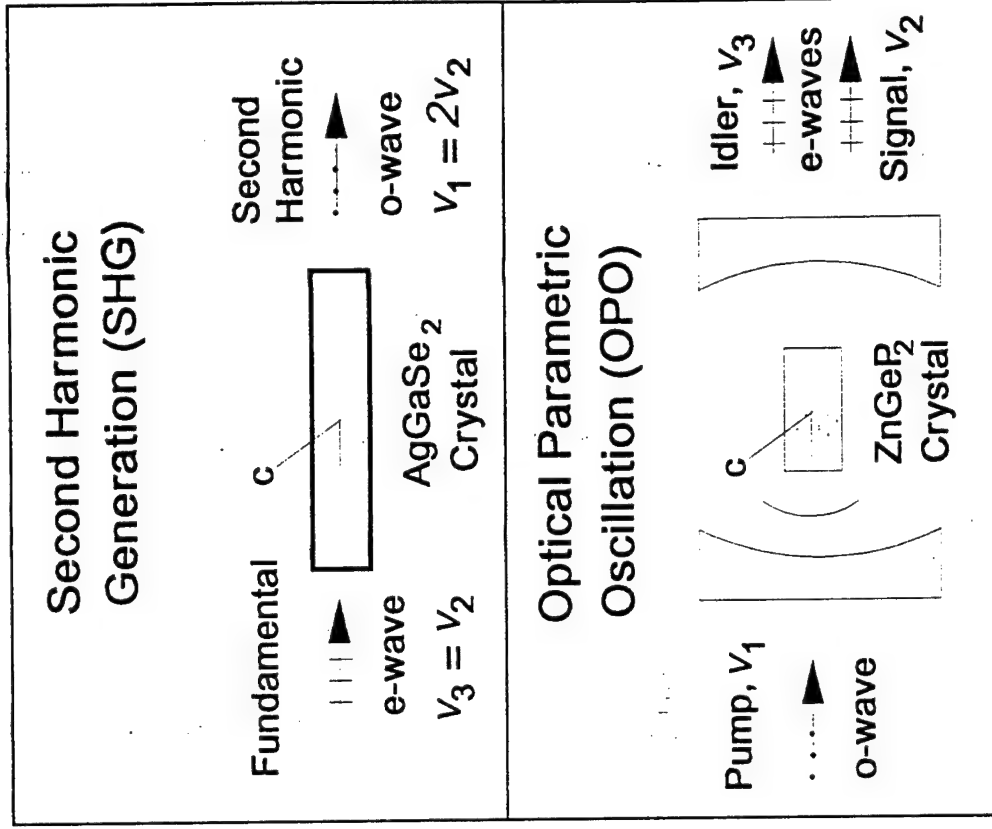


Presented at the 1999 Nonlinear Optical Materials
Workshop, (NLO 99), DERA, Malvern, UK, Sept. 20, 1999

Work supported L.N. Durvasula at DARPA (via the Air Force Research Laboratory Materials Directorate
contract No. F33615 -94-C-5415) and Sanders Internal R&D Funding

Chalcopyrite Crystal Growth at Sanders

- For the past 10 years we have focused on crystal growth and processing of bulk chalcopyrites for nonlinear optical (NLO) frequency conversion:
 - Frequency doubling of CO₂ Lasers (SHG)
 - "Wavelength doubling" of 2um solid state lasers (OPO)
- The Goal:
 - Produce efficient mid-IR lasers operating in regions of high atmospheric transmission
- Applications:
 - Laser radar, remote sensing, etc.



Strategies for Improved Infrared NLO Materials

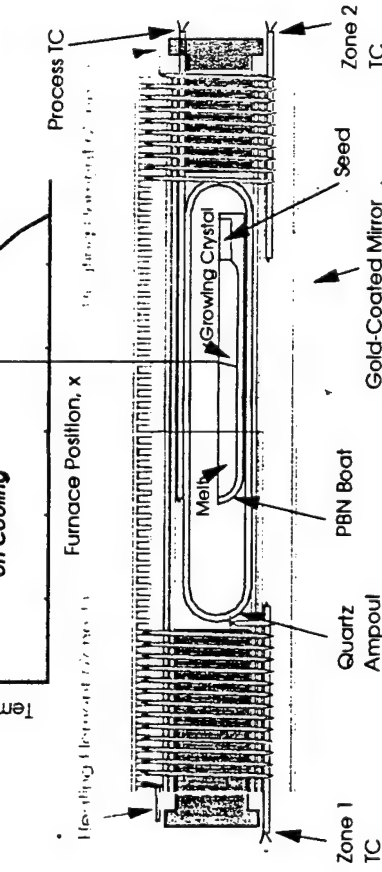
2um-pumped OPO's

- Material of Choice: ZnGeP₂.
 - Highest NLO Coefficient with sufficient band gap ($d_{14}=75$ pm/V)
 - High Thermal Conductivity (0.35W/cmK)
 - Reduced Losses -----> Efficient, High Power Output
- Alternatives for better performance:
 - **None:** Continue to Reduce ZnGeP₂ Near-IR Absorption

CO₂ Doubling

- Material of Choice: AgGaSe₂.
 - Respectable NLO Coefficient (39 pm/V)
 - Wide transparency and phase-matching range (.78-18um)
 - Low absorption Losses
- Alternatives for better performance:
 - CdGeAs₂: Highest Nonlinearity ($d_{14}=236$ pm/V) ► Reduce Absorption Loss
 - Ag(Ga,In)Se₂: Adjust Birefringence for Noncritical Phase-Matching (NCPM)
 - ABX₂: Continue Search for New Materials

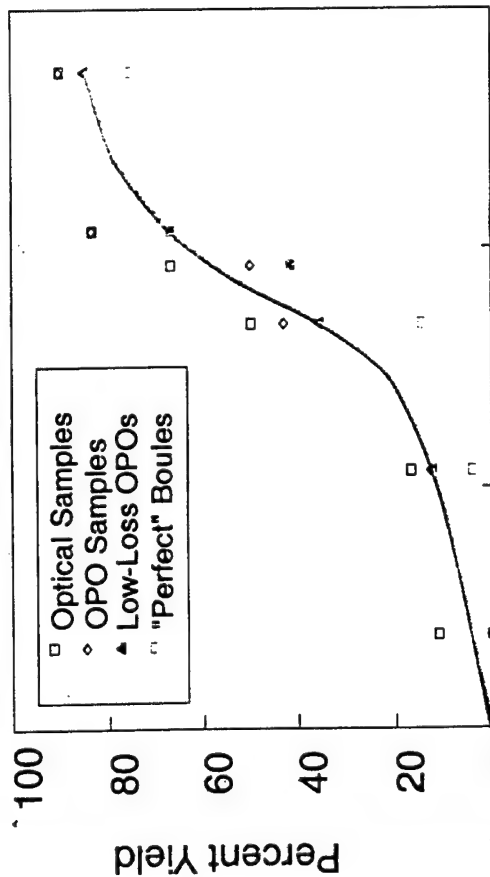
Horizontal gradient freeze growth led to advances in NLO chalcopyrites



HGF Approach: Key Aspects

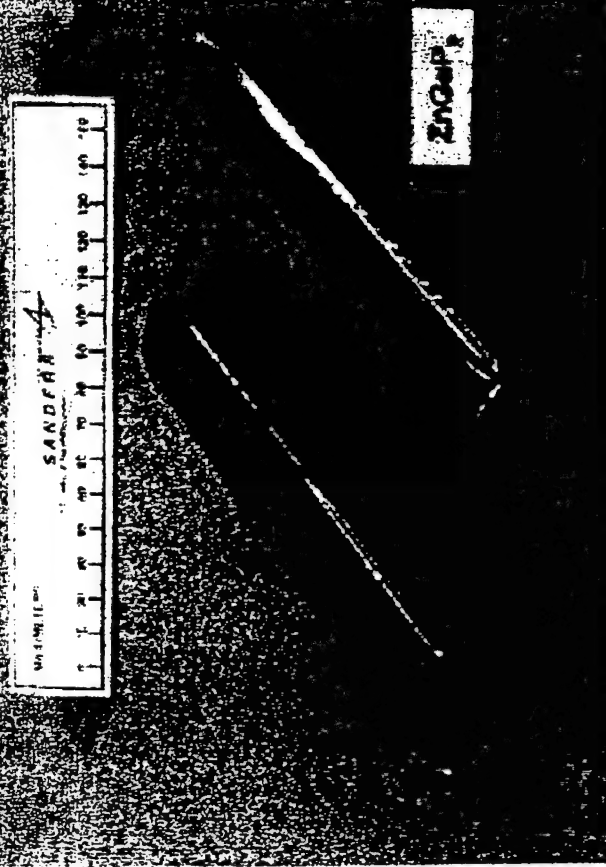
- **Low thermal gradients**
 - Minimize vapor transport
 - Eliminate cracking due to anisotropic thermal expansion
- **Transparent Furnace**
 - Simplifies the seeding process
 - Allows *in situ* monitoring of the S/L interface shape & position
 - Facilitates interactive growth (secondary grains can be re-melted)
- **Seeded growth**
 - Eliminates initial polycrystallinity due to supercooling
 - Optimizes orientation to accommodate negative c-axis thermal expansion
 - Enables growth along phase matching direction for max. device length & yield

Improved Single Crystal Yield

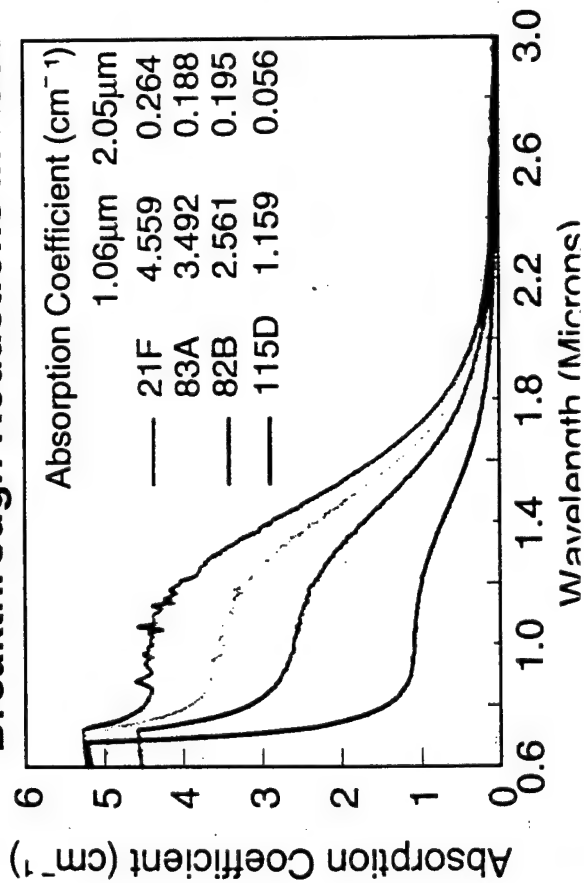


Dec-88 Sep-91 Jun-94 Mar-97
Program Time Line

300mm ZnGeP₂ Crystal Growth



Breakthrough Reductions in Loss

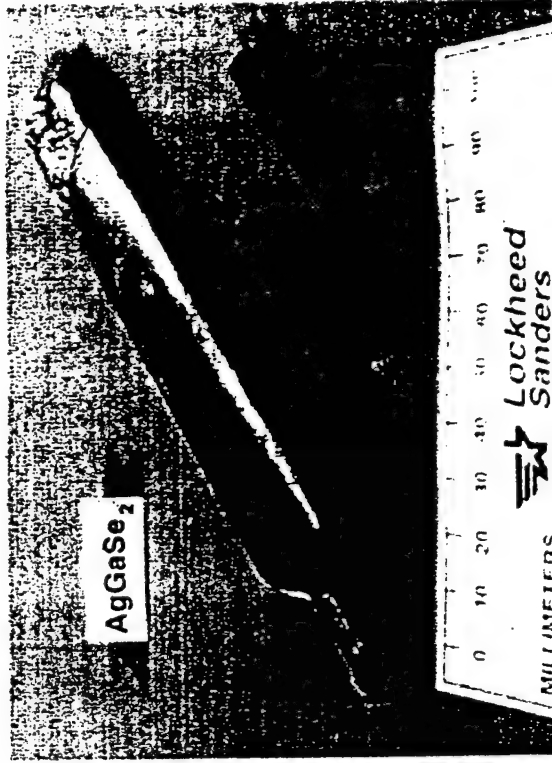
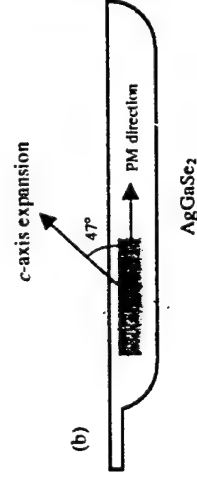
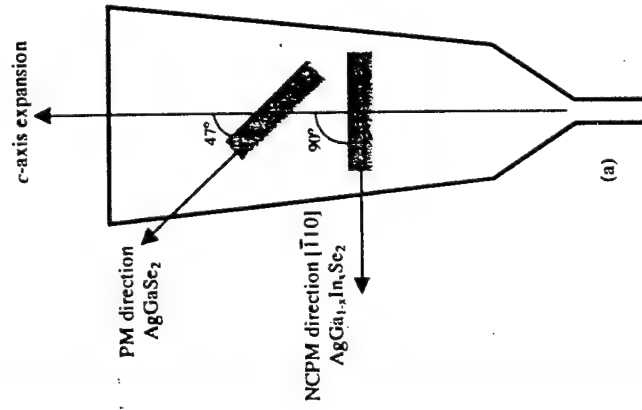


Absorption Coefficient (cm⁻¹)

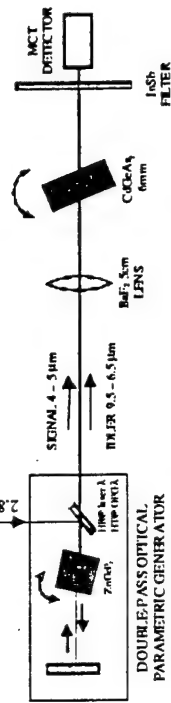
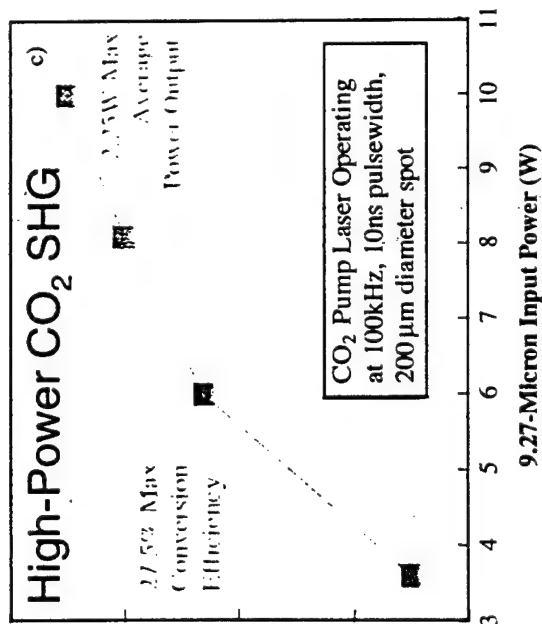
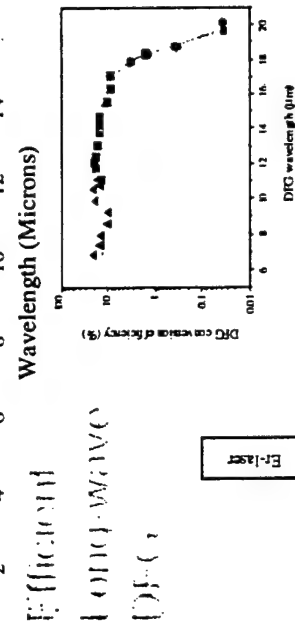
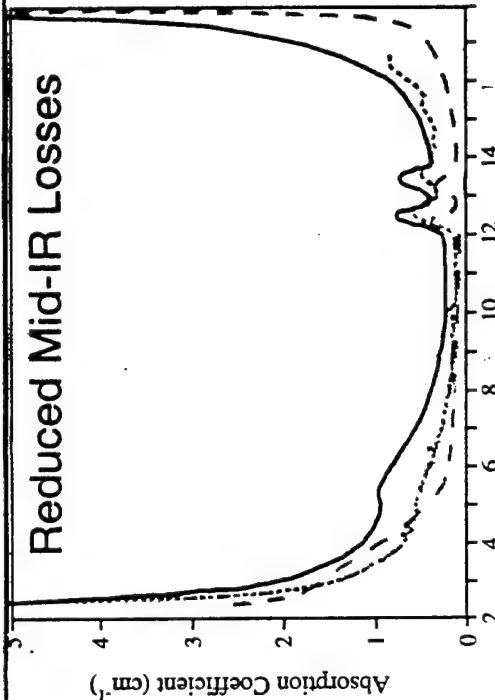
	1.06μm	2.05μm
— 21F	4.559	

“Phase-Matched” Crystal Growth of AgGaSe_2

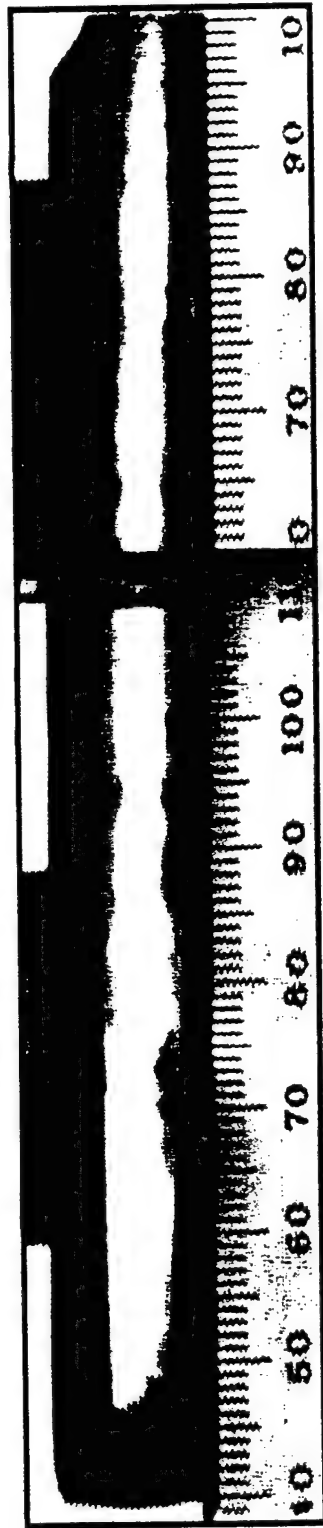
- Vertical Bridgman growth of AgGaSe_2 requires seeding along c-axis for unconstrained thermal expansion during cool-down
- The Horizontal Gradient Freeze (HGF) technique allows “phase-matched” growth along device orientation, yielding longer interaction lengths and minimal waste



CdGeAs₂: Development Milestones



Segregation of Absorbing Defects in CdGeAs₂



Growth Direction [001]



[112] facets

Dark Regions

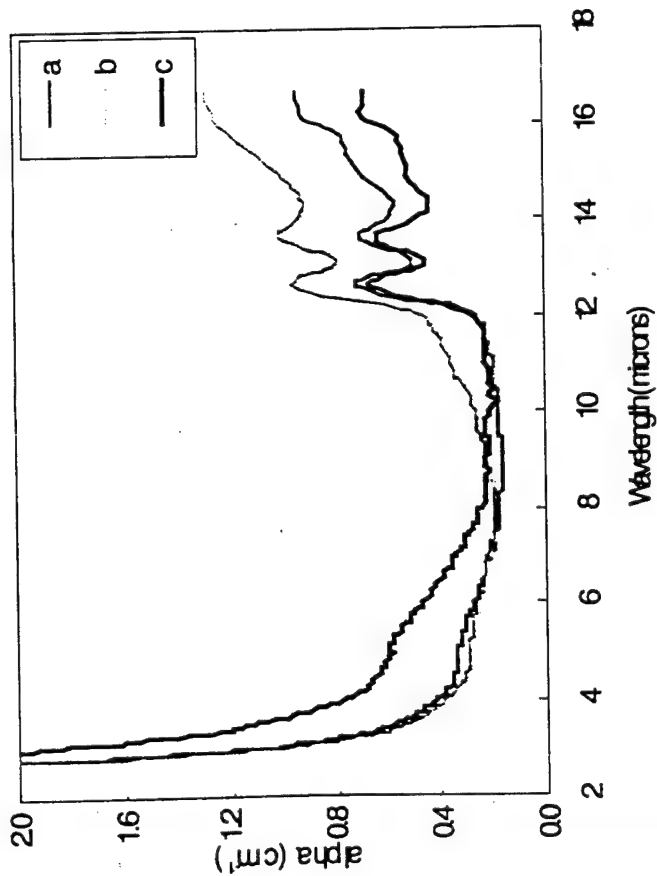
Growth Direction [001]

Light Region

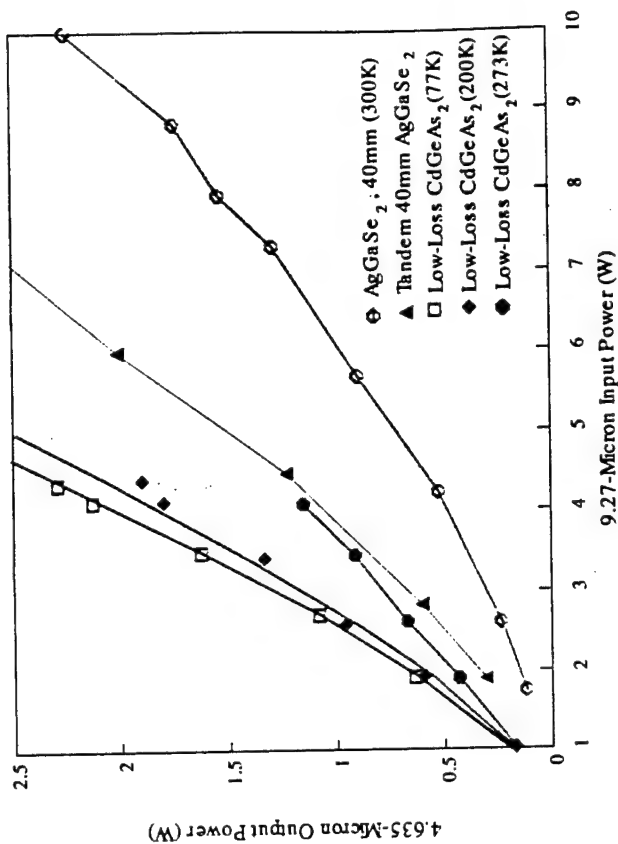
(c)

CdGeAs₂: Recent Advances

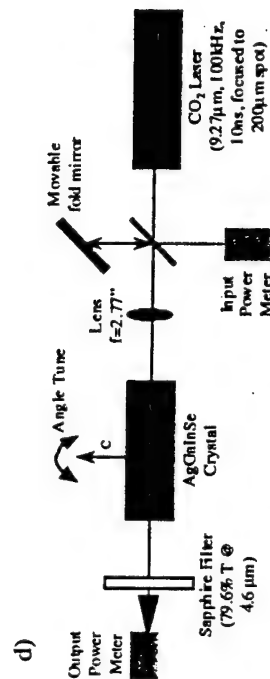
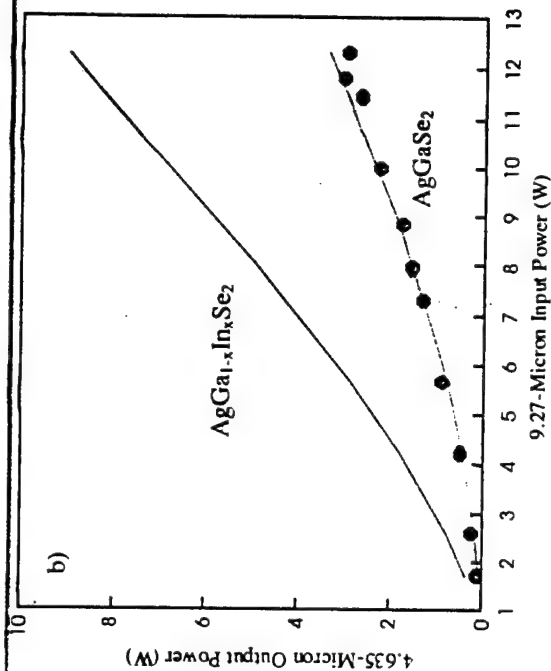
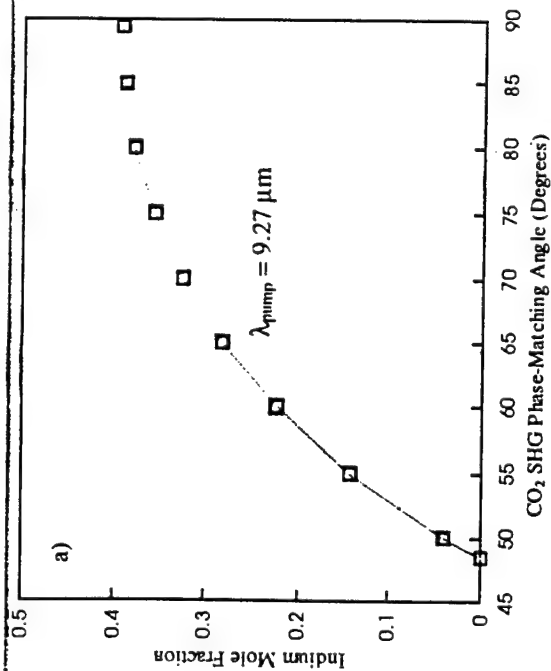
Reduced Mid-IR Absorption
(Low-Loss Central Core)



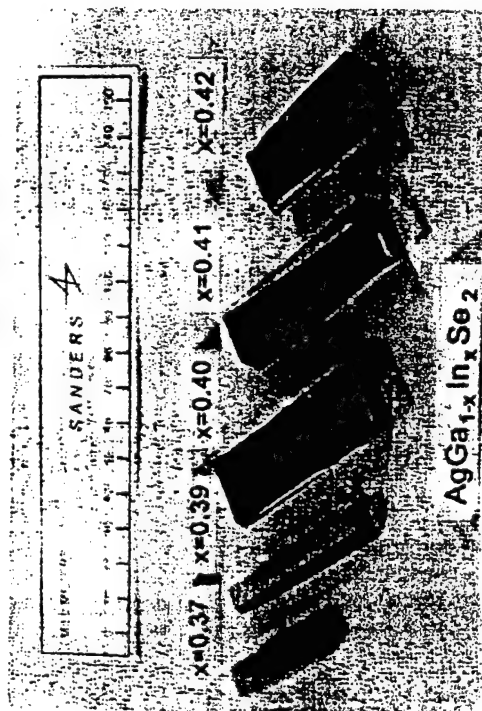
Efficient CO₂-Doubling:
 $\eta = 53\%$ at 77K
 $\eta = 28\%$ at 273K



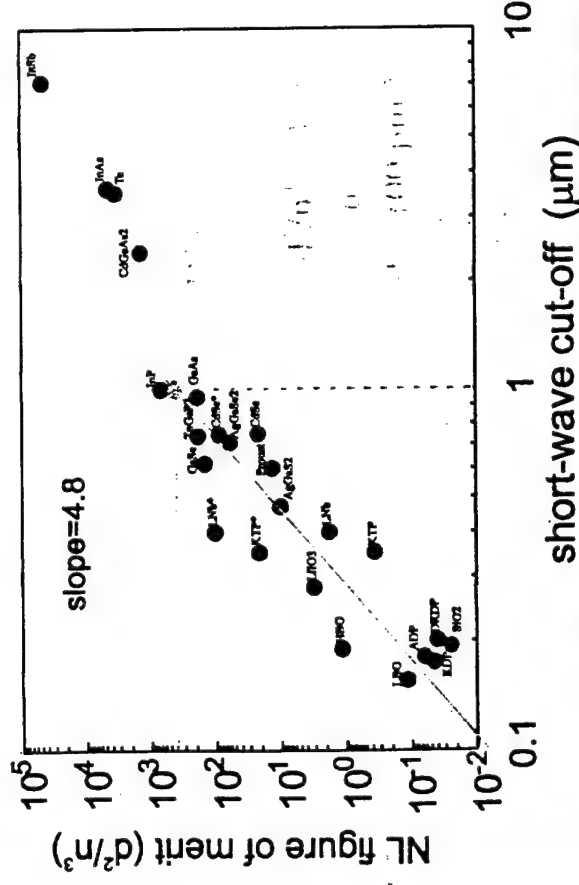
AgGa_{1-x}In_xSe₂: Engineered Birefringence for NCPM



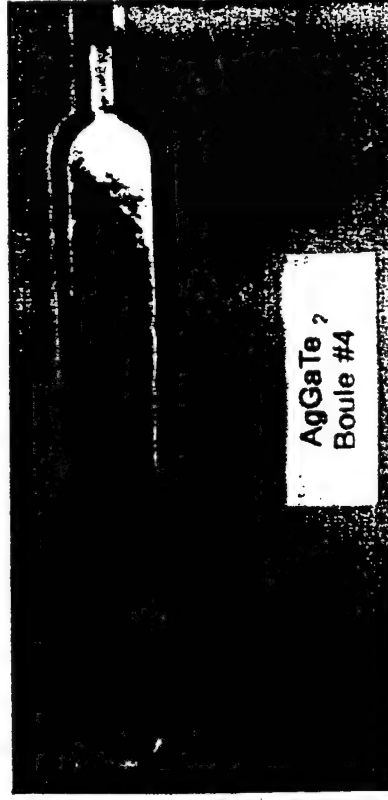
NCPM at $x=0.42$ (melt)
Reflection & Scattering Losses $\rightarrow \eta = 1.8\%$



AgGaTe₂: a promising new nonlinear optical crystal



- Motivation:
 - Telluride analog of AgGaS₂ & AgGaSe₂
 - Substitution by Te should triple the NL coefficient and shift the transparency range further into the IR ($\sim 1\text{-}20\mu\text{m}$)
- Objectives of Research:
 - Produce large, crack-free single crystals
 - Determine if birefringence is sufficient for phasematching
- Approach:
 - HGF Growth in Transparent Furnace
 - Fabricate prism, measure Δn



Summary

- Recent crystal growth advances have established chalcopyrites as the NLO materials of choice for mid- to far-IR laser frequency conversion:
 - Large crack-free single crystals (up to 16x28x140mm³) of ZnGeP₂, AgGaSe₂, and CdGeAs₂ can be reproducibly grown by the HGF technique
 - Substantial reductions in absorption and/or scattering losses have been achieved by feed purification, compositional control, & post-growth annealing
 - Improved crystal quality has resulted in outstanding NLO device performance
- The birefringence of mixed crystals (AgGa_{1-x}In_xSe₂) can be engineered to achieve non-critical phase-matching (NCPM)
- The search for new materials has led to promising NLO crystals such as AgGaTe₂, CdGa₂S₄, and CdGa₂Se₄
- Dy³⁺:CaGa₂S₄ was demonstrated as the first sulfide mid-IR laser host

**Development of Technology of ZnGeP₂ Single Crystal at
Institute for Optical Monitoring SD RAS**

By Alexander I. Gribenyukov, Galina A. Verozubova, and Valentina V. Korotkova

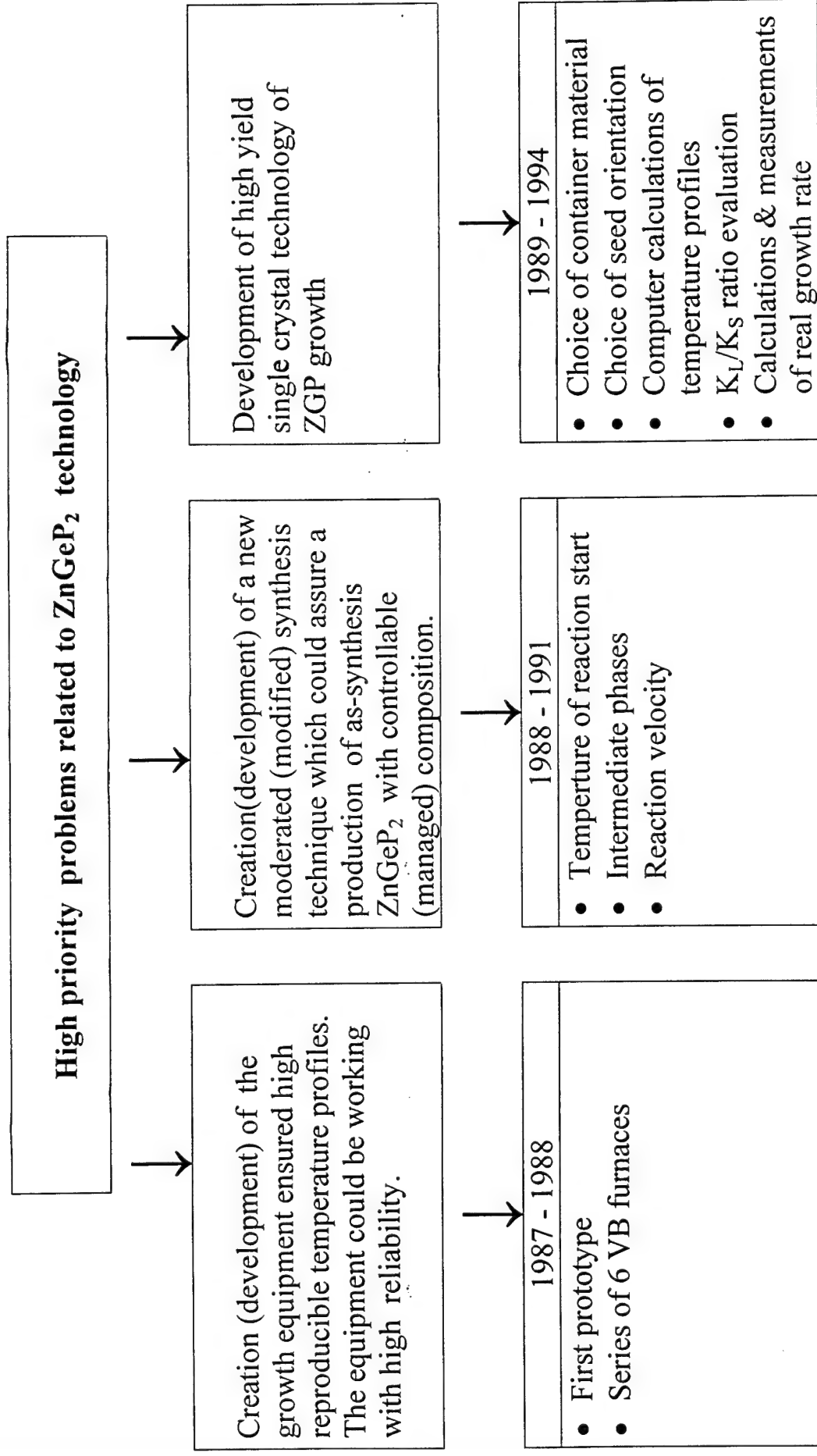
Laboratory of Optical Spectroscopy

Institute for Optical Monitoring

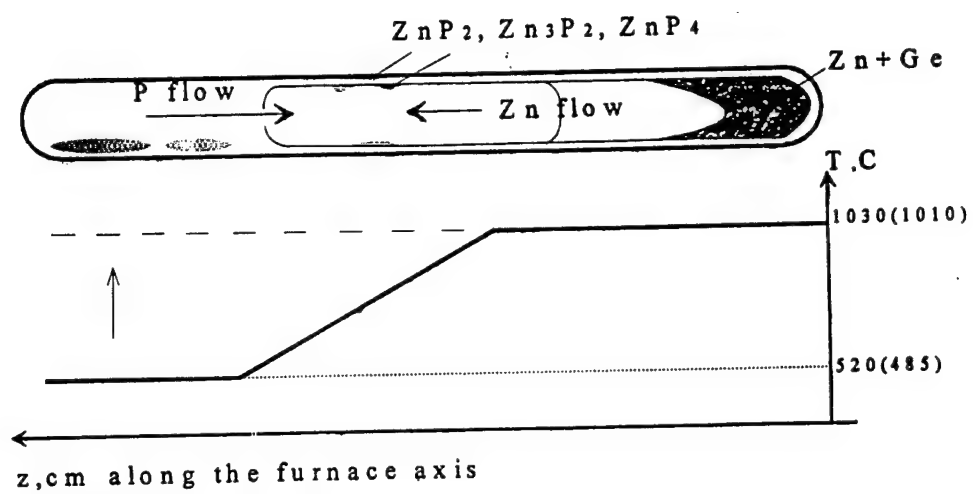
Tomsk Branch of Siberian Division

Russian Academy of Sciences

IOM	The main directions of IOM activity & interests	<ul style="list-style-type: none"> • Theoretical and experimental investigations of climatic and ecological changes under effect of natural and human factors •
	The basic theme of the noted direction of IOM's activity	<ul style="list-style-type: none"> • Development of new techniques and technologies for environment remote sounding •
	Divisions of the basic theme	<ul style="list-style-type: none"> • Development of optical monitoring systems based on new generation of tunable coherent radiation sources working in the middle IR spectral range. •
	The main task	Provision of IOM works on development and multiplication of the new optical systems by optical materials needed
LOS IOM	The basic theme	Development of high yield and reliable technologies for production optical materials with controllable physical properties
	The main points of contents of basic theme	<ol style="list-style-type: none"> 1. Development of high yield technology of single crystal growth 2. Investigations of possibilities of controllable manage by physical properties of material due to purposeful changes (variations) of technological parameters on all stages of crystals production – at synthesis, at crystal growth, at postgrowth annealing

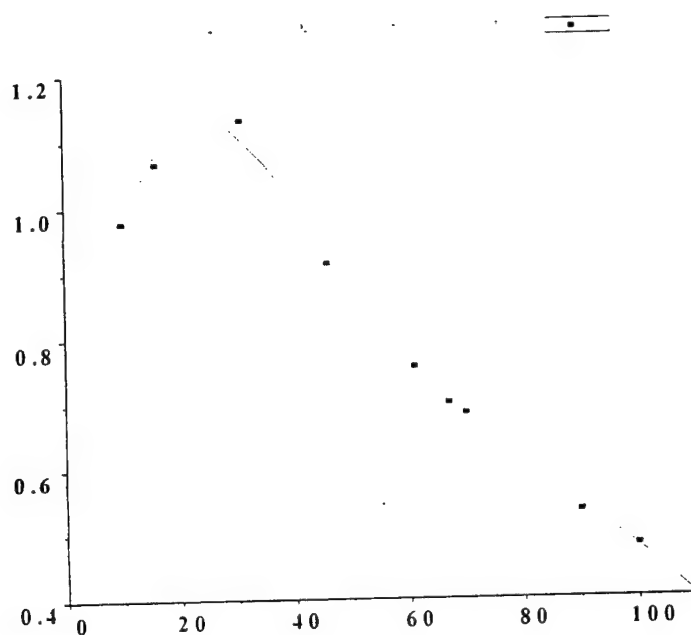


TR9. P_4 and Zn flows in non-isothermal closed synthesis system.

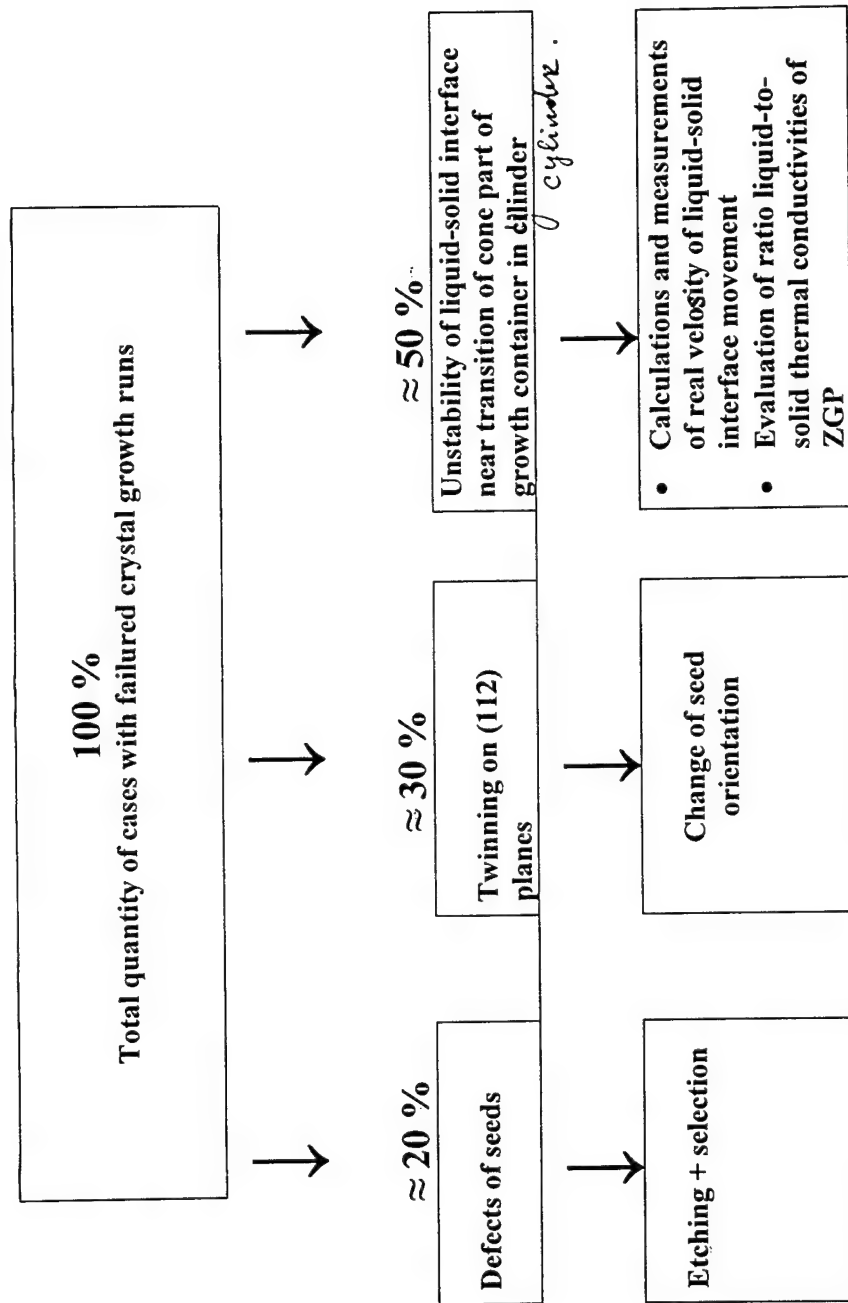


TR10 – Time dependence of expenditure velocity of P4 vapour
under pressure of 10-12 atm with Zn-Ge melt at 1010 C .

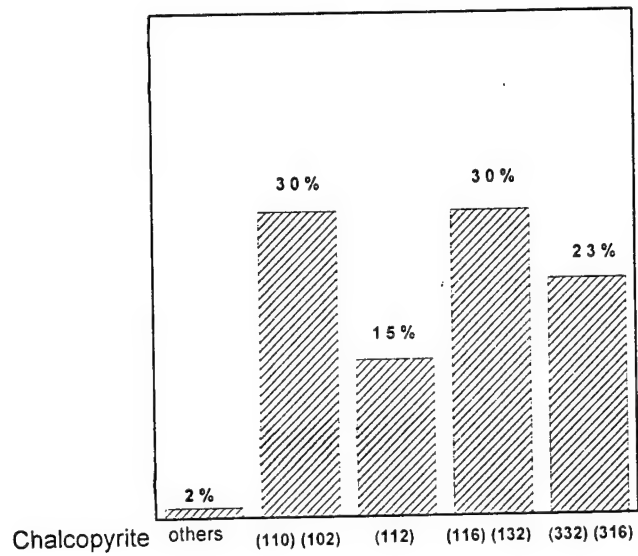
Hot zone temperature - 1010 °C
Cold zone temperature - 515 °C ($P_{P4} = 10$ atm)



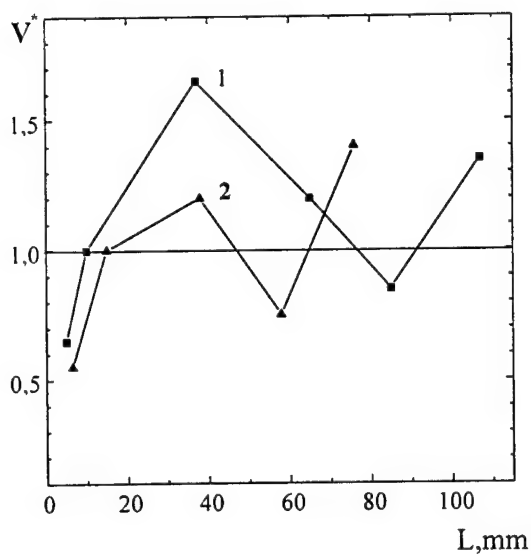
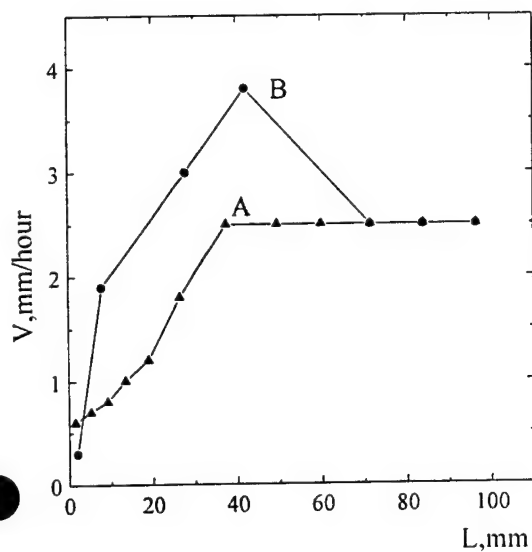
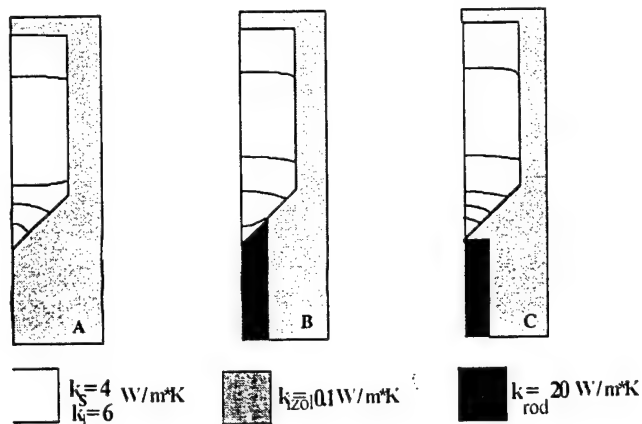
Distribution of growth failures on causes



TR12 – Probability distribution of ZGP crystalline blocks enlarged along growth axis in VB-method with spontaneous nucleation.



TR14 – The image of growth container surrounding structure for computer calculations.



GF method:

The isotherm crystallization rate for container with A and B surrounding structure.
Cooling rate – 1 °/hour.

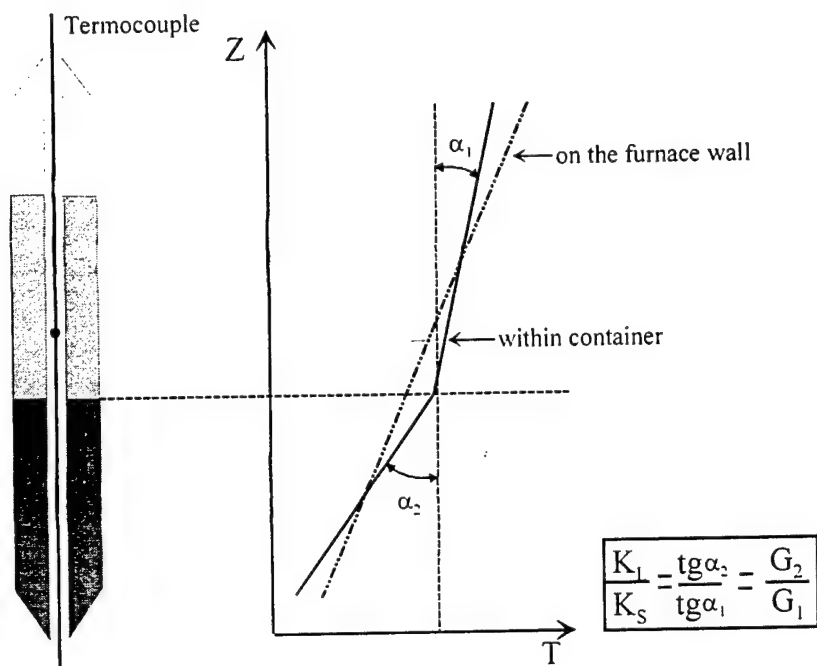
VB method:

Distribution of isotherm crystallization rate (in units of mechanical movement rate) along crystal axis.

A-type of surrounding structure, $\varnothing_{\text{furnace}} = 6 \text{ cm}$;
1 – calculation's data, $\varnothing_{\text{ampoule}} = 3 \text{ cm}$;
2 - experiment's data, $\varnothing_{\text{ampoule}} = 2 \text{ cm}$;

steady

R15. Diagram of stady state temperature distribution

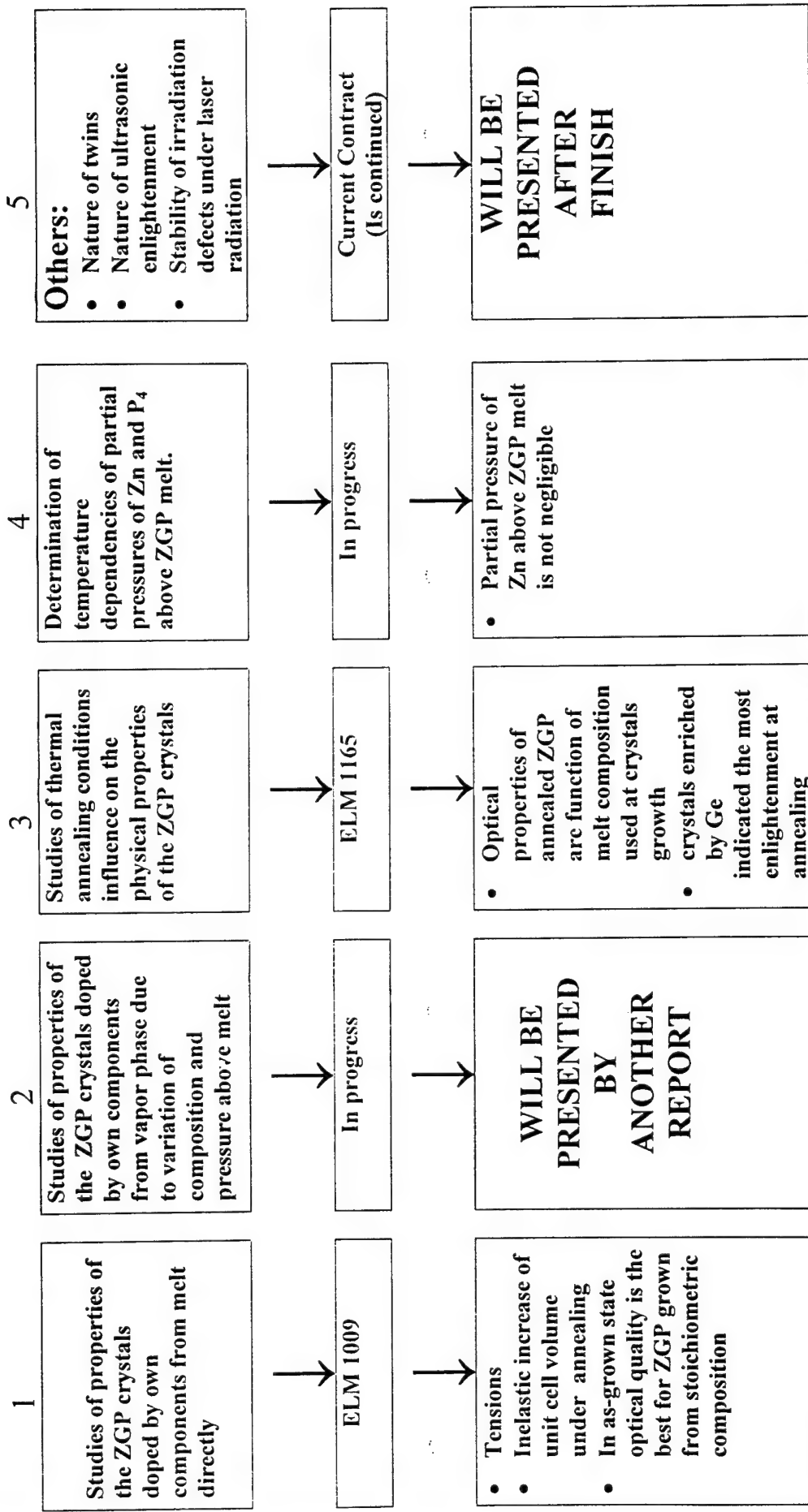


Material	Linear regression coefficients				Calculated values	
	Ts	Gs	TL	GL	T _{mel}	K _L /K _S
Ge	942.42	4.6	940.51	2.7	937 ± 1	1.7 ± 0.1
● GeP ₂	2009.9	16.24	1807.53	12.9	1027 ± 1	1.3 ± 0.1

Literature data for Ge : K_L/K_S = 2.93 [3]

Corrected ratio for ZnGeP₂ : K_L/K_S = 2.3

The Second Long-term Program



TR17 Some Results of investigations of ZGP crystals doped from melt. Measurements were made in DERA. The crystals were grown in IOM

Crystal	Dopant (P ₄ -pres. atm)	Temperat gradient DT/dx, °C/cm	Unit cell volume, Å ³	Unit cell volume difference (V _{irr} - V _{nr}) Å ³	Absorpt. coeff. at 2.06 μm cm ⁻¹	Absorpt. coeff. difference α _{irr} - α _{nr} cm ⁻¹	Derivative dα/dV, cm ⁻¹ Å ⁻³	Unit cell volume after annealing Å ³	Absorpt. coeff. after annealing cm ⁻¹
89/3 ltf	0.2 wt%Ge	5.2	319.94861	-0.03872	0.431	0.016	<u>-0.465</u>	320,234	0.27 -meas. <u>0.298-calc</u>
89/3 ltf	(7.5)	15.4	319.90989		0.449				
91/2 ftf	Stoich	1.5	319.92818		0.332		<u>+1.07</u>	320,332	0.36 -meas. <u>0.764-calc.</u>
91/2 ltf	(7.1)	7.5	320.04824	+0.12000 6	0.461	0.129			
93/3 ftf	0.2 wt%Zn	2.5	319.98361		0.615		<u>+2.4</u>	320,190	0.53-meas. <u>1.11-calc</u>
93/3 ltf	(3.8)	>20	319.93989	-0.04372	0.510	-0.105			

Seeds orientation is (116) for all grown crystals.

Annealing result in an increase of unit cell volumes, but expected change of absorption coefficient with the unit cell volume indicated only for sample enriched by Ge.

**ZGP GROWTH FROM MELT:
THE VAPOUR PHASE COMPOSITION AND CRYSTAL
PROPERTIES**

**G.A. Verozubova
A.I. Gribenyukov
Yu. F. Ivanov***

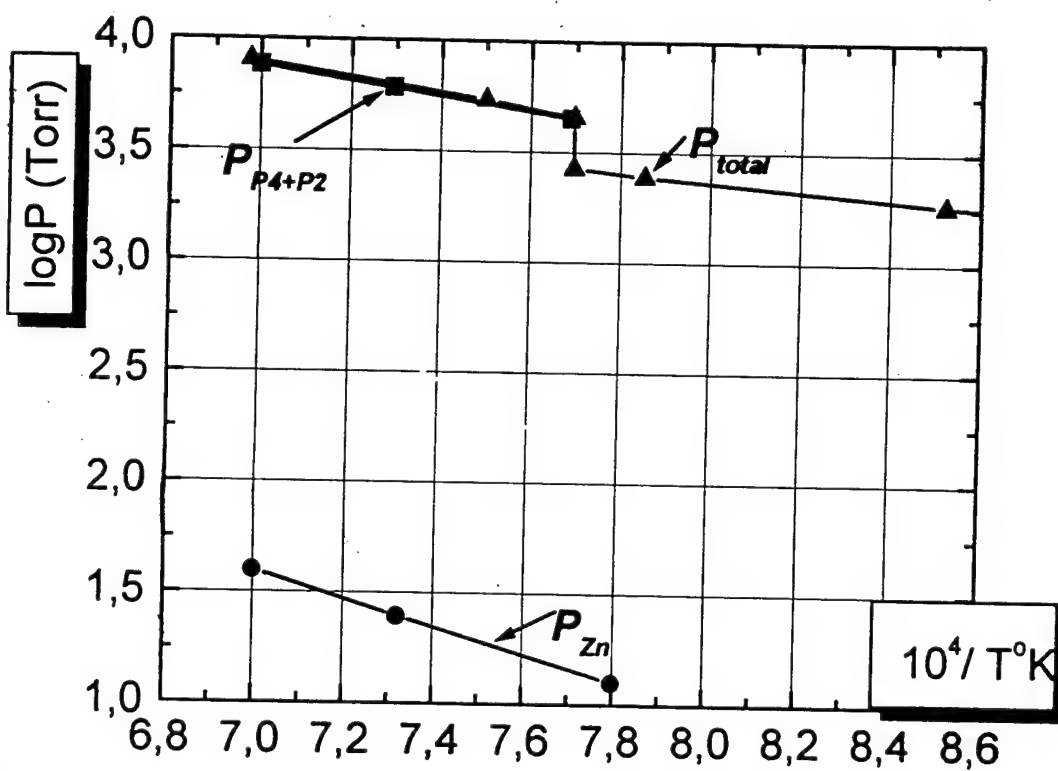
**Institute for Optical Monitoring SD RAS
*Tomsk Polytechnical University**

in collaboration with A.Vere, DERA, Malvern

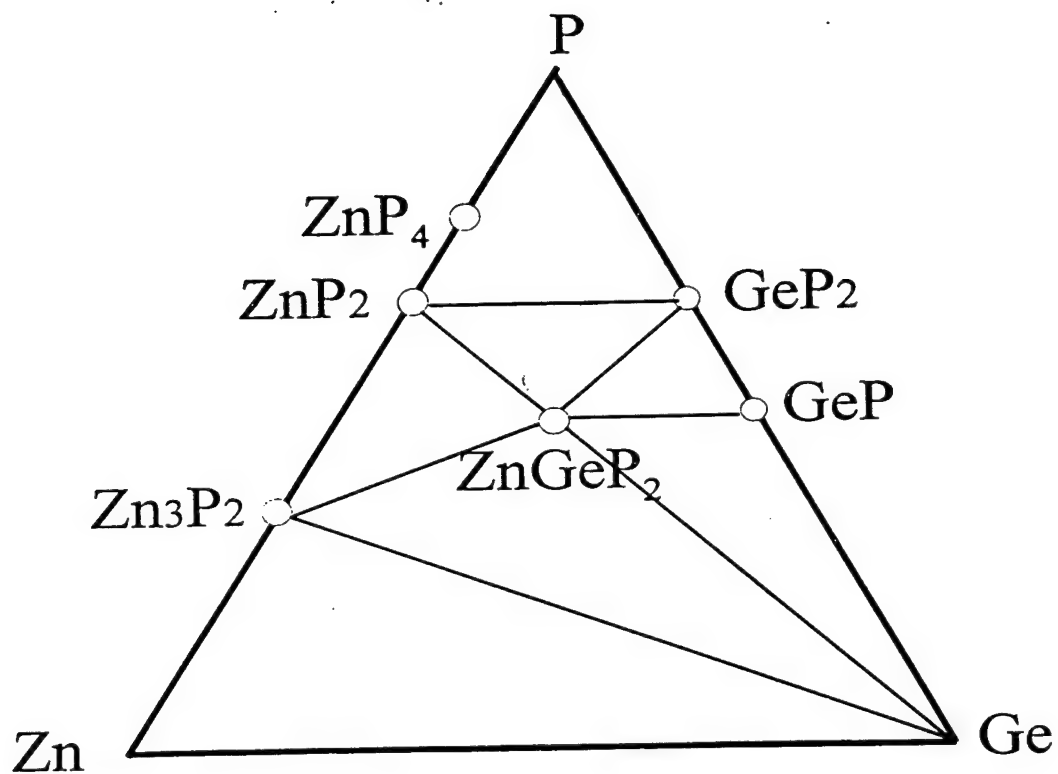
***The work was fulfilled under financial support
DERA, United Kindom***

327°C – ZnGeP_2 starts to decompose

1038°C – ZnGeP_2 melting point (Seb Fiechter, 1996)



The total pressure above ZnGeP_2 - P_{total} (Buehler, 1971) and partial pressures of Zn - P_{Zn} and P - P_{P4+P2} calculated from the regular solution theory (Roenkov, 1975): $P_{Zn} = 18$ Torr at 1068°C



The Zn-Ge-P phase triangle

Experimental details

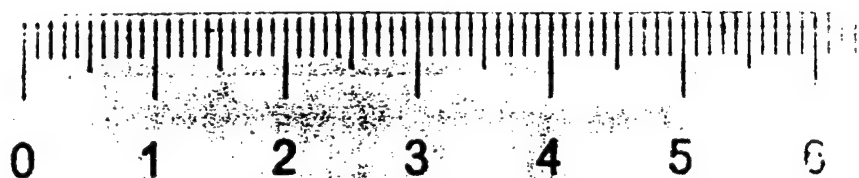
Synthesis: modified two-temperature technique, allowing to produce more then 500 gms of the material in one process

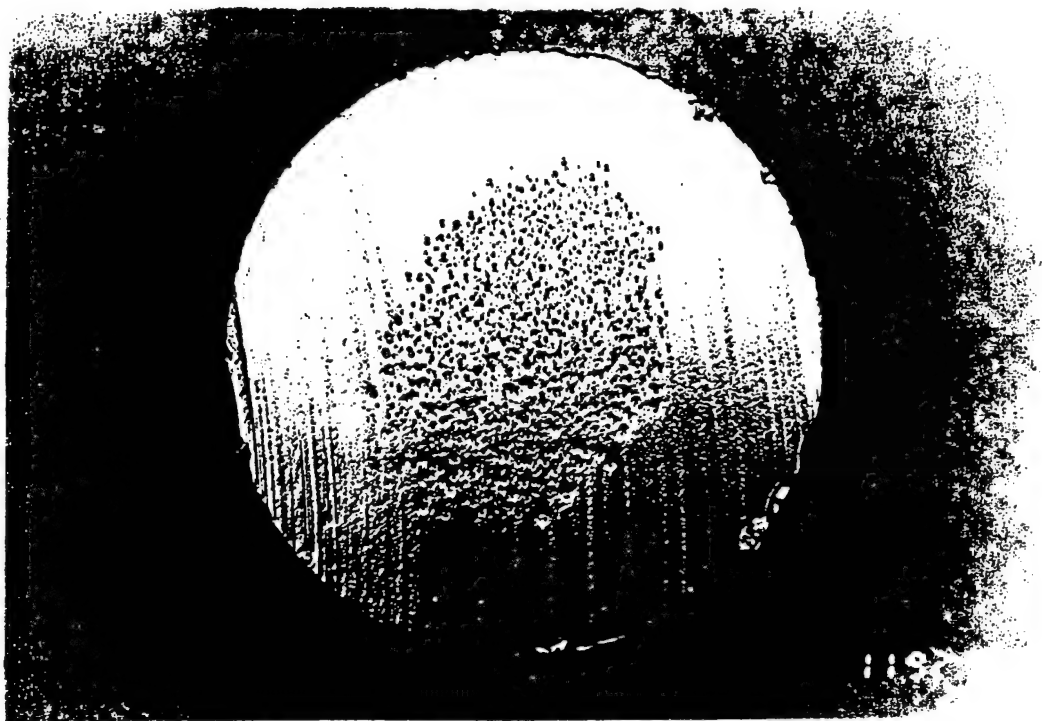
Growth: vertical Bridgman technique, (100) seeds

TABLE 1. Crystal growth conditions.

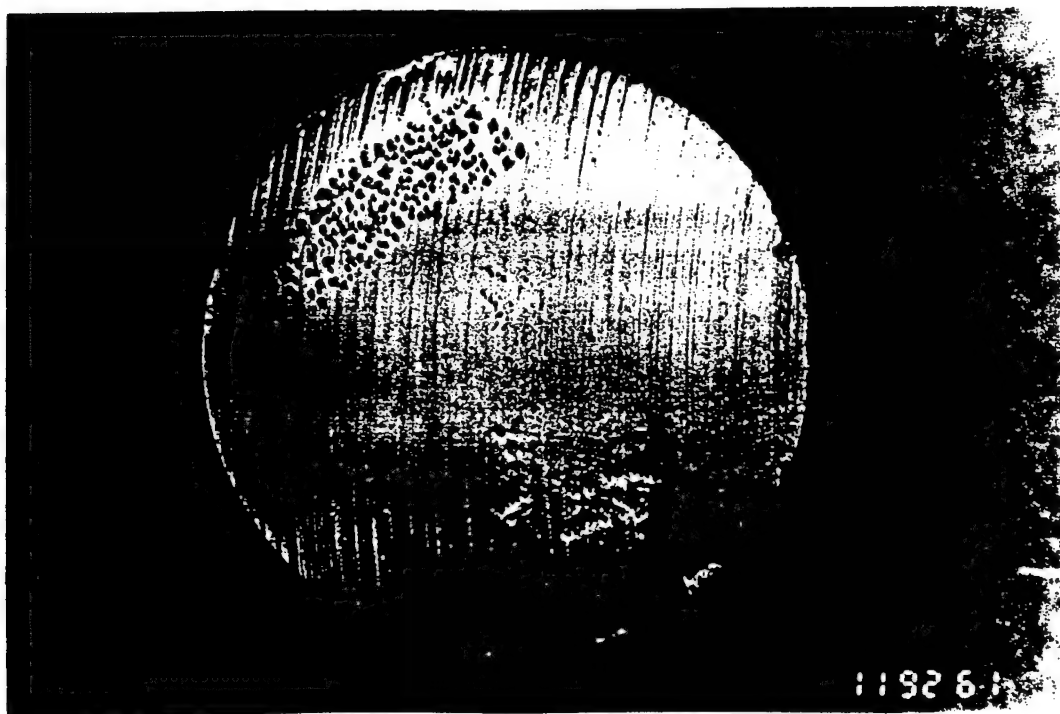
NUMBER OF CRYSTAL	HOT ZONE TEMPERATURE °C	COLD ZONE TEMPERATURE °C	WATER HEATING POINT °C	PHOSPHORUS PRESSURE MPa	ZINC PRESSURE MPa	PHOSPHORUS PRESSURE MPa	EXTERNAL VIEW OF THE GROWN CRYSTAL
1	1060	990	6	0.5	6.9	1.1	Gas pockets
2	1060	1000	3.5	1.0	7.2	-	No pockets Single phase
3	1060	950	10	0.5	-	-	Ge eutectic on the top of the crystal

* P_{P_4} (P_{Zn}) - pressures of phosphorus (zinc), created by additional charges of P (Zn), and calculated from the ideal gas law.

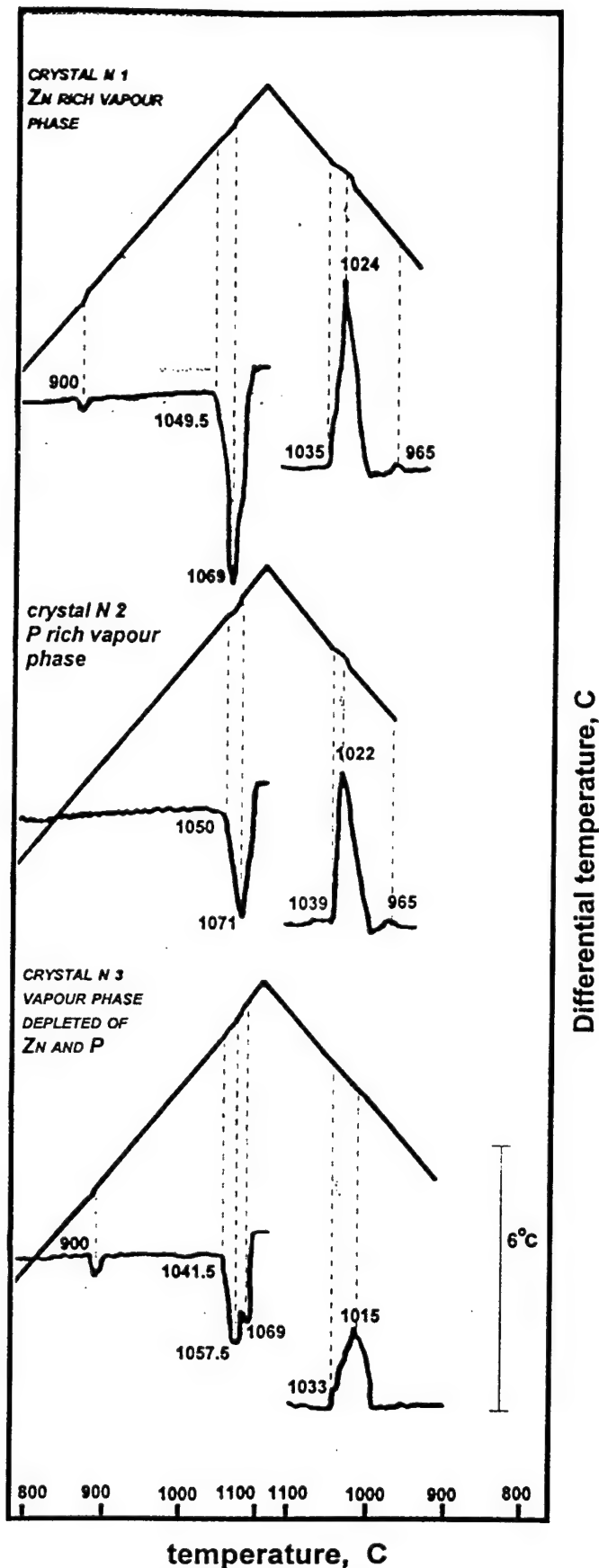




1 cm

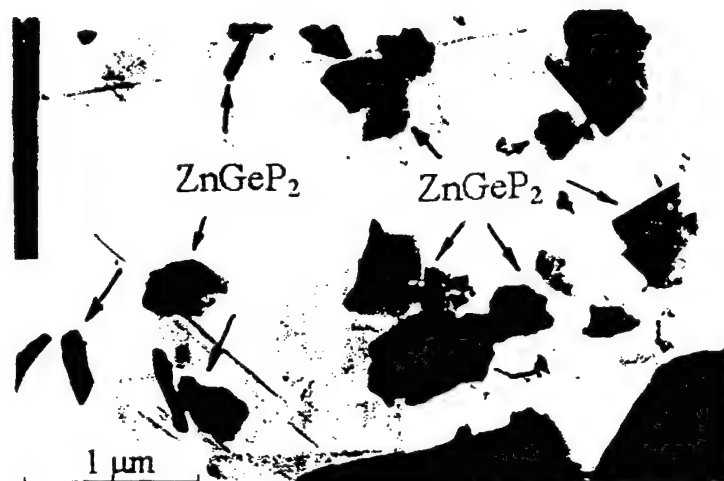


ZnGeP₂ slices after chemical etching



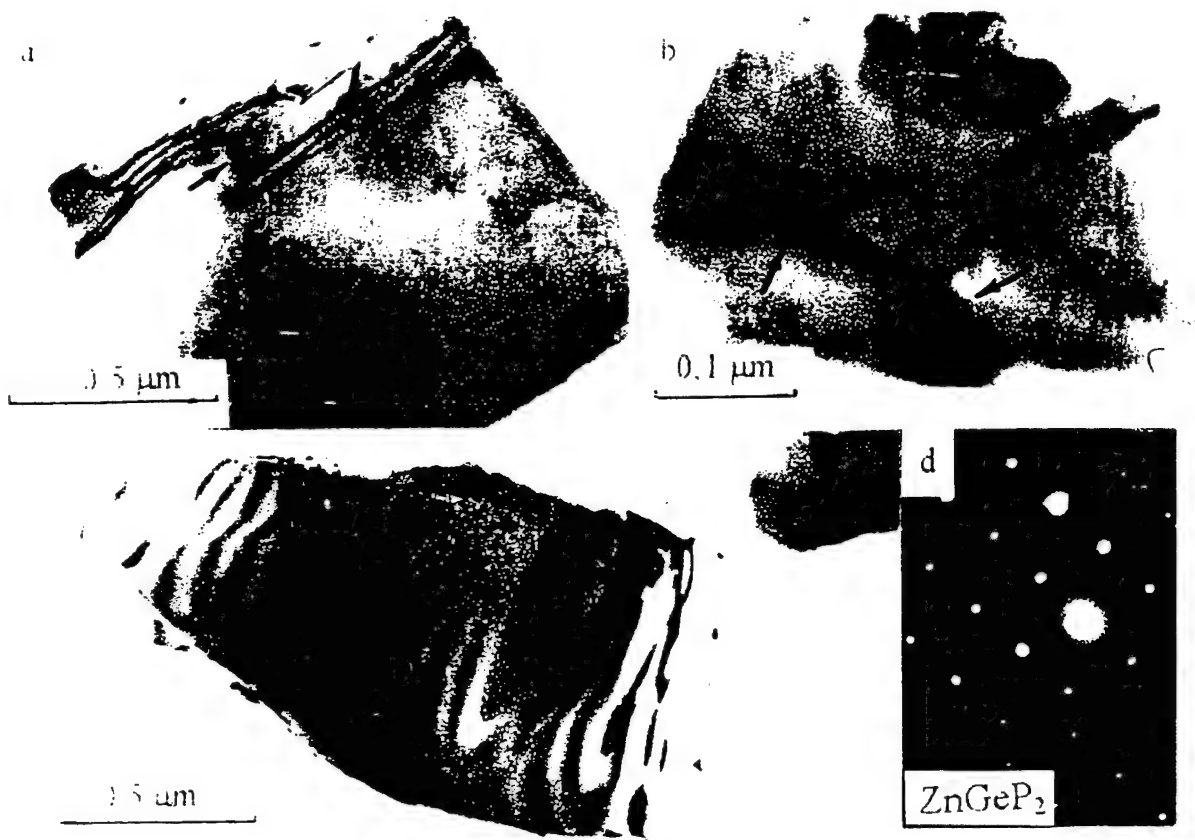
DTA curves of ZGP grown under
various pressures of Zn and P

Experimental details: the weight of the studied samples - 0.5 g, heating and cooling rates - 7.5 deg/min
reference material - Al_2O_3 , speed of the paper movement - 1 mm/min



Fragments of failure (damage) of the bulk ZGP specimen
arranged on the carbon substrate

*Electron microscope EM-125
Accelerating voltage 125 kV
Working Magnification 65-85 000
Resolution 7-10Å*



Microscopic image of ZnGeP_2

A Theoretical Study of Defects in ZnGeP_2 and CdGeAs_2

Ravi Pandey

Michigan Tech., Houghton, MI 49931
(pandey@mtu.edu)

(AFOSR-F49620-96-1-0319)

Approach : calculations of defect configurations and energetics in the framework of the atomistic model.

Results :

- (i) Cation sublattice disorder is predicted to be the dominant native defect in both ZnGeP_2 and CdGeAs_2 .
- (ii) The nature of defects responsible for the near-IR absorption band in ZnGeP_2 and CdGeAs_2 appears to be different -

ZnGeP_2 : zinc vacancy (localized hole)

CdGeAs_2 : cadmium antisite (delocalized hole)

Defect-induced lattice distortion plays a key role in stabilizing the hole states in the lattice.

Based on the size argument, antisites in ZGP are not expected to introduce significant lattice distortion while those in CGA would be expected to cause significant distortion in the lattice.

$$R_{\text{Zn}} = 1.23 \text{ \AA}, R_{\text{Ge}} = 1.23 \text{ \AA}, R_{\text{Cd}} = 1.41 \text{ \AA}$$

Dopant Binding Energies in ZnGeP_2 and CdGeAs_2

– selective doping of ZnGeP_2 to reduce the concentration of the dominant native acceptor level via charge compensation in the lattice.

–

ZnGeP_2

» Au, Cu : inactive Se, Ga, In : acceptor (Gigoreva 73)

»

» Au, Cu, Ga, In, Se, Pt : acceptor (Rud 97)

»

CdGeAs_2

» Cu, Ga : acceptor In, Te : donor (Bairamov 98)

Summary

- Both Cu and Ag always act as acceptors.
- small hole binding energies for Cu and Ag at the Zn site.
- large hole binding energies for the group III dopants at the Ge site except B which shows a distinct behavior.
- donor levels for B, Al, Ga, In predicted to be near middle of the gap.

DEFECT IDENTIFICATION IN ZnGeP_2

K. J. Nash
DERA Malvern

Discussions, exchange of unpublished
results, with

M. Fearn, A. W. Vere (DERA)

L. E. Halliburton, K. T. Stevens
(WVU, Morgantown)

SYMMETRY THEORY

Which defect symmetry groups are possible in the ZGP structure?

- Determination of symmetry from experiments.
- Which defects have a particular symmetry?
Which of these are consistent with
- the spin Hamiltonian?

DEFECT SYMMETRY IN ZGP

4 possibilities

- - tetragonal

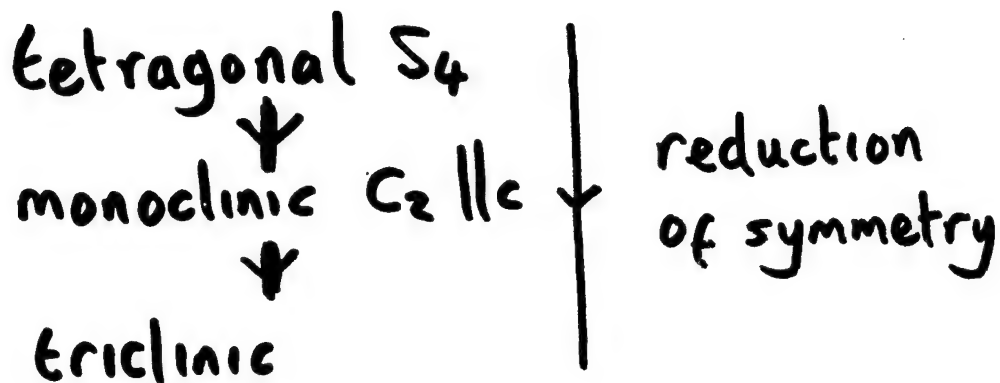
- monoclinic ($C_2 // a$ or b)

ENDOR on the main defect in ZGP
(Halliburton et al)

⇒ monoclinic symmetry ($C_2 || a$ orb)

suggested identity: V_{Zn}

- But the Zn site has tetragonal symmetry

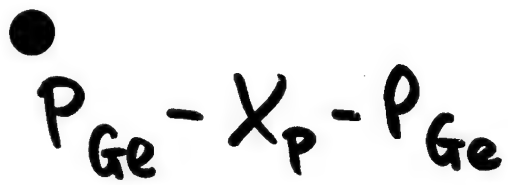


- So V_{Zn} does not have the right symmetry

Other Models



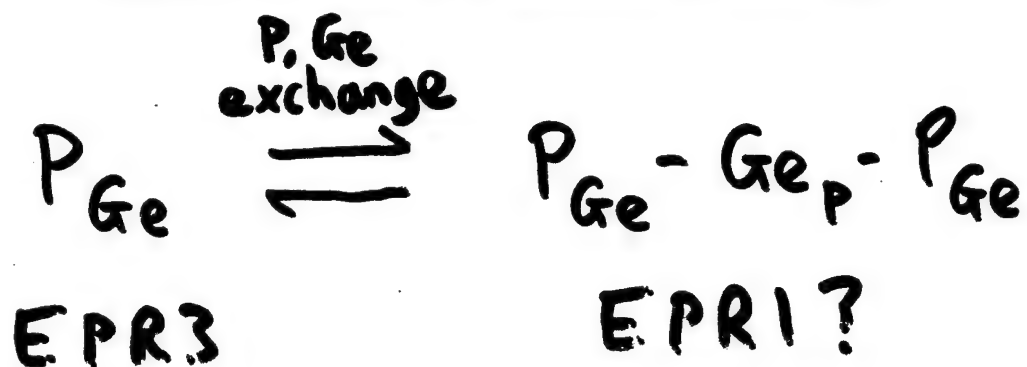
where D is a defect site that is close to one P atom and D, E are related by the C_2 symmetry axis



(CI = interstitial site on cation sublattice)

- - ↳ unpaired spin localised on X;
two P atoms related by symmetry

SPECULATION



●
no evidence for this! but...

- P_{Ge} has already been found in ZGP
- $P_{Ge} - Ge_P - P_{Ge}$ would explain the
- EPRI signal, if the unpaired spin is localised on Ge_P .

● ●

Optical Properties of Tellurium Rich $\text{Te}_x\text{Se}_{(1-x)}$ Nonlinear Optical Semiconductors

G.J. Brown*, Cindi L. Dennis*,
M. C. Ohmer*, and Arnold Burger**

*Air Force Research Laboratory, Materials & Manufacturing Directorate,
AFRL/MLPO, Wright-Patterson AFB, OH 45433-7707

** Fisk University, 1000 17th Ave., N, Nashville, TN 37208-3051

ASC-99-1822

Outline

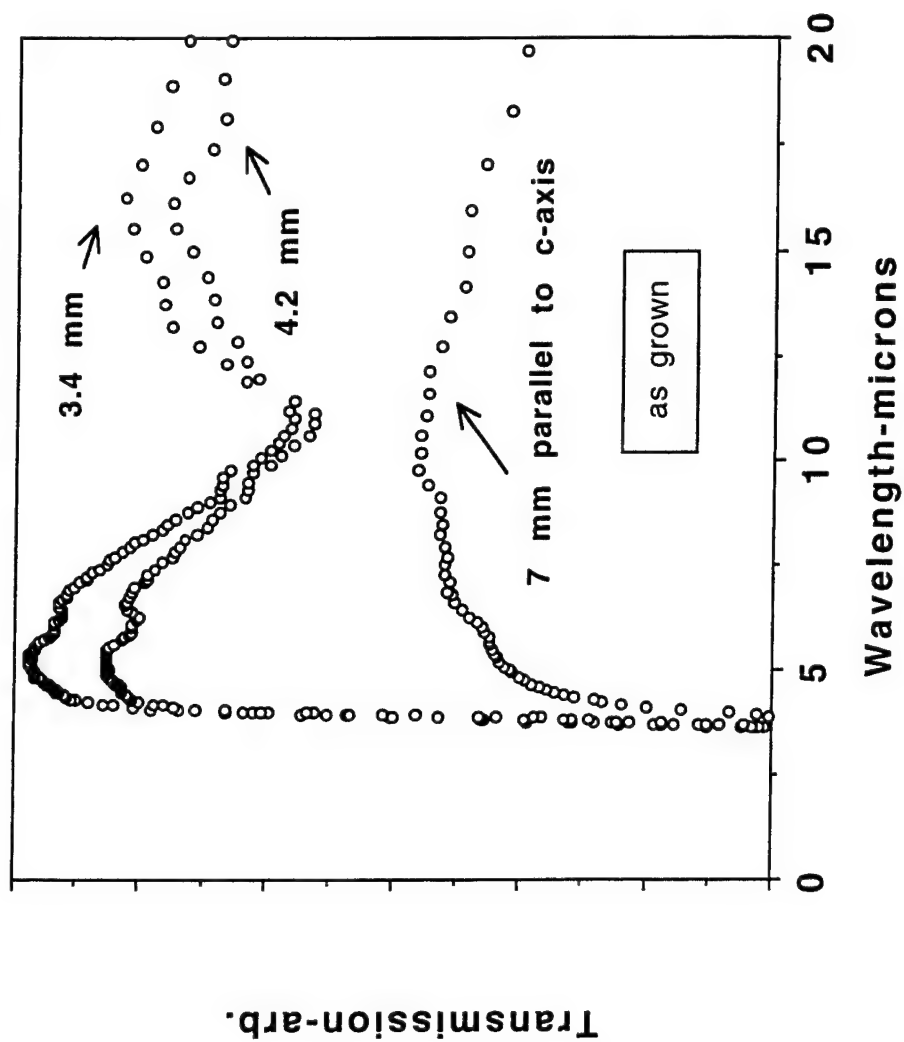
- Infrared photoresponse and the energy gaps of tellurium rich oriented crystals of the form $\text{Te}_x\text{Se}_{(1-x)}$ for $x=1, 0.9$, and 0.8 are reported.
 - Band gaps are compared

– Te	0.33 eV	3.76 microns
– $\text{Te}_{0.9}\text{Se}_{0.1}$	0.38	3.26
– $\text{Te}_{0.8}\text{Se}_{0.2}$	0.498	2.48
– Se	1.7	0.73
- The composition $\text{Te}_{0.286}\text{Se}_{0.714}$ is estimated to have an energy gap of 1 eV or 1.24 microns from literature data

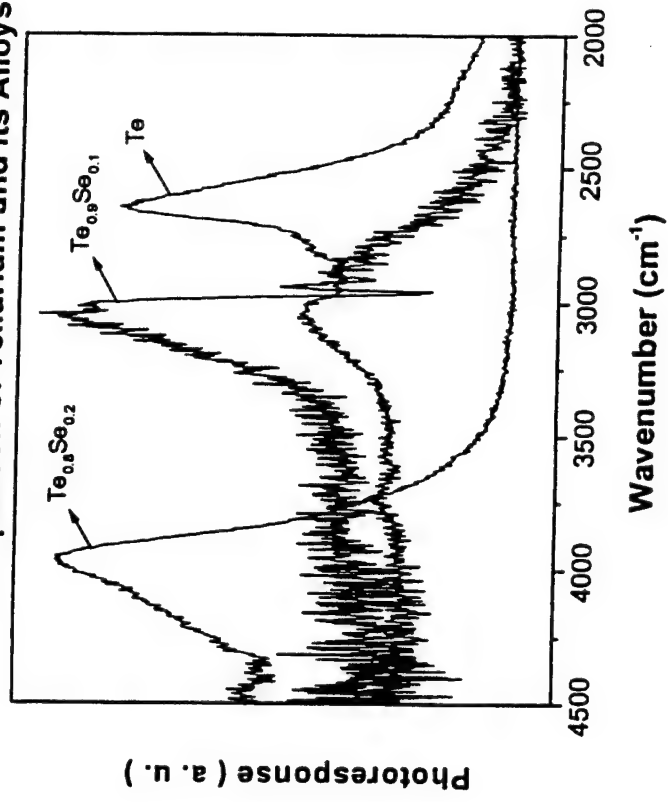
WHAT IS A LARGE SECOND ORDER NONLINEAR SUSCEPTIBILITY (a.k.a. CHI2)?

- The largest reported value for a birefringent element is 650 pm/V for Te. The value for Se is 97 pm/V.
- The largest reported value for a birefringent compound is 470 pm/V for CdGeAs₂
- The value of 11 pm/V for lithium niobate (LiNbO₃) is usefully large for optical signal processing applications
- Two state of the art IR materials, AgGaS₂ and AgGaSe₂ have Chi2 values of respectively 36 pm/V and 66 pm/V
- ZnGeP₂ has a very respectable value of 150 pm/V, but not birefringent
- The above numbers are normalized to GaAs at 180 pm/V
- Upper limit for bound electrons is 4000-5000 pm/V

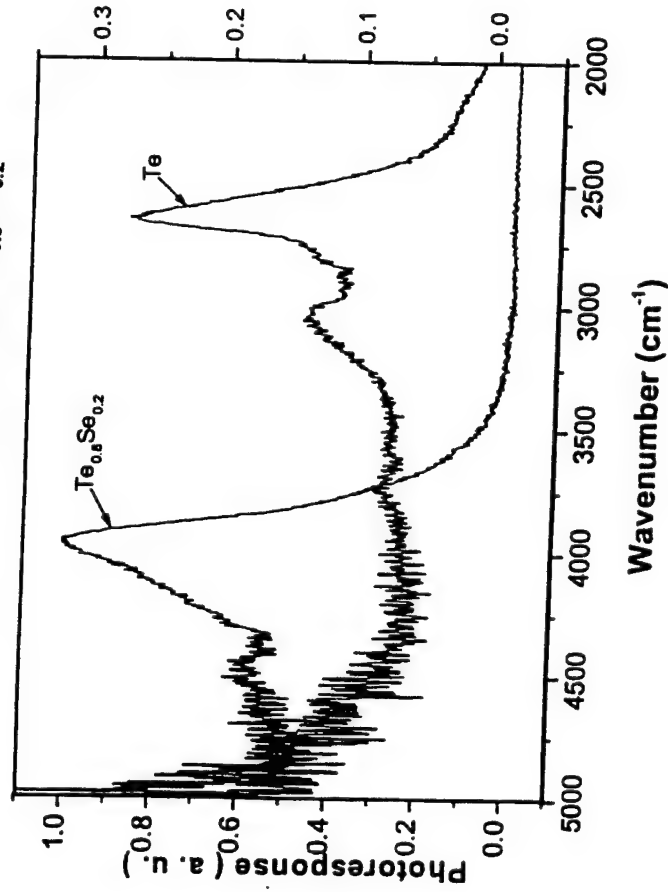
Oriented Tellurium Crystal
Perkin Elmer FTIR (Raw Source Beam)



Comparison of Tellurium and Its Alloys



Photoreponse of Te and Te_{0.8}Se_{0.2}



AFRL Materials Directorate Efforts in Nonlinear Optical Crystal Development for Laser Wavelength Shifting

**NILS C. FERNELIUS*, F.K. HOPKINS,
& M.C. OHMER**

*Materials Directorate,
Air Force Research Laboratory,
Wright Patterson Air Force Base,
Dayton, Ohio 45433*

DESIRED PROPERTIES FOR NLO UNOBTAINIUM

BROAD WAVELENGTH OPTICAL TRANSMISSION

LOW LOSS: ABSORPTION & SCATTER

LARGE NONLINEAR SUSCEPTIBILITY or d

rather d_{eff}^2/n^3

**NEED LARGE BIREFRINGENCE FOR PHASE MATCHING
(or USE QUASI-PHASE-MATCHING STRUCTURES)
TOO LARGE LEADS TO BEAM WALK-OFF PROBLEMS
NEED UNIFORM REFRACTIVE INDEX THROUGHOUT**

CRYSTAL

LASER DAMAGE RESISTANCE

WANT SMALL dn/dT TO AVOID SELF-FOCUSING

WANT HIGH THERMAL CONDUCTIVITY

WANT STRONG MECHANICAL PROPERTIES

STABLE CHEMICAL PROPERTIES

CRYSTALS EASY TO GROW

INEXPENSIVE

THRUSTS OF BULK CRYSTAL PROGRAM

BIREFRINGENT CRYSTALS:

KTP {KTiOPO₄} ISOMORPHS- KTA {KTiOAsO₄},
RTA {RbTiOAsO₄}, CTA {CsTiOAsO₄},
KRTA {K_{1-x}Rb_xTiOAsO₄}

KTP GREY TRACK

CHALCOPYRITES- ZnGeP₂, CdGeAs₂, AgGaS₂,
AgGaSe₂, AgGa_{1-x}In_xSe₂, AgGaTe₂

GaSe

HgGa₂S₄

CGC {CsGeCl₃}

CGB {CsGeBr₃}

UV MATERIALS(borates) - LBO {LiB₃O₅} ,

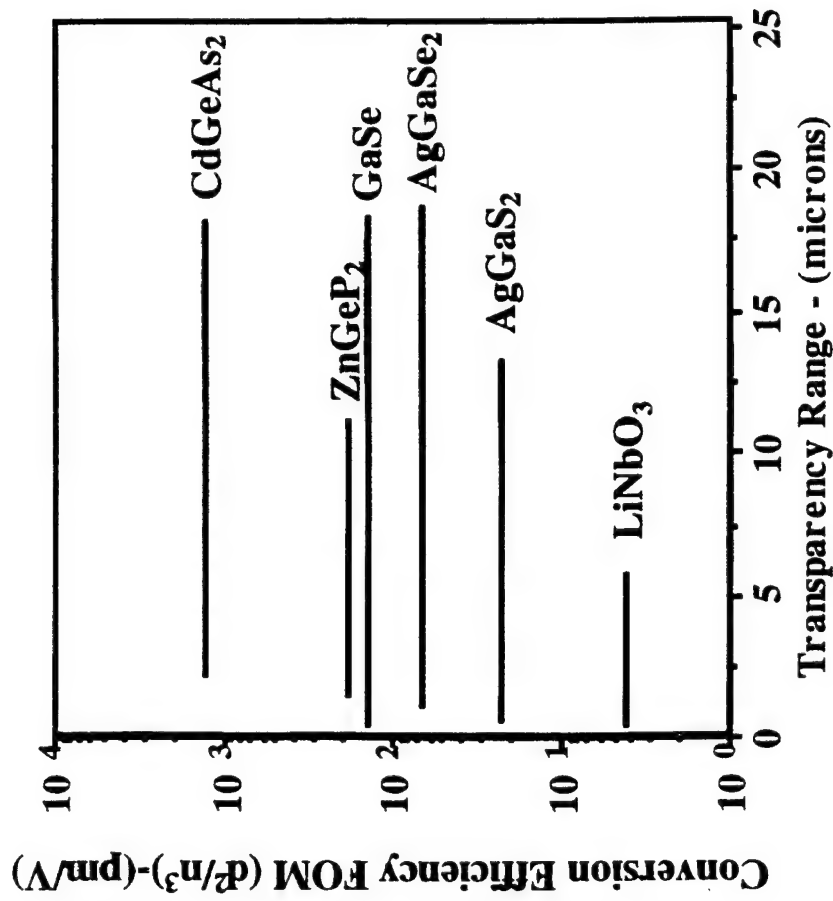
BBO { β-BaB₂O₄}, CLBO { CsLiB₆O₁₀},

KBBF {KBe₂BO₃F₂}, CsLaB₇O₁₃,

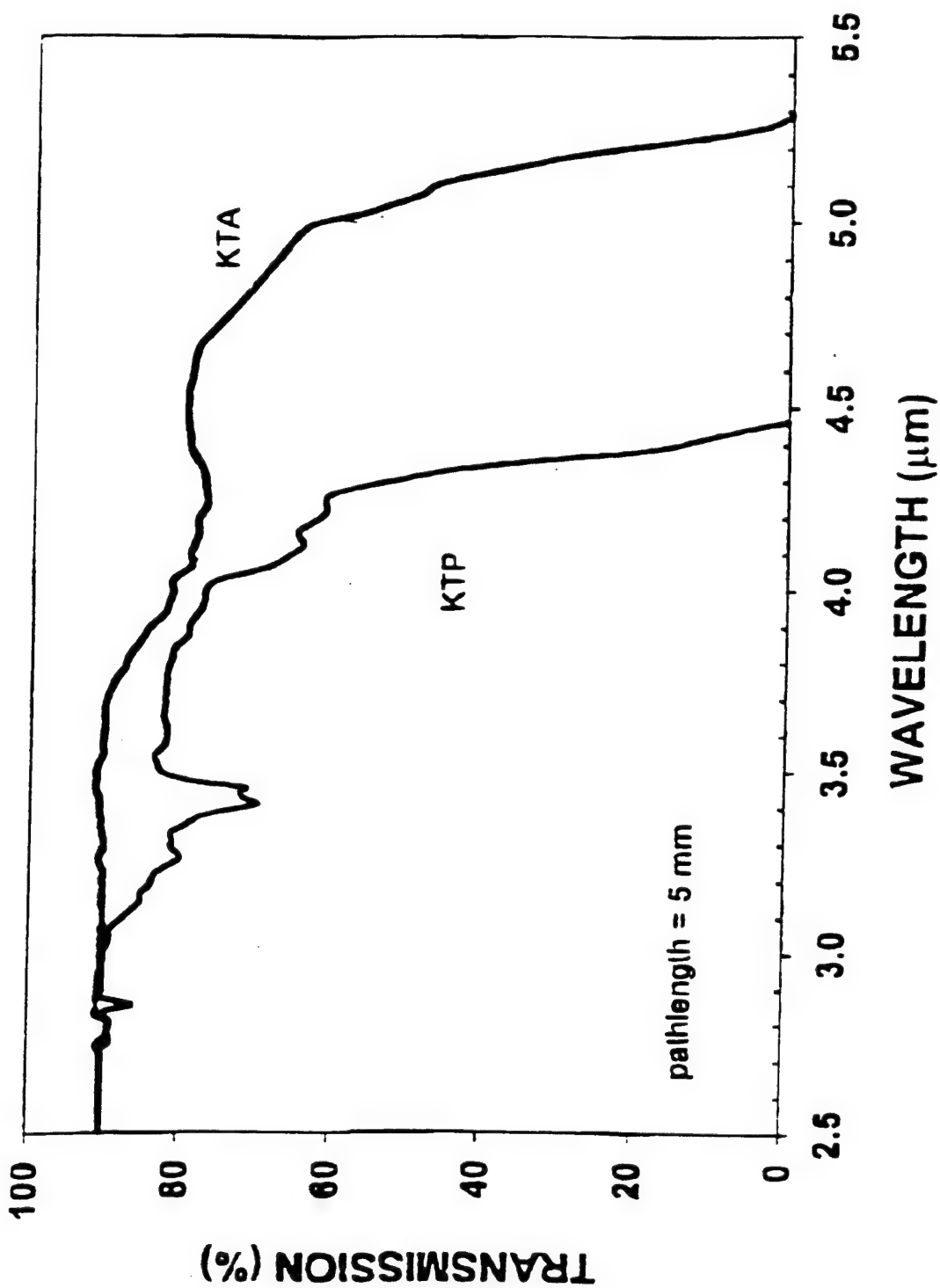
low birefringence: SBO {SrB₄O₇} & PBO {PbB₄O₇}

MM'(B₃O₅)₃ where M = Sr, Ba, Pb; M' = Li, Na

Figure of Merit for Many Common NLO Materials



TRANSMISSION
KTA vs. KTP



CRYSTAL ASSOCIATES, INC.

GRAY TRACKS IN KTP

Nd:YAG laser produces 355 nm photons (third harmonic generation or sum of fundamental & second harmonic)
 KTP room temperature band edge at 360 nm.
 The above-band-gap photons generate electron-hole pairs.
 Many recombine but a portion are trapped at stabilizing defects such as vacancies or impurities to form "stable" gray tracks. When these complexes contain an unpaired electron, they can be studied by ESR and ENDOR.

Flux grown KTP: $\xrightarrow{\text{formation}}$ $\text{Fe}^{3+} + \text{h}^+ < \text{decay}$ Fe^{4+}

$\text{Ti}^{4+}\text{-V}_\text{O} + \text{e}^- \xrightarrow{\text{formation}} < \text{decay} \text{Ti}^{3+}\text{-V}_\text{O}$

Hydrothermal grown KTP: $\xrightarrow{\text{formation}}$ $\text{Fe}^{3+}\text{-OH}^- + \text{h}^+ < \text{decay} \text{Fe}^{4+}\text{-OH}^-$

$\text{Ti}^{4+}\text{-OH}^- + \text{e}^- \xrightarrow{\text{formation}} < \text{decay} \text{Ti}^{3+}\text{-OH}^-$

Halliburton & Scripsick, SPIE Proc. 2379 235 (1995)

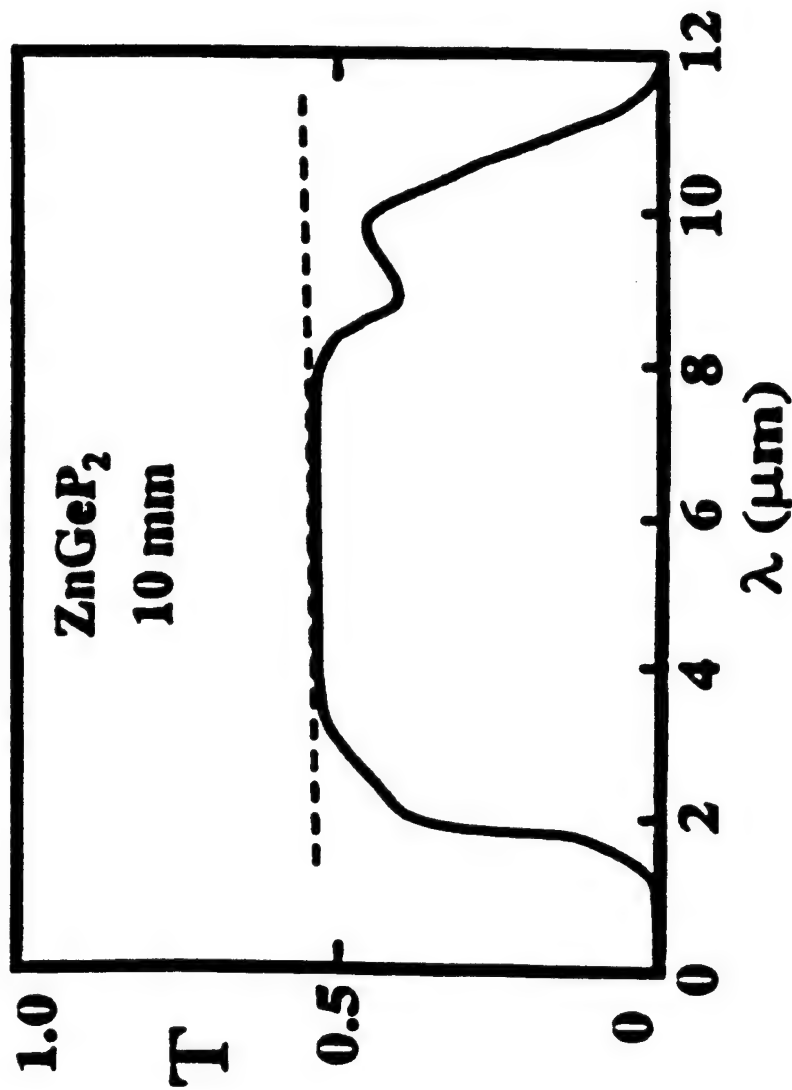
CHALCOPYRITES



Some examples for IR NLO:

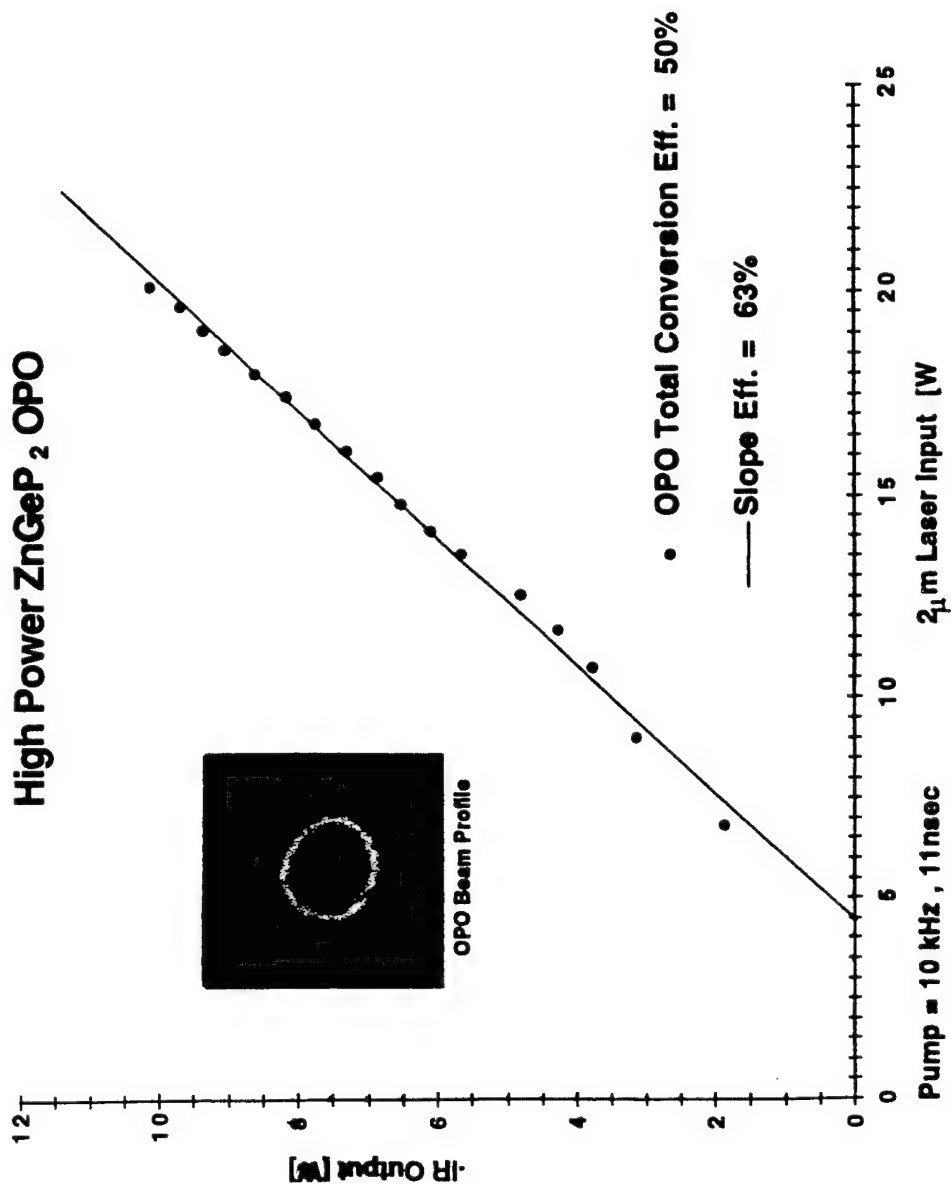


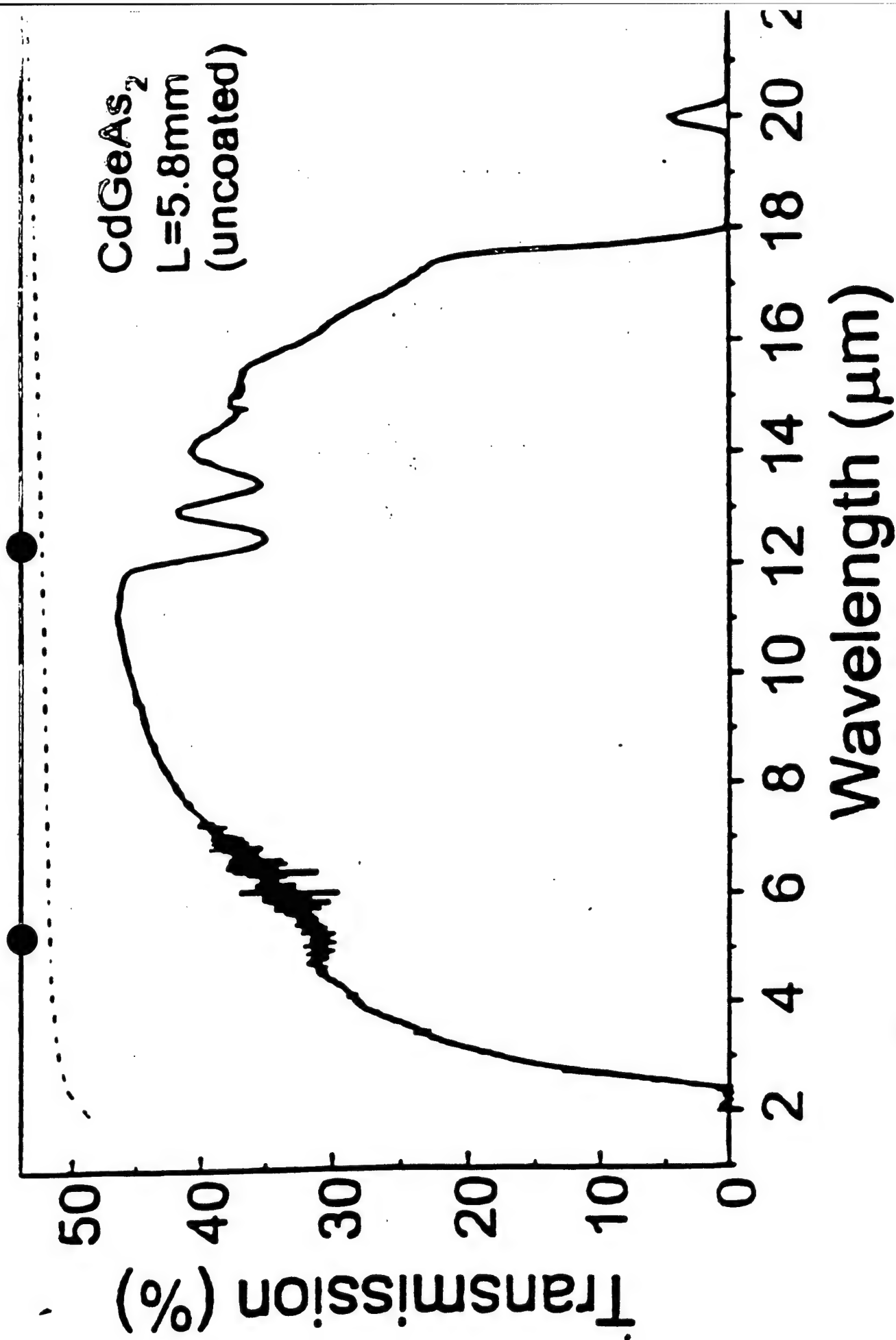
See July, 1998 issue MRS Bulletin 23(7)



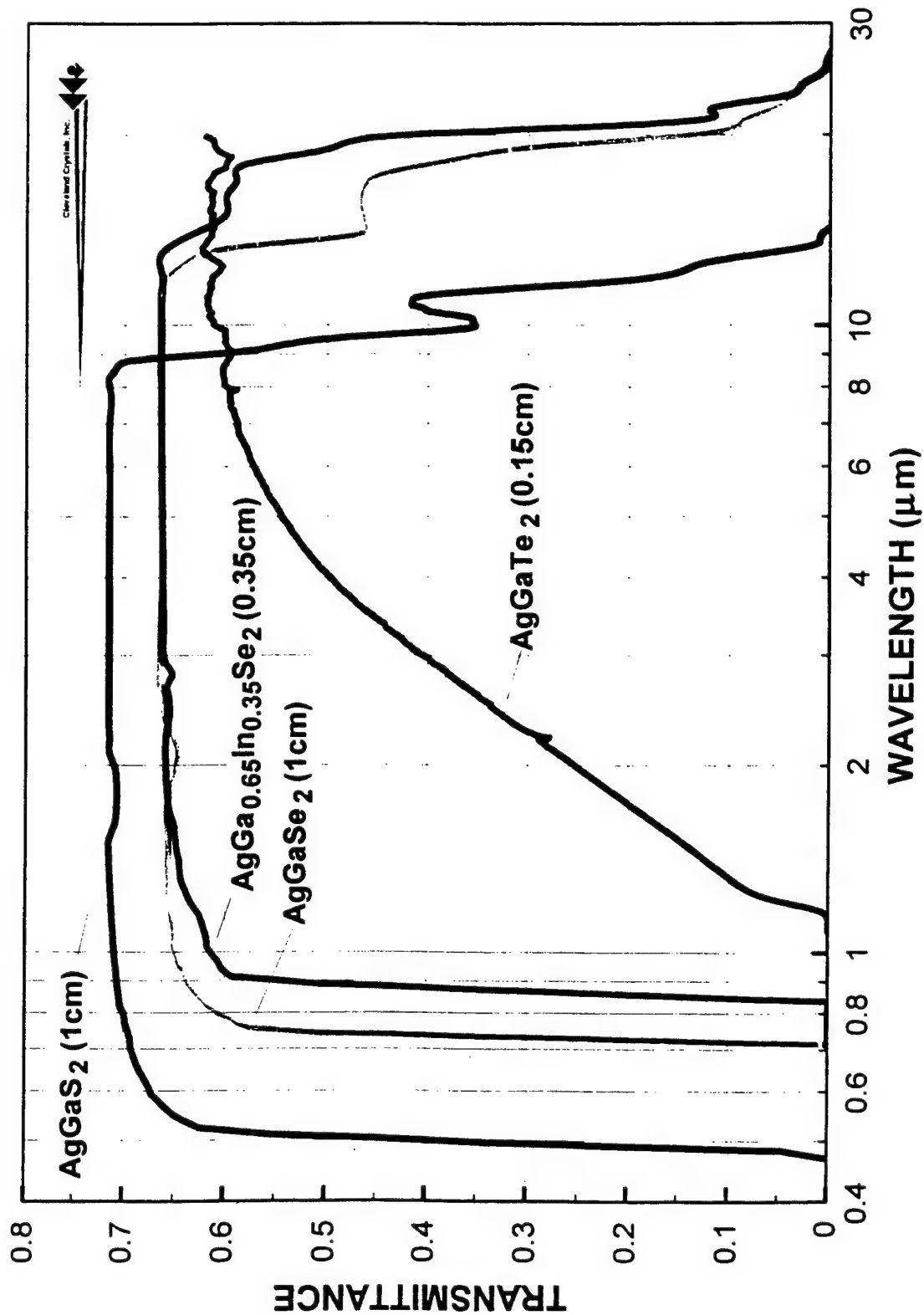
Transmission spectra taken at room temperature.
ZnGeP₂ ($L = 10$ mm). Dashed curves, Fresnel losses.

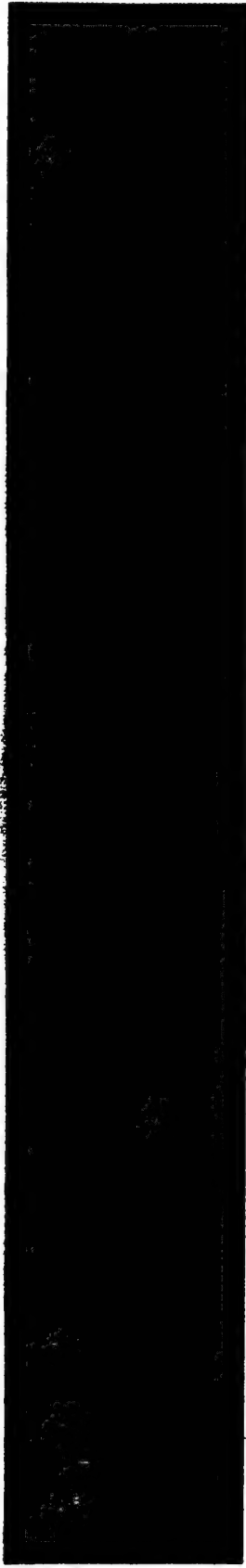
High Power ZnGeP₂ OPO





Measured transmission spectrum of an uncoated, 5.8 mm long CdGeAs₂ sample.



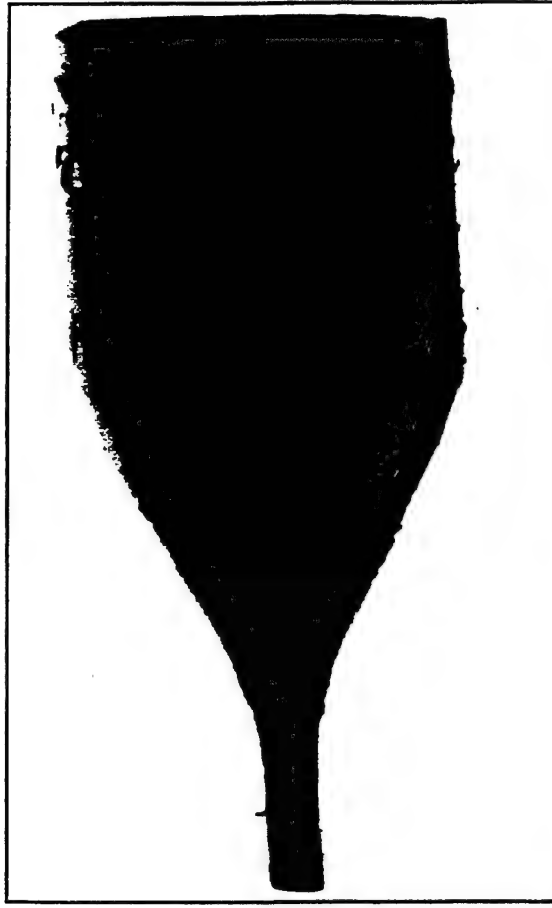
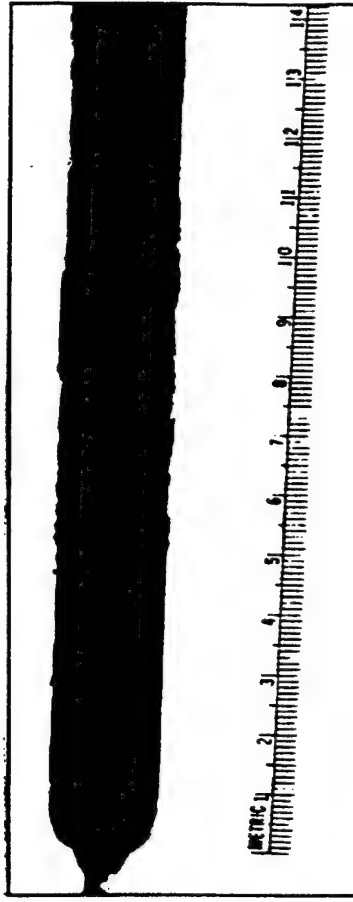


- ◆ GaSe has extremely high NLO coefficient (76 pm/V) and merit (d^2/n^3 331) compared to ZGP, TAS and AgGaSe₂ crystals.

- ◆ GaSe transmits between 0.65 to 20 micrometer wavelength region without any absorption band.

- ◆ GaSe has very high damage threshold and did not damage up to 180 MW/cm² power

NORTHROP GRUNNAN

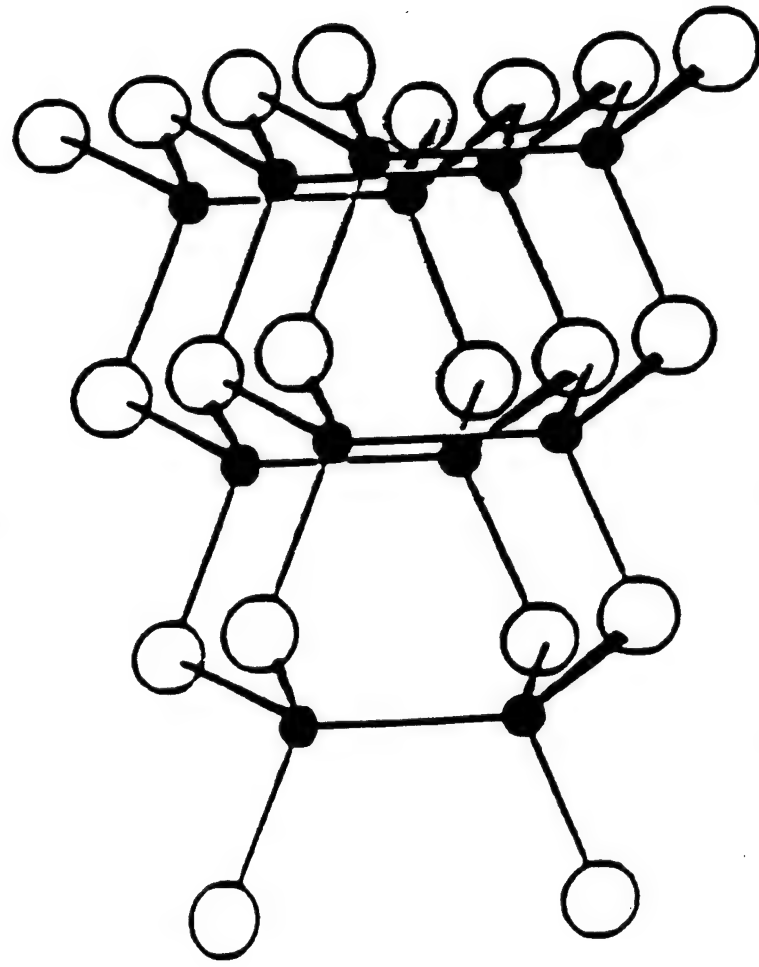


AF-1 Gas Crystal

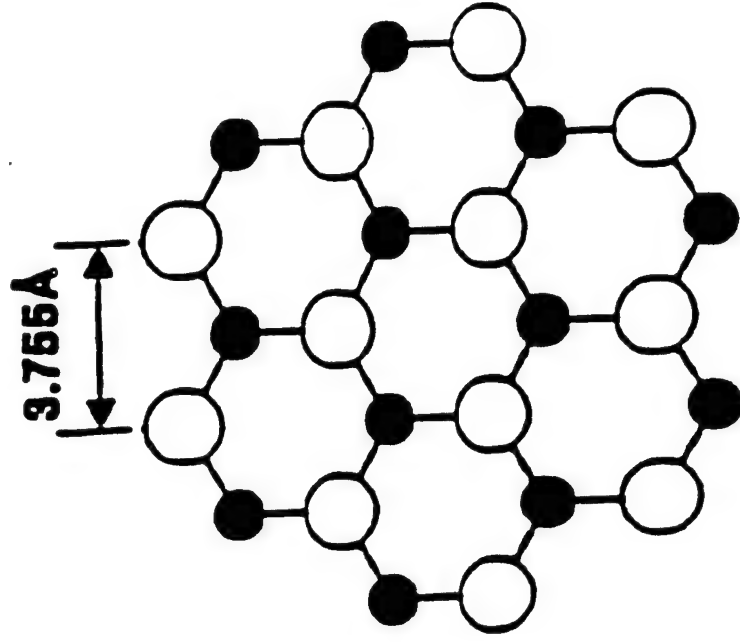
METRIC 11

2





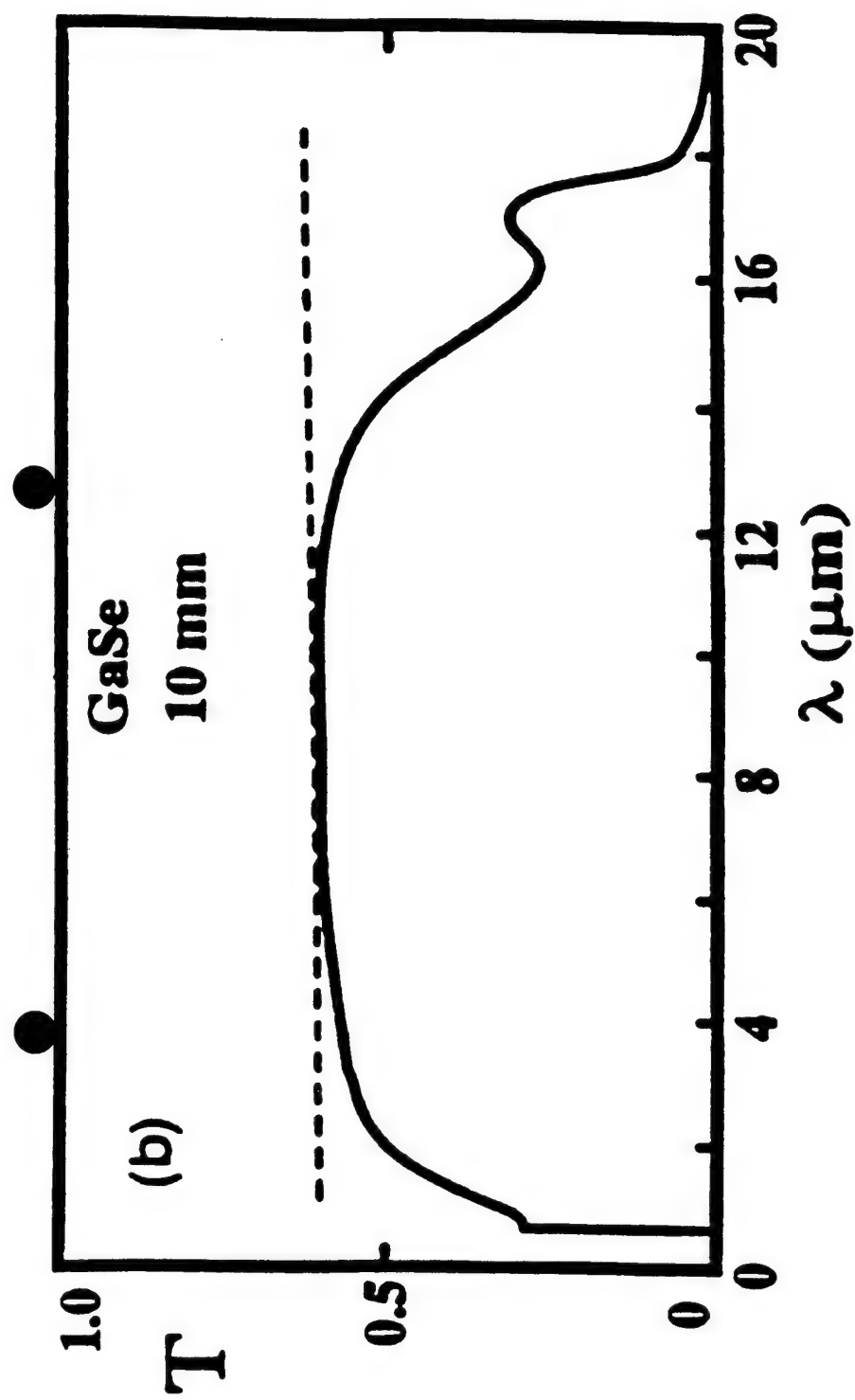
Perspective view



Top view

Perspective and top views of a unit layer of GaSe.

Uneo, Abe, Suiki & Koma, Jap. J. Appl. Phys. Lett., 30 L1352 (1991)



Transmission spectra taken at room temperature. GaSe ($L = 10$ mm). Dashed curves, Fresnel losses.

K. L. Vodopyanov

RECENT GaSe USES

W.C. Eckhoff, R.S. Putnam, S. Wang, R.F. Curl, F.K. Tittel
A continuously tunable long-wavelength cw IR source
for high-resolution spectroscopy and trace-gas detection
Appl. Phys. B 63, 437-441 (1996)

Difference frequency generation (DFG) of two
synchronously pumped Ti:sapphire lasers yields continuously
tunable light over 8.8-15.0 μm region.

K.L. Vodopyanov & V. Chazapis
Extra-wide tuning range optical parametric generator
Optics Communications 135, 98-102 (1997)
Optical parametric generator (OPG) yields continuously
tunable light over 3.3-19 μm range.

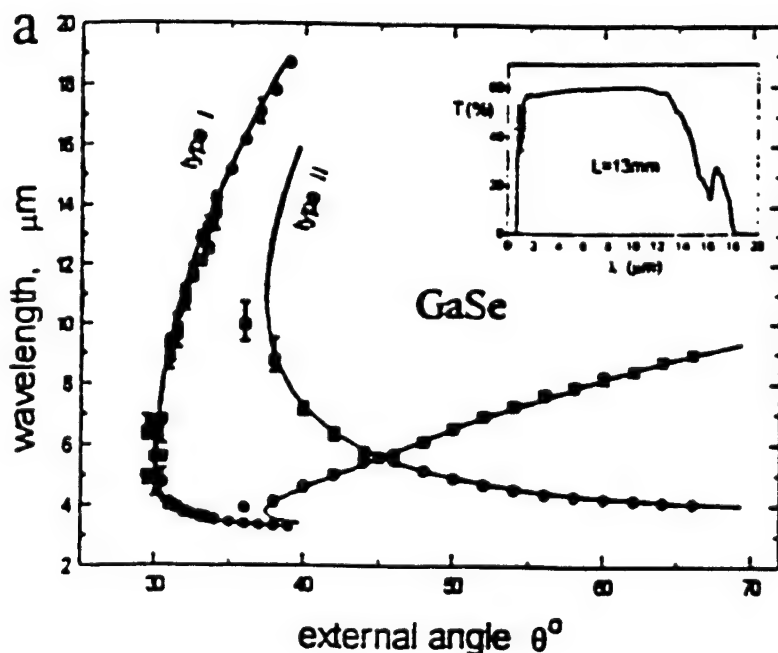
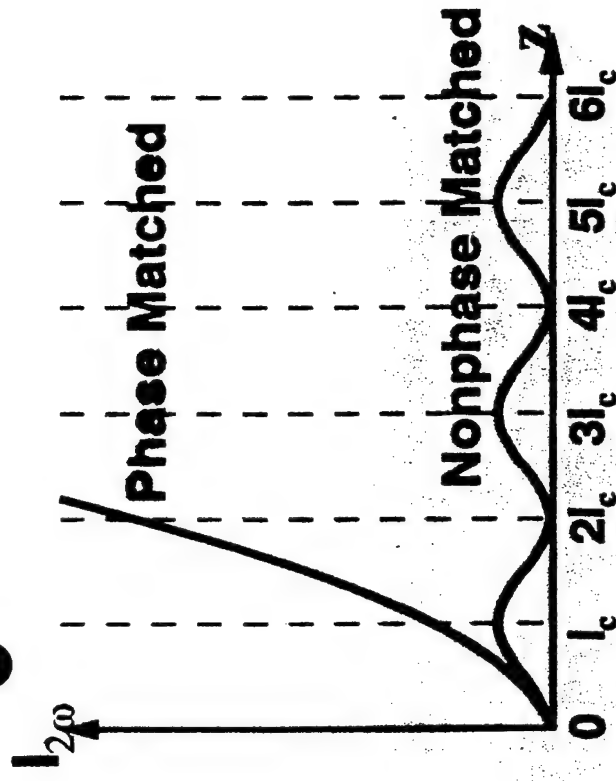
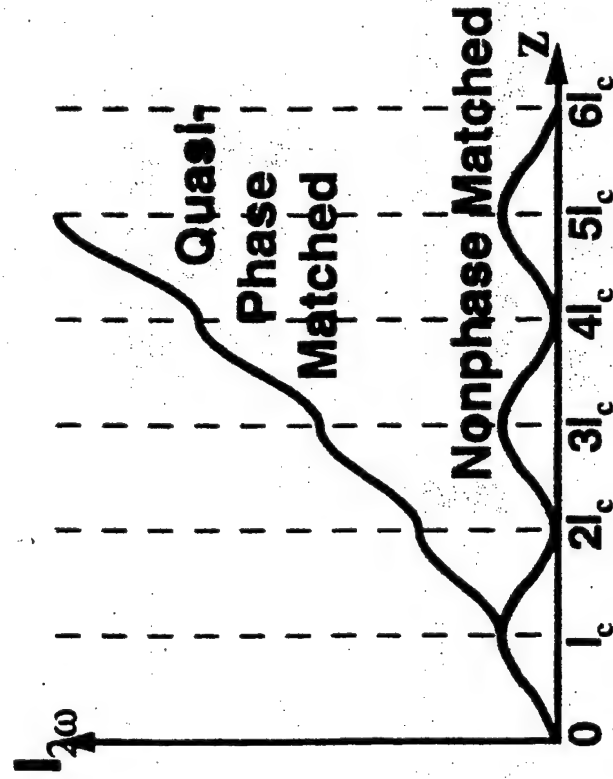


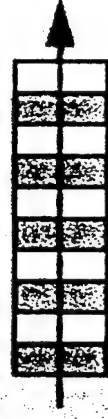
Fig. 2. GaSe and ZnGeP₂ angular tuning curves at $\lambda = 2.8 \mu\text{m}$ pump for the two types of phase-matching. Vertical bars correspond to experimental half-maximum linewidths. Solid lines - calculated tuning curves. Insets show linear transmission spectra for the two crystals;

Quasi-Phase Matching



QUASI-PHASE-MATCHING TECHNIQUES

Inverted Segments



Diffusion bonded - GaAs
 Periodically poled - LiNbO_3 ,
 LiTaO_3 , KTP, RTA, KTA, SBN
 Periodic doping

- diffusion exchange
- ion implantation

Total Internal Reflection Devices



- GaAs, ZnSe

THRUSTS OF BULK CRYSTAL PROGRAM

QUASI-PHASE-MATCHING TECHNIQUES:

INVERTED SEGMENTS

DIFFUSION BONDED - GaAs

PERIODICALLY POLED- 3-5 μ m: LiNbO₃{PPLN},

LiTaO₃ {PPLT},

KTP, RTA, KTA

Pb_xBa_{1-x}Nb₂O₆ (PBN)

8-12 μ m: CsGeCl₃, CsGeBr₃

Tl₃PbBr₅, Tl₄PbI₆, Tl₄HgI₆

PERIODIC DOPING - diffusion exchange

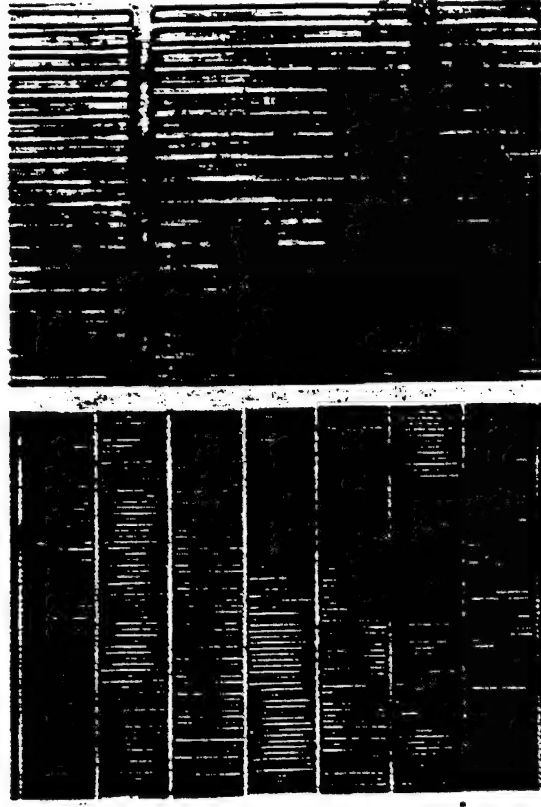
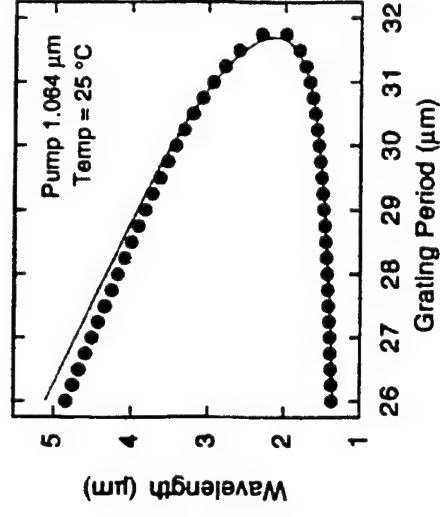
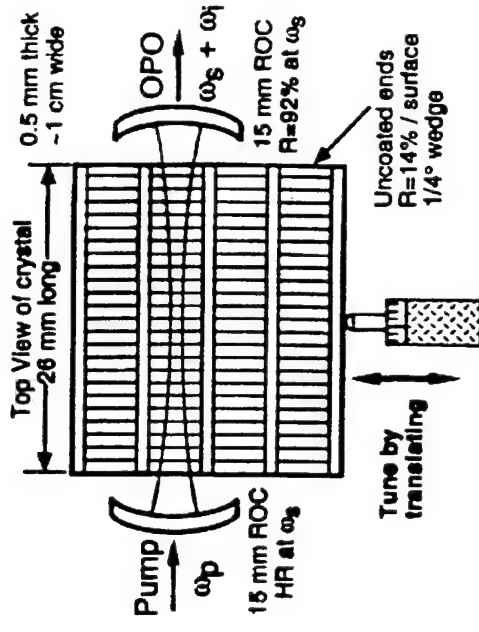
ion implantation

PERIODIC PRESSURE TO INVERT DOMAINS

TOTAL INTERNAL REFLECTION DEVICES - GaAs, ZnSe

Mid IR Multigrating PPLN

Tuning from $\sim 1.4 - 4.8 \mu\text{m}$
 Multi - Watt Output Power
 Suffers from Photorefractive Effects
 Low Cost Material
 Uses $1.06 \mu\text{m}$ Laser Pump



● ●

MATERIALS WHICH HAVE BEEN PERIODICALLY POLED

LiNbO_3 (PPLN)

LiTaO_3 (PPLT)

KTiOPO_4 (KTP)

RbTiOAsO_4 (RTA)

KTiOAsO_4 (KTA)

$\text{Sr}_{0.6}\text{Ba}_{0.4}\text{Nb}_2\text{O}_6$ (SBN)

BaTiO_3 (PPBT)

PERIODICALLY POLED LITHIUM NIOBATE-LiNbO₃ (PPLN)

GOOD POINTS:

**USE $d_{33}= 42$ pm/V INSTEAD OF $d_{31}= 5$ pm/V AS IN
BIREFRINGENT PHASE MATCHING**

IMPROVES FIGURE OF MERIT BY ~ 25

NO WALK OFF PROBLEMS

CAN USE Nd:YAG 1.06 μ m AS PUMP

BAD POINTS:

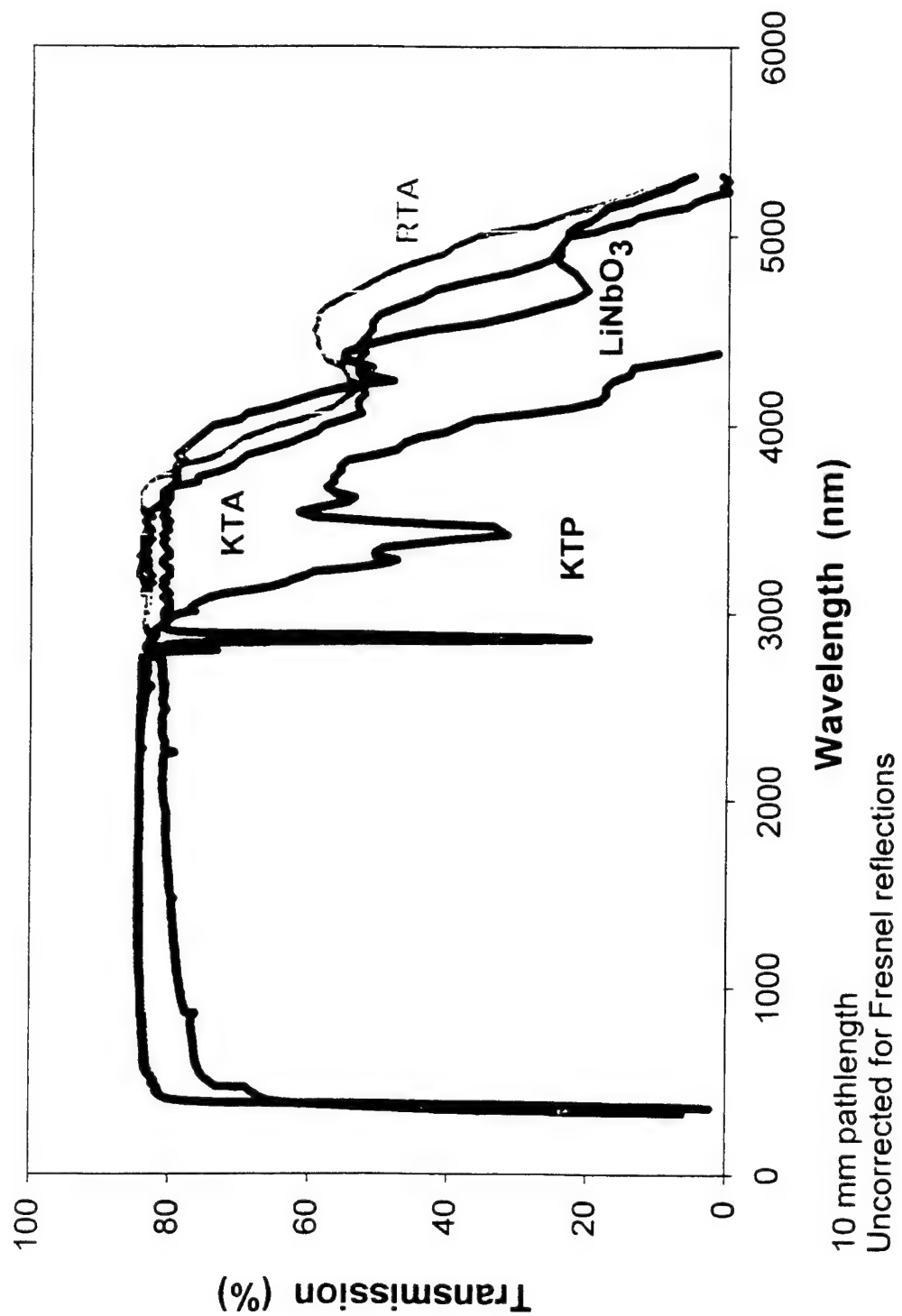
SMALL INPUT APERTURE WHICH LIMITS POWER OUTPUT

SO FAR SAMPLES 0.5-1 mm THICK

UNLESS DIFFUSION BOND A STACK

**M² PROBLEMS OF OUTPUT BEAMS EVEN WITH STACK
PHOTOREFRACTIVE DAMAGE**

**HEAT SAMPLE IN OPERATION TO ANNEAL OUT
DAMAGE**



MWIR (3-5 μm) THRUSTS

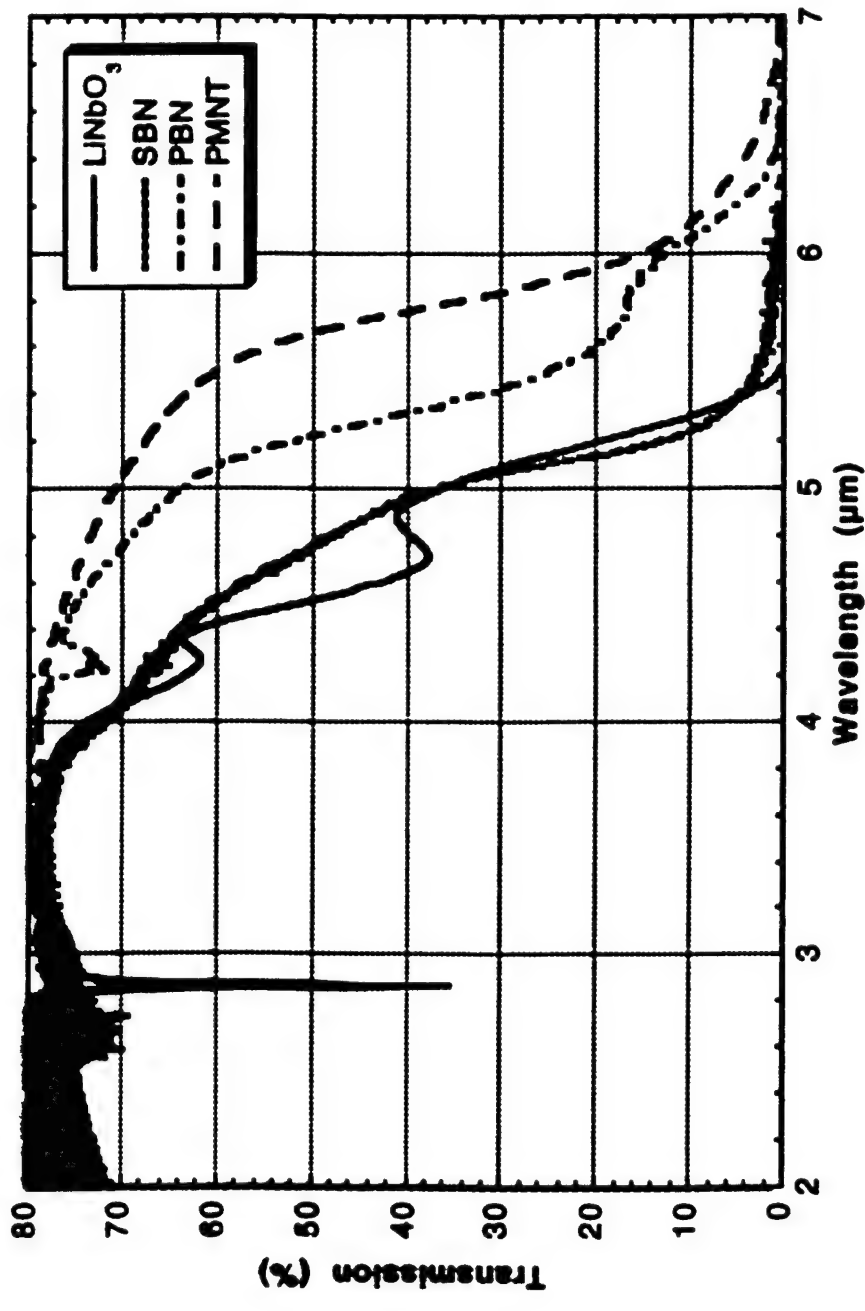
PMNT : $\text{Pb}\{\text{Mg}_x\text{Nb}_y\text{Ti}_{1-x-y}\}\text{O}_3$ Rockwell Science Center
(PMNT) to cover 4.5-6 μm band
Difficult to grow optically clear. Switch to
 $\text{Pb}_x\text{Ba}_{1-x}\text{Nb}_2\text{O}_6$ (PBN) to cover 4.5-5.5 μm band

KRTA : $\text{K}_x\text{Rb}_{1-x}\text{TlOAsO}_4$ Crystal Associates
Best for $x = 0$

LWIR (8-12 μm) THRUSTS

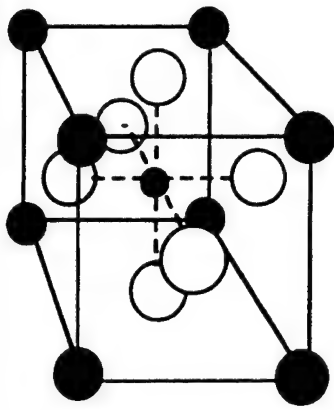
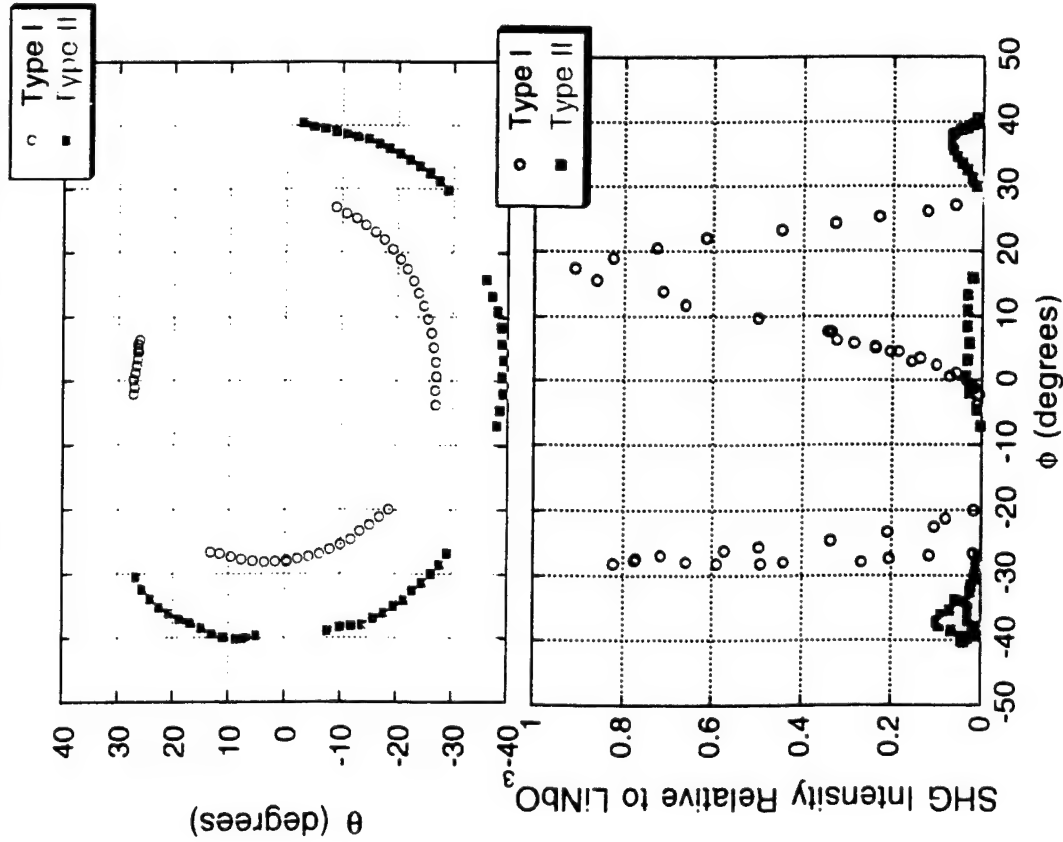
CsGeCl_3	Rockwell Science Center
CsGeBr_3	
Tl_3PbBr_5	Northrop Grumman
Tl_4PbI_6	(Pittsburgh) \rightarrow (Baltimore)
Tl_4HgI_6	

Comparison of Spectral Transparencies in Ferroelectric Oxides



New Family of NLO Materials: CGX

DPM Loci & d_{eff} in CsGeCl_3



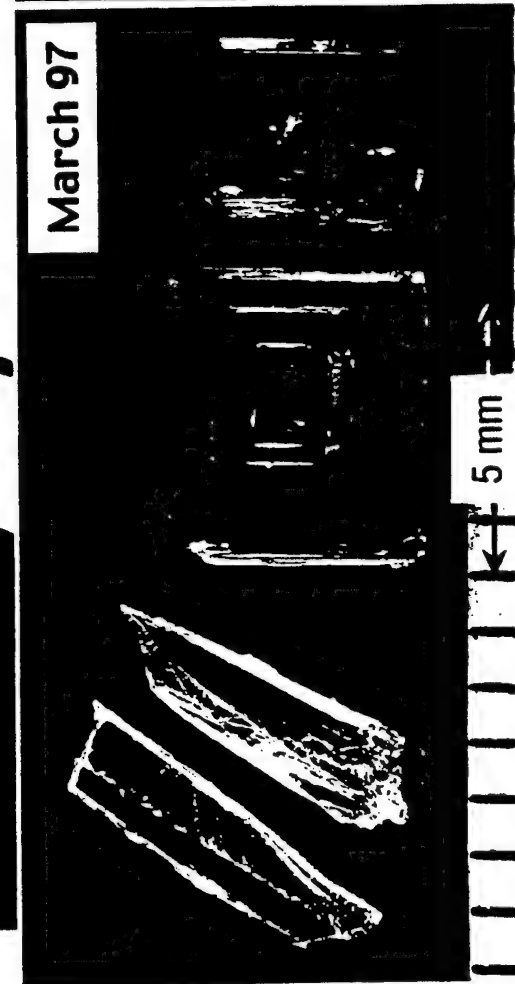
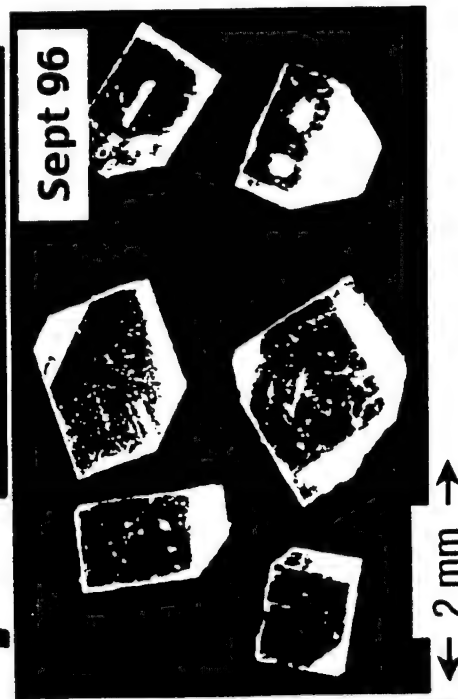
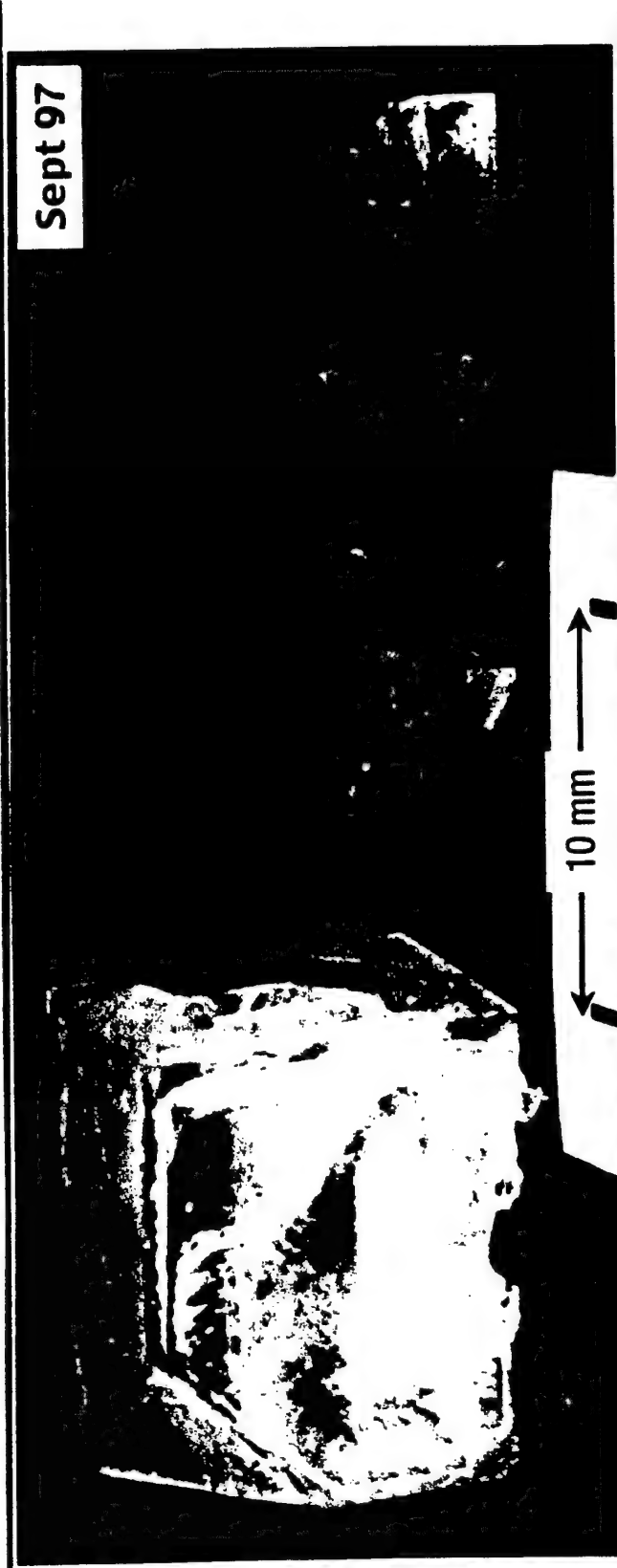
- Ge, Sn, Pb (2+)
- Cs, Rb (1+)
- Cl, Br, I (1-)

Ferroelectric Halides

- Perovskite structure
- Wide IR transparency
- Solution-grown semiconductor
- Mechanically robust
- Nonlinearity $\sim \text{LiNbO}_3$
- Periodically poled?

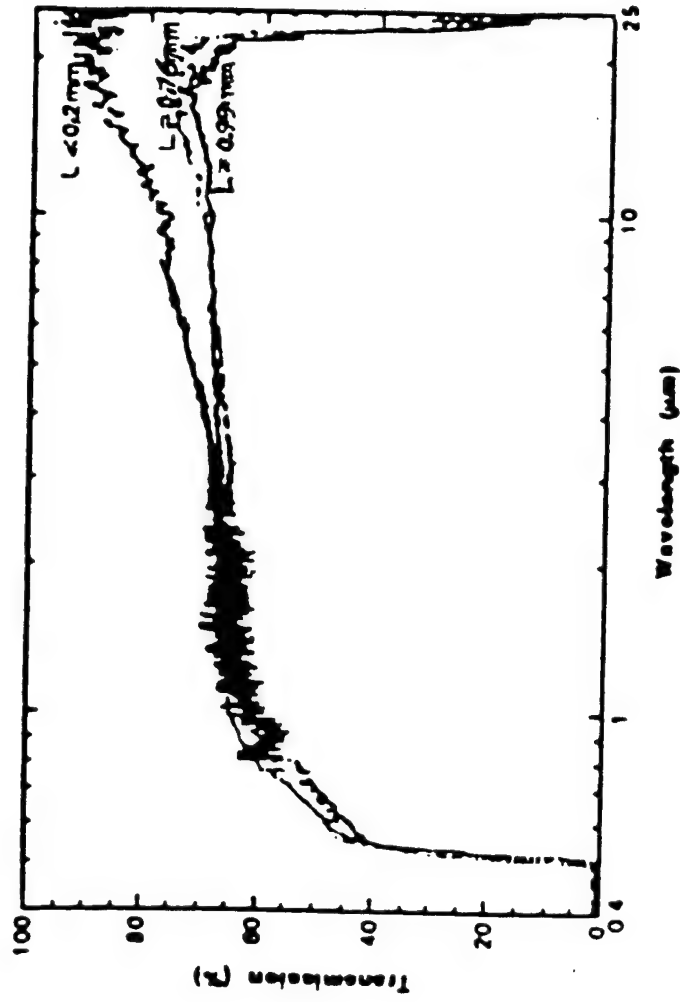
**Rockwell
Science Center**

Progress in Crystal Growth of CsGeCl_3



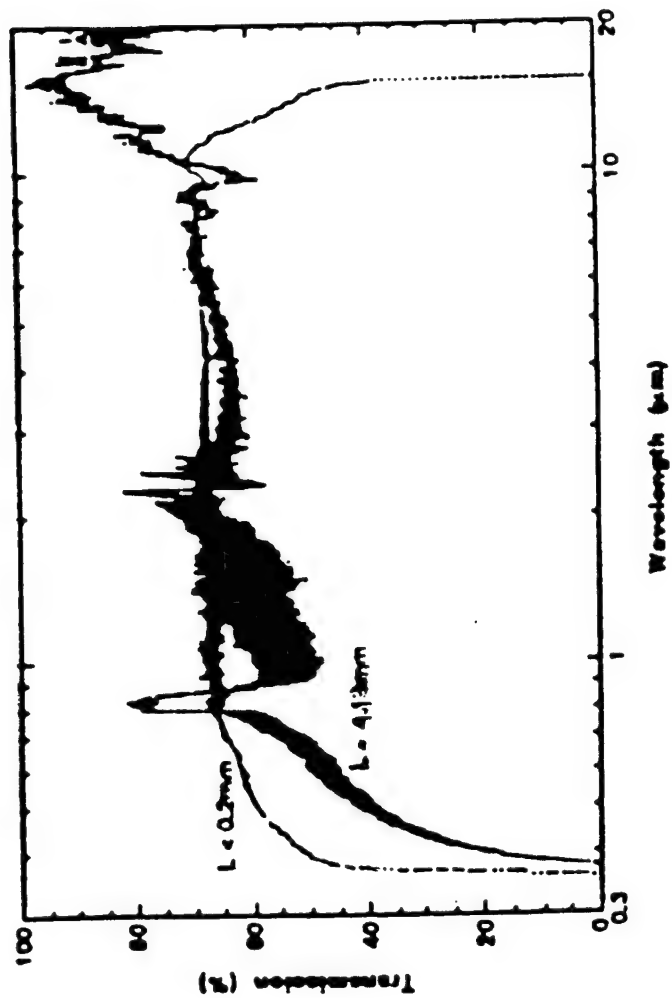
Rockwell
Science Center

CsGeBr₃ Transmission Spectra



Rockwell
Science Center

CsGeCl₃ Transmission Spectra

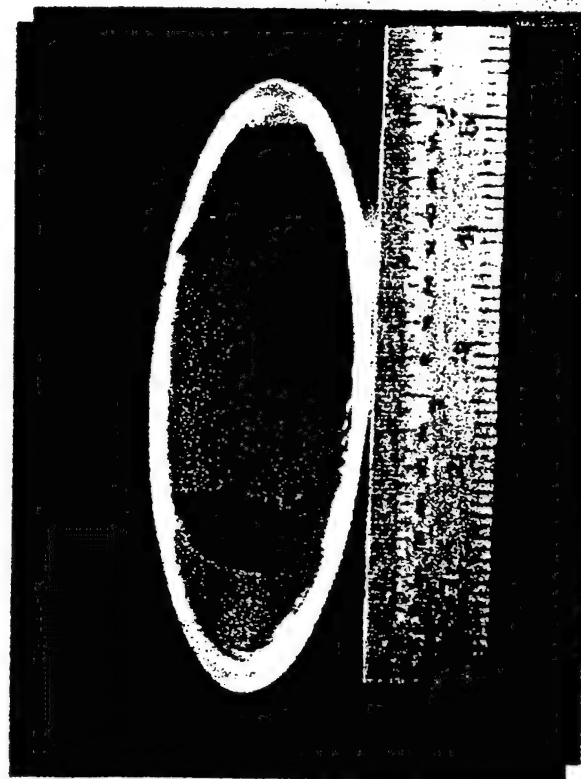


Rockwell
Science Center

We disclose a novel class of binary halides for the tunability of dielectric constant. This will enable very efficient tunable devices suitable for radar applications. These materials are combinations of $A^+ B^{n+} X$ (where A is monovalent, B is divalent and $X=F, Cl, Br$ and I). We have experimentally demonstrated the growth feasibility of $Tl_3 PbBr_5$, $Tl_3 PbI_5$ and $Tl_4 Hgl_6$ stoichiometry. Many other compounds such as $Rb_2 ZnCl_4$, $K_2 ZnF_4$, $K_2 ZnBr_4$ and $K_2 ZnCl_4$ also belong to this category. These compounds were grown by Bridgman method in large sizes and were fabricated in desired shape and sizes. The devices of these crystals will provide high performance rf tunable filters for radar receivers and communications for receivers such as SC-21 and JSF.

TOTAL INTERNAL REFLECTION QUASI PHASE MATCHED WAVELENGTH CONVERTER

- GaAs TIR QPM Converter
- Couple Pump Into Plate With GaAs Prism
- Output Via Prism Also Allows Use Of High CHI Two Materials With Little Or No Birefringence



Non-linear for IR
region in DTIM

L. I. Isaenko

Design & Technological Institute of Monocrystals SB RAS, 630090,
Novosibirsk, Russia, E-mail: lisa@lea.nsk.su



Outlines

I. Design & Technological Institute of Monocrystals SB RAS:

- field of activity, main crystals;
- contacts and collaborators;

II. Crystal real structure.

1. Investigation techniques;
2. Pyroelectric properties effect on processes of crystallization and defect formation (on example of KTA, LiInS_2);
3. Defects, appearing at deviation from stoichiometry (KTA, AgGaS_2 , LiInS_2);

III Structural investigation

1. Structural features responsible for spontaneous polarization P_s in KTA, LiInS_2
2. Structural simulation of doping process:
 - KTA, doped by Nd and Yb;
 - LiInS_2 , doped by Nd;
 - AgGaS_2 , doped by Yb

IV. Spectroscopic parameters of polyfunctional crystals

V. Double chlorides as active media for IR region

VI. Conclusions

Design & Technological Institute of Monocrystals,
Russian Academy of Sciences, Siberian Branch,
founded in 1978

The main trends of the scientific research:

- 1** The complex physic-chemical study of the growth processes of the optic quality single crystals for the laser technique and optoelectronics.
- 2** Experimental modeling of the diamond crystallization processes and the refinement of the methods of diamond instruments manufacturing.
- 3** Experimental modeling of the natural mineral formation processes and the improvement of the methods of gem crystals growth..

Main growth techniques:

TSSG, Czochralski, Bridgeman-Stockbarger, Kyropulos,
low temperature growth from aqueous and organic solutions

The main groups of crystals under consideration:

- Oxides; halogenides, chalcogenides (Tables);

Foreign collaborators:

1. The Lawrence Livermore National Laboratory, U.S.A.;
2. Tohoku University, Japan;
3. Observatory of Paris, Bureau of Metrology, Paris, France;
4. University of Bourgogne, Dijon, France,

Financial support:

1. Grant of the Civil research and Development Foundation (CRDF);
2. INCO-Copernicus grant;
3. Contracts with the LLNL beginning from 1992;
4. Contracts with other universities/ companies all over the world.

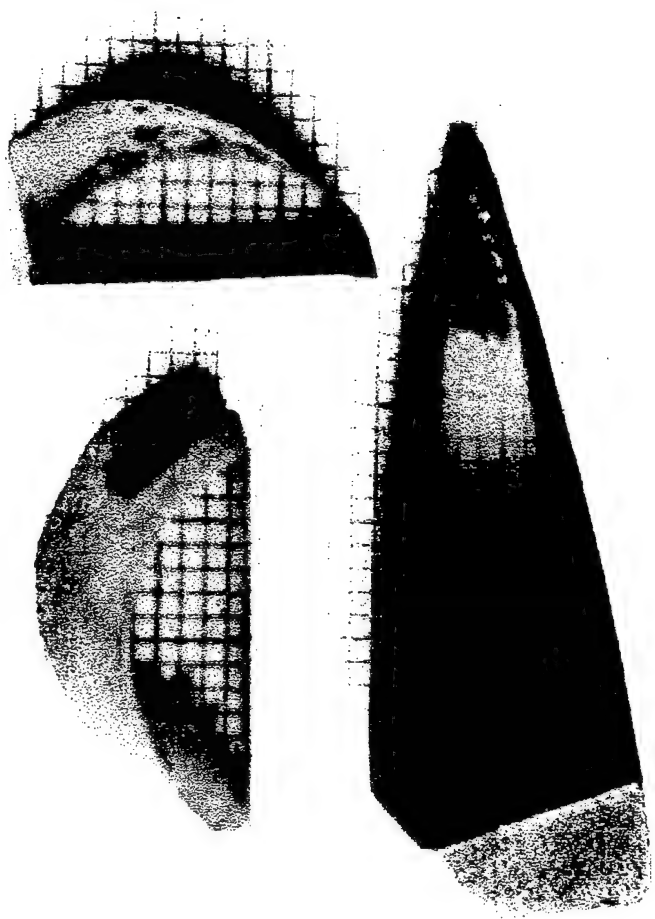
Table 2. SOME CHARACTERISTICS OF OBTAINED NONLINEAR SINGLE CRYSTALS

Crystal	Transparency μm	Max size of element (mm)	SHG cut off (nm)	Walk off angle (degree)	Optical damage threshold (MW/cm^2)	Conversion efficiency (%)
LBO	0.16 - 2.6	10 x 10 x 20	554	0.43(I) 0.22(II)	>10 000 (1.064 μm , 20 ns, 50 Hz)	70(1.064 μm , 20ns, 50Hz, 2W) 30(0.8 μm , 20ns, 50Hz, 2W) 55(1.064 μm , quasi CW, 2W) 50(1.064 μm , 20ns, 3W)
BBO	0.19 - 2.6	4 x 4 x 20	411	4.80	>2000 (1.064 μm , 10 ns)	30(1.064 μm , 20ns, 3W)
CLBO	0.18 - 2.8	5 x 5 x 15	471	1.83	>10 000	1.064 μm , 2W-5W
α-LiIO₃	0.28 - 5.6	30 x 30 x 30	630	4.0	500 + 100 (1.064 μm , 20ns)	50(1.064 μm , 20ns, 50Hz, 2W) 35(0.780 μm , 20ns, 10Hz, 2W) 20(1.064 μm , 20ns, 50Hz, 3W)
KTP	0.35 - 4.5	5 x 5 x 15	990	0.06	500 (1.064 μm , 20ns)	60(1.064 μm , 10ns, 50Hz, 2W)
KTA	0.35 - 5.5	5 x 5 x 20	1083	0.06	>10 000 (1.064 μm , 70 ps)	OPO pumping by 20-30 (1.064 μm , 20ns) to 3-5 μm
POM	0.44 - 2.1	8 x 8 x 8	1000		2000(1.064 μm , 15ns) 75(0.53 μm , 15ns)	20(1.32 μm , 10ns, 10MW/ cm^2 L=4mm
BLAP	0.23 - 1.95	10 x 10 x 10	532	2.0	>10 000 (1.064 μm , 20ns)	
LiInS₂	0.4 - 12	5 x 5 x 10			>100 (1.064 μm , 10 ns)	OPO up to 10 μm
LiInSe₂	0.6 - 15	5x5x5			>50(1.064, 10 ns)	
AgGaS₂	0.46 - 12	10 x 10 x 20	1736		8000(1.06 μm , 15ps, 10Hz) 75(1.06 μm , 10ns, 20Hz)	OPO up to 10 μm (1.064 μm , 20ps, 10mJ)
AgGaSe₂	0.65 - 18	5x5x5			>50	OPO up to 10 μm DFG up to 18 μm
GaSe	0.7 - 18	5x5x5			3.7 J/ cm^2 (9.25 μm) 0.5 (cw 10.6 μm)	1 (OPO 2.94 μm , 100 ps) DFG up to 18 μm

Specific effects at crystallization/cooling of pyroelectric (ferroelectric) crystals

1. **A strong anisotropy in growth rates** along and across polar axis;
2. **Self-organization of extended defects** structure directed to lower or compensate completely the large pyroelectric fields inside crystal appearing at crystallization or cooling:
 - Formation of **twin or domain structures** from several blocks with different (opposite) direction of spontaneous polarization vector P_s .
 - Formation of **channel type defects** extended along polar axis and filled by different phases with lower melting temperature which operates as a conductor removing the fields appearing in the «ideal» pyroelectric lattice.
3. **Cracking of the crystals** is particularly dangerous in temperatures where pyroelectric coefficient γ has maximum.
4. Pyroelectric fields stimulate **migration of alkali cations** and **formation of defects** in the cation sublattice.
5. The electric discharge as a result of huge pyroelectric fields inside crystals is one of the mechanisms of their **mechanical damage** at cooling or during operation in laser schemes.







Single crystals



pyroelectrics
ferroelectrics



pyroelectrics



nonpyroelectrics

Symmetry

(point group)

$\text{mm}2$

$\text{mm}2$

$\bar{4}2\text{m}$

Lattice parameters

$a = 13.103 \text{ \AA}$

$b = 6.558 \text{ \AA}$

$c = 10.746 \text{ \AA}$

$d = 3.45$

$a = 6.887 \text{ \AA}$

$b = 8.05 \text{ \AA}$

$c = 6.474 \text{ \AA}$

density (G/cm^3)

$d = 3.5$

$a = 5.757 \text{ \AA}$

$c = 10.305 \text{ \AA}$

$d = 4.56$

Growth techniques

($T_{\text{cryst.}} = 850\text{--}1000 \text{ }^\circ\text{C}$)

TSSG

with pulling
from selfflux
in $\text{K}_2\text{O}\text{--}\text{As}_2\text{O}_5\text{--}$
 TiO_2 system

Bridgeman-

Stockbarger

from melt

Bridgeman -

Stockbarger

from melt

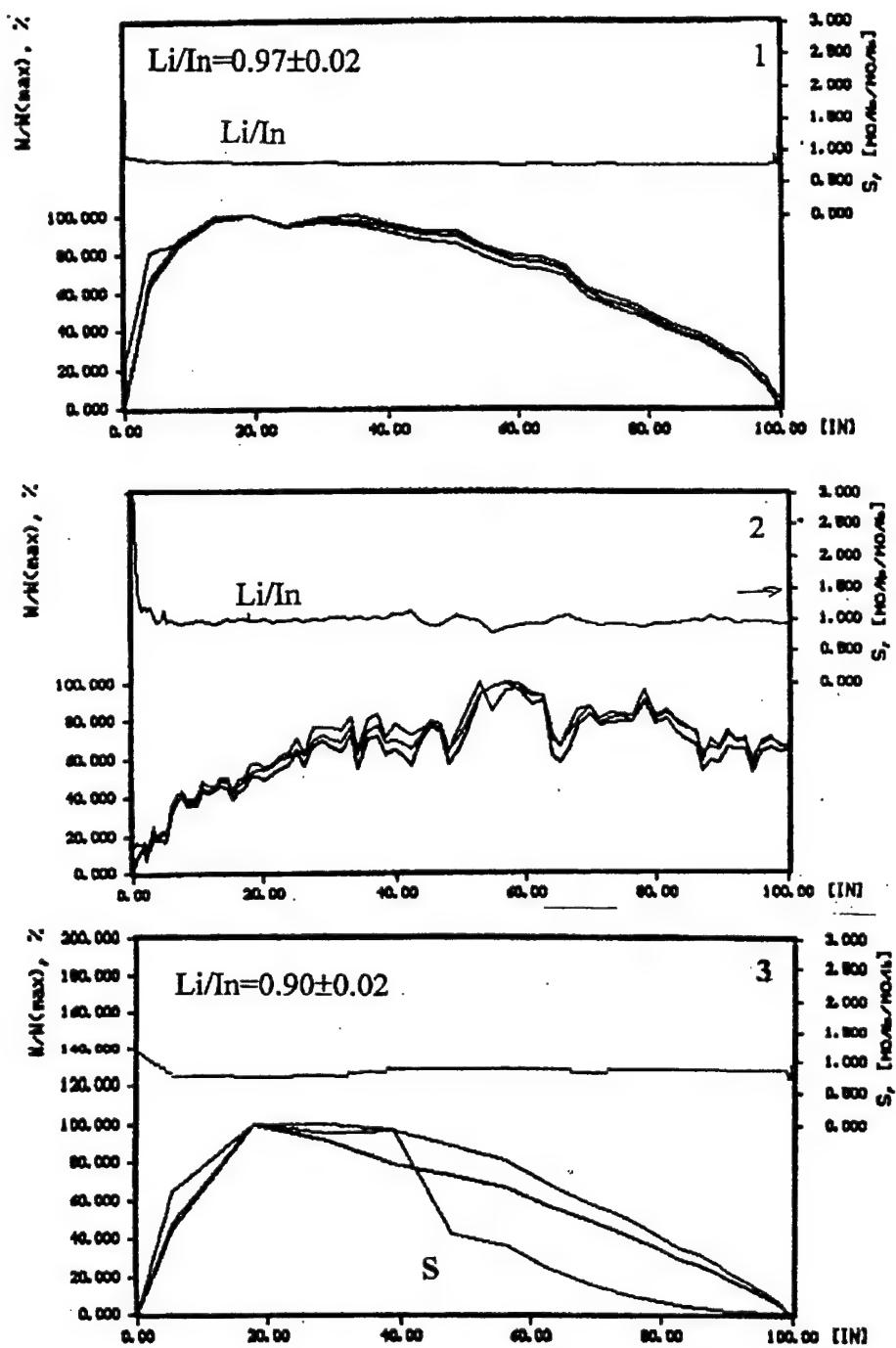
Boule size (mm^3)

$50 \times 55 \times 45$

$20 \times 20 \times 50$

$25 \times 25 \times 100$

The technique of differential dissolving combined with the ICP analysis
(inductively coupled plasms)



Kinetic curves of dissolving, Li/In stoichiogramms for:
1, 2 – grown samples, 3 – annealed in S_2 sample

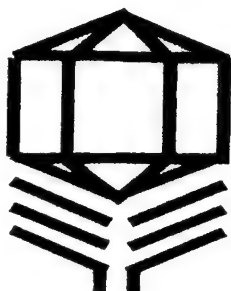
	KTA		LiInS ₂	AgGaS ₂	
Dopant	Yb	Nd	Nd	Yb	Nd
Segregation coefficient C _{cryst} /C _{melt}	0.2	10 ⁻³ -0.1*	0.02	0.02-0.3**	<10 ⁻³
Possible position of dopant ion in the lattice	Distorted TiO ₆ prism, two sites: Ti(1),Ti(2)	K-O(8,9) polyhedral Formation of NdO ₇	Octahedral cavity	Octahedral cavities Distorted octahedral	
Absorption cross-section, cm ² (300K)	1.2 x10 ⁻²⁰		2x10 ⁻²⁰		

Notes: * for KTA:Me²⁺

** for milky as grown AgGaS₂ sample

Necessary conditions for dopant stability in the crystal structure:

- Coordination number ≥ 6 ;
- Similarity of sizes for dopant ion and host site;
- Charge compensation



**Design & Technological Institute
of Monocrystals SB RAS**

43 Russkaya str.,
Novosibirsk 630058 Russia
E-mail: alex@elis.nsk.ru

**Spectroscopic properties
of pure and Rare Earth-doped
nonlinear crystals for the mid-IR**

A.Eliseev

Outline:

A. Spectroscopic features of pure nonlinear crystals

**1. Absorption /luminescence of pure nonlinear single
crystals for the mid -IR: excitation mechanisms**

- **KTiOAsO₄ (KTA);**
- **AgGaS₂;**
- **LiInS₂.**

B. Spectroscopic properties of RE-doped crystals

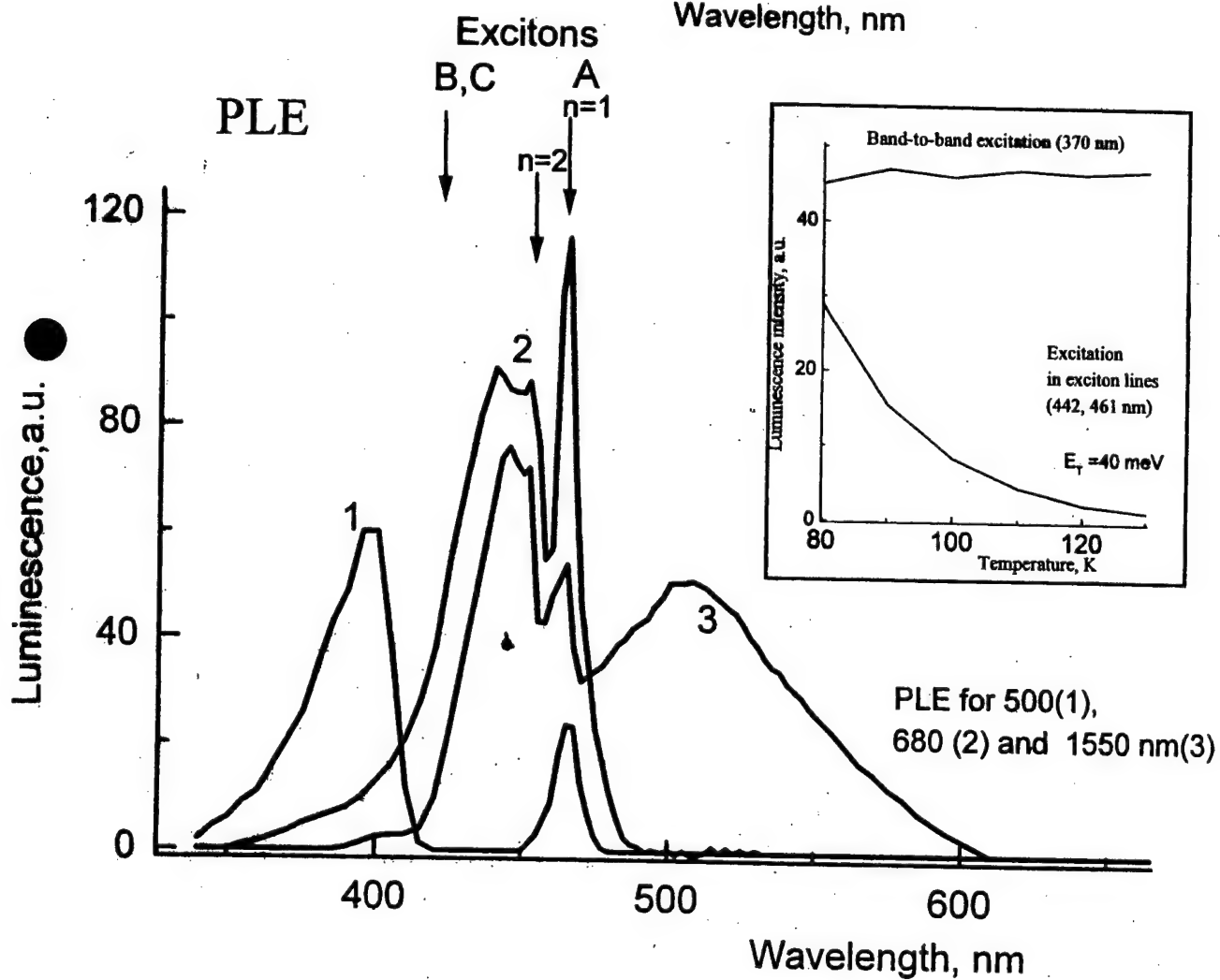
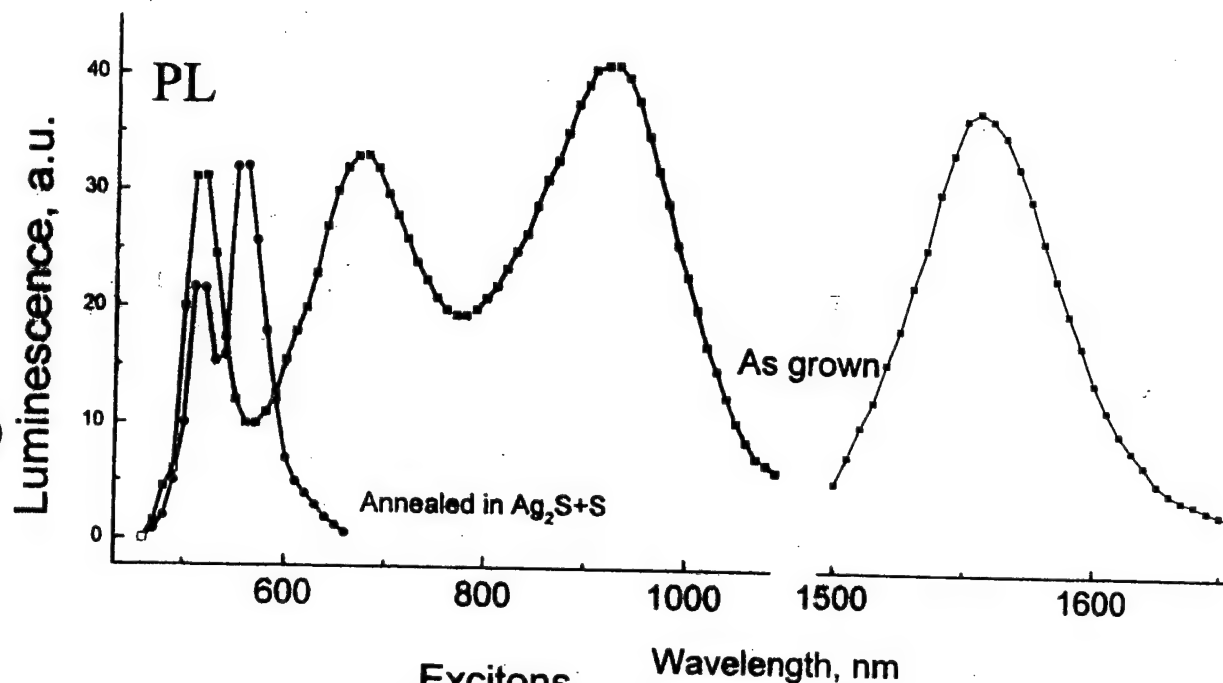
1. Option of RE dopants for nonlinear crystals as

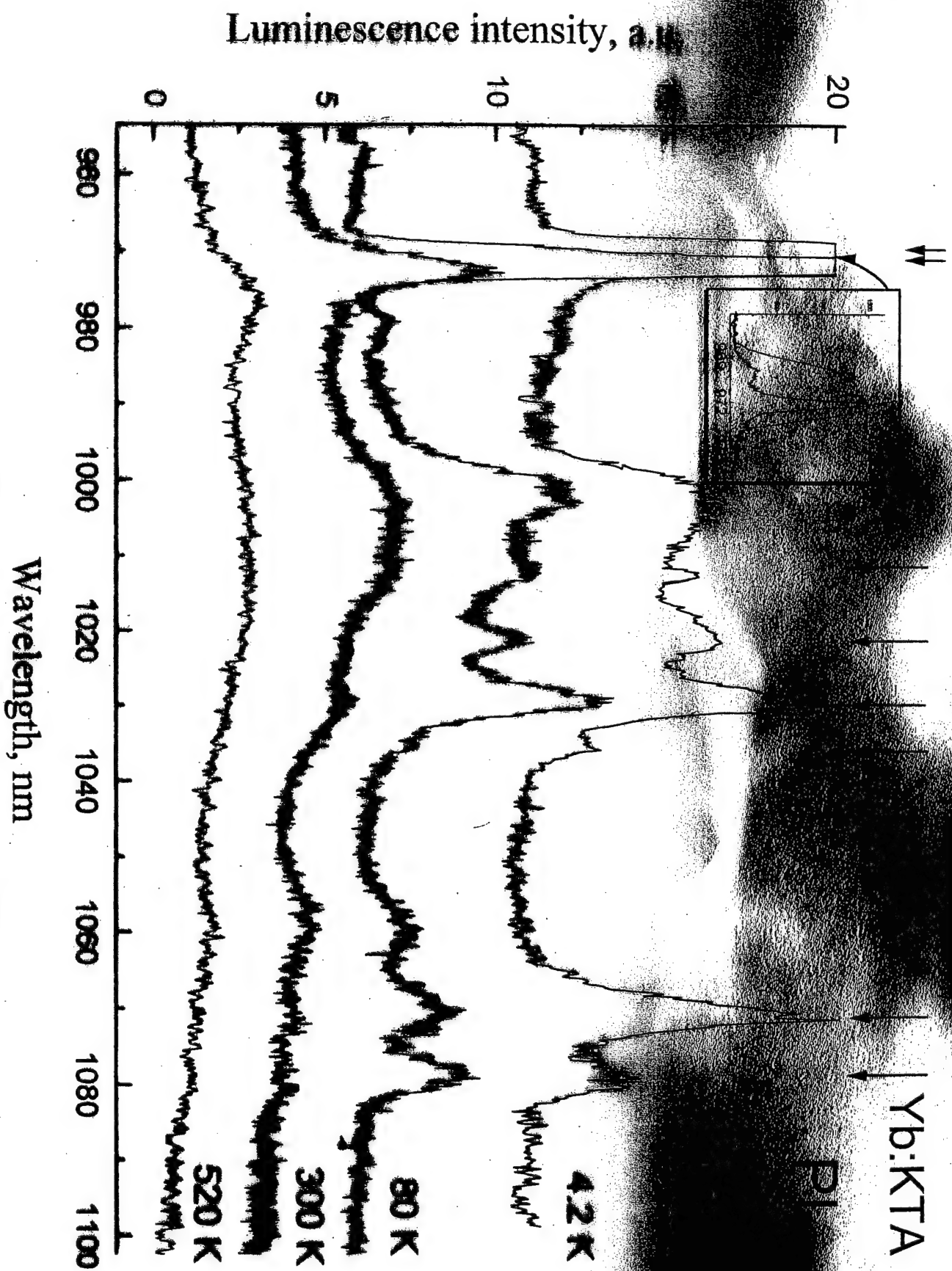
- **Polyfunctional laser elements;**
- **Chalcogenides as an active media for the mid IR;**

2. Spectroscopy of Nd and Yb: spectra, decay times,

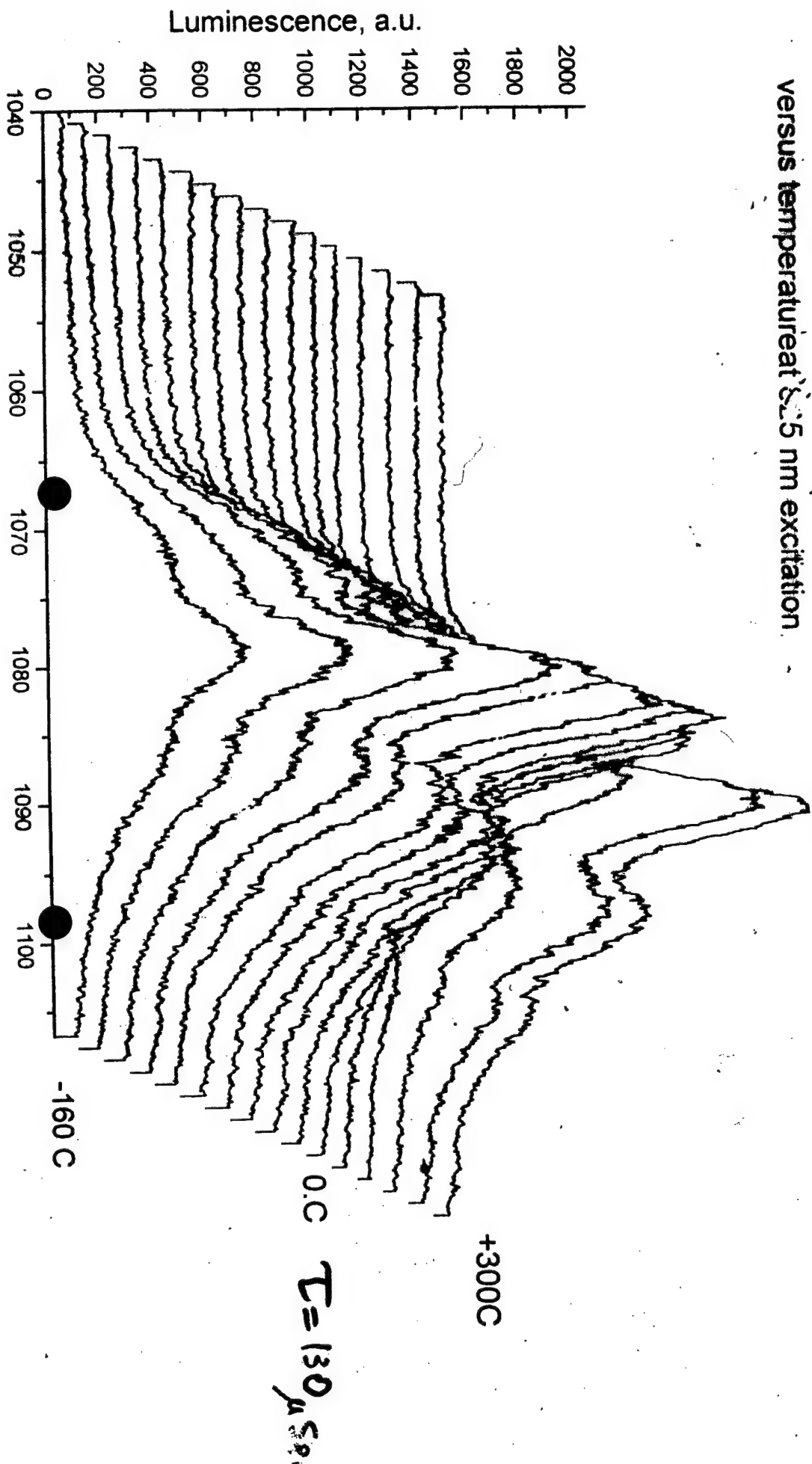
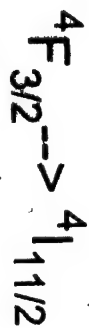
**3. Radiation and radiationless multiphonon
relaxation, stimulated emission in the mid-IR**

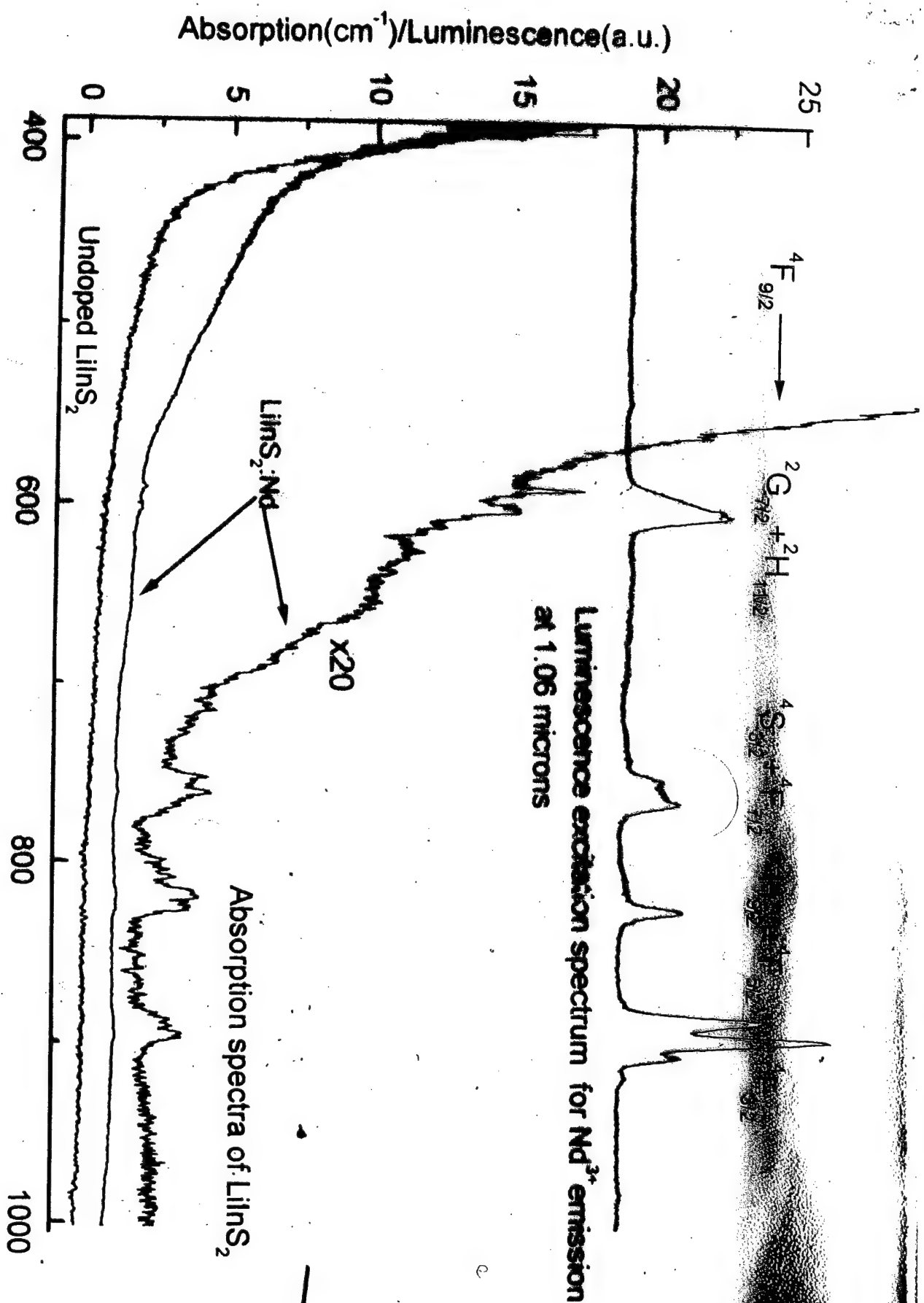
Photoluminescence in AgGaS_2 , $T=80\text{K}$





Luminescence spectra of $\text{LiInS}_2:\text{Nd}$
versus temperature at 825 nm excitation





Growth and Optical Properties of $\text{LiNbO}_3\text{-WO}_3$ and $\text{LiNbO}_3\text{-MoO}_3$ solid solutions

A. Hill, A. Pirie, T. P. J. Han and H. G. Gallagher

Optical Materials Research Centre
Department of Physics and Applied Physics
University of Strathclyde
Glasgow G1 1XN, Scotland, UK

Tel: +44-141-548 4015 ; Fax: +44-141-553 4162

E-mail: h.g.gallagher@strath.ac.uk

Crystal Growth

- Method: Czochralski

- Composition: $X < 10 \text{ mol\%}$

Solid solution range of $\text{Li}_{1-x}\text{Nb}_{1-x}\text{W}_x\text{O}_3$:-

At $T = 860^\circ\text{C}$, $X = 0 - 50 \text{ mol\%}$

Blasse et al, 1970

At $T = 750^\circ\text{C}$, $X = 0 - 20 \text{ mol\%}$

Foulon et al, 1998

Solid solution range of $\text{Li}_{1-x}\text{Nb}_{1-x}\text{Mo}_x\text{O}_3$:-

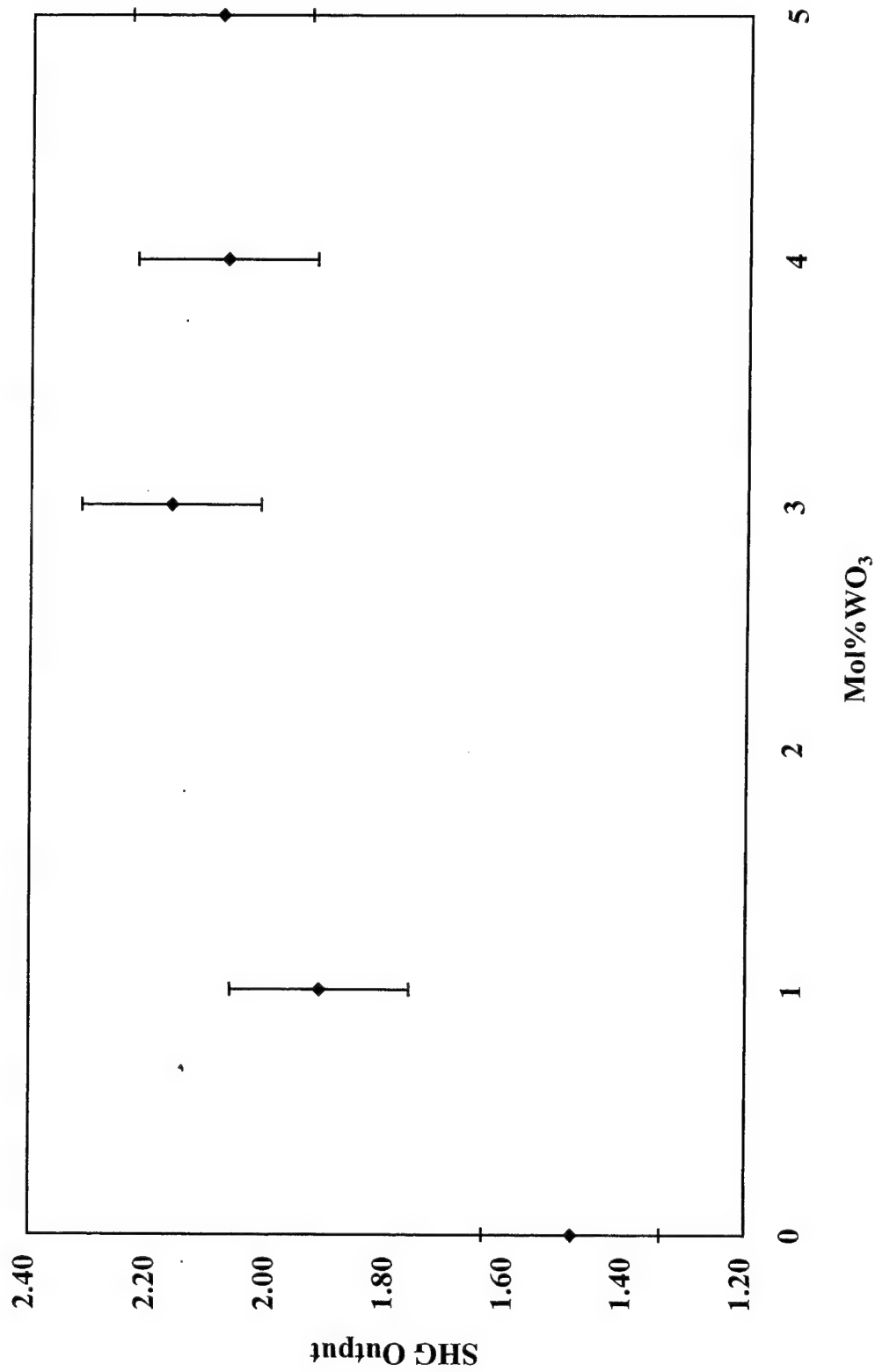
At $T = 860^\circ\text{C}$, $X = 0 - 30 \text{ mol\%}$

Blasse et al, 1970

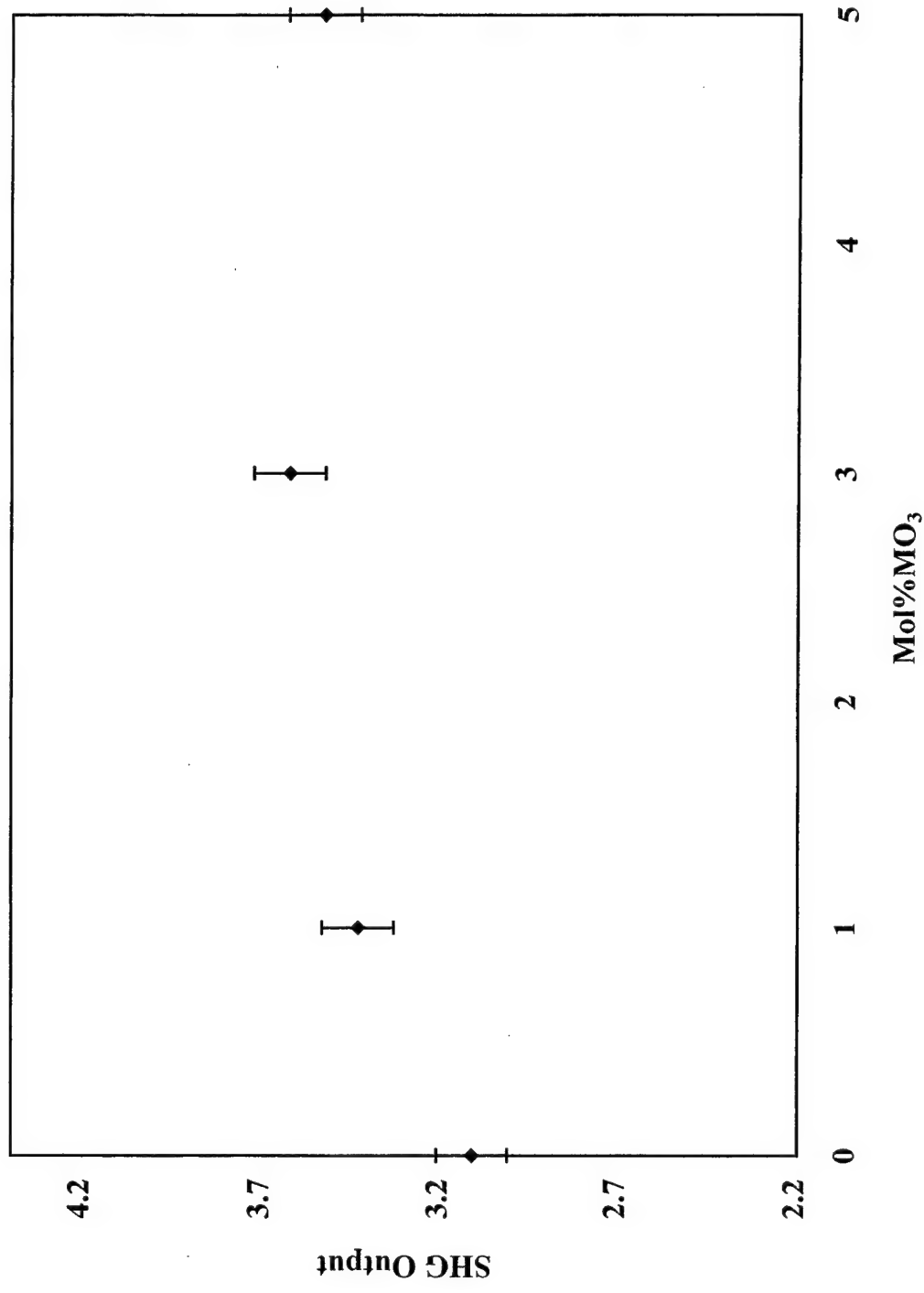
- Melting temperature: $1180 - 1250^\circ\text{C}$

- Poling: $1 - 2 \text{ mA/cm}^2$ at 1200°C

Variation in Powder SHG for LiNbO₃ Doped with Various Concs. of WO₃

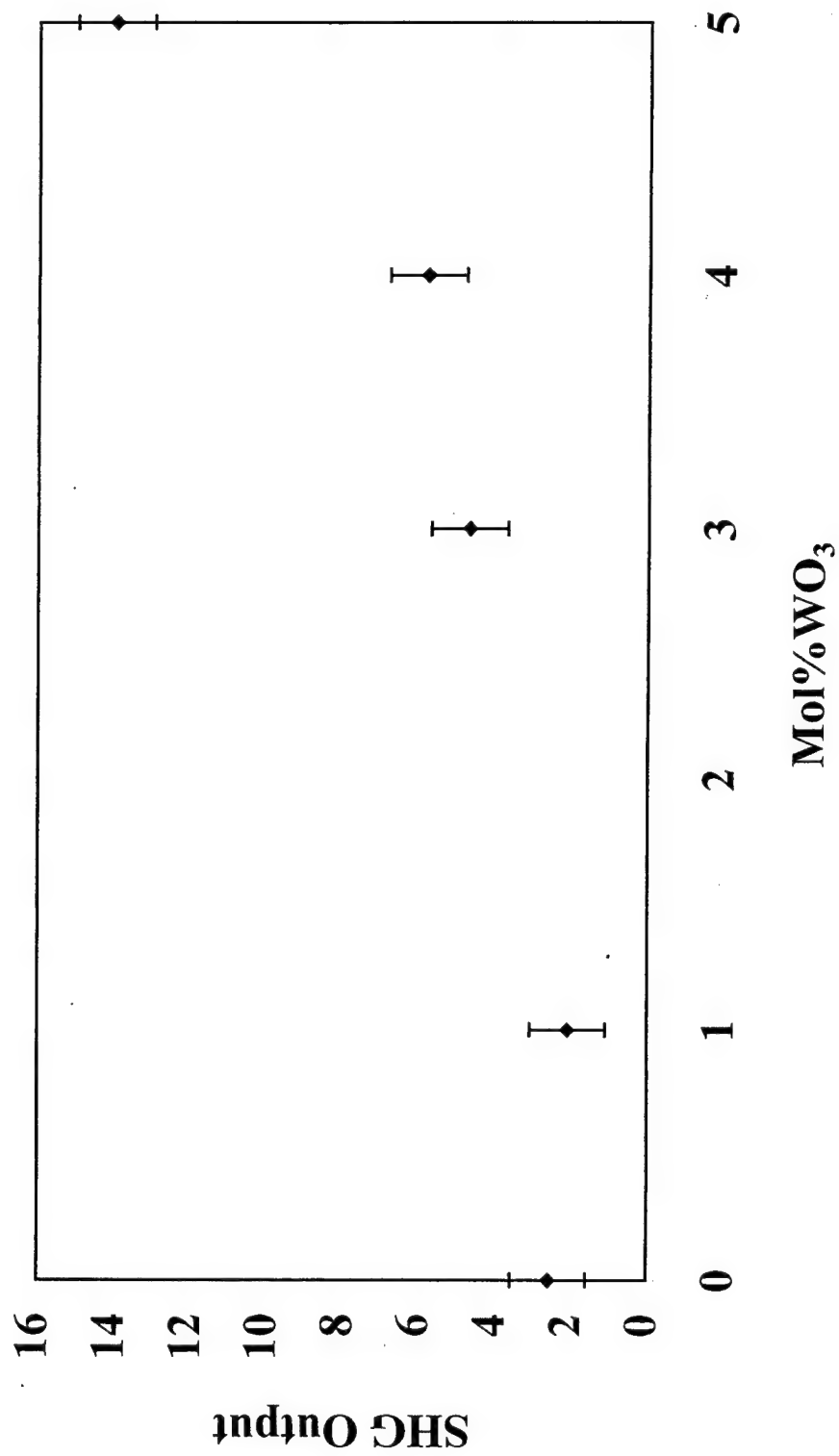


Variation in Powder SHG for LiNbO₃ Doped with Various Concs. of MO₃

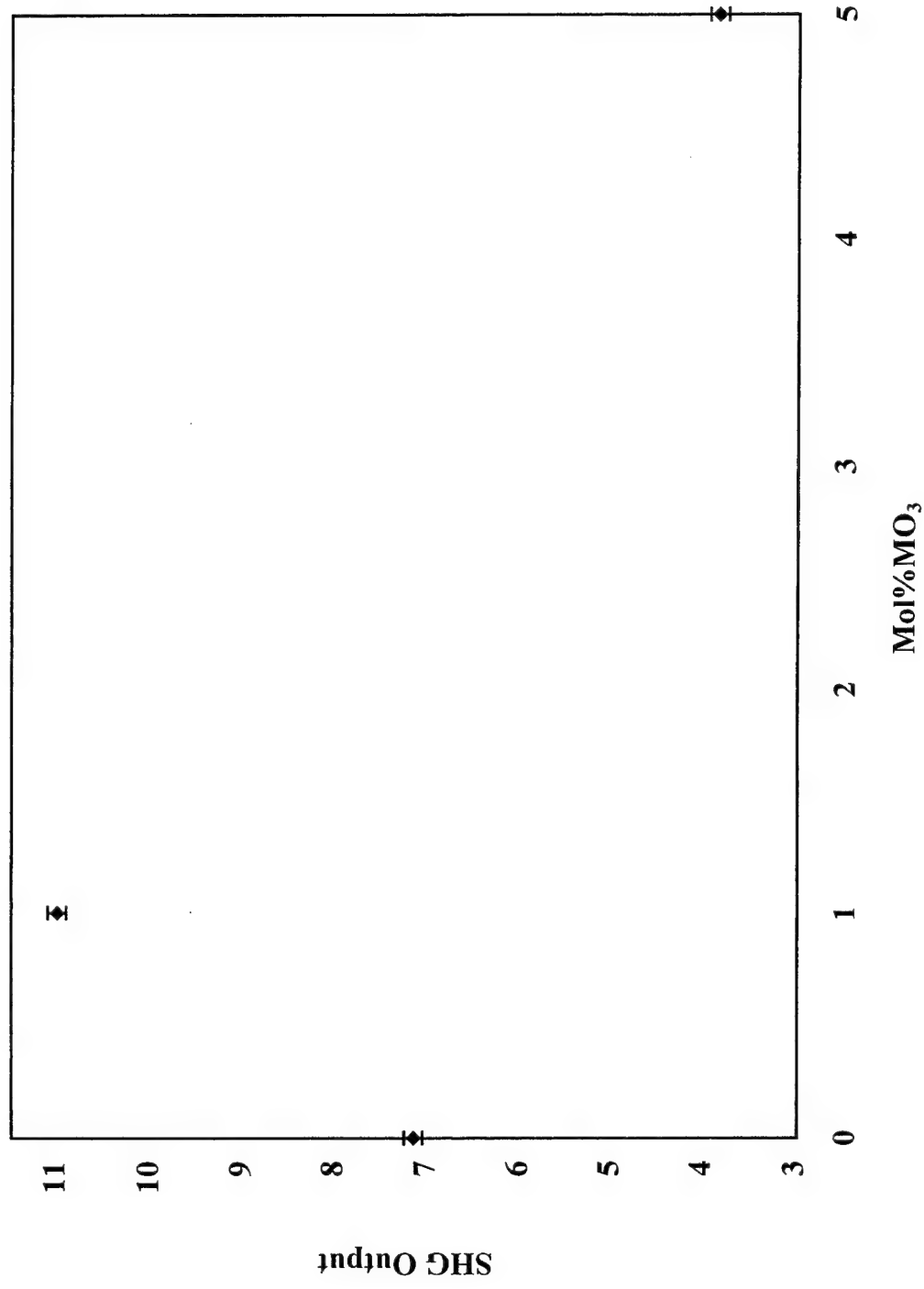


● ●

Variation of d_{33} Coefficient for LiNbO_3 Doped with Various Concentrations of WO_3



Variation of d_{33} Coefficient for LiNbO_3 Doped with Various Concs. of MO_3



Conclusions

- The solid solution range for growth of $\text{Li}_{1-x}\text{Nb}_{1-x}\text{W}_x\text{O}_3$ and $\text{Li}_{1-x}\text{Nb}_{1-x}\text{Mo}_x\text{O}_3$ crystals is limited to $x = 0.5$ due to cracking and constitutional cooling, respectively
- Optical properties vary (linearly?) with concentration of WO_3 and MoO_3
- Further work is required to refine growth conditions and eliminate optical defects
- More detailed optical characterisation is necessary

Growth and Characterisation of Photorefractive Materials

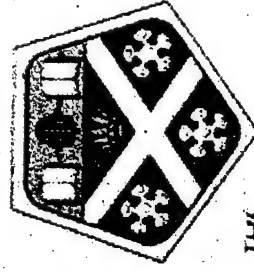
Craig.J. Finnan, H.G. Gallagher, T.P.J. Han.

Optical Materials Research Centre (OMRC),

University of Strathclyde

G. Cook, D. Jones

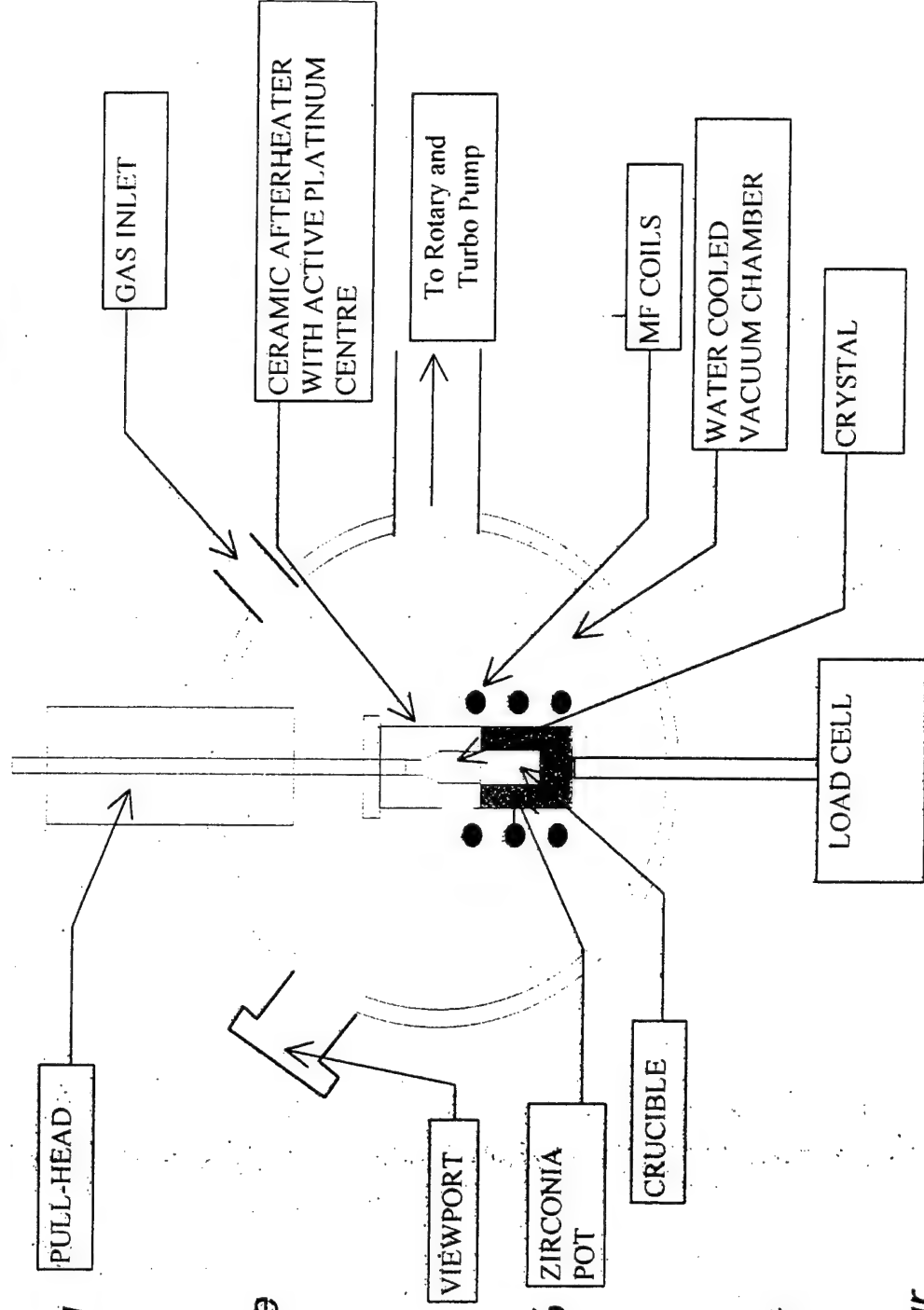
DERA Malvern



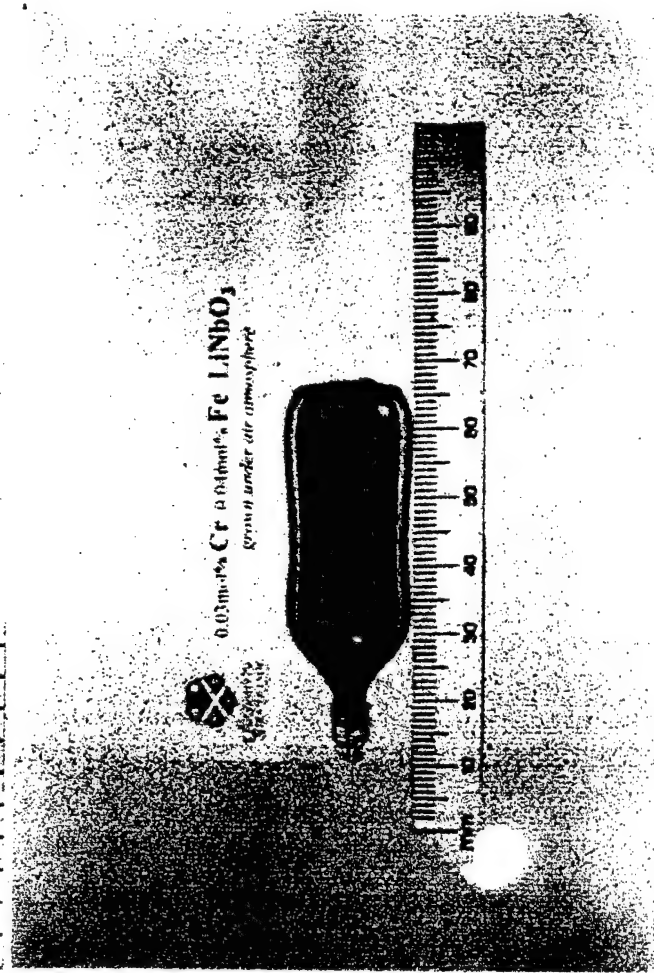
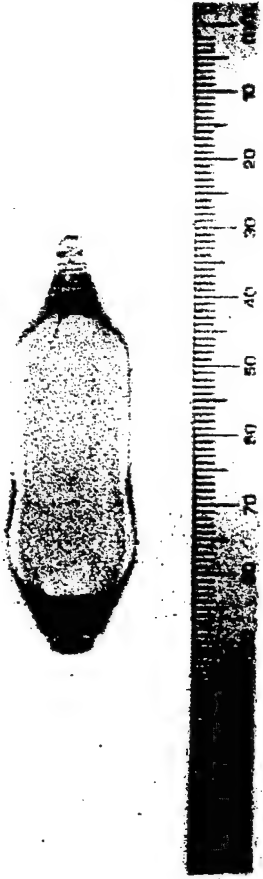
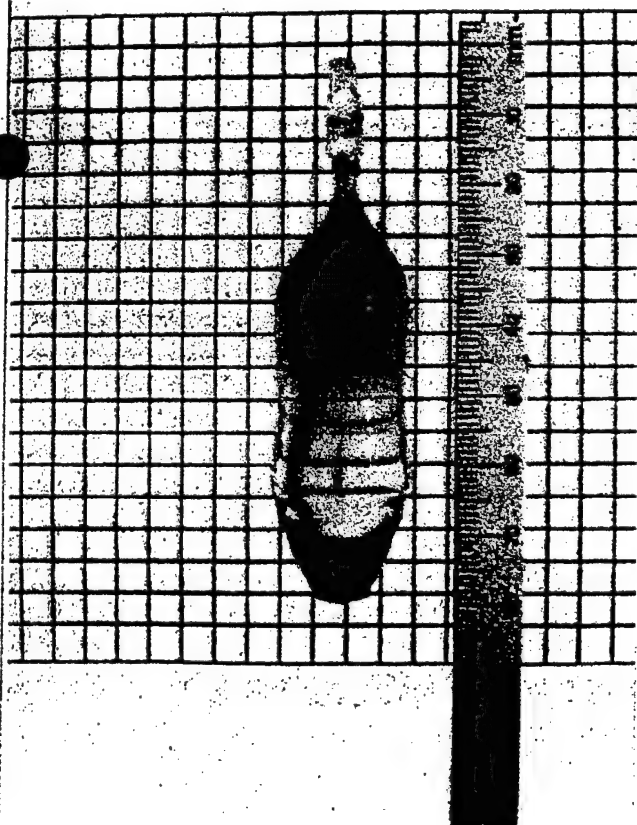
**THE
UNIVERSITY OF
STRATHCLYDE
IN GLASGOW**

DERA

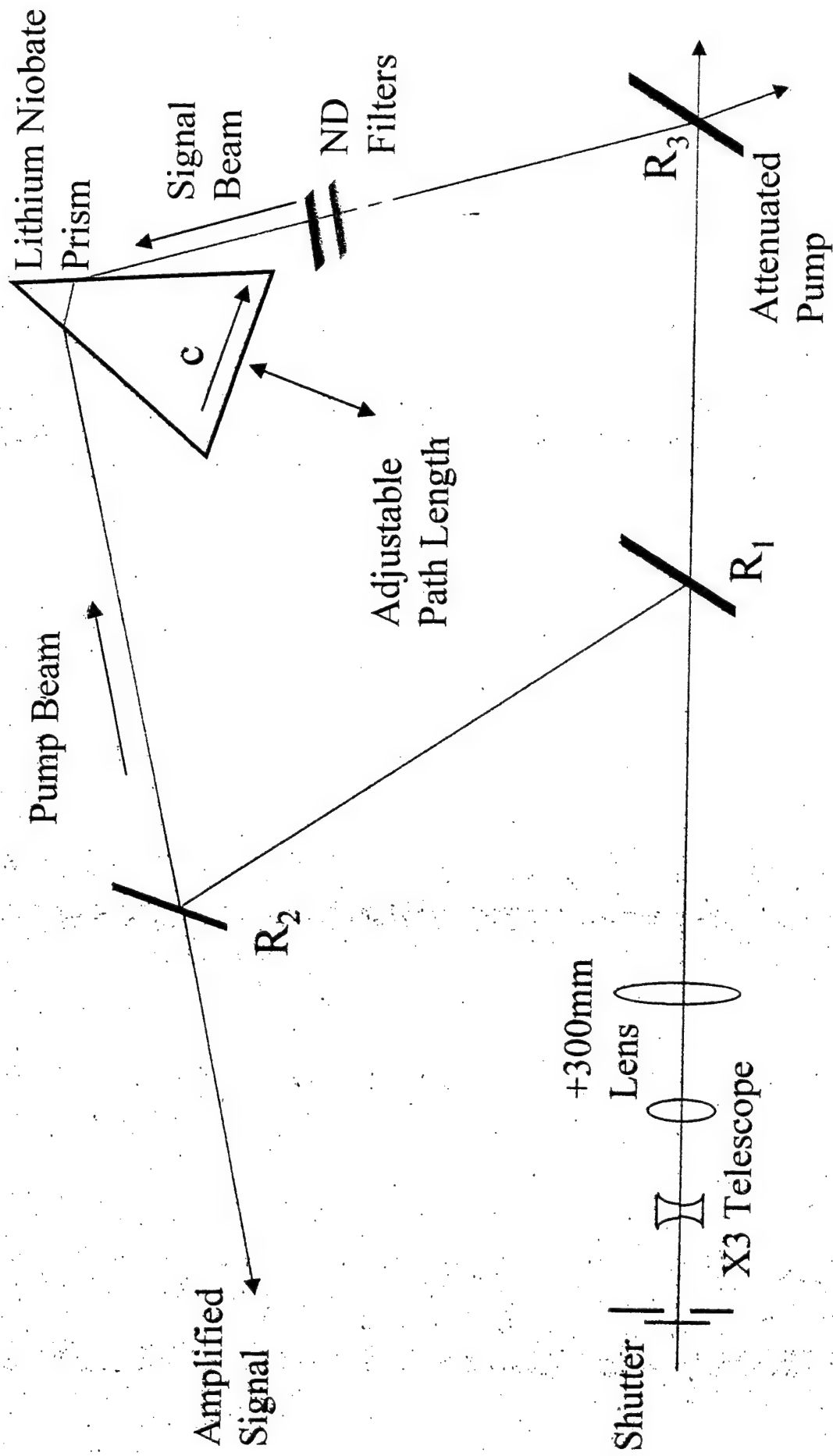
Czochralski Growth Technique



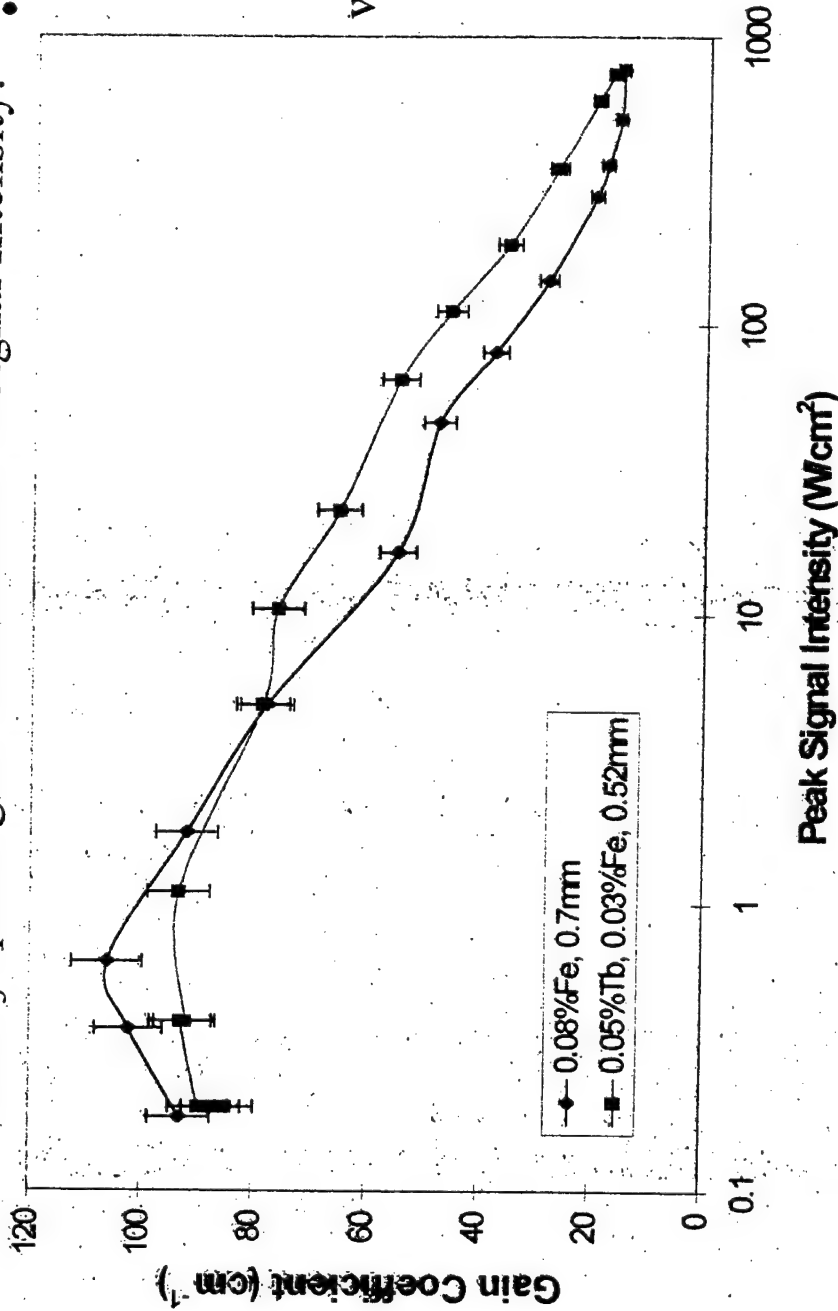
- ◆ Both single and co-doped Fe:LiNbO_3 samples have been grown.
- ◆ Congruent Lithium Niobate is best grown from a melt by the Czochralski technique.
- ◆ Congruent composition is 48.6mol% Li_2O , 51.4mol% Nb_2O_5 .
- ◆ To reduce thermo-Mechanical Strain, a Platinum Afterheater must be used.
- ◆ Surface cracking can occur due to Li_2O evaporation.



EXPERIMENTAL SETUP



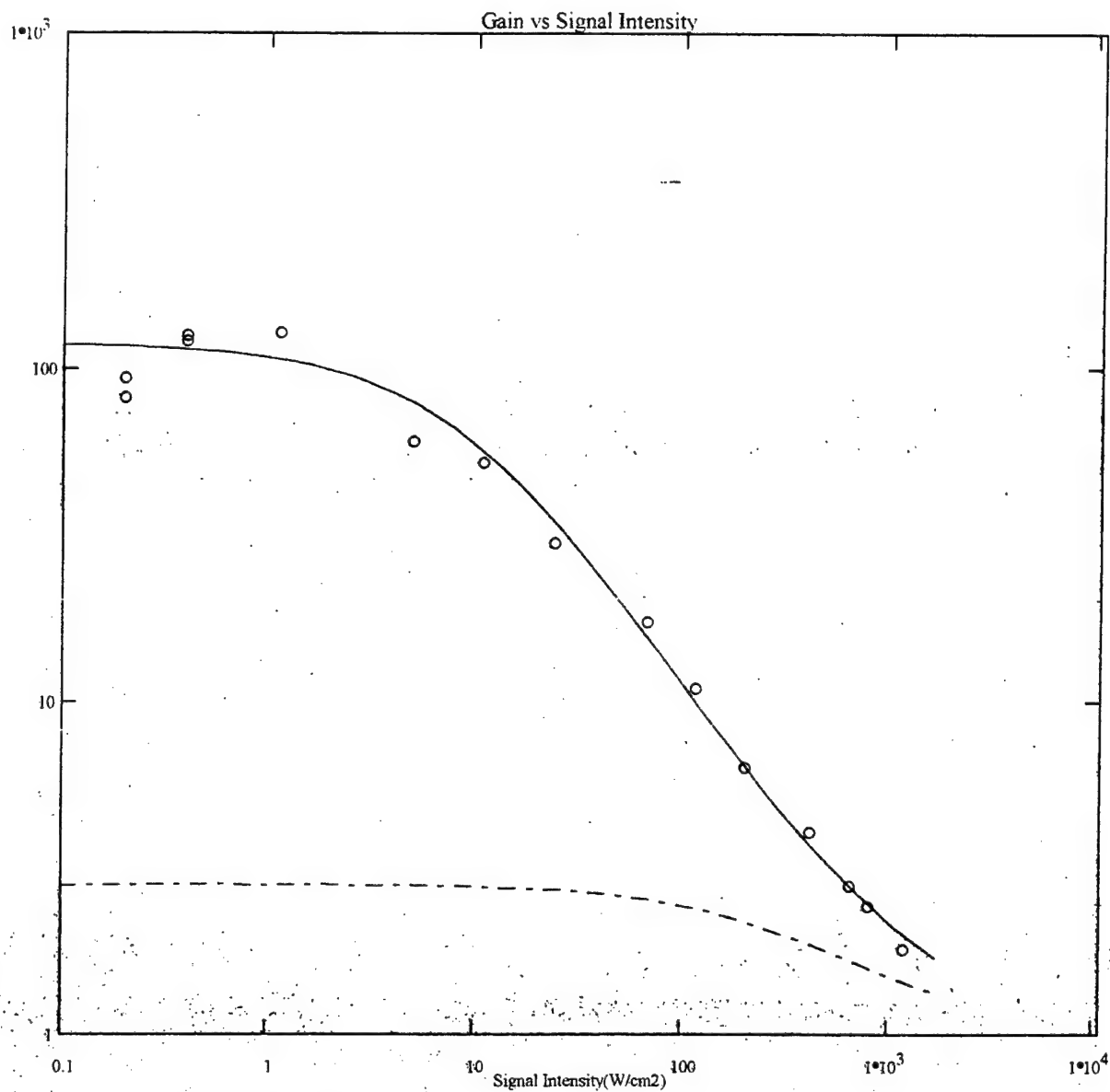
LiNbO₃ optical gain as a function of Signal Intensity.



- Pump intensity is constant at 1kW/cm².
- Gain Coefficient is calculated from,

$$G = \frac{\ln \left[\frac{(I_a - I_b)}{I_s} \right]}{l}$$

where I_B is the background intensity with no pump beam, I_S and I_A are the intensities of the transmitted signal beam in the presence and absence of the pump, and l is the sample thickness



— Fit to Data($\Gamma=92\text{cm}^{-1}$)
-- Normal Diffusion Theory($\Gamma=20\text{cm}^{-1}$)
ooo Data

Developments in PPLN Fabrication at the ORC

Dr. Peter G.R. Smith

Prof. D.C. Hanna, Prof. D.J. Richardson

Dr R.W. Eason, Dr. Graeme Ross, Dr. Neil Broderick

Dr. H.L. Offerhaus

Paul Britton, Cowin Gawith, Joyce Abernethy, Ian Barry

Outline

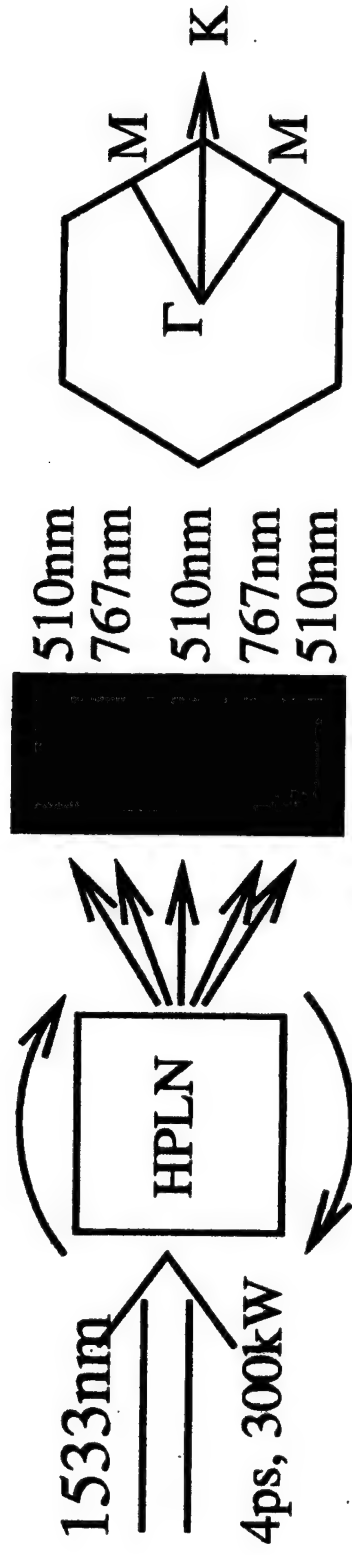
- PPLN Fabrication 1mm material
- PPLN OPOs and fibre lasers
- Etched PPLN microstructuring
- HeXLN

PPLN Fabrication 1mm material

- **DERA Supported Project**
- **Constructed a current controlled poling rig for 1mm samples**
- **Successfully fabricated 1mm thick PPLN at coarse periods $>25\mu\text{m}$.**
- **Issues are breakdown through the material, electrode design, yield.**
- **Future - how to improve quality, how to improve yield? Can push to 2mm?**



Experimental Setup



- A schematic of the experimental setup is shown above. The pulse source is a high power all-fibre CPA source.
- The input pulses were ~ 3 ps long with a bandwidth of 2nm and a maximum peak power of 300kW.



2D patterned PPLN

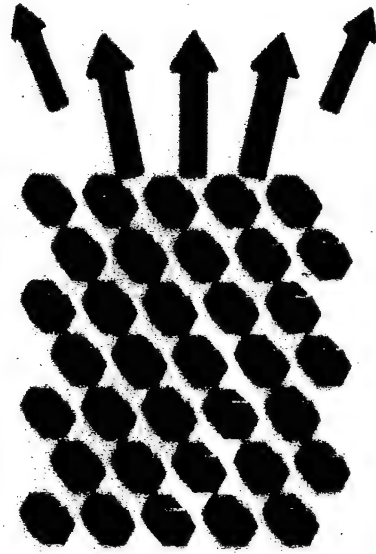
Light

Inverted domains

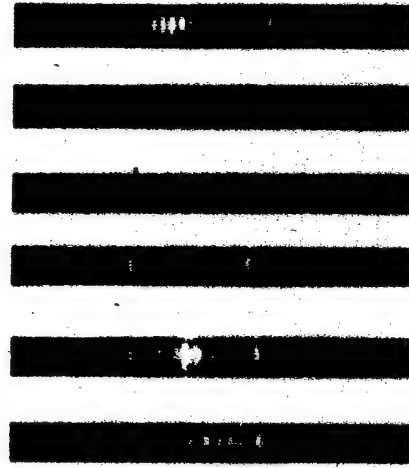
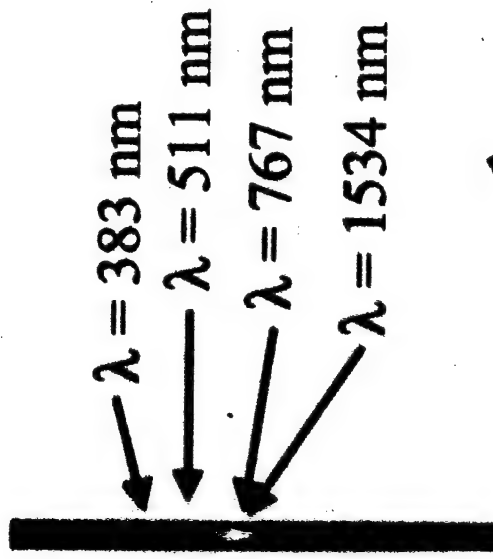
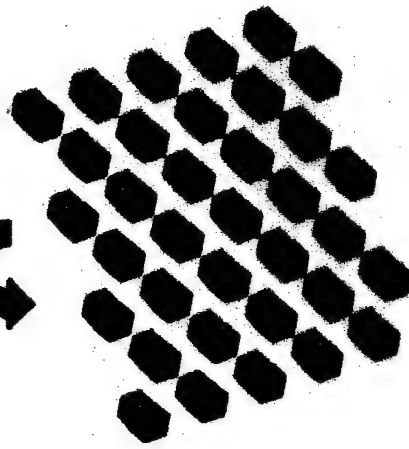
Normal incidence



$\lambda = 1.534 \mu\text{m}$
4ps, 300kW



Angled



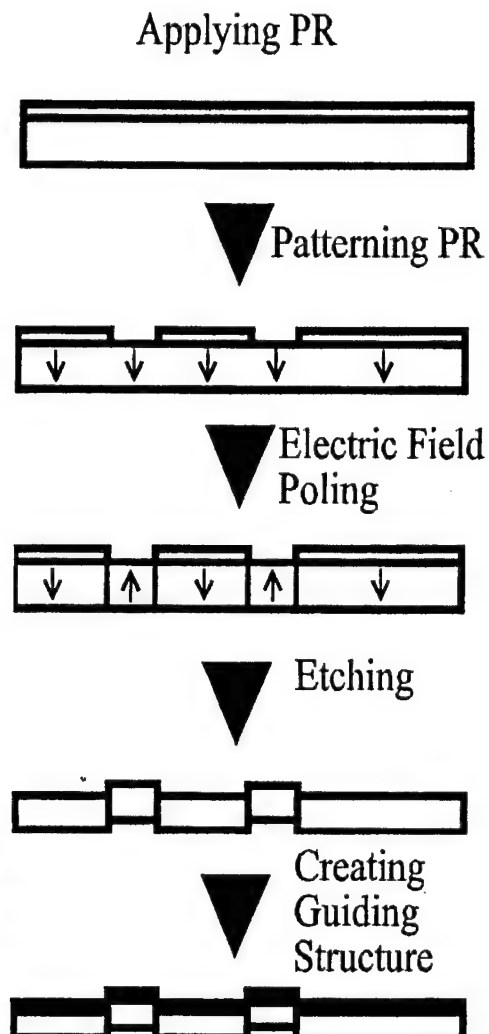
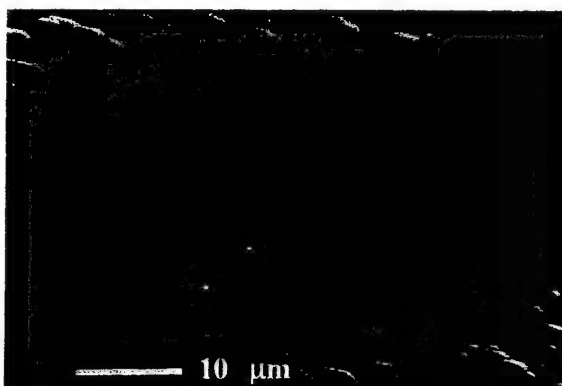


Introduction

- Recently V. Berger [Phys. Rev. Lett. **81**, 4136 (1998)] developed the idea of a nonlinear photonic crystal in which the linear refractive index is constant but the nonlinear susceptibility varies periodically.
- We have fabricated such a crystal in Lithium Niobate. Due to the crystal symmetry of LiNO_3 our crystal has hexagonal symmetry – hence HeXLN.
- Such a crystal is able to phase-match nonlinear interactions in any direction where there is a suitable reciprocal lattice vector (RLV).
- For certain angles of incident this should result in multiple output beams for a single input beam. Or it could phase-match multiple wavelengths at different angles simultaneously.

Lithium Niobate: differential etching

- +z untouched
- -z etches
700nm/hr
(room temp.)



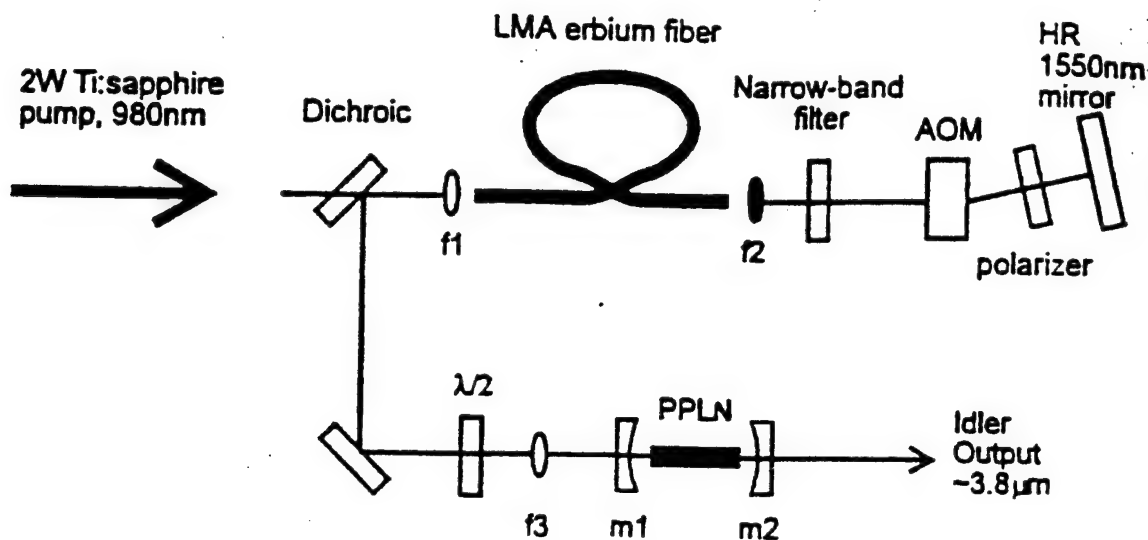


Fig. 1. Schematic of the setup: LMA, large-mode-area. AOM, acousto-optic modulator; HR, highly reflecting.

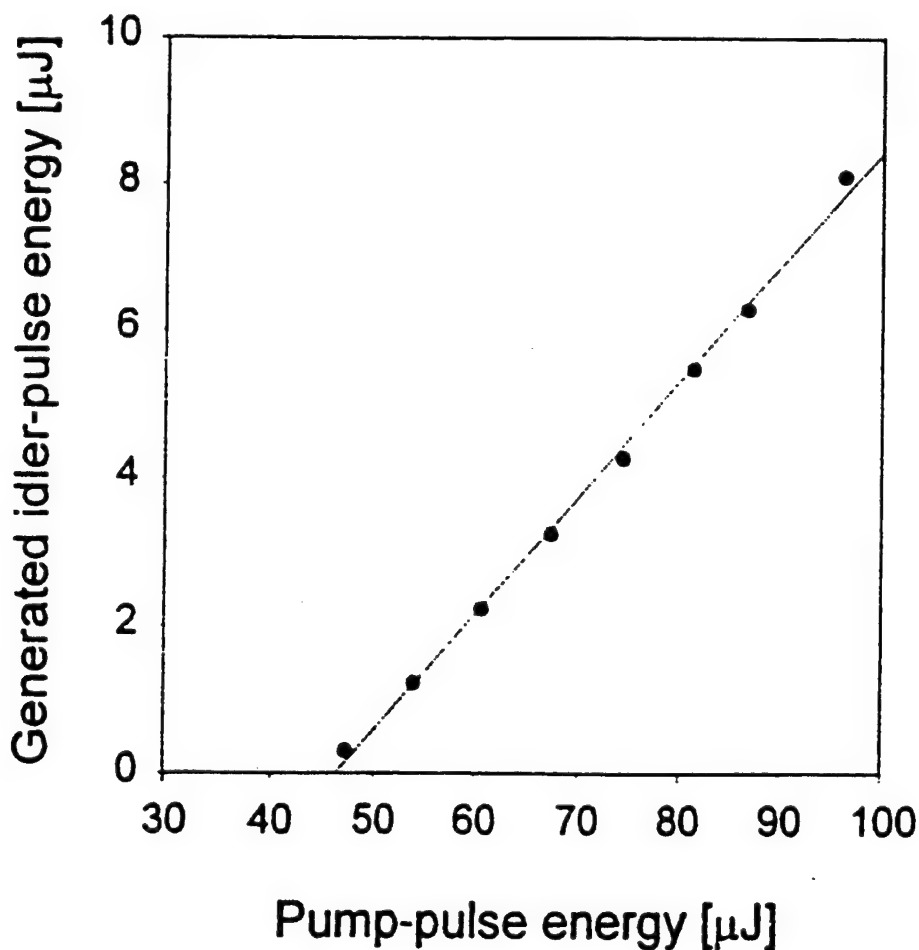
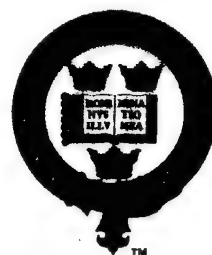


Fig. 2. Energy characteristics of the generated idler output at $2.61\mu\text{m}$.

Oxford Crystal Growth Group



Growth of phosphates and arsenates for periodic poling

K.B.Hutton and R.C.C.Ward

Clarendon Laboratory, Parks Road, Oxford OX1 3PU

- **Properties of phosphates and arsenates**
- **Material requirements for periodic poling**
- **Growth programme using self fluxes**
- **Assessment of results**

Collaborators

P.A.Thomas, Warwick Univ.

D.C.Hanna, P.Smith, Southampton ORC

M.H.Dunn, St.Andrews Univ.

Acknowledgements

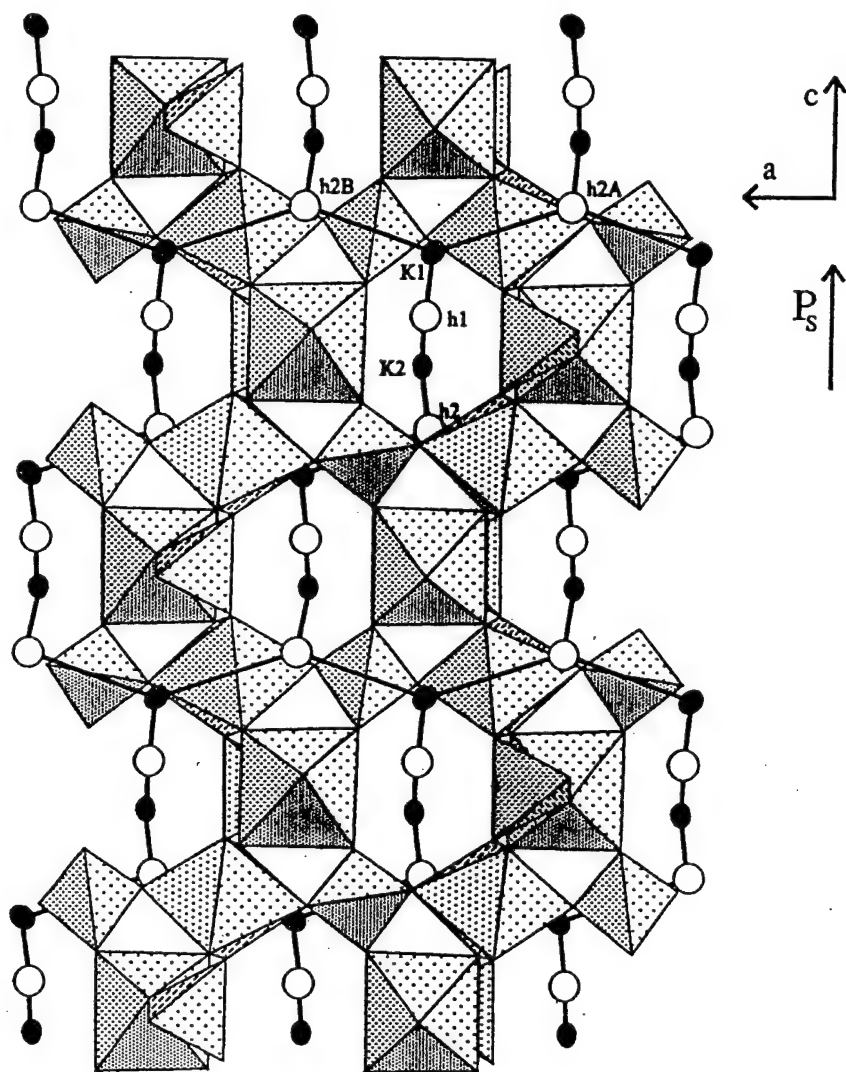
EPSRC, DERA Fort Halstead

Optical and electrical properties of KTP isomorphs

	KTP	RTP	KTA	RTA
Curie point (°C)	946	785	873	750
Trans. range (μm)	0.35 - 4.3	0.35 - 4.3	0.35 - 5.3	0.35 - 5.3
SHG NCPM y cut-off (nm)	994	1038	1075	1138
1.06 μm PM ϕ°	25	60	-	-
d_{33}	16.9	17.1	16.2	15.8
$d_{\pi\pi}$ type II, 1.06 μm	3.3	2.4	-	-
ionic conductivity 0.1kHz (S/cm)	$5 \times 10^{-7}^*$	2×10^{-8}	2×10^{-7}	10^{-11}

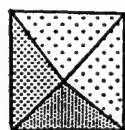
* Can be reduced to 2×10^{-9} by doping with trivalent ions

Sources : Cheng et al, J.Crystal Growth 137 107 (1994)
Cheng & Bierlein, Ferroelectrics 142 209 (1993)

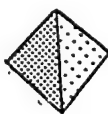


Crystal structure of $\text{K}^+\text{Ti}^{4+}\text{OP}^{5+}\text{O}_4$

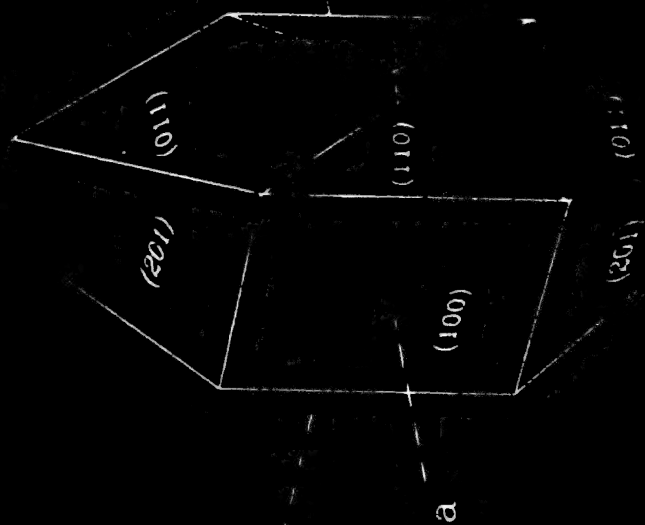
(from P.A.Thomas & A.M.Glazer, *J.Appl.Cryst.* 24 968 (1991))



TiO_6 octahedra



PO_4 tetrahedra



Morphology, growth, and orientation of crystals in solution

Electric field poling of KTP and analogues

- Electric field poling of hydrothermal KTP
Q.Chen & W.P.Risk, Electron.Lett. 30 1516 (1994)
- Periodic poling of RTA
H.Karlsson, F.Laurell et al, Electron.Lett. 32 556 (1996)
- Periodic poling of flux-grown KTP with Rb-exchanged layer
H.Karlsson & F.Laurell, Appl.Phys.Lett. 71 3474 (1997)
- Low-temperature poling of flux-grown KTP
G.Rosenman et al, Appl.Phys.Lett. 73 3650 (1998)

Advantages of KTP analogues for periodic poling

- Lower poling voltage than LiNbO_3
- Highly anisotropic crystal structure inhibiting domain broadening
- Stable device operation due to small dn/dT

Growth of KTP analogues for periodic poling

● Objectives

1. Production of high-quality, flux-grown KTP for poling trials
2. Investigate methods of lowering conductivity of KTP
Doping - Ga^{3+} (ref: Morris et al, *J.Cryst.Growth* **109** 367 (1991))
 Ce^{4+} (correlation with increased transmission?)
 Rb^{+} (ref. RTP properties)
3. Establish UK source of KTA and RTA
Extended IR transmission and inherently low conductivity (RTA)
4. Investigate in-situ poling techniques

● Growth methods

TSSG method using self fluxes



Synthesis of high-purity arsenate starting material

Production of arsenate seed crystals by spontaneous nucleation

Optimisation of growth conditions

flux composition, growth temperature, doping

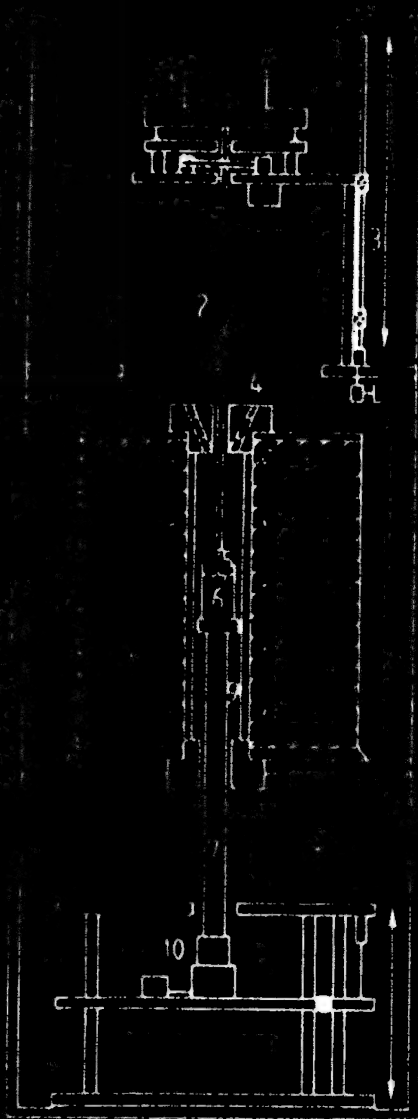


Fig. 1 Top Weighing TSSG Furnace

1. Electronic Balance
2. Seed Rod
3. Vertical Adjustment Stages
4. Optical Windows
5. Seed Crystal
6. Platinum Crucible
7. Alumina Crucible Support Rod
8. Three Zone Furnace
9. Silica Liner
10. ACRT Motors

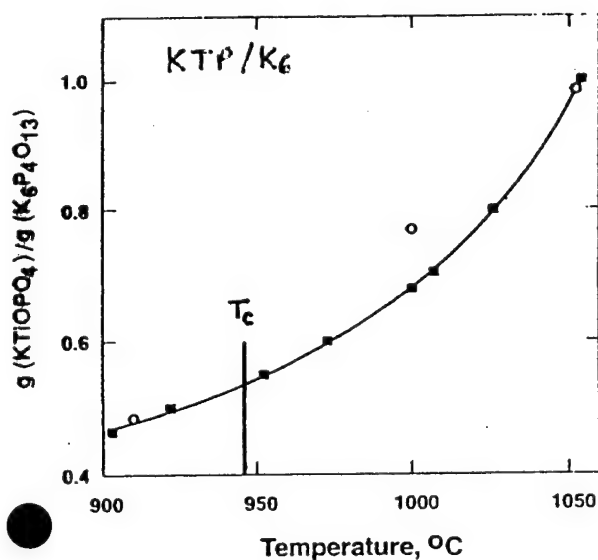
Self fluxes for KTP and analogues

Polyphosphate $K_2O - P_2O_5$ solvents :

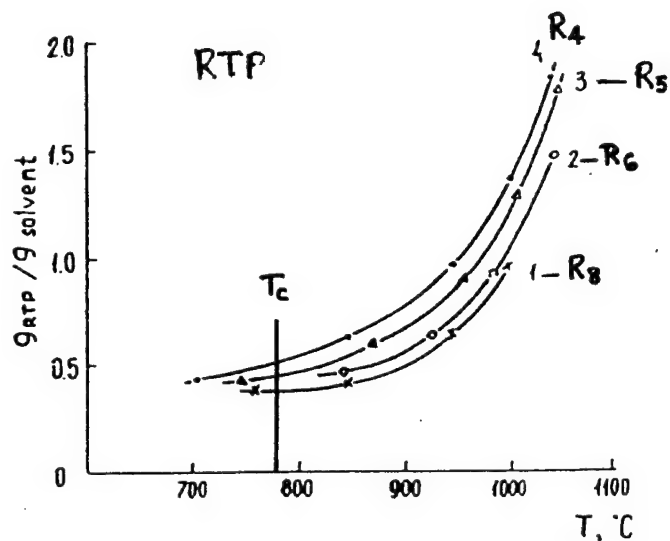
K_2O / P_2O_5	Flux
2	$K_4P_2O_7$
1.67	$K_5P_3O_{10}$
1.5	$K_6P_4O_{13}$
1.33	$K_8P_6O_{19}$

Corresponding
Rb and As analogues.

Solubility curves for KTP/ K_6 and RTP/ R_n



Ref: Angert et al, J.Cryst.Growth 137 116 (1994)



Ref: Oseldchik et al, J.Cryst.Growth 125 639 (1992)

Viscosity

- KTP/ K_6 – viscosity increases from 75cP at 950°C to 300cP at 800°C

High viscosity and flat solubility curve set limits for very low temperature growth

Results to date of growth programme

- Undoped KTP, Ga:KTP, Ce:KTP

Routine production of large crystals ($\approx 100\text{g}$) established

- Rb-doped KTP

5, 10, 20 mol% concentrations, growth temp. $\approx 860^\circ\text{C}$

Growth rate low along a-axis

Quality appears higher than undoped KTP

- RTP crystals

Growth along a-axis enhanced ($a:b:c \approx 1:1:1$)

Melt very viscous at 830°C - higher temp. under test

- Arsenates

Synthesis of starting materials established

KTA run in progress (886°C using K_6 flux)

Volatility of solution higher than KTP

RTA - small crystal grown at 893°C (R_5) to provide seeds

Evidence that a-axis growth enhanced in arsenates



Shekhar Guha and Chris Reyerson*
AFRL/MLPJ

Wright Patterson Air Force Base, OH 45433-7702
* Anteon Corporation

shekhar.guha@afrl.af.mil

NLO99 Workshop, DERA, Malvern, UK, 20 - 21 September, 1999



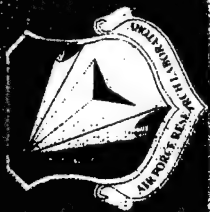
AR coating wafers:

1. Coating 2 inch diameter single wafer, dicing in oriented pieces and stacking three coherence length thickness 320 micrometers
2. Growing 100 wafers 1 inch diameter, three coherence length thick
Then IR AR coating at 5.3 and 10.6 micrometer

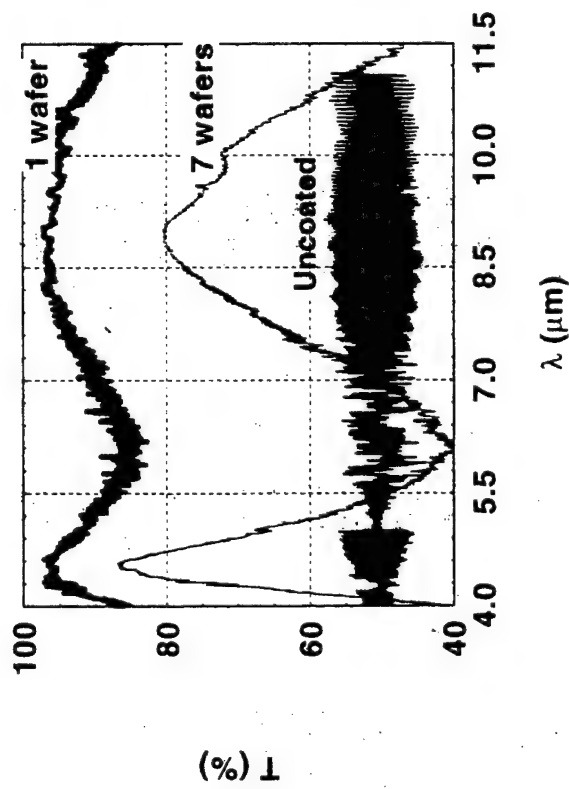
Results:

1. Up to 5 μ J of MWIR energy generated
2. Saturation of generated power observed

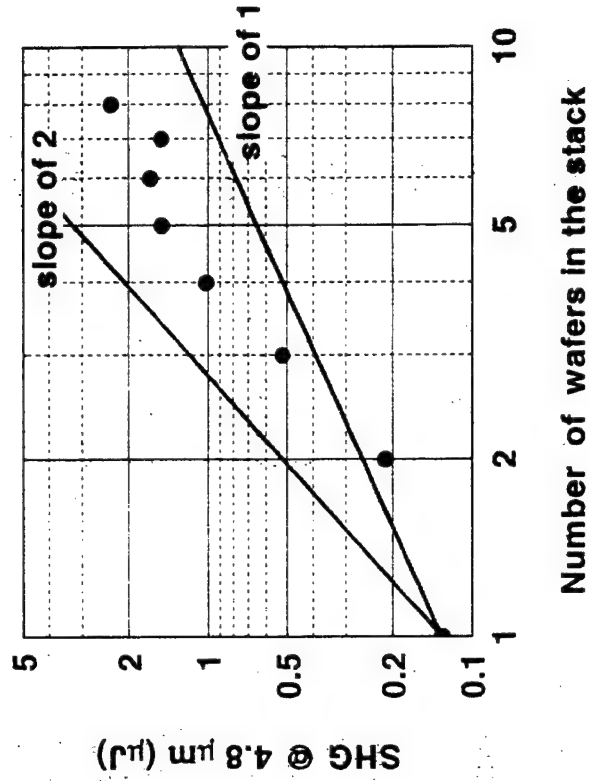
Possible causes of saturation being investigated



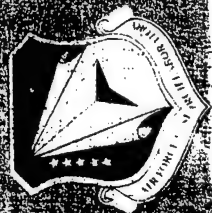
AR coated 320 μm GaAs wafers



SHG of 9.6 μm laser



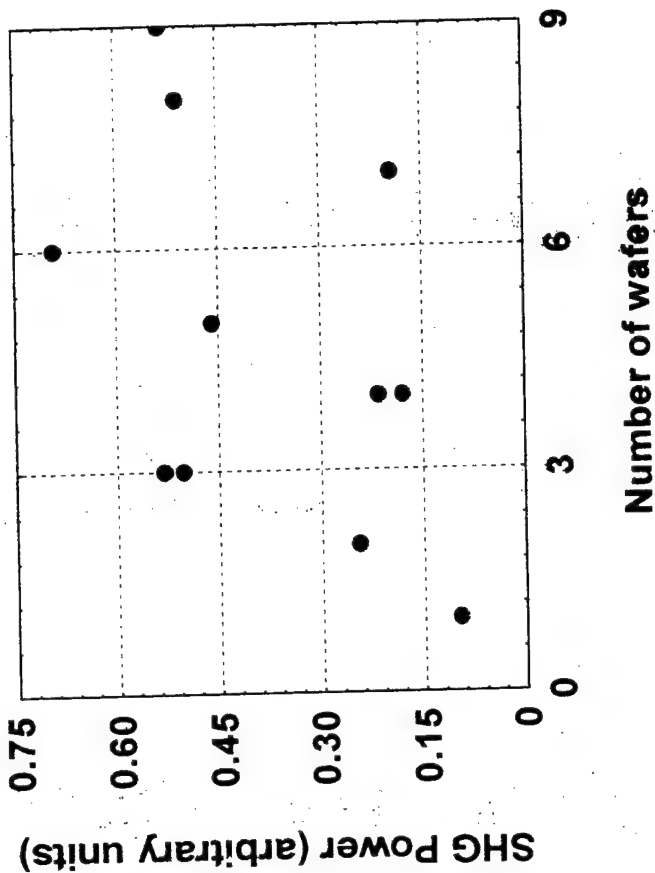
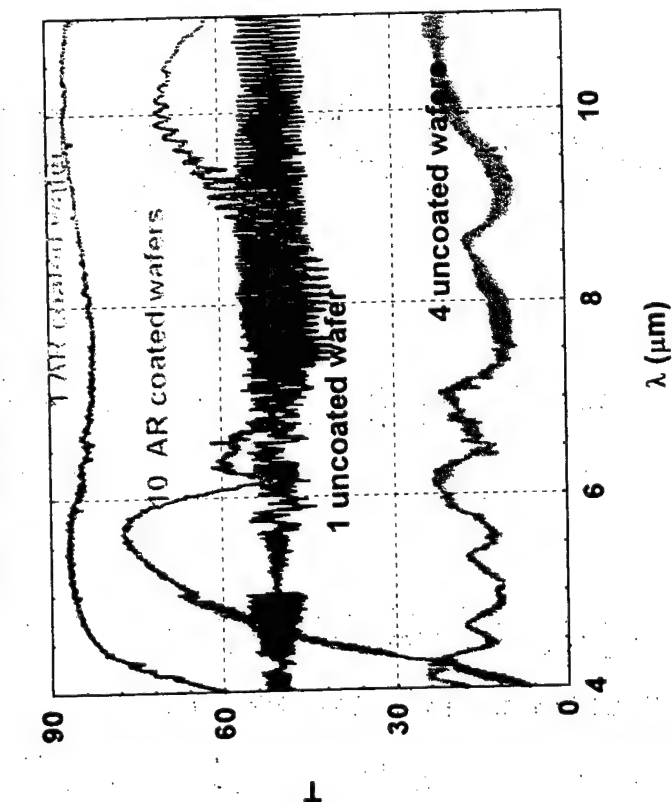
- SHG is not increasing quadratically
- Saturation of generated signal



SHG in AR coated GaAs Wafers of 107 μm

1 Coherence length each

1 inch diameter, 107 μm GaAs Wafers



Worse SHG performance



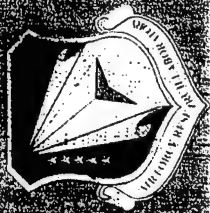
	d_{eff}	n	K	α	dn/dT	FOM_1	FOM_2
GaAs	61	3.3	55	0.01	1.5	2.5	633
ZnSe	37	2.4	18	5×10^{-4}	0.64	2.4	9333
CdTe	28	2.7	6.3	0.001	0.5	1	867

ZGP	70	3.1	35	0.1 (1996)	1.7	4	55
CGA	154	3.5	4.2	0.2 (1996)	5	13.5	5
AgGaSe ₂	27	2.6	1	0.01	0.7	1	1

d : pm/V
 K : W/m/K
 α : cm⁻¹
 dn/dT : 10⁻⁴ K⁻¹

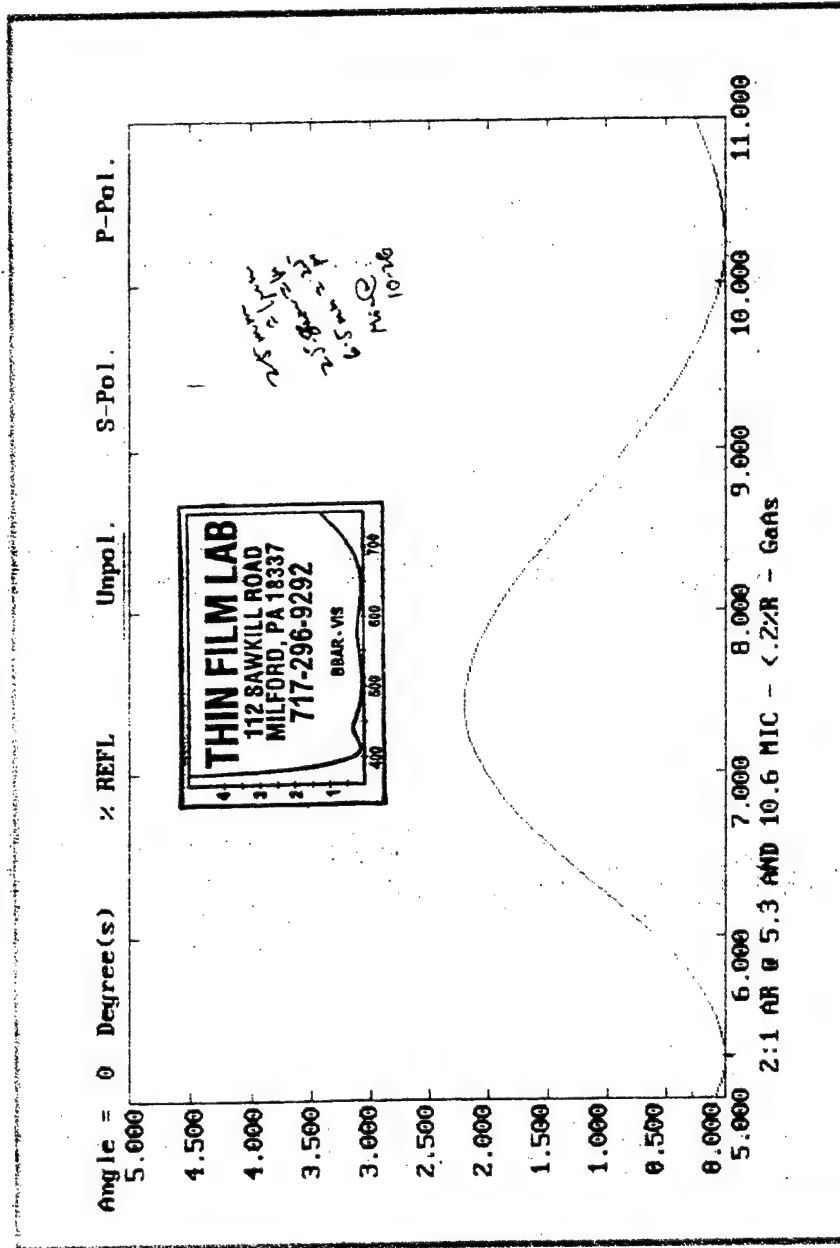
$$FOM_1 = \frac{d^2}{n^3}$$

$$FOM_1 = \frac{d^2}{n^3} \times \frac{K}{\alpha} \frac{dn/dT}{\alpha}$$



Reflectivity of a single AR coating GaAs window

1 coherence length ($106 \pm 10 \text{ } \mu\text{m}$)



Very low reflectivities shown at 5.5 and 10.26 μm

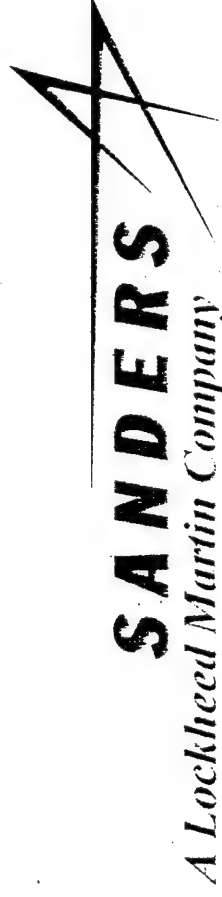


AR coating GaAs for efficient QPM SHG of CO₂ laser was attempted

Coating performance still not adequate

A New Nonlinear Optical Material: Periodically-Poled Barium Titanate (PPBT)

P. G. Schunemann, S. D. Setzler, T. M. Pollak



Presented at the 1999 Nonlinear Optical Materials
Workshop, (NLO 99); DERA, Malvern, UK, Sept. 21, 1999

Work supported L.N. Durvasula at DARPA (via the Air Force Research Laboratory Materials Directorate
contract No. F33615 -94-C-5415) and Sanders Internal R&D Funding

Periodically-Poled Barium Titanate

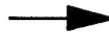
SANDERS

A Lockheed Martin Company

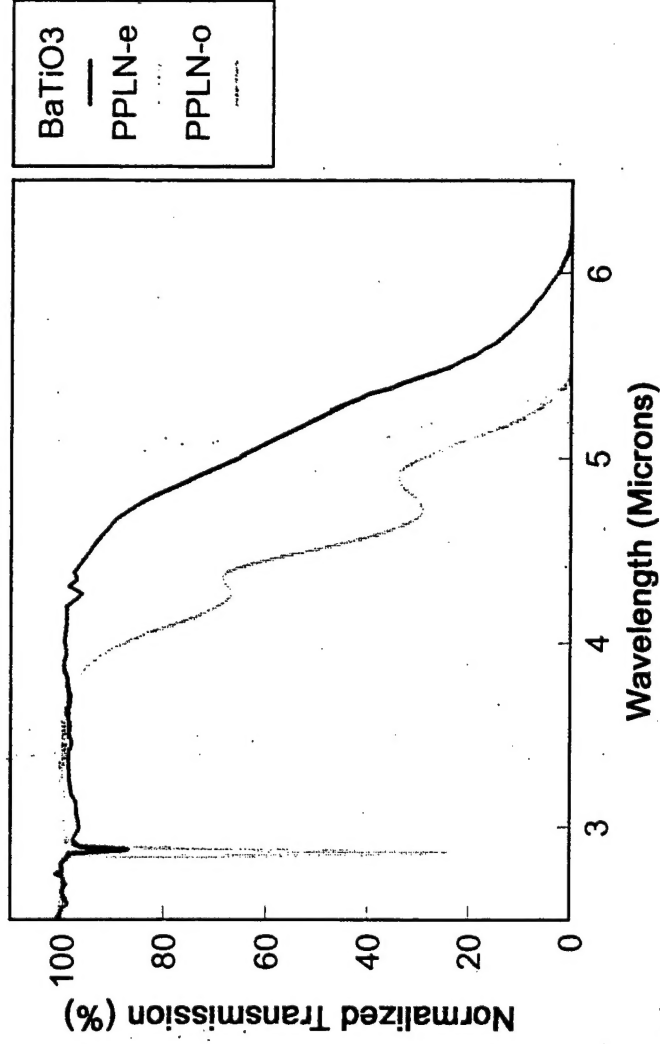
Advanced Engineering and
Technology Division

BaTiO₃ Offers Very Attractive Properties for Periodically-Poled OPOs

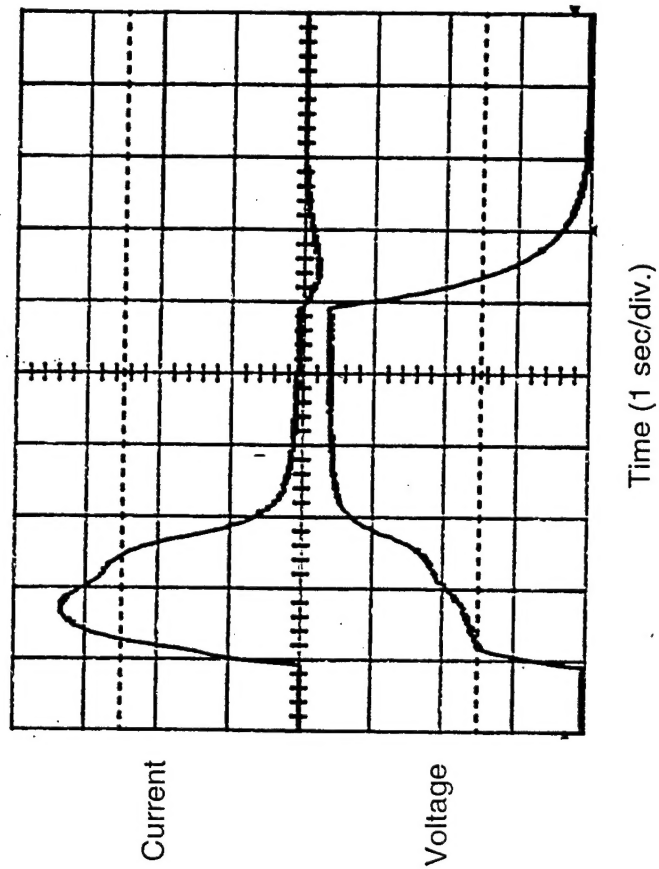
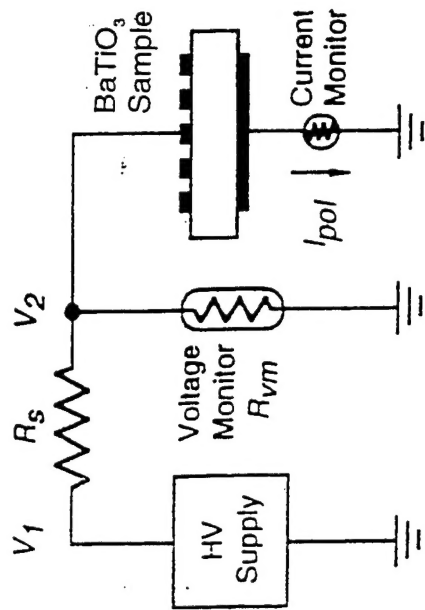
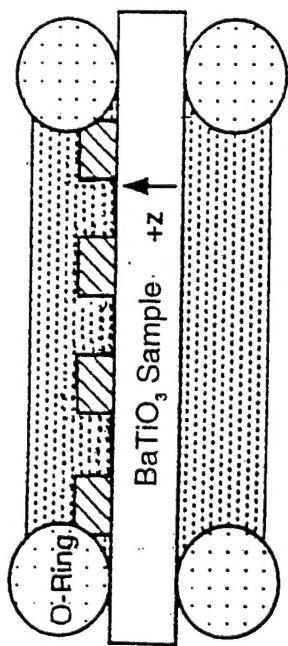
- Longer IR cut-off than PPLN (allowing full 3-5 micron coverage)
- Low Coercive Field (100V/mm, 200x lower than PPLN)



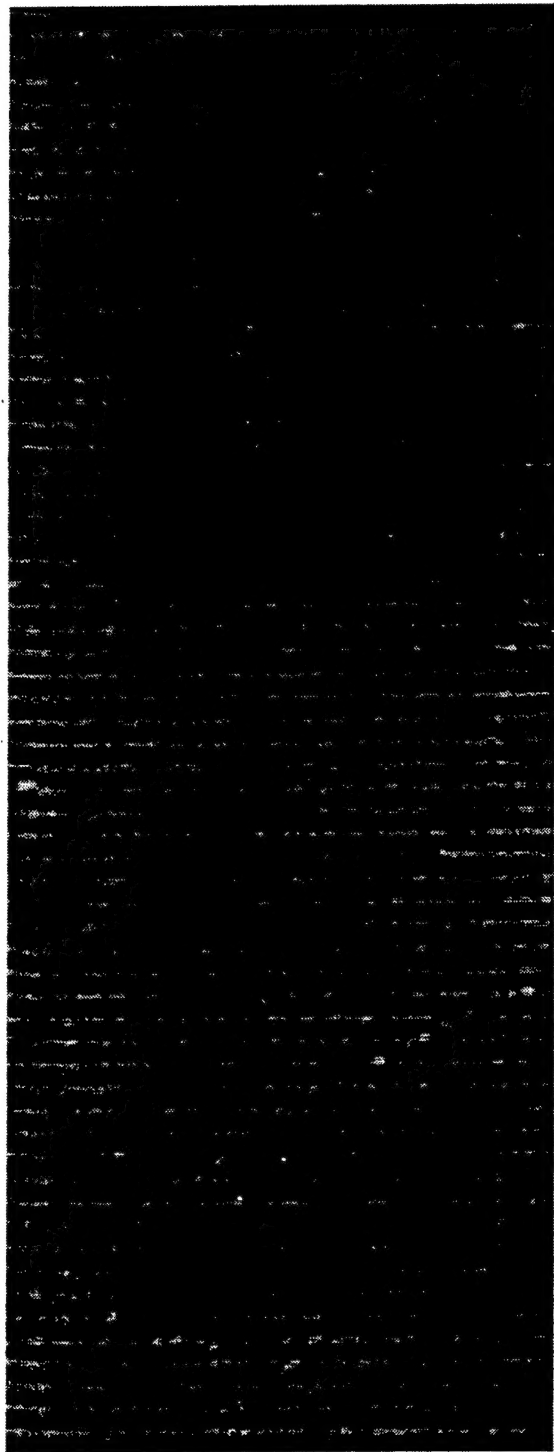
- Larger Apertures
- Large Nonlinear Coefficient
 $d_{15}=17\text{pm/V}$



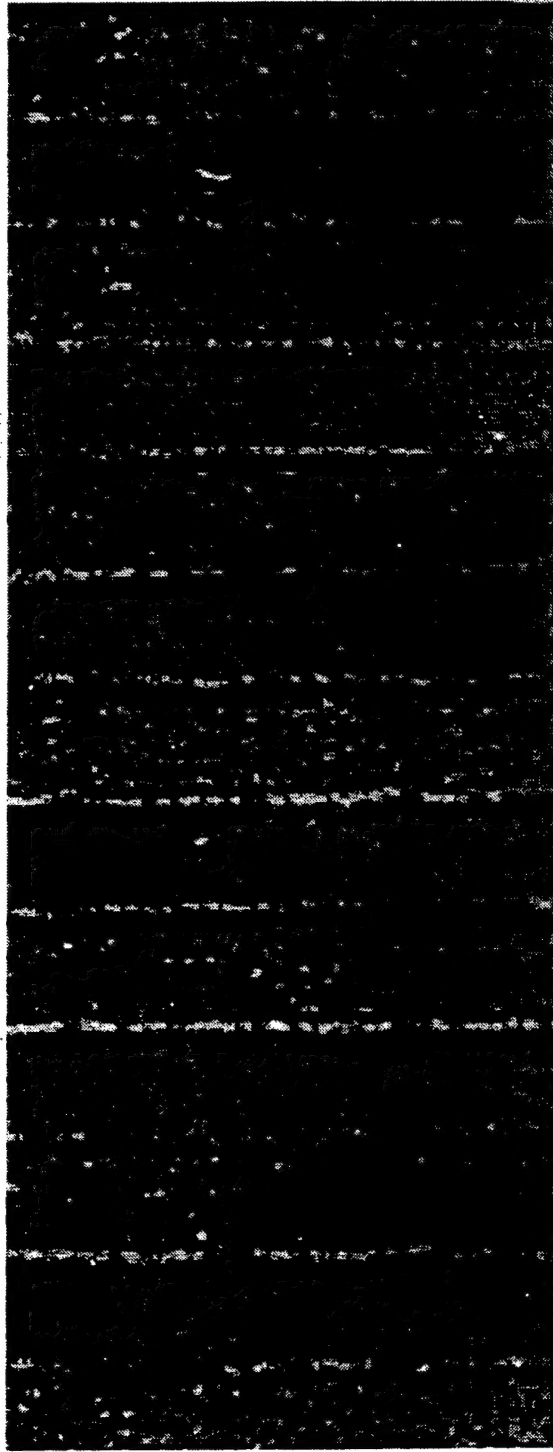
-  Liquid Electrolyte
-  Insulator (Photoresist)



Images of sample #296G (Total poling depth ~0.5 mm)



150X magnification



1500X magnification

17 μm

Periodically-Poled Barium Titanate

SANDERS

A Lockheed Martin Company

Summary

Advanced Engineering and
Technology Division

- Barium Titanate single crystals were grown by the TSSG technique
- New refractive index measurements revealed insufficient birefringence for phase-matching, allowed determination of QPM grating spacings
- Periodic poling of bulk BaTiO₃ successfully demonstrated for the first time
 - Wafers survived photoresist patterning and bake-out
 - Domain reversal achieved at low E-fields (200X lower than for PPLN)
 - Mask grating pattern reproduced on wafer (no spreading of domains under photoresist unless overpoled)
 - Large thickness (1.4 mm) poled in first trial
- Quasi-phase-matched SHG demonstrated in PPBT
 - 10W of 2.05um input (10kHz, 10ns) produced 300mW at 1.025um from an uncoated, 8mm-long sample at ~55° C (4% conv. eff. after refl. loss)
 - No evidence of photorefractive damage or thermal lensing was observed